TWIN SCREW RANULATION: UNDERSTANDIN THE MECHANICAL PROPERTIES OF PHARMACEUTICAL EXCIPIENTS FROM POWDER TO TABLET

Bilal Khorsheed

Department of Chemical and Biological Engineering

The University of Sheffield

A thesis submitted in partial fulfilment of the requirement for the degree of Doctor of philosophy

January 2019

Publications related to this thesis

- B. Khorsheed, I. Gabbott, G.K. Reynolds, S.C. Taylor, R.J. Roberts, A.D. Salman, Twin-screw granulation: Understanding the mechanical properties from powder to tablets, Powder Technol. 341 (2019) 104–115.
- B. Khorsheed, I. Gabbott, G.K. Reynolds, S.C. Taylor, R.J. Roberts, A.D. Salman, Twin screw granulation: understanding the mechanical properties from powder to tablets. The 8th international granulation conference, Sheffield, UK J, 2017, paper number 68.

Other publications

- W.H. AlAlaween, B. Khorsheed, M. Mahfouf, I. Gabbott, G.K. Reynolds, A.D. Salman, Transparent Predictive Modelling of the Twin Screw Granulation Process using a Compensated Interval Type-2 Fuzzy System, European Journal of Pharmaceutics and Biopharmaceutics. 124 (2017) 138–146.

Contents

List of Figures

List of Tables

Nomenclature

P	Compaction Pressure
K	Heckle Coefficient
D	Relative Density
F	Tablet Crushing Force
H	Tablet Diameter
εT	Tablet Porosity
σ_T	Tablet Tensile Strength
T	Tablet Thickness
Y_p	Yield Pressure

Abbreviations

ANN	Artificial Neural Network
APIs	Active Pharmaceutical Ingredients
BA	Bonding Area
BET	Brunauer–Emmett–Teller Equation
BS	Bonding Strength
BSA	Bonding Surface Area
DAWB	Dry And Wet Bond
HPC	Hydroxypropyl Cellulose
HSM	High Shear Mixer
K60°	Kneading Disc At 60° Pitch
L/S	Liquid To Solid (Ratio)
MCC	Microcrystalline Cellulose
MP	Mechanical Properties
PAT	Process Analytical Technology
QSARs	Quantitative Structure-Activity Relationships
SB	Solid Bridge
SEM	Scanning Electron Microscope
SPCE	Short Pitch Conveying Screw Elements
SSA	Specific Surface Area
TS	Tablet Strength
TSG	Twin Screw Granulation
UCC	Unified Compaction Curve
Yp	Yield Pressure

Abstract

In the pharmaceutical industry, tablets are the most widespread oral dosage form. Tablets make approximately 70-80% of all administrated medications. Tablets are normally manufactured either by direct compression of powder or granular intermediate. Granulation is a technique commonly used before tabletting in order to solve powder handling problems and ensure uniform filling of the compression dies. However, granulation can have an impact on powder transformation into a tablet; i.e. tabletability.

The overall aim of this work is to understand the effect of the mechanical properties of the primary powder and the granulation process on granules and tablets properties, most importantly tablet tensile strength. The study investigated the mechanisms that dictate the change in tabletability before and after wet granulation using twin screw granulation (TSG). Additionally, the research focused on improving the understanding of the relationship between the properties of the compressed materials and their tablet strength.

To achieve the aims of the project four pharmaceutically-relevant excipients with different mechanical strength and water solubility were granulated in a TSG at a variety of stresses using a range of screw speeds and screw configurations. The mechanical properties of the powder were characterised by Heckel analysis and work of compaction. A regime map that enables the prediction of the percentage of change in tabletability after TSG compared with direct compression is proposed. The materials were classified by the yield pressure of the primary powder. A mitigation strategy to reduce the loss of tabletability after granulation was proposed based on the regime map.

In addition, an empirical equation to predict the tabletability of powders and granules is proposed which provides a mechanistic understanding of the origins of tablet tensile strength. It was found that the specific surface area available for bonding in association with the moisture content of the compressed materials (granules and powders) are capable of explaining the tabletability of mechanically different materials. Moreover, the model can successfully predict the tabletability of plastically-deforming materials such as MCC, as well as brittle materials such as mannitol and even blends of them.

Lastly, a modelling approach using artificial neural network was developed to predict the granules size and their tablets strength. The developed model helps in reducing the development times by removing the need for trial and error which is common in the pharmaceutical industry.

Acknowledgements

Doing a PhD is not a smooth journey at all, anyone who has done a PhD would relate to what I mean. Without great family, lovely friends, and the help of so many sincere and supportive people my PhD would have been impossible.

Firstly, I would like to thank Prof Agba Salman for his great support during my PhD under his supervision. He always pushed me further to reach new limits of my capabilities. His unique open-door policy is very appreciated. Especial thanks are reserved to Dr Ian Gabbott. He was a great friendly supervisor always there to support and engage in great scientific discussions. He always believed in me and supported me, he added a new dimension to my journey, I am eternally grateful to him. I also would like to thank Prof Gavin Reynolds, he always finds time to help. Also, extended thanks go for all AZ friendly staff.

My Parents are indeed the main people who were behind my achievement. My amazing Dad was the first and main believer in me, without him, I would have not achieved anything on my academic achievements. He taught me how to aim for the Sky, he overwhelmed me by his unconditional support. In addition, my mom and her endless emotional support, I would have not been able to keep up my journey. I am forever grateful for you Both, Lina and Mohamad. My lovely brothers and sisters Bader, Batool, Amr, and Raghad, enormous thanks for being a great support and source of motivation. I love you to bits.

To all my amazing friends, I am so lucky and delighted to have you all. Every one of you supported me to his/ her limits with loads of care and love, for that I am always grateful to you all, and I always love you.

Finally, I would like to thank AstraZeneca and EPSRC for their financial support.

Chapter 1   Introduction

1.1   Tabletting and granulation

Powder pressing is a widely used process in several industries, such as pharmaceuticals, industrial ceramics, batteries, detergents, and food. In the pharmaceutical industry, tablets are the most widespread oral dosage form. Tablets make about 70-80% of all administrated medications [1,2]. Tablets are widely used because of their ease of administration, packing, handling, manufacture and distribution [3,4]. Good-quality tablets must meet several criteria including good chemical and physical stability, content uniformity of the constituents – including the active pharmaceutical ingredients (APIs), intended API release profile and adequate tabletability [5].

Tabletability is defined as the ability of powder or granules to transform into a tablet of adequate strength due to compression. It is usually presented as a plot of the tablet tensile strength vs compaction pressure. The adequate physical strength of tablets is essential to maintain the quality of tablets by resisting fracture, abrasion, and chipping during manufacturing processes, transportation and shelf-life [6,7].

Tablets are manufactured by either direct compression of powder or compression of a granular intermediate. Direct compression of powders is preferable as it reduces cost and minimises any potential physical or chemical change of the APIs. Some APIs and excipients have inherent flow, compressibility and/or segregation issues, which make granulation a necessary step before tabletting [8]. Granulation is mainly used to improve one or more of the properties of the starting materials namely flow, handling, dustiness, uniformity (reduction of segregation) [9]. Figure 1.1 is a schematic illustration of the possible processes available to transform powder into a tablet. Route A is the direct compression of powders, which is usually applied for powders that have good flowability, good compactability and a low tendency to segregate. While route B is usually applied for powders that are hard to flow and tend to segregate.
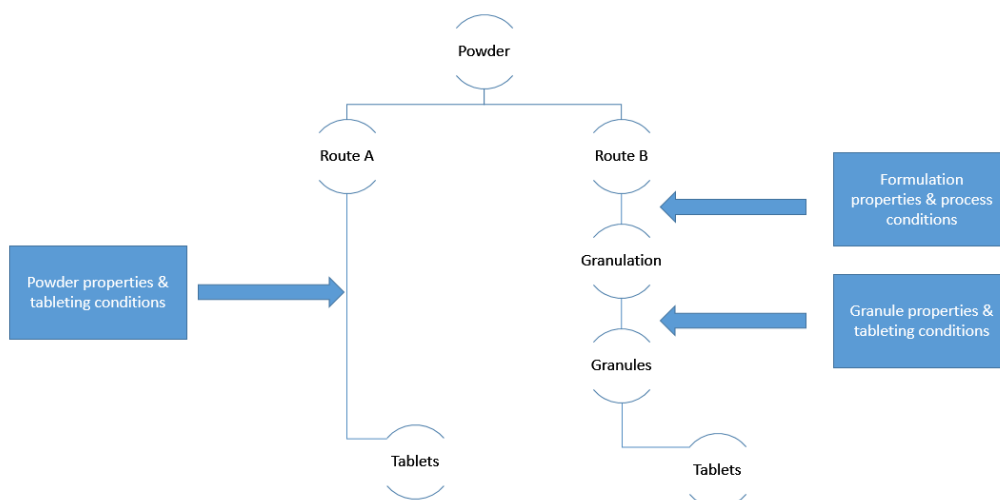
Figure 1.1 Flow chart of tablet manufacturing selection process based on powder properties.

Granulation is the process of particle size enlargement, in which materials consisting of small particles are aggregated to produce large particles (granules) [10]. Granulation can be either a dry or wet process. Wet granulation is commonly used as a granulation method, in which liquid binder is added to the powder to form interparticle bonds. The powder-liquid mass is agitated in order to promote particle agglomeration and granule growth. The focus of this research is wet granulation using twin screw granulation (TSG).

Even though wet granulation can improve the processability and powder handling, It can add more cost for manufacturing compared with the direct compression. Most importantly, it can influence the quality attributes of the final products (i.e. tablets) [11].

Granulation can have an adverse effect on the tablet tensile strength, whereby tablets produced from granules generally have lower tablet strength compared with tablets produced by direct compression. This phenomenon is usually referred to as the loss of tabletability [12,13]. The loss of tabletability after dry granulation has been investigated by several studies [14–17]. Some work was done to understand the effect of wet granulation using high shear mixer (HSM) on the tabletability of the granulated materials. It was reported that the porosity, strength, and the size of the granules is related to the change in tabletability after granulation [18,19].

TSG is distinctly different from roller compaction and HSM in the mechanisms of size enlargement, type and extent of the compression and shear stresses, and the residence time during granulation. The use of a granulation liquid can have a significant impact on

4

the process when compared with roller compaction. Hence, the mechanisms that describe the reduction of the tabletability of granules made using roller compaction and wet granulation by HSM should not be extrapolated to wet granulation by TSG without a thorough investigation. There appear to be no reports in the available literature to date about the mechanisms which describe the change in tabletability of the granulated material using TSG which was part of the motivation for this work was to try to investigate such mechanisms. More importantly, three is still a need for more research to understand the mechanisms that lead to a change in tabletability and correlate it with the properties of the compressed materials.

Rational tablets development should be based on a profound understanding of the material properties and the processing conditions that affect the tabletting process, to ensure good quality tablets [20]. Several models have been used to predict the compaction behaviour of powders/ granules based on the data analysis (load and displacement data during compression) [19,21,22]. Despite the usefulness of the compaction data analysis, which was the focus of several studies [23–25], these studies did not provide a direct correlation between the material properties and tablet strength.

It is widely accepted that two factors are primarily responsible for the tablet strength, which are the surface area available for bonding and the dominating mechanisms for bonding [26–28]. However the direct effect of the moisture on the total strength of tablet has been overlooked. This research aims to deconvolute the effect of the factors which dictate the tabletability such as specific surface area, particle size, granule porosity, plasticity and elasticity of powders and granules, moisture content and the primary mechanisms of bonding. This research proposed a mechanistic equation based on powder/granules properties to predict the tablet tensile strength. Additionally, a data-driven model was developed to predict the tablet strength.

1.2 Aim and objectives

The overall aim of this work is to understand the effect of the mechanical properties (MP) of the primary powder bed and the granulation process parameters on the granules and tablets properties, mainly tablet tensile strength. Consequently, providing the necessary knowledge for better prediction of the quality attributes of granules and tablets. Twin screw granulation was used as a model for wet granulation process.

The first objective of this research is to investigate how the mechanical properties of the primary powder influence the granulation process and consequently the quality attributes of granules and tablets. Secondly, to investigate the mechanisms that dictate the change in tabletability after wet granulation using twin screw granulator and provide mitigation strategies for the loss of tabletability. Thirdly, improving the current understanding of tabletability by investigating the effect of the bonding surface area and the main bonding mechanisms. Lastly, providing predictive models for both powder and granules based on a rigid mechanistic understanding of the granulating proses and the material properties.

1.3 Thesis overview

Chapter 1: A brief introduction to the importance of tabletting and granulation.

Chapter 2: The scope of this chapter focuses on the available literature about wet granulation and the tabletability of powders/granules. In addition, it explains the main mechanisms of tablet formation and highlights the predictive models of tabletability. Also, it covers one of the main drawbacks of granulation which is the loss of tabletability after granulation.

Chapter 3: This chapter focuses on the materials used in this study, and the experimental and analysis methodology used.

Chapter 4: This chapter investigates the loss of tabletability after twin-screw granulation. A regime map of the reduction in tabletability after twin-screw granulation was proposed. Furthermore, a predictive model based on a material property (yield pressure of primary powder) is suggested.

Chapter 5: This chapter investigates the mechanisms that control the tabletability of powders and granules. A novel universal predictive compaction model was proposed.

Chapter 6: This chapter provides a solution to control the change in tabletability after twin screw granulation. In addition, the dissolution rate of the granulated formulation was investigated.

Chapter 7: In this chapter, a data-driven model using an artificial neural network was developed to predict the granules size represented by its D values (D_{10}, D_{50}, and D_{90}), and the tablet strength of powder and granules.

Chapter 8: An overall summary of the main findings of each study was provided.

Chapter 9: Further work that can be conducted to improve the current understanding of the main mechanisms that control tablet strength and the change in tabletability after granulation is suggested.

Chapter 2   Literature Review

Tablets are the most widespread oral dosage form, which makes about 70-80% of all administrated medications [1,2,29]. Tablets are made either through direct compression (DC) or granulation [30]. The DC method is suitable for the materials that have good properties including but not limited to the following: good flowability, low tendency to segregate, good mechanical properties [31]. However, not all powders have good flowability and compressibility properties. Bad flow properties can lead to variation in tablet weight if the material is compressed directly. Therefore, some powders need to be granulated to improve their properties, so the powders become suitable for tabletting.

In this literature review, a brief introduction about twin screw granulation is provided. Then the effect of the granulation process and the properties of the primary materials on the quality of resulted granules and tablets is discussed. Also, the mechanisms of the loss of tabletability after granulation are explained and the possible solutions to mitigate the loss of tabletability. The review also covers the main factors and mechanisms that dictate the formation of a tablet. The prediction models for tablet strength are reviewed. Lastly, the factors that affect the dissolution behaviour of tablets made from granulated materials are discussed.

2.1   Twin screw granulator

In 1986, Gamlen and Eardley were the first to report using single screw extruder to produce Paracetamol extrudates [32]. Shortly afterwards, Lindberg et al. used a twin screw extruder to produce effervescent tablets [33]. Between 1987 and 1988 Gamlen published a series of papers on the effect of process variables on the granules properties [33]. In 2002, Ghebre-Sellasie et al. were awarded a patent on the use of twin screw granulator (TSG) in a single pass continuous pharmaceutical granulation process, which led to an increase in the interest and the depth of research in TSG [34].

TSG is a machine with a pair of co or counter-rotating screws, which are housed inside a longitudinal barrel. The screws are composed of different elements which are designed to perform different process steps inside the barrel including feeding, mixing, granulation, conveying and discharging [35].

TSGs are built with a variety of designs and fields of application. Chan et al. provided a good review article about the variability in the types of twin screw granulation and the effect of the equipment/process parameters on the quality of the granules. The most commonly used type of TSG is the co-rotating self-wiping, Figure 2.1 presents an example of the TSGs different designs:
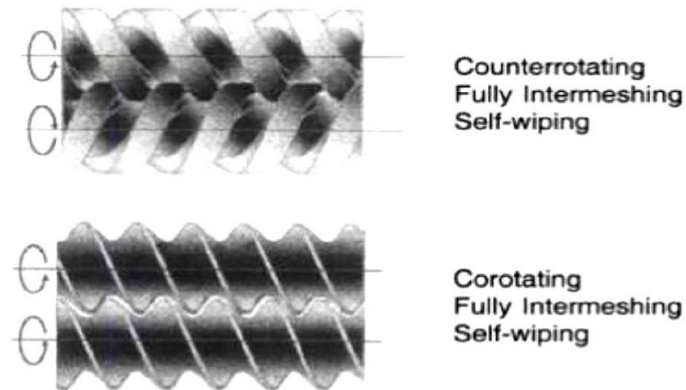
Figure 2.1 Counter and co-rotating fully intermeshing self-wiping twin screw. Adapted from [1].

The screws of the twin screw can be configured into endless possibilities by changing the arrangement of the screw elements as presented in Table 2.1. The change in the screw configuration is expected to change the granule formation rate.

Table 2.1 Description of the screw elements used in the granulation process.

Screw element type	Ratio of length of the element to its diameter	Element Image
Short pitch conveying element (SPCE)	L=D	
Long pitch conveying element (LPCE)	L=2D	
Kneading disc with 60° staggering angle	L=D/4	

2.1.1 Mechanism of wet granulation including the twin screw granulator

Wet granulation process starts with the addition of a liquid, which functions as a binder, to the dry powder. The liquid will then be distributed among the powder particles by mechanical agitation generated via the granulator. The particles start to adhere to each other because of the liquid bridges. The addition of more binder and the mechanical agitation promote further adhesion between the particles [2].

The type of granulation equipment affects the mechanism by which the dry powder transforms into granules [3]. Nevertheless, the wet granulation mechanism can be divided into four stages which include nucleation, consolidation, coalescence/ growth, attrition and breakage [2]. Figure 2.2 is a schematic drawing of the mechanisms of the granulation process.
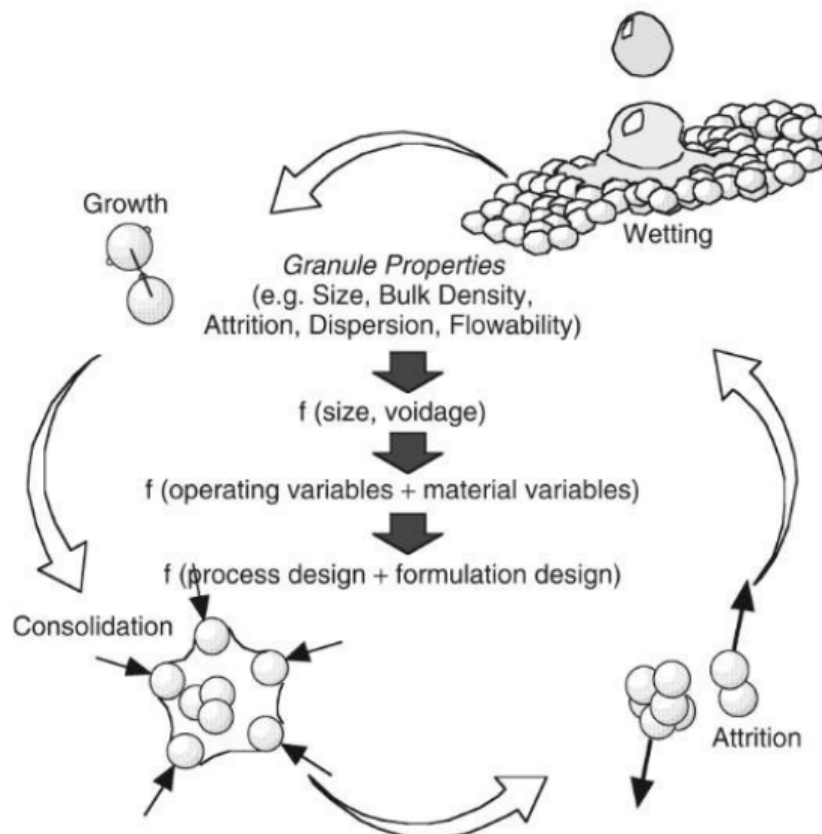
Figure 2.2 The mechanisms of granulation [2].

Twin screw granulation (TSG) was used in this study as a continuous granulation technique. The mechanism of granulation inside the TSG was investigated by Dhenge et al. (2012). They divided the granulator barrel into several compartments as shown in Figure 2.3.

Dhenge et al. (2012) concluded that granulation takes place in a series of steps in compartments along the length of the screw. C1 is the segment at which the liquid binder is added to the powder. Nucleation happens in C1 (conveying elements) where big agglomerates are formed, consolidation and breakage take place in C2 due to the kneading elements. In C3, some coalescence and breakage happen leading to an increase or decrease in the size of the granules depending upon which mechanism is dominating. In C4 coalescence and consolidation is dominant and breakage in C5 is causing decrees in the mean granule size [1].
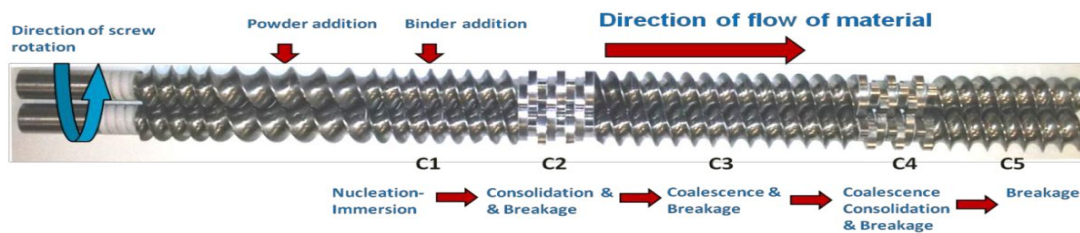
Figure 2.3 Mechanism of granulation in twin screw, adapted from [1].

2.1.2 Granulation regime maps for twin screw granulators

Dhenge et al. developed two regime maps for granule growth using TSG. The first one using conveying elements only [5] and the second using both conveying and kneading elements [6]. Both maps were developed based on the deformation value and the pore saturation of the granules as presented in Figure 2.4.

The deformation value (β) was determined by dividing the stresses acting on the wet mass by the strength of the dry granules [6]. Ideally, the strength of the wet granules should be used instead. A small deformation value indicates a strong granulation system while a large value represents a weak one. The stresses that the wet mass experience in the granulator barrel was calculated by dividing the torque of the twin screw by the volume of the material in the twin screw barrel. The pore saturation of the granules is affected by the liquid to solid ratio (L/S) as well as the viscosity of the binder [6].
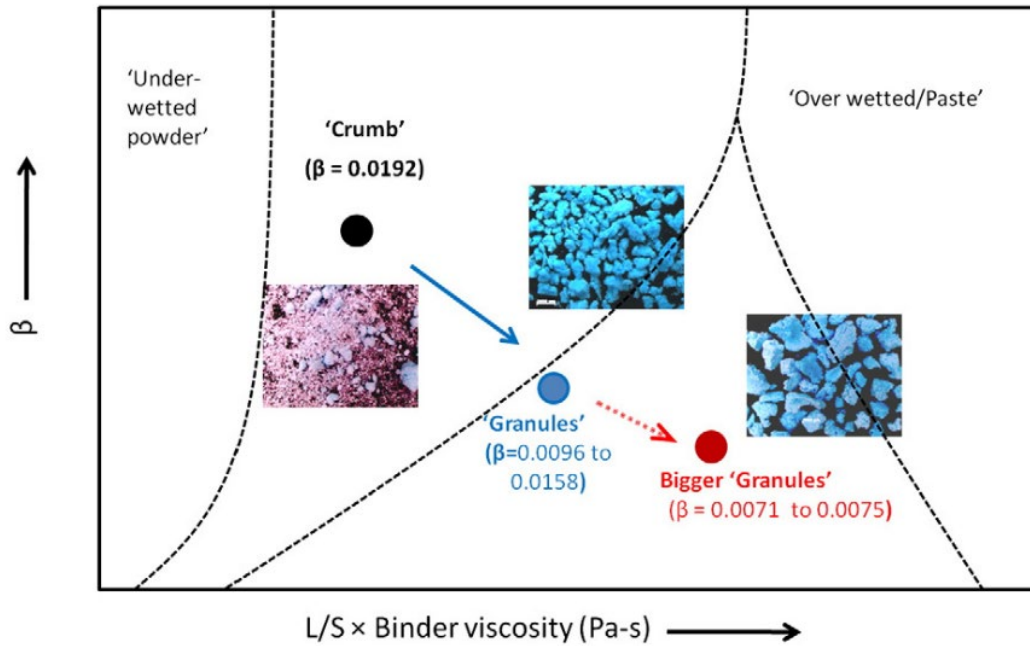
Figure 2.4 Granule growth map for twin screw granulation, adapted from [7].

Tu et al. proposed a regime map for granulation using twin screw [8]. The study covered three parameters; the L/S ratio, screw speed and screw configuration and used the screw speed and the motor torque as scale-dependent parameters [8]. The study found that an increase in the screw speed leads to a reduction in the fill level of the granulation barrel [8]. Another regime map was suggested by Kumar et al. whereby the regime map was based on the correlation between the L/S ratio used for granulation and the specific mechanical energy. The specific mechanical energy expressed by the screw speed, material throughput and the troupe needed to move the screws [9].

The suggested regime maps help in obtaining granules with the required granule properties such as granule size distribution, flowability, shape, strength and compressibility [6,10].

The papers reported in this section demonstrate that the process and formulation parameters could directly affect the granules properties. The granule properties have a significant effect on the tablet attributes, i.e. tablet strength and dissolution rate [11,12]. In the following two sections the effect of the granulation process on the granule and tablet attributes will be discussed.

2.2　Twin screw granulation parameters and granule attributes

Several researchers investigated the effect of liquid to solid ratio, screw speed, screw configuration, and powder feed rate on the granule properties [7,13–16].

Keleb et al. investigated the effect of the liquid to solid (L/S) ratio and the screw speed on the quality of alpha-lactose monohydrate granules. It was found that the water content has a significant effect on the granulation process and the granules size distribution. The screw speed had a significant effect on granules friability when polyvinylpyrrolidone (PVP) was used as a binder. However, no effect was observed on the granules friability when lactose was granulated without PVP. On the other hand, the size distribution was affected by increasing the screw speed [17].

Djuric et al. were the first to highlight the effect of screw configurations on the granule properties. It was reported that the conveying elements resulted in the highest value of friability of lactose granules whereas, using kneading elements produced the lowest value of friability. The implementation of the combing mixer elements resulted in granules with moderate porosity values [14]. In addition, Djuric et al. investigated the effect of screw diameter, in which two granulators with 19 and 27 mm screw diameters were used [18]. Djuric reported that the screw diameter significantly affected the median size and the friability of the granules [18].

The effect of the primary material on granules properties produced using TSG was investigated by several researchers [19,20]. Fonteyne et al. studied the effect of six different grades of microcrystalline cellulose, manufactured differently, on the quality of the granules using a powder-to-tablet wet granulation line (ConsiGma^{TM} 25). They found that the water binding capacity and the degree of crystallinity elucidated the difference in the granules size distribution [21]. The effect of the properties of two water-soluble materials, lactose and mannitol, on granule attributes were investigated. It was found that the primary powder morphology, size and compressibility have a significant effect on the size and structure of the granules [20]. The aforementioned observation can be expected as the size of the starting materials has a critical role in defining the size of the nuclei during the nucleation stage in wet granulation [22].

Dhenge et al. investigated the effect of screw speed, feed rate and L/S ratio on the granule attribute [23]. It was found the L/S ratio has the most pronounced effect on the granule

size distribution, flowability, and strength. The granule strength was found to be a function of the barrel fill level and significantly affected by the L/S ratio. Whereas the screw speed had a minor effect on the granule properties [23]. It was reported that increasing the screw speed from 400 to 550 RPM caused a drop in the granule size of lactose-microcrystalline cellulose based formulation. This maybe because at low speed the channel fill is increased as well as the residence time of the material inside the TSG allowing more granules growth [23]. In another study, Dhenge et al. reported that the dissolution and release rate of the granules decreases as the density of granules increases [13].

The effect of the binder addition to the TGS on the granule attributes was investigated [24]. It was reported that the binder addition method influences the size distribution, and strength of MCC- lactose granules. Adding the binder (hydroxypropyl methylcellulose) in solid form resulted in a narrowest granule size distribution, and lower variation in the granules strength compared with the liquid binder addition method.

It could be concluded that the effect of the process and formulation parameters on the quality attributes of granules are well studied by several researchers whereby several regime maps for TSG was established, which help to produce granules with the specific attributes as seen in section 2.1.

2.3   Twin screw granulation parameters and tablet attributes

The effect of wet granulation process on tablet strength has been studied extensively using high shear mixers as well as fluidised bed granulator [15,25–27]. However, limited work has been carried out to study the effect of twin screw granulation process on tablet attributes.

It was reported that the quality of theophylline-lactose tablets can be optimised by changing the number of kneading elements[28]. For example, decreasing the number of kneading elements yielded with lower granules density tablets, which resulted in higher tablet strength [28]. A similar observation was reported by Djuric and Kleinebudde who studied the effect of screw configuration on the tensile strength of the lactose tables [14]. It was reported that the conveying elements produced the strongest tablets comparing with the kneading and the combining mixer elements. However, a different trend was

seen when mannitol and dicalcium phosphate were used. Djuric did not report the effect on the disintegration and dissolution rates in his studies [14,29].

Melkebeke et al. studied the effect of screw configuration and the staggering angle of the kneading block on the strength and disintegration time of lactose formulation [30]. The study reported no significant effect on the tensile strength of the tablets. However, the disintegration time/rate of the tablets was significantly affected (became shorter) only when an extra conveying element was used after the kneading block [30].

Lute et al. studied the tabletability of six grades of mannitol and lactose with different particle size, structure and compressibility. They concluded that the L/S ratio resulted in an increase in the granule size and weaker tablets for all the granulated powders [20]. This may be explained by the reduction in the granular porosity as the L/S ratio increased for all the powders. In another study, the effect of the seven theophylline grades, different in particle size, on the quality of the granules and the final tablet product was investigated. It was found that the differences in the primary material properties affect the processability, tablet strength and disintegration time [31].

Keleb et al. studied the effect of water and polyvinylpyrrolidone (PVP) on the properties of strength and dissolution of lactose tablets [16]. The authors reported that increasing the liquid to solid ratio (amount of water) resulted in an insignificant increase in the tensile strength while using an extra amount of PVP caused a significant increase in the tablet strength [16].

Meier et al. granulated Ibuprofen with several disintegrants via twin screw. The study reported that the tablets with high tensile strength, fast disintegration and dissolution rate could be produced depending on the type of disintegrant and the liquid to solid ratio used for the granulation [32].

When comparing MCC tablets produced by TSG and high shear mixer (HSM), it was found that the tablets made by HSM are weaker [11]. The previous observation could be due to the over granulation by the HSM resulting in denser and harder granules compared to those made via twin screw [11].

Based on the studies presented above, it can be realised that the effects of the granulation/ processing variables on the tablet attributes have been investigated. However, there is a need for systematic studies to build a profound understanding of how different materials

behave after granulation based on the main material properties such as mechanical properties or water solubility. Therefore, one of the aims of this work is to investigate how brittle and deformable materials that have different water solubility behave during granulation and to study their tabletability before and after granulation.

2.4   Tabletting

Powder pressing is widely used in several industries, such as pharmaceuticals, batteries, detergents, food, and ceramics [33]. Tablets are most commonly made by either direct compression of powder or compression of a granular intermediate.

The tabletting process can be divided into three sequential phases: die filling, tablet formation, and tablet ejection. Tablets can be produced using a single punch or rotary presses. Figure 2.5 illustrates the steps of tablet formation using a single tablet press.
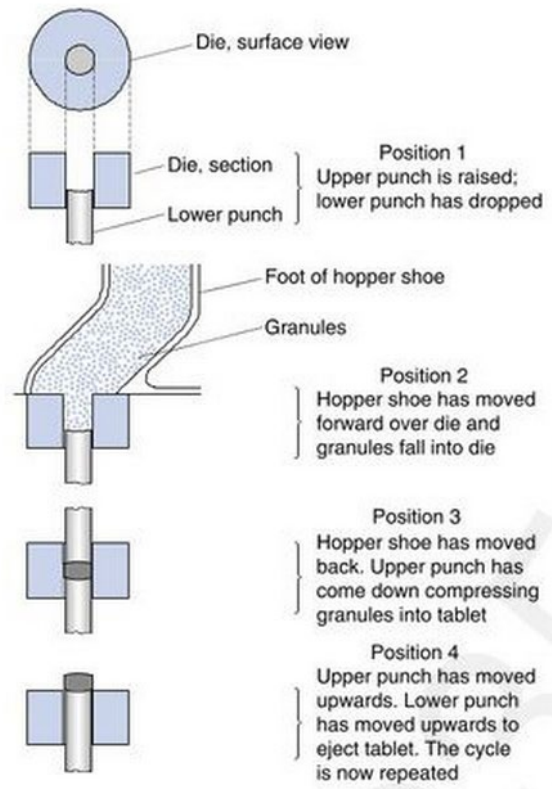
Figure 2.5 The sequence of events involved in the formation of tablets, adapted from [34].

The adequate physical strength of tablets is essential to maintain the quality of tablets by resisting fracture, abrasion, and chipping during manufacturing processes, transportation and shelf life [35,36]. Tabletability is defined as the ability of powder or granules to transform into a tablet of adequate strength due to compression [37]. It is usually presented as a plot of the tablet tensile strength vs. compaction pressure [38,39].

The relationship between tablet strength and compression pressure is complex; it can be divided into three stages as presented in Figure 2.6. Firstly, no coherence is established, then at the intermediate stage, the tablet strength will increase by increasing the compression pressure. In the third stage, strength will be independent of the compression pressure [40].
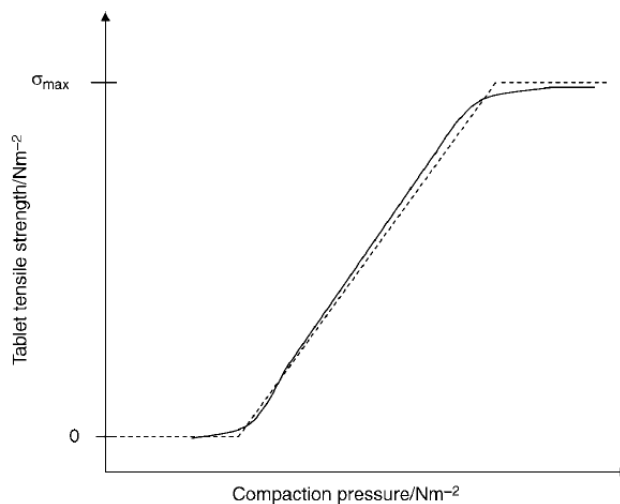
Figure 2.6 Illustration of a sigmoidal compactability profile, adapted from [40].

2.4.1 Tablet compression

During tablet compression, particles and/or granules are forced into close proximity to each other due to the application of a compression force, which causes a decrease in the volume of the powder. As particles approach each other, inter-particle bonds are formed providing cohesion between the particles, and thus a compact is formed. During compression the materials progress by [33,41]:

1   Particle rearrangement.

2   Deformation at the contact points

3   Reversible deformation (elastic deformation).

17

4   Irreversible deformation (plastic deformation and/or particle fracture)

5   Formation of interparticulate bonds.

At the beginning of any compression process, the particles (powder/ granules) are rearranged resulting in a closer packing structure. At a certain compression force, the characteristic of the particles or the interparticulate friction between them prevents any rearrangement of the particles. The subsequent reduction in the volume of the powder bed is accompanied by elastic and plastic deformation of the original particles. Several particles will be fragmented into smaller particles, which will rearrange leading to further reduction in volume. If the compression pressure is further increased the smaller particles could undergo deformation. The contribution of these mechanisms changes as the pressure applied increases and varies according to the material properties [33].

The type of interaction between neighbouring particles dictates the response of the material to any compaction process. At low compression load, the interaction between particles is predominantly elastic. Plastic material densifies because of plastic deformation while powders with low fracture toughness densify by particle crushing or splitting. These effects are illustrated in Figure 2.7. Microcrystalline cellulose, starch and sodium chloride are examples of predominantly plastically deforming materials. On the other hand, crystalline lactose and calcium hydrogen phosphate are examples of materials that fragment due to compression [41,42]. It is crucial to keep in mind that all materials have some degree of plastic, elastic, viscoelastic and brittle behaviour [41].
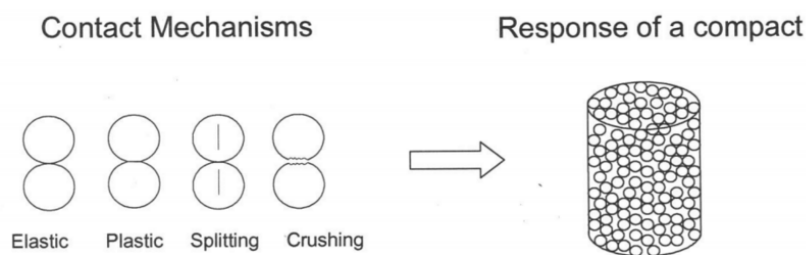
Figure 2.7 Compaction mechanism [33].

2.4.2 Tablet strength

The mechanical strength of a tablet is defined by the force needed to fracture the tablet across its diameter. However, the breaking force does not take into consideration the dimensions and the shape of the tablet. The conversion of the fracture load to tensile strength enables the comparisons between tablets of different shapes or sizes [33].

The diametrical compression test is the most commonly used for strength measurements of tablets. The underlying mechanism of the test is to place the tablet against a platen (usually made of strong material like steel) then the force is applied along an axis of the tablet, the diameter of the tablet in case it is cylindrical [40]. The force is continuously increased at a fixed rate until the tablet fails. A schematic illustration of the diametrical test is depicted in Figure 2.8.
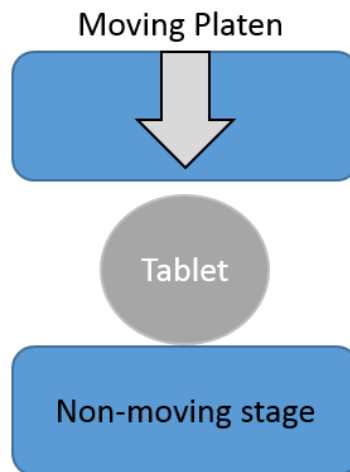
Figure 2.8 Schematic illustration of the diametrical compression test of a cylindrical flat-faced tablet.

The use of a compression test to calculate tablet tensile strength requires the tablets to fail by a normal tensile failure or double or triple cleft failure. The test is not valid when tablets fail by shear or compressive failure [33].

The tensile strength of a flat face tablet is calculated using Eq (2.1) [43].

$$\sigma_T \ = \frac{2F}{\pi HT} \qquad\qquad \text{Eq 2.1}$$

Where σ_T is the tablet tensile strength in MPa, H is tablet diameter in mm, and T is the tablet thickness in mm.

2.5   Fundamental bonding mechanisms relevant to tablets

There are two main groups of bonds that keep matter together. The stronger one is called the primary bonds[1], which include the ionic bonding, covalent bonding and metallic bonding. The second category, which is weaker than the primary bond is often denoted as secondary bonds or long range attractive forces or intermolecular (van der Waals) [44,45]. The distance between the centres of the atoms is shorter for the stronger bonds [44].

For covalently or ionically bonded substances, the strength of the bulk material is highly dependent on whether the covalent and ionic bonds form a network between all atoms (e.g., diamond and sodium chloride crystals) or whether they are confined to individual molecules (e.g., water and carbon dioxide). This distinction forms the primary basis for the behaviour of materials during compaction and the range of compact tensile strengths that can subsequently be achieved.

While the bonds holding the molecules themselves together are very strong, the bonding between molecules is much weaker, and in the form of one or more of the intermolecular (van der Waals) types/secondary bonds. Tablets to a large extent are held together by the secondary bonds [45], as described below. The maximum achievable bonding force will depend on how many of the following mechanisms are active and are discussed in the sub-sections below:

2.5.1   Van der Waals forces

The van der Waals forces between atoms or molecules describe a class of interactions where the interaction force varies as $1/r^7$ with separation distance [46]. The three (four if hydrogen bonding is included) sub-types of van der Waals forces are additive (i.e. multiple ones can exist simultaneously). Therefore, the maximum achievable bonding force will depend on how many of the following mechanisms are active.

---

[1] More details about the primary bonds are provided in appendix A.

2.5.1.1 Orientation (Keesom) interaction, between two freely rotating polar molecules (permanent dipole-permanent dipole).

Permanent dipoles exist in a molecule if the centres of gravity of the positive and negative charges do not coincide (e.g., H_2O). A sort of permanent magnet is formed, and molecules arrange themselves around each other to align the positive and negative charges. This is known as the orientation or Keesom interaction between molecules.

2.5.1.2 Hydrogen bonding

Hydrogen bonds are a strong type of orientation (permanent dipole-permanent dipole) interaction which occur when a hydrogen that is covalently bonded to an electronegative atom (e.g. O, N, S) is shared with another electronegative atom (in an adjacent molecule). Hydrogen bonds are stronger than most other van der Waals forces at around 20-40 kJ/mol [47]. In the case of higher molecular weight and more complex substances, hydrogen bonding can also occur intra-molecularly [48].

2.5.1.3 Induction (Debye) interaction, between a polar and a non-polar molecule (permanent dipole-induced dipole).

Induced dipoles can be generated in neutral molecules if a molecule with a permanent dipole is brought into close proximity. The permanent dipole and induced dipole then result in mutual attraction. This is known as the induction or Debye interaction between molecules.

2.5.1.4 Dispersion (London) interaction, between two non-polar molecules (induced dipole-induced dipole).

Dipoles can be induced in two otherwise neutral molecules in close proximity due to the probabilistic nature in which the electrons in their atoms orbit the nuclei. Continually changing dipoles in neighbouring atoms will find a 'rhythm', which results in stabilisation of the induced dipole and consequent mutual attraction. This is known as the dispersion or London interaction and is considered to be the most important of van der Waals attraction forces because [49]:

- It is always present (i.e. in and between all materials).
- It does not decrease with temperature, unlike the orientation force.

- It is usually the largest contributor to the total van der Waals force, except in the case of highly polar molecules, such as water.

2.5.2 Repulsive atomic potentials

When two atoms are brought close enough together, their electron clouds overlap. Since this overlapping is energetically unfavourable (except for the case of chemical reaction in which covalent bonds are formed and thus new molecules are formed), a repulsive force is generated, which rises steeply with decreasing separation distance [47]. This is the force, which prevents two atoms or molecules from occupying the same space, and together with the applied compaction force, promotes plastic deformation or brittle fracture at contact asperities [49].

2.5.3 Contact-separation induced electrostatics

Electrostatic forces arising from triboelectric charging due to the movement of the particles against each other during mixing and transport lead to attractive and repulsive forces between particles. However, the distances involved during compaction are small, and the electrostatic forces dissipate with time, especially at ambient or higher relative humidity in which liquids such as water are absorbed in or adsorbed onto solid particles [50]. Therefore, electrostatics are not thought to represent a significant contribution to bonding in a powder compact [51].

2.6 Liquid-mediated bonding of solids

2.6.1 Effect on van der Waals bonding

The presence of a liquid between two solids can change the nature (typically reduces the strength by an order of magnitude) of the van der Waals forces between the solid surfaces. This reduces their significance (placing greater emphasis on capillary or meniscus forces – discussed in section 2.6.2) but may not eliminate them entirely. The magnitude of the reduction depends on the number of layers of liquid molecules present in the separation distance between the solid surfaces [49].

2.6.2 Capillary/meniscus forces

The energy required to form a material surface exposed to a gas or vacuum is known as the surface energy (for solids) or the surface tension (for liquids). It quantifies the strength of the internal inter-molecular forces keeping a molecule at the surface interface part of the solid lattice or liquid rather than being allowed to move away. When a liquid droplet forms, the liquid molecules rearrange themselves to a specific shape that minimises the surface area (often a sphere). Therefore, the surface energy is required to prevent any molecules from leaving the bulk. The pressure associated with the curved surface of a liquid is called the capillary or Laplace pressure as described by the equation developed by Young & Laplace in 1805 [49]. The capillary pressure can be positive or negative (i.e. greater than or less than that of the surrounding environment).

In powder and granule compaction, we are interested in what happens to liquids trapped in the confined spaces between particles. Liquids such as water could be presented through adsorption on the surfaces of the particles prior to compaction, absorption within (particularly higher molecular weight) materials, which are then squeezed as a result of the compaction pressure applied, or could be pulled in by capillary condensation under high humidity conditions [52,53]. If the surfaces between which the liquid finds itself have a favourable surface energy (e.g. water with a hydrophilic material such as lactose), the radius of the liquid meniscus formed between those surfaces will be negative (curves inwards) and a negative capillary pressure acts to pull the surfaces even closer together (and resist any tensile stress applied to try and pull them apart). If the opposite is true (e.g., water between two hydrophobic surfaces such as magnesium stearate), a positive capillary pressure will result in acting to push the surfaces away from each other, reducing composite strength.

A comparison between capillary and van der Waals forces acting between a rough particle and a surface shows that capillary forces can be of a similar if not greater magnitude than van der Waals forces of attraction [54]. However, this requires the quantity of water to be in an optimum region. For example, too little liquid will reduce the significance of the capillary bonding component, whereas, too much liquid will flood the space between all particles, which can cause sticking of the material to the tabletting machine and particle-particle lubrication during strength testing (resulting in lower strength values) [55].

2.7 Primary and secondary factors for tablet strength

Two factors are primarily responsible for the tabletability of powders: the dominating bond mechanism, and the surface area over which these bonds are active [50] (i.e. the number and strength of bonds). Due to considerable experimental difficulties, these factors have not been evaluated before for pharmaceutical materials [56].

Secondary factors such as particle size, shape, surface texture and the volume reduction behaviour (i.e. the elastic and plastic deformation and particle fragmentation) have been studied in detail [50,57]. These secondary factors are usually studied to make correlations with tablet strength.

2.7.1 Bonding surface area

The bonding surface area (BSA) is usually used to refer to the effective surface area that takes part in the interparticulate interaction. In other words, it is the true interparticulate contact area. During compaction, particles consolidate through rearrangement, slippage and deformation/fragmentation. The bonding surface area is the net result of the particles deformations [58]. For a plastic material, most of the bonding area, which is created during the compression phase survives after the decompression phase. However, it is not necessary for the resulting dense compact to be strong as other factors could influence the bonding area and consequently the final compact strength. These factors are particle size, shape, surface texture, the amount of the applied pressure, and the mechanical properties of the compressed particles [58]. In general, a decrease in the particle size and an increase in the surface roughness result in an increase in the tablet strength [59].

On the other hand, the compression of brittle materials leads to an increase in the BSA due to fragmentation. The plastic deformation of the fragmented particles leads to the formation of a strong compact/ tablet. Otherwise, the resulting tablet would be weak as the elastic deformation can eliminate most of the bonding area. To summarise, the effective bonding area is affected by both the particles characteristic and their behaviour during and after compression [59]. It is very difficult to define the exact bonding surface area directly, instead the factors (mentioned earlier), which affect the bonding area are used for correlation with tablet strength [60]. Some researchers reported a correlation between the tablet surface area of lactose and microcrystalline cellulose and the tablet strength [61,62].

2.7.1.1 Surface area measurements

Surface area is an important material characteristic during the development, formulation and manufacturing of particles [63]. The surface area of a solid material (powder/ granules) is obtained by measuring the void spaces on the surfaces of that material [63], which is usually expressed as m²/g.

Gas adsorption has been widely used to measure the specific surface area (SSA) of particles and tablets [61,64,65]. Other methods are also used to measure the SSA such as mercury porosimetry [66], recently the tetra-hertz spectroscopy was used as well. More details about the pros and cons of each technique are provided in the literature [67].

In this work, the gas absorption technique was used to measure the specific surface area using a method developed by Brunauer–Emmett–Teller (BET) [68]. The BET theory is covered in the methodology section **Error! Reference source not found.**.

2.7.2 Bonding mechanisms & tabletability

Several bonding mechanisms describing the cohesion of particles have been proposed historically, such as those by Rumpf [69], which include:

1. Solid bridges (including by crystallisation, melting, sintering and/or hardening 'binders').
2. Movable liquids (capillary and surface tension forces).
3. Non-freely movable binders (viscous binders and aqueous adsorption layers).
4. The attraction between solid particles (molecular and electrostatic forces).
5. Mechanical interlocking (shape-related bonding).

The relative magnitude of the bonds mentioned above as a function of particle size is presented in Figure 2.9.
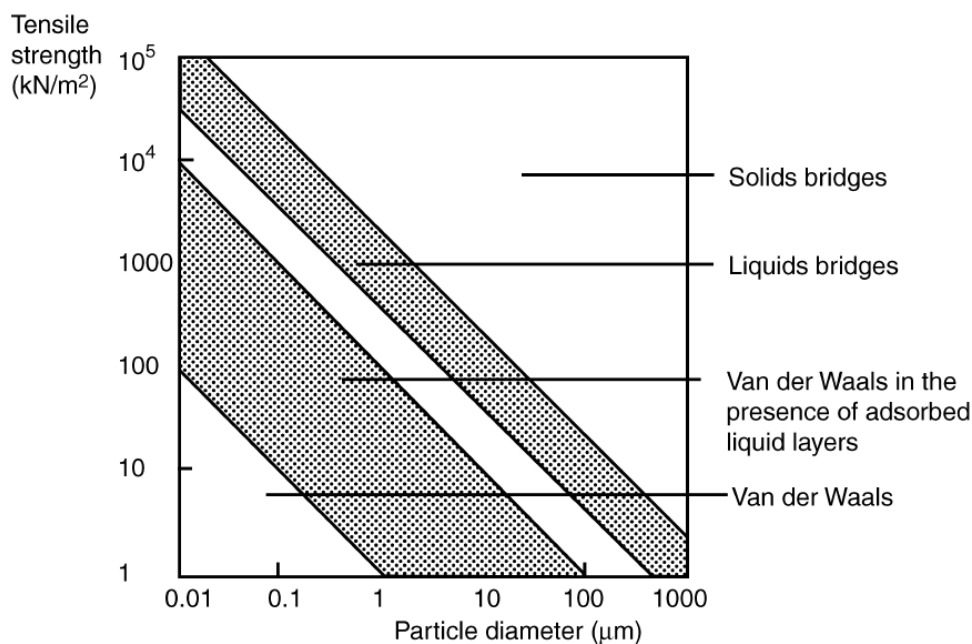
Figure 2.9 Theoretical tensile strength of agglomerates with different bonding mechanisms, adapted from [70].

It is widely reported that the significant mechanisms for tablet formation are mainly the solid bridges, the attraction between solid particles due to the interparticulate attraction forces and to a lesser extent the mechanical interlocking of irregular particles [41,45,50,71,72]. Nonetheless, the presence of liquid/moisture in the compressed materials or the tablets (absorbed during storage) may have a significant effect on the tablet strength [73–75].

A brief review of the main bonding mechanisms of tablets, which are accepted in the literature are provided below:

2.7.2.1 Solid bridges

The mechanical treatment of materials such as tabletting leads to the removal of the interparticle faces of the contact area by sintering or by recrystallisation [76]. Solid bridges (SB) should be expected to form if the material has certain mobility at the contact areas over a limited period of time. Solid bridges can be formed due to the asperity melting at the extreme local stresses combined with local heating. The combination of high local stress and heat is sufficient to cause a molecular movement facilitating the return of the particles to the liquid state. The subsequent crystallisation of solid bridges between adjacent particles results in a network structure, which gives the tablet pronounced strength [45,76]. Another way for particles to gain mobility is under the

influence of the dissolved state due to the solvent sorption layer (mainly water) [76]. Sebhatu et al. reported that the water uptake of spray dried lactose before compression lead to a significant increase in the tablet strength due to crystallisation and the formation of solid bridges [75]. Solid bridges contributing to the overall tablet strength are considered the areas of real contact at the atomic level between surfaces [41]. In many occasions, SB has been ambiguously used, without a clear explanation of what does it mean especially on the molecular level [77–79], since there is no such bond called solid bridge at the molecular level. Olsson et al. reported a clear and accurate definition of the solid bridges. Solid bridges were defined as a continuous phase of powder between particles, in which there is a particle to particle contact on the atomic level. The molecules or ions between the particles are assumed to be bonded in the same manner as those inside each particle [48], Van der Waals forces are the dominating bonding mechanisms between the surfaces of the solid particles when the surrounding medium is air[48]. The phenomena that is typically considered to result in 'bridge' formation such as crystallisation, sintering, melting-solidification etc, only act to increase the surface area of contact that is sufficiently close for van der Waals bonding.

2.7.2.2 The attraction between solid particles

Interfacial forces (also known as long-range forces) exist between all solids regardless of whether a material bridge exists between particles or not [69]. Tablet formation occurs due to the interparticulate attraction that arises partially from the interfacial forces also called intermolecular forces, which act over very short distances [41]. Interfacial forces have lower energy than covalent bonds. The most influential long-range forces during the tabletting process are van der Waals (VDW) and hydrogen bonding forces for molecular solids, which may occur intra and intermolecularly [41,45]. These forces are important for directly compressible materials such as MCC, lactose and polyvinyl pyrrolidone [80]. Many excipients and active pharmaceutical ingredients have the potential to form hydrogen bonds such as cellulose and sugars [45]. Whereas for ions, ion-dipole and, ion-induced dipole interaction, and Columbic forces also contribute to tablet strength [58]. The strength of VDW forces depends on the material properties being compressed and on the surface area over which bonding can take place [45]. It is assumed that the strength of a plane within the tablet is defined by the sum of all the attractions between the particles in that plane [80]. The VDW forces become negligible when the

separation distance between adjacent surfaces is more than a few nanometers, such as the case of loose powder [58].

2.7.2.3 Mechanical interlocking

The mechanical interlocking can happen during tabletting due to plastic flow and brittle fracture of particles where particles hook and twist together. Consequently, assisting in increasing the surface area for inter-particulate bonding [45]. This mechanism of bonding is dependent on the shape and surface structure of particles. Irregular particles and needle shaped particles are more likely to hook and twist compared with smooth spherical ones leading to an increase in the potential for VDW forces between particles [50,81].

2.8   Prediction of the tensile strength of compacts

Several factors are affecting the efficiency of the compaction process. They can be related to the formulation, process, and/or the environment (relative humidity) [41]. Figure 2.10 presents the main factors, which affect the tabletting process and compression efficiency such as granule porosity, compression force and moisture. The former factors have been investigated by several researchers in order to enhance the understanding of the factors that affect the creation of a tablet and to build predictive models for tablet strength [20,42,58,62,82].
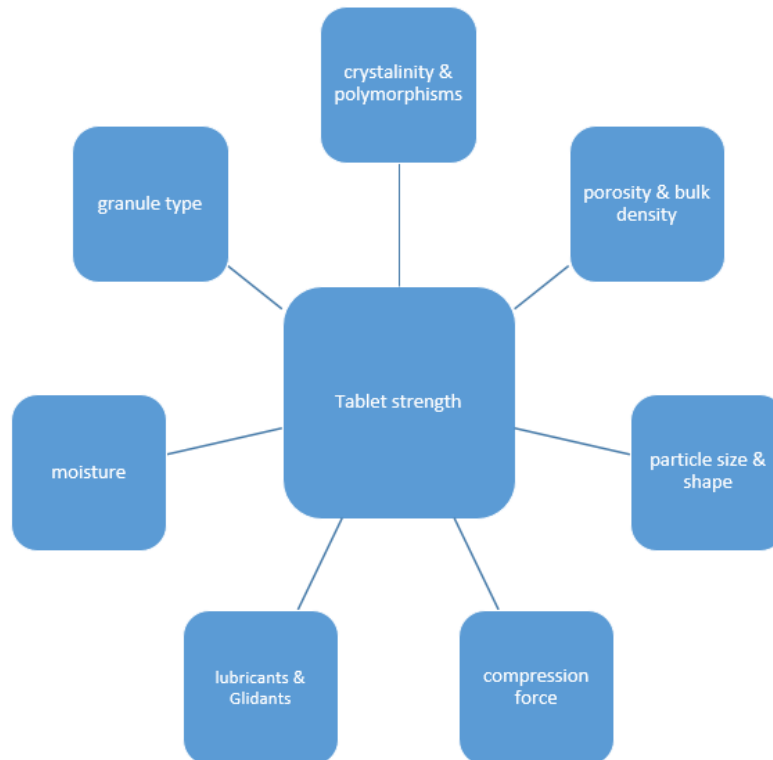
Figure 2.10 Main factors affecting the efficiency of tablet strength, adapted from [41].

2.8.1 Compaction-based predictions

Traditionally several models have been proposed to predict the compaction behaviour of powders or granules based on compaction data analysis (load and displacement or stress/strain data during compression). The tabletability of powders/ granules is governed by the compressibility and the compactability [83].

Walker, Heckel and Kawakita equations have been used by several researchers to describe the porosity/volume reduction of a compact as a function of pressure, which is referred to as compressibility [33,84–86]. Compactibility elucidates the tablet tensile strength as a function of the compact density, which can be described by Ryshkewitch-Duckworth equation [87–89]. Adam et al. proposed a model to estimate the fracture strength of a single granule from in-die compression data [90].

These approaches are all useful in enabling researchers to understand the gross behaviour of different materials under compression [41]. The previously mentioned models have been critically compared by several researchers [91–93]), but provide no insight into the fundamental mechanisms of tablet formation.

29

Sun et al. suggested a qualitative model explaining the tablet strength based on inferred inter-particulate bonding area and bonding strength [39]. In this model, the authours classified the compactibility profiles of powders into six categories based on the assumed (i.e. not directly measured) roles of bonding strength and bonding area [39]. In another study published recently, this concept of bonding area (BA) and bonding strength (BS) on the tabletting behaviour of powders was tested [94]. In the study, a polymer (polyvinyl caprolactam-polyvinyl acetate-polyethylene glycol graft copolymer) was compressed systematically at different temperatures during tabletting in an attempt to qualitatively describe the role of bonding area and bonding strength interplay in tabletting [94], although the results still relied on interpretation of compaction profiles rather than direct measurements [94].

Al-Nasassrah et al. predicted the tensile strength of polyethene glycol tablets at zero porosity as a function of the strain energy release rate and the molecular weight of several polyethene glycol grades [95], but one of the grades did not follow the trend, and the applicability to other materials was not explored. Also, the authors did not specify the steps taken to control sample moisture content.

Farber et al. proposed the unified compaction curve (UCC) model, which describes the relationship between the roller compaction conditions and the tabletability of granules [96]. This model has been subsequently applied to wet granulation using a high shear mixer (HSM) by Nguyen et al. [97]. For wet granulation, the UCC enables the prediction of tablet strength as a function of liquid level, wet massing time or binder flow rate [98], but specifically for predominantly plastically-deforming materials such as MCC. It has been reported that brittle materials such as mannitol can display increased tabletability following wet granulation [82], which is not explicable using the UCC approach.

While each of these approaches has its uses (they are a significant step forward from traditional experimental trial and error), they all tend to be specific to a particular material or set of 'calibrated' materials, and are therefore all incapable of predicting the tensile strength of a new compact based on the properties of the input material(s). They also provide little or no insight into the bonding mechanisms at work, which means that development of future products (assuming a change in materials, which is very common in the pharmaceutical industry) must also be done empirically.

2.8.2 Powder and granule property-based predictions

2.8.2.1 Particle size

The effect of particle size and size distribution of powders or granulated materials on tablet strength has been investigated by several researchers, with varying conclusions.

For example, in one study, it was found that decreasing the particle size of lactose powder results in stronger tablets, whereas microcrystalline cellulose was unaffected by variations in particle size [99]. The difference in behaviour was attributed to differences in deformation behaviour (i.e. brittle vs plastic) as characterised by Heckel analysis. In another study, Walker et al. reported a trend of increasing tablet strength with decreasing granule size for melt-granulated lactose and PEG [100]. Conversely, a complex granulated mixture dominated by lactose monohydrate and microcrystalline cellulose was found to have size-dependant compactibility, whereby larger particles showed higher crushing strength of tablets [86].

Kelemen et al. reported a general decrease in tabletability with increasing particle size for sorbitol, although the authors reported that the correlation was insignificant [101]. Paluch et al. [102] were firmer in their conclusions and reported that particle size did not affect the tabletability of chlorothiazide sodium and chlorothiazide potassium powders. Keleb et al. also reported no effect of particle size for tablets produced from different grades of lactose [103]. Khorsheed et al. reported no effect on tabletability of different sieve cuts of granules made from MCC [82]. Fichtner et al. reported no influence in the spread of particle size on tablet porosity and tensile strength immediately following the compaction for paracetamol, sucrose and sodium chloride powders [104].

It could be concluded based on the variation in study outcomes that the particle size of granules or powders does not have a clear and direct relationship with tabletability behaviour.

2.8.2.2 Granule strength/porosity/density

Macias and Carvajal did find an inverse power law relationship between granule strength (determined by confined uniaxial compressive tests) and tablet strength for granulated MCC [105]. Similarly, Morkhade [106] reported a correlation between granule friability and tablet tensile strength, whereby more friable granules resulted in stronger tablets for

a range of different formulations. Gabbott et al. also found that granules with lower density correlated with stronger tablets [107]. Johansson and Alderborn reported increased tablet tensile strength with increasing intragranular porosity for a wide range of materials tested. However, granules with the same porosity still showed a material dependence on tablet tensile strength [108]. Badawy et al. found that tablet compaction was more likely to be impacted by granule density than granule size [109].

Ganderton and Hunter found that for systems containing lactose and calcium phosphate, granule strength had no correlation with tablet strength. This was attributed to the fragmentation of granules during compression [110].

In conclusion, it seems quite common (although not exhaustive) for a trend of increasing granule strength or density or decreasing granule porosity to be correlated with decreasing tabletability. However, where multiple materials have been studied side-by-side, these properties are unable to explain material-to-material differences in tabletability.

2.8.2.3   Surface area

Shi et al. measured the specific surface area of MCC granules made by wet granulation and found decreasing tabletability with increasing wet massing time [111]. The authors observed a corresponding reduction in the specific surface area of granules with increasing wet massing time, although these results were confounded by similar decreases in granule porosity. Interestingly, however, they observed no change in tablet porosity at a given applied compaction pressure, which suggests that any increase in granule strength is not having a significant impact, although this was not commented on by the authors. Grote and Kleinebudde also found a good correlation between the primary material surface area and the tabletability for two types of DCPA, milled and agglomerated grades [112]. They also reported a loss in tabletability with increasing roller compaction pressure applied to the materials but did not report the ribbon surface area.

Yoshinari et al. investigated the effect of granulation on different polymorphs of mannitol and showed a very good correlation between the specific surface area of the mannitol powders and the strength of tablets manufactured from these powders [113].

Nystrom et al. presented a very strong correlation between the specific surface area of tablets manufactured from different lactose grades and their crushing strength in which

greater surface area resulted in higher compact tensile strength [42]. Riepma et al. studied the tabletability of binary powder mixtures of four different types of lactose. The authors found that there is a proportional relationship between the internal specific surface area of tablets and their crushing strength [114]. It is also suggested in their follow-up publications [115,116] that the majority of the surface area for the different grades of lactose tested came primarily from fragmentation during compaction, since the tablet specific surface areas were consistently significantly higher than that of the primary powder and correlated well with tablet crushing strength. Paluch et al. found that the internal surface area of tablets was not a reliable predictor of tablet tensile strength across a range of different materials, although the authors did find that in general powders with higher specific surface area compact better than those which have the lower surface area, even at low compression forces [102].

To summarise, the work discussed in this section generally shows a correlation between the specific surface area of either the primary material or the compact itself and the tensile strength of the tablet.

2.8.2.4 Moisture / liquid content

The percentage of the moisture content in the compressed materials is associated with variation in the tablet strength, and as shown by Gabbott et al., can even overshadow the effect of granulation [39,73,75,107]. Moisture can affect tablet strength by the following mechanisms:

1 The formation of liquid bridges, which cause particles to adhere to each other due to capillary forces [69,117] adding strength to the tablet. Attractive capillary forces are created when the liquid pressure is less than the air pressure, which leads to the formation of a concave meniscus and a state of tension [117].

2 The presence of moisture in the compressed solids results in a lower yield pressure of individual particles by facilitating plastic deformation [73,118]. Probably, this is primarily achieved when the moisture is absorbed into the particle structure [73], which is most likely the case with long-chain molecules like MCC.

3 Moisture acts as a lubricant to reduce friction [73,119]:

   (a) Aiding particle rearrangement during compaction.

   (b) Aiding tablet ejection from the die post-compaction.

4   The recrystallisation of dissolved material leading to increased areas of intimate solid:solid contact, resulting in greater tensile strength. This would take time and would most likely be observed during the post-compaction storage period for soluble materials in an environment with fluctuating humidity [120].

5   Moisture could increase the inter-particulate bonding area in a tablet [73] as it works as a plasticising agent promoting molecular mobility [121], but only if given the time to do so (such effects may most likely be observed over the course of a tablet's shelf life).

The mechanisms 1-3 are related to the short-term phenomena occurring during and immediately following the compaction event- which are relevant to data presented in this work. Mechanisms 4 and 5 relate to longer-term, stability effects which are only detectable over longer time periods.

The effect of moisture on tablet properties immediately following compaction (i.e. mechanisms 1-3 above) has been reported for both hygroscopic and non-hygroscopic materials [55,73,75].

Gabbott et al. [107] reported that the residual moisture content remaining in non-hygroscopic mannitol-based granules after drying has a significant effect on the tablet crushing strength, whereby increased moisture content results in increased tablet tensile strength. The authors attributed the increase in strength to plasticisation of the material resulting in greater contact surface area for van der Waals attraction.

Ahlneck and Alderborn [73] studied a number of different non-hygroscopic materials over a wide range of humidities. They found that some materials showed a linear increase in tensile strength with humidity and moisture content, others displayed an optimum relation, and a few showed no significant effect. They attributed this behaviour to adsorbed moisture at the particle surface which aids dissolution/recrystallisation of molecules at particle-particle contact points leading to greater contact area for van der Waals forces of attraction. However, they also tentatively acknowledge the possibility of water vapour bridges forming and contributing to tablet strength. Interestingly, they also tested the effect of powder conditioning and moisture content on tablet porosity and concluded that "water adsorbed at particle surfaces has a very limited effect on the volume

reduction behaviour of a particulate solid" [73], suggesting that the lubrication or plasticisation effects are negligible.

Stubberud et al. reported that increasing the moisture content of hygroscopic MCC powder before compaction leads to an increase in the tablet strength up to about 70% relative humidity, after which a reduction was observed [122]. Similarly, Sun et al. have studied the effect of moisture content of MCC powder on its mechanical properties, including tabletability and plasticity [55]. Peak tablet tensile strength was achieved between 3 and 5% w/w moisture content, and the effect was attributed solely to plasticisation of the material since the yield pressure was observed to decrease significantly with increasing moisture content [55].

A frequently-cited explanation for ruling out the possible effect of liquid bridges is that the environmental conditions are less humid than that of the critical humidity required for condensed liquid bridges to be stable [53]. However, compaction is a fast process (relative to capillary condensation and evaporation), and moisture can come from sources other than capillary condensation (such as that adsorbed onto surfaces or absorbed into long-chain polymers), so it is possible that this assumption may not hold.

Moisture content has a significant contribution to the tensile strength of agglomerates. Several researchers have investigated the direct effect of material moisture content on tablet tensile strength, immediately following compaction and on extended storage [104,120,123]. However, the effect of the liquid on tabletability as a discrete mechanism (i.e. its ability to form liquid bridges with negative capillary pressure) has so far been largely overlooked.

2.8.2.5   Other properties

Roberts et al. proposed a model to predict the extrapolated tensile strength at zero porosity as a function of the cohesive energy density for 12 materials including MCC.). Whilst the brittle materials were described well by the linear relationship found, MCC (a plastically deforming material) was not described well by this approach [124].

2.9 Change of tabletability after granulation

Granulation is commonly performed before compression because it helps to improve the flowability, ensures more uniform filling of the tablet dies, and helps to prevent segregation during the tabletting process [125,126]. However, both wet and dry granulation processes can affect (both positively and negatively) the tabletability of granulated powders [37,127–129]. The substantial loss of the ability of granulated materials to be compressed into tablet compared with the non-granulated materials is known as loss of tabletability or over-granulation in the case of wet granulation [127].

The effect of granulation on the tabletability of several materials using dry granulation (roller compaction or slugging) has been thoroughly investigated [38,130–133]. It is reported that dry granulation causes a reduction in tabletability and compactability of the granulated powder. Two principal mechanisms for the deterioration of compactability after dry granulation have been proposed:

1 Size enlargement (difference in size among granules, and between the granules and the primary powder) [37].
2 Material hardening which is usually accompanied by an increase in granule strength [129].
3 A combination of both mechanisms [131].

The effect of wet granulation on the tabletability has been studied in a high shear mixer (HSM). It was reported that increasing the granules size caused a deterioration of the granule tabletability after granulation using HSM [127]. Johansson et al. reported the tabletability of pellets made from MCC based formulations is directly related to the pellets' porosity [134]. Osei-Yeboah et al. reported that the decrease in the tablet strength of MCC granules produced using HSM correlates with the size enlargement, specific surface area, and porosity of the granules [128]. Part of the motivation for this work was to try to deconvolute these effects.

Comparison of the tabletability of MCC granules made using a continuous TSG and HSM showed that tablets produced from granules manufactured using the HSM were weaker in comparison to those generated by the TSG, due to over granulation in the HSM [11].

TSG is distinctly different from roller compaction and HSM in the mechanisms of size enlargement, type and extent of the compression and shear stresses and the residence time during granulation [4,11]. Also, the use of a granulation liquid can have a significant impact on the process when compared with roller compaction. Hence, the mechanisms that describe the reduction of the tabletability of granules made using roller compaction and wet granulation by HSM should not be extrapolated to wet granulation by TSG without a thorough investigation. There appear to be no reports in the available literature up to date, about the mechanisms involved in changing the tabletability of the granulated material using TSG. Therefore, this work will investigate these mechanisms in TSG.

2.10 Solutions for loss of tabletability

Several approaches have been used to reduce the loss of tabletability or restore some of the lost tabletability. Modifying the granules attributes such as porosity, surface, and specific surface area lead to a reduction in the ratio of the loss of tabletability after granulation, which could be achieved by milling or surface coating [135,136]. Badawy et al. granulated MCC with hydroxypropyl cellulose (HPC) using HSM with different granulation parameters. By milling the over granulated MCC granules, it was feasible to restore significant amount of the reduced tablet strength of MCC after granulation. The improvement in the tabletability of the MCC granules is associated with an increase in granule porosity and the specific surface area [135].

A more formulation based approach involves the incorporation of brittle materials such as dibasic calcium phosphate or lactose into MCC granules (prepared by HSM) to resolve the loss of tabletability [137]. Improved tabletability was also reported after wet granulation (using TSG) due to polymorphic transition, which caused a change in the morphology of the mannitol crystals and an increase in the specific surface area [138]. An improvement of tablet strength of acetames after roller compactor compared with the tablet strength of the unprocessed powder was reported [139]. It was found that the improvement in the acetames tablet strength is associated with an increase in the specific surface area due to the brittle fragmentation after the roller compaction process [139].

2.11 Dissolution of solid particles

To understand the dissolution of a material, it is important to define the parameters that control the dissolution process. Several theories were developed to understand the mechanism of dissolution including the interfacial barrier model, the Danckwert's model, and the diffusion layer model. The theories which explain dissolution conclude that the main factor affecting dissolution is the interface between solid and liquid; this relationship is expressed through the Noyes-Whitney equation as illustrated in equation 2.2 [3].

$$\frac{dm}{dt} = \frac{DA(Cs - C)}{L}$$
Eq 2.2

Where dm/dt is the dissolution rate,

D is the diffusion coefficient,

A is the surface area of the solid,

Cs is the concentration of the solid in the diffusion layer surrounding the solid,

C is the concentration of the solid in the bulk dissolution medium and

L is the diffusion layer thickness

Based on the Noyes-Whitney equation, the dissolution rate could be increased by increasing the drug saturation solubility and/or by increasing the particle surface area. The thickness of the boundary layer is affected by the degree of agitation and the viscosity of the dissolution medium [3].

The dissolution process of a tablet made from granules starts by the disintegration of the tablet into granules. The latter will start to disintegrate into smaller particles and the drug particles will be released into the solvent medium as illustrated in Figure 2.11.
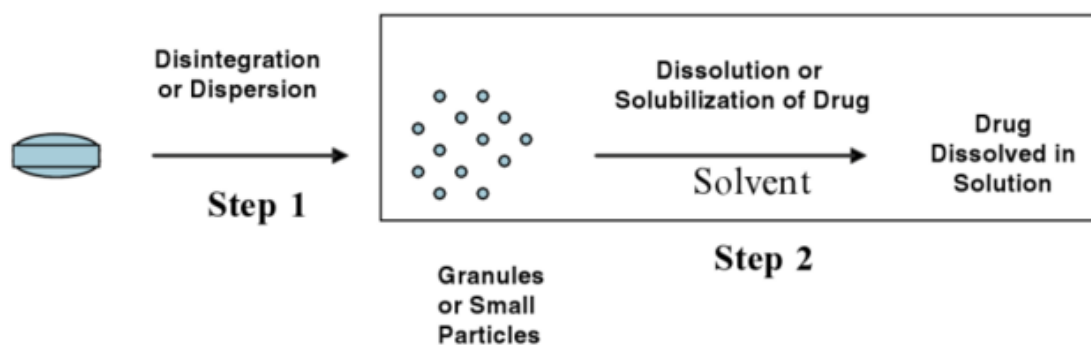
Figure 2.11 The process of drug dissolution into the solvent medium from the wet granulated tablet [140].

2.12 Granules and tablets: The balance between mechanical strength and dissolution

Compression pressure has an effect on the porosity of a tablet. This means the amount of air inside the tablet will change in correspondence to the applied pressure [141]. Similarly, tablet tensile strength is affected by the compression pressure. An increase in compression pressure will cause an increase in the tensile strength of the tablet and a decrease in the tablet porosity. When tablets are designed to have a fast disintegration rate, it is not desirable to produce the tablets with the minimal percentage of pores. Therefore, it is important to have a balance between the mechanical properties of a compact and it's dissolution characteristics, which are related to the porosity of the compact [142].

It was reported that there is a clear trade-off between the granule strength and the dissolution rate of the granules produced using a HSM [143]. Granules were either strong and slow dissolving or weak and fast dissolving [143]. It was reported that an increase in granule fracture load is associated with a decrease in the dissolution rate of calcium carbonate granules using a high shear mixer [143]. Increasing the surface area of granules results in an increase in the dissolution rate [144].

The process parameters of the TSG showed an effect on the dissolution rate of granules [13]. Dhenge et al. reported that high powder feed rate resulted in denser granules, which took longer time to release the salt embedded in the granules [13]. It was also found that the tablet strength and disintegration rate depend on the number of the kneading elements used during granulation [28]. The TSG was used to produce controlled release tablets by controlling the viscosity of the used binder [145,146]. The work conducted by Vanhoorne

et al. highlights the significance of the deep understanding of the TSG process on the dissolution behaviour of granules and tablets [145]. However, there is a need to understand further the effect of the formulation properties on the dissolution behaviour of tablets made from granulated materials using the TSG. Therefore, the dissolution behaviour of nine different formulations that have different mechanical and water solubility behaviour was investigated in this work.

2.13 Artificial neural network

Recently, neural computing has emerged as a practical technology with successful applications for several fields such as chemistry, dentistry, and powder technology [147–149]. Artificial neural network (ANN) is a mathematical representation inspired by the neural structure of the human brain [150]. By mimicking the structure and function of the human brain, the ANN is adaptive, self-organising and fault tolerant. The ANN usually maps the inputs space to the outputs space [147]. In general, an ANN can be a single layer or multiple layers. The structure of the ANN is built of interconnection of nodes analogous to the biological neural network. Any neural network consists of three components: node character, network topology, and learning rules [151]. A basic model for a node in the ANN is presented in Figure 2.12.
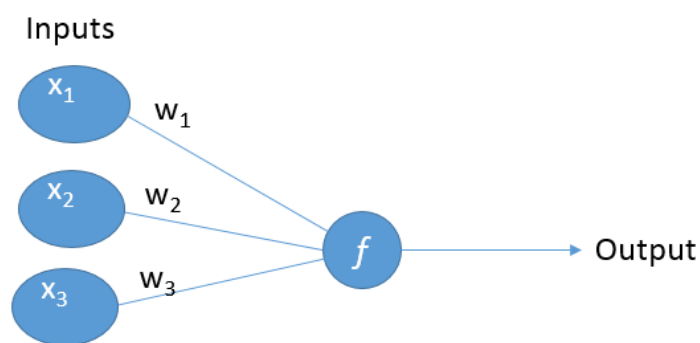
Figure 2.12 A basic model of single node neural network. X_i=input, w_i=weight, f is the activation/transfer function.

2.13.1 Node character

The character of the node determines the way signals are processed by the node including: the number of the inputs and outputs associated with the node, the weights allied to the inputs, and the activation function. Each node receives multiple inputs that have associated weights. When the sum of the multiplication of each input by its weight exceeds the threshold value of the node/neuron, the node is activated and passes the signal to neighbouring nodes through an activation function [151]. The activation function has many forms, such as linear and nonlinear functions. The nonlinear functions are more common in the engineering applications than the linear functions; this is due to the ability of the nonlinear functions to model complex processes with an acceptable degree of accuracy. Among these nonlinear functions, the sigmoid function has been utilised in different applications; this can be attributed to being mathematically convenient (i.e. derivatives are continuous), such a function is described by Eq (2.3).

$$Output = \frac{1}{1 + e^{-(\sum_i w_i \, x_i + w_0)}}$$
Eq 2.3

Where x_i is the ith input, w_i is the ith connecting coefficient and w_0 is the bias.

2.13.2 Network topography

In a neural network, the neurons/ nodes are organised into linear arrays called layers. The architecture of an ANN is made of an input layer, an output layer and one or more hidden layers.
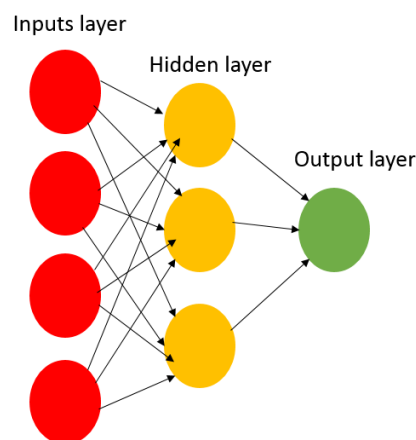
Figure 2.13 A schematic illustration of an artificial neural network. The network cosset of one inputs layer (four inputs), one hidden layer that contains three neurons, and one output layer (one output).

41

2.13.3 Learning rules

The ANN uses the so-called training data set to learn the relationships between the inputs space and the outputs one; this process is called learning [152]. Mathematically, training is done by adjusting the weights to desired values (i.e. the target/experimental outputs). In general, training can be supervised or non-supervised. In the supervised training, the ANN is provided by the inputs and the associated output. During the training process of the supervised network, the weights are tuned to reduce the error between the network output and the target output. Whereas in the unsupervised training the desired output is unknown, the network tries to capture the trends and patterns in the input data alone [151,152].

2.13.4 Pros and cons of the ANN

Compared to traditional regression, the main advantage of a neural network is its ability to model complex nonlinear relationships [149]. Additionally, it is fast and highly scalable which can be run within seconds unlike the mechanistic models which make the ANN more suitable for industrial applications [148,151]. One of the main drawbacks of ANNs is that they are considered as a "black box". If the analytical form of the relationship that link samples in the data set is essential, then ANN is not the best suitable tool due to the opaque nature of the decision-making algorithm [149]. Nonetheless, ANN can be coupled with other modelling approaches such as neuro fuzzy logic. The combination enables the generation of rule sets representing the cause-effect relationships contained in the analysed data [153].

2.14 Application of artificial neural network in powder processing and granulation

Since ANN is a powerful tool that can capture complex patterns and highly nonlinear relationships in an available data set that was collected from a process, it has been used in several areas of science such as analytical chemistry, biomedical and powder technology [149,154]. An ANN has been used in the field of processing powders, granules, and tablets [148,155–157]. Barmpalexis et al. studied the effect of formulation on the release rate of nimodipine from tablets. It was found that using ANN with eight hidden neurons provide better fit compared with multiple linear regression [158]. Sajjia

et al. investigated the effect of the roll force and screw speed of roller compactor on the ribbon density [159]. ANN has been useful in predicting the particle size of granules [160]. Ye et al. predicted the mean particle size and the span of granules made using a high shear mixer with an average absolute relative error of 7.18% and 5.75% respectively [160].

Behzadi et al. showed that the neural network can be a reliable method to predict the size and flowability of granules produced using fluid bed granulation [161].Murtoniemi et al. studied the effect of several independent variables which are inlet air temperature, atomising air pressure and binder amount on the granule size and friability [155]. A 486 personal computers were used to perform the analyses with a special accelerator card. The results showed that the ANNs are more accurate than the multilinear regression analysis [155]. Kesavan and Peck investigated the effect of formulation and granulation technique (high shear mixer and fluidised bed granulation) on several outputs including tablet strength and disintegration. It was found that the correlation coefficients are higher when the data is analysed using ANN compared with regression analysis model [162].

Shirazian et al. (2017) were the first to study the applicability of ANN modelling to predict the particle size of granule made using twin screw granulation [148]. The ANN inputs in Shirazian's study were screw configurations, liquid to solid ratio, screw speed and powder feed rate while the output was the particle size distribution of the microcrystalline cellulose represented by the d-values (d_{10}, d_{50}, and d_{90}) [148]. The ANN could be a powerful tool to help in reducing the amount of trial and error in product development and predicting the quality attributes of granules and tablets. However, there is a strong need to examine the applicability of the use of ANN in twin screw granulation.

Chapter 3   Materials and Experimental Methodology

3.1   Materials

The materials used in this study are pharmaceutical grade materials which are used as excipients in the pharmaceutical industry. The materials were selected for their different mechanical properties and water solubilities. The used materials range from plastically deformable to brittle and from water soluble to water insoluble.

3.1.1   Microcrystalline cellulose

Microcrystalline cellulose (MCC) is a purified partially depolymerised cellulose. MCC is a white, powder which is composed of porous particles. MCC is practically insoluble in water, but it is a hygroscopic powder. The typical water content of MCC powder is approximately %5 w/w when the MCC is exposed to 25 °C and 50% relative humidity [163]. MCC is commonly used in the pharmaceutical industry as well as in the food and cosmetic industries [164].

In the pharmaceutical industry, MCC is used as binder or diluent for oral dry formulations including tablets and capsules. Also, MCC is commonly used for granulation and direct compression [164]. In addition, MCC is used as a tablet disintegrant, and also to reduce the friction during tablet manufacturing [164]. Figure 3.1 presents the structural formula of MCC, which is a cellulose chain bonded together by strong hydrogen bonds [163].
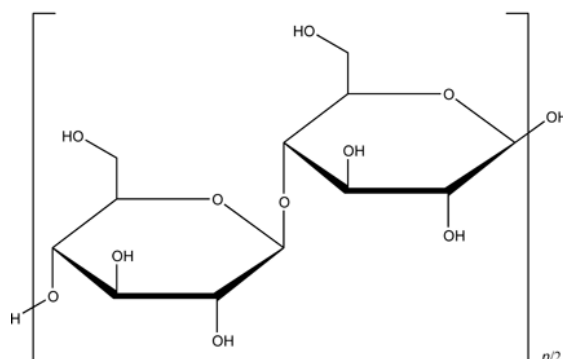
Figure 3.1 The structural formula of microcrystalline cellulose, adapted from [164].

Figure 3.2 presents a scanning electron microscope (SEM) image of MCC particles which are made of elongated particles and aggregates.

SEI   10kV   WD16mmSS50   x370   50µm

Jun 02, 2016
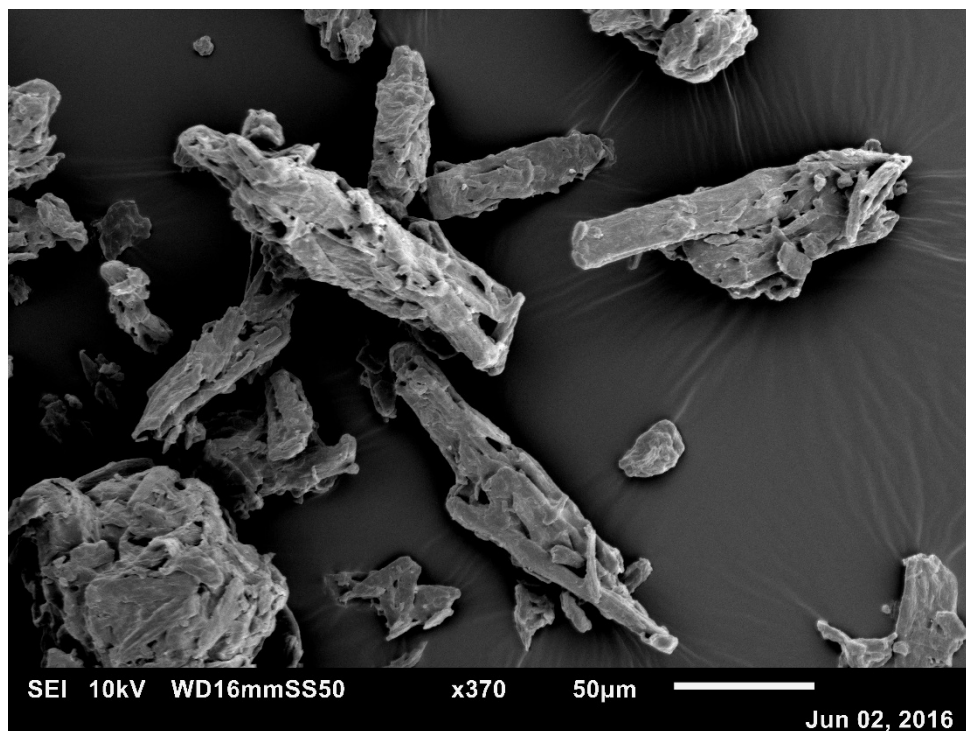
Figure 3.2 Scanning electron microscope image of microcrystalline cellulose (Avicel PH-101)

3.1.2 Mannitol

Mannitol is a white or white off crystalline water soluble and free-flowing powder. It is a hexahydric alcohol as presented in Figure 3.3. Mannitol shows polymorphisms, and it is not a hygroscopic material. Mannitol is commonly used in food and pharmaceutical industries. In pharmaceutical formulations, mannitol is mainly used as a diluent in tablet formulations, and as a carrier in dry powder inhalers [164].
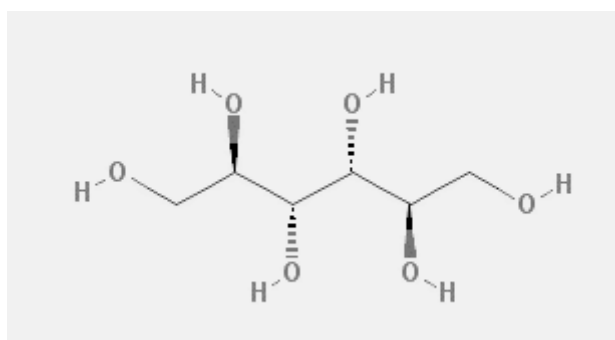
Figure 3.3 The structural formula of mannitol, adapted from [164].

In this research, two types of mannitol were used. The first one is crystalline mannitol (Pearlitol® 160 C - mean diameter 160 μm, Roquette, France). This grade of mannitol has a brittle nature which deforms by fragmentation [82]. Figure 3.4 presents a SEM image of 160 C mannitol. The crystalline mannitol is made of large square or rectangular shaped crystals that have a relatively flat surface.
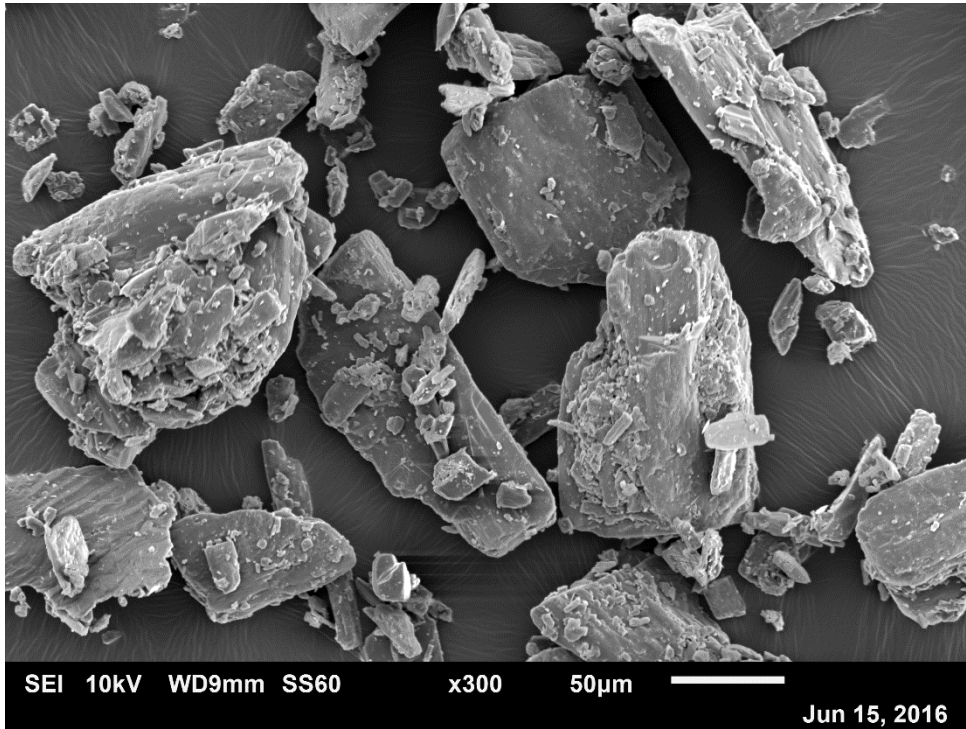
Figure 3.4 Scanning electron microscope image of crystalline mannitol 160C.

The second type of mannitol is the spray-dried mannitol (Pearlitol® 100 SD -mean diameter 100 μm, Roquette, France). This grade of mannitol has better compression properties compared with the 160 C mannitol [82]. Figure 3.5 presents a SEM image of the 100 SD mannitol. As it could be seen from Figure 3.4 Figure 3.5 the mannitol particles have different shapes which is expected as the two mannitol types are manufactured in different methods. The mannitol 160C is made by crystallisation while the mannitol 100 SD is made using spray drying. More photos of the crystalline mannitol are provided in Appendix B.
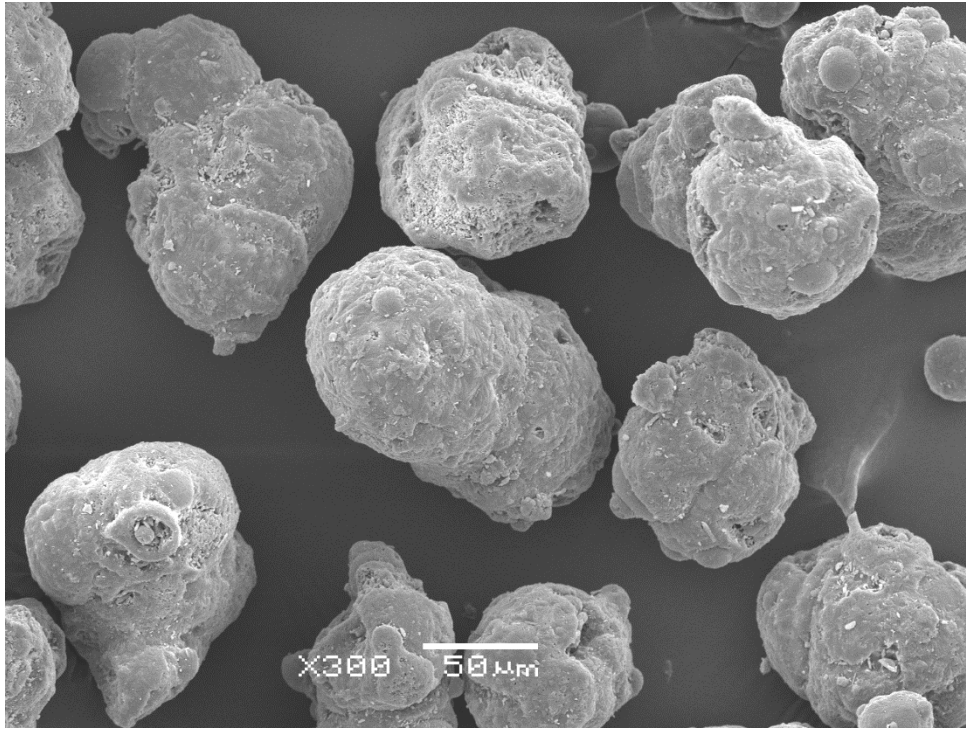
Figure 3.5 Scanning electron microscope image of spray dried mannitol 100SD.

3.1.3 Dibasic calcium phosphate anhydrous

Calcium phosphate, dibasic anhydrous which is also called dibasic calcium phosphate (DCP) is a white non-hygroscopic powder or crystalline solid which is practically insoluble in water [164]. It is used as an excipient and a source of calcium in the nutrition sector. In the pharmaceutical industry, it is used in wet granulation, roller compaction, and direct compression formulation. The predominant deformation mechanism of DCP coarse grade is brittle fracture thus it is used to reduce the strain rate sensitivity of formulation [165]. The inorganic nature of the DCP is presented in Figure 3.6. SEM image of the DCP powder is presented in Figure 3.7. The DCP particle looks like an aggregate of smaller particles.
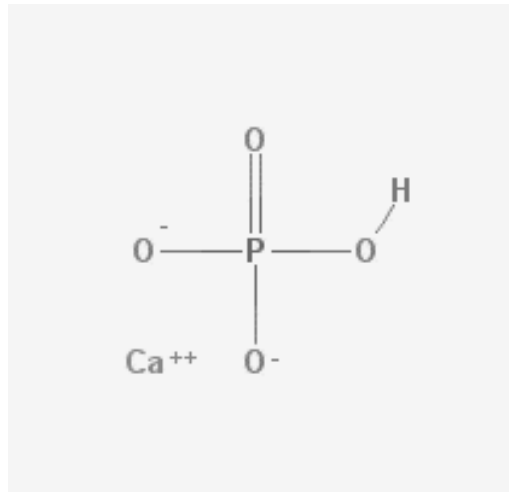
Figure 3.6 The structural formula of dibasic calcium phosphate, adapted from [166].
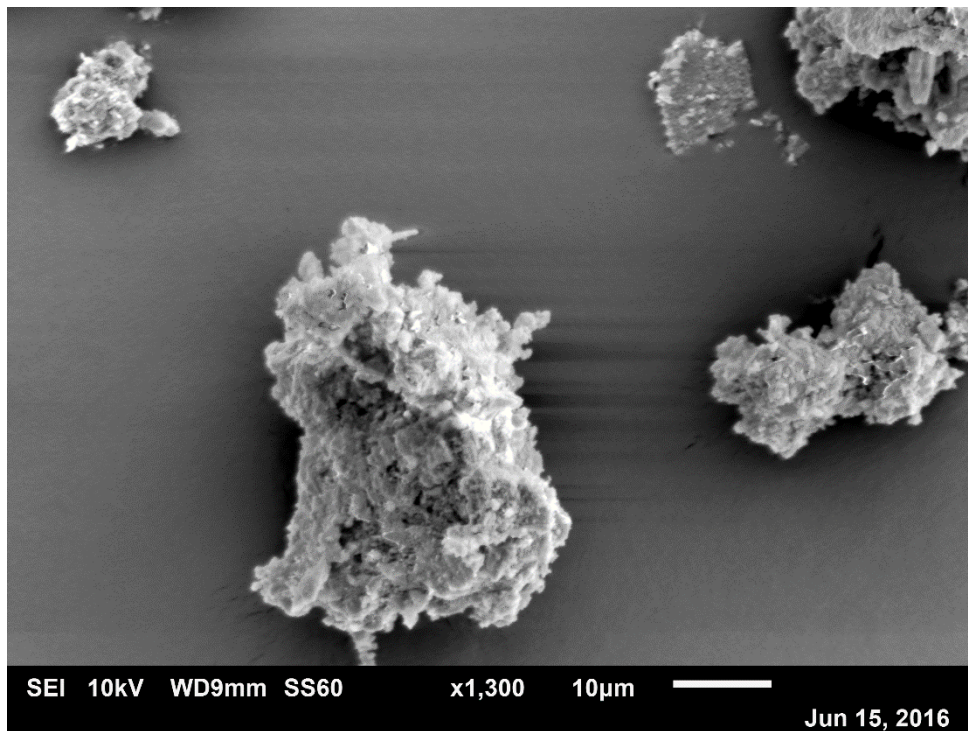
Figure 3.7 Scanning electron microscope image of dibasic calcium phosphate.

3.2 Methods

3.2.1 Primary powder characterisation

3.2.1.1 Heckel analysis

A materials testing machine (3367, dual column, Instron®, USA) with data logging capability was used to compress the powders. A flat-face upper punch and a fixed 12 mm internal diameter cylindrical die were used. The compression speed was 1 mm/second, a pre-load of 1 N was used. Each of the primary powders was compressed at a range of compression forces from 5-20 kN (44-176 MPa). Out-of-die Heckel analysis was used to analyse the powder compaction data - this analysis is based on the assumption that the process of pore reduction during compression follows first order kinetics [167]. The Heckel coefficient (K) was calculated using Eq (3.1) [33].

$$Ln\left(\frac{1}{1-D}\right) = K.P + A \qquad\qquad Eq\ 3.1$$

This equation is in the form $y = mx + c$, where D is the relative density (the density of the tablet divided by the true density of the powder) at any given compaction pressure P, K is the Heckel coefficient (the slope of the line), and A is a constant (and the y intercept). The reciprocal value of the Heckel coefficient is the yield pressure, Y_p, which is a measurement of the compressibility of the material. The smaller the Y_p of a material the more deformable it is.

3.2.1.2 Work of compaction

The work of compaction of the primary powder was measured using the same Instron materials testing machine and the same punch and die set as for the Heckel analysis. A compression-decompression method was used, using the same compression speed (1 mm/second) and a pre-load of 1 N was applied. Once a compression force of 10 kN (88 MPa) had been reached, the punch direction was reversed at the same speed until the load was removed (0 N). The force-displacement data during the compression and decompression was plotted as shown in

Figure 3.8, where A is displacement at the beginning of the test, B is the maximum compression load, C is the displacement at the maximum compression load, and D is the displacement corresponding to 0 N load at the end of the test. The area ABC is the total

work of compaction. The elastic work is represented by the area DBC which is the energy recovered during the decompression phase. The subtraction of the elastic work from the total work represents the apparent net work (plastic work) [33,41,168]. The plastic work is a good indicator of a material's plasticity [168]. The area under the curve was calculated using the trapezium rule using a simple function in spreadsheet software (Excel 2013, Microsoft, USA). The percentage of the plastic and percentage of the elastic work was calculated by dividing each work by the total area under the curve. Five replicates were performed for each sample.
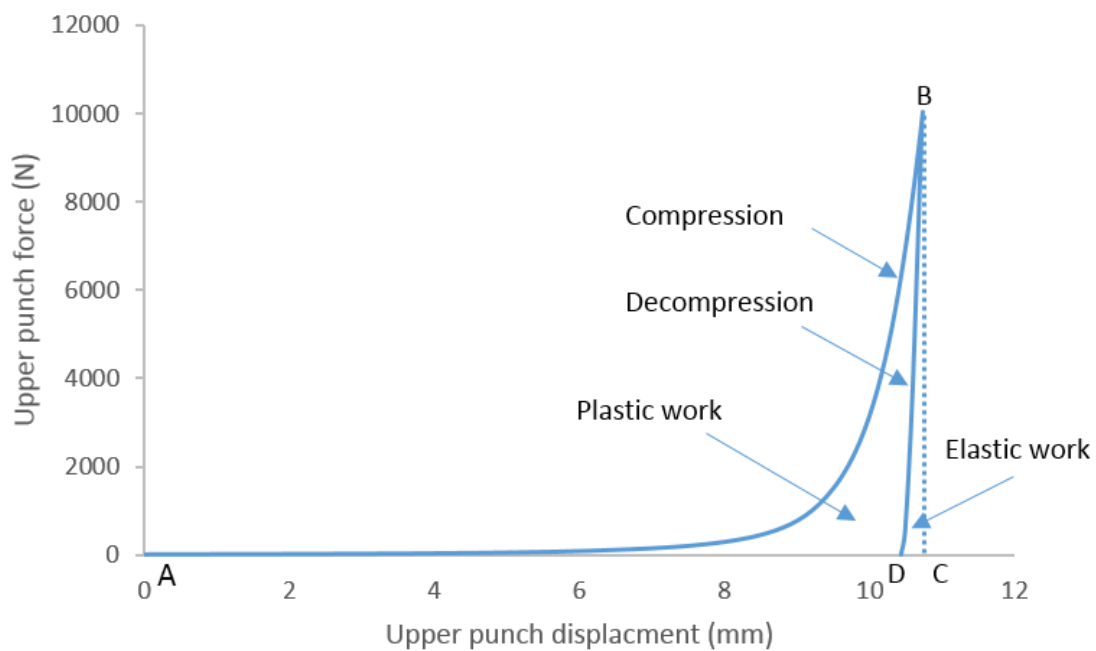
Figure 3.8 Force vs displacement data during the compression-decompression method. The area ABC is the total area of compaction, the DBC area is the elastic work and the area ABD represents the apparent net work (plastic work).

3.2.2 Powder blending

In the case of a formulation, the powders were mixed using a Y-shaped mixer to prepare powder mixtures. The mixer rotated at a constant speed (60 r/min). The powders were mixed for five minutes to improve the uniformity of the mixtures.

3.2.3 Twin screw granulator & granulation process

Powders were granulated using an open channel (no die at the end), co-rotating twin-screw granulator (Euro-lab 16, Thermo Fisher Scientific, USA). The barrel length is 400 mm, and the diameter is 16 mm (the length-to-diameter ratio is 25:1).

The granulator is a lab-scale granulator that is built for pharmaceutical wet granulation. The granulator is a co-rotating intermeshing self-cleaning twin screw granulator. The twin screw can achieve a maximum speed of 1000 RPM and 12 Nm of torque. The granulation equipment consists of a motor, pair of co-rotating intermeshing screws placed in the granulator barrel, powder feeder, and liquid peristaltic pump. The granulation barrel temperature was kept constant at 25 °C using a temperature control unit. A schematic illustration of the granulator is depicted in Figure 3.9
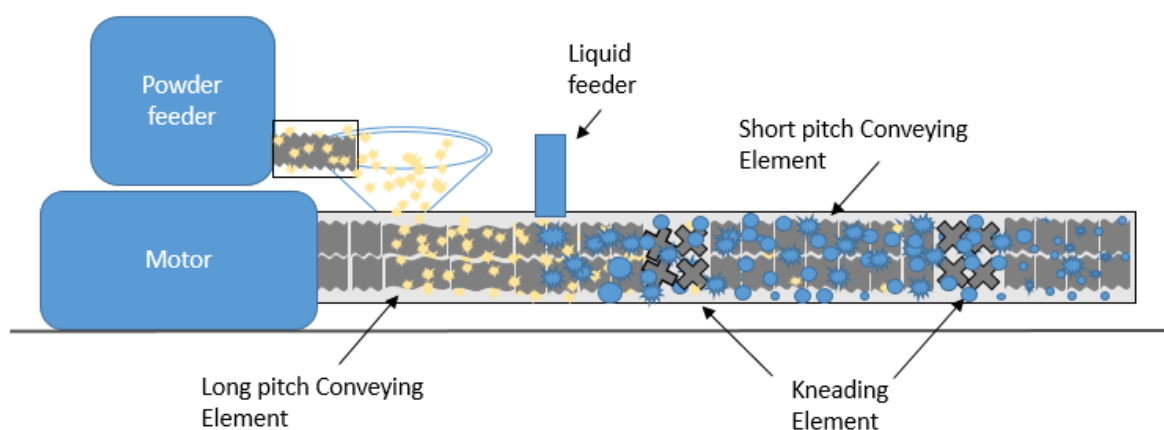
Figure 3.9 Schematic draw of a continuous twin screw granulator.

Each powder was fed into to the barrel of the granulator using a gravimetric twin-screw feeder (K-PH-CL-24-KT20, K-Tron, USA). The powder feed rate was fixed at 1 kg/h. De-ionised water was used as a liquid binder for all the granulation experiments. The de-ionised water was fed into the system using a peristaltic pump (101U, Watson-Marlow, UK). The optimum liquid-to-solid ratio (L/S) for each material was used (determined by prior experiments to allow using the same L/S ratio while changing the processing conditions). The twin screw elements can be configured in many ways allowing the use of conveying elements only, kneading elements only or a combination of both. For this study, three screw configurations were used as presented in Figure 3.10.

For instance, in set 1 each screw contains two short conveying elements, two long conveying elements and 19 short conveying elements, while in set (2) and (3), 8 and 16

51

kneading discs were added in each screw respectively [153]. A brief description of the screw elements used is provided in Table 3.1.
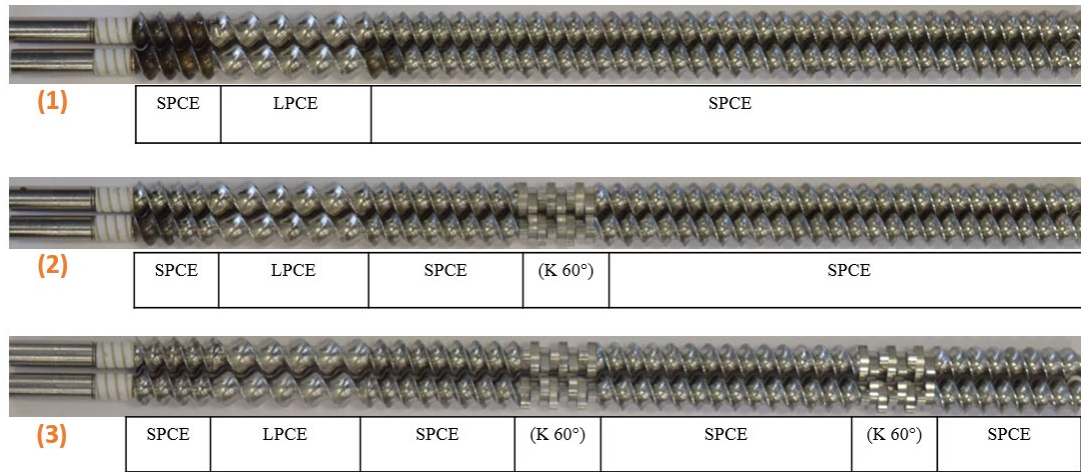
Figure 3.10 (1) The screws configured with conveying elements only. (2) The screws configured with conveying elements and 16 kneading discs. (3) The screws configured with conveying elements and 32 kneading discs. LPCE: Long pitch conveying element (Length=2 x diameter), SPCE: Short pitch conveying element (length = diameter) and K 60° staggering angle: Kneading disc at 60° pitch (length=diameter/4).

Table 3.1 Description of the screw elements used in the granulation process.

Screw element type	Ratio of length of the element to its diameter	Element Image
Short pitch conveying element (SPCE)	L=D	
Long pitch conveying element (LPCE)	L=2D	
Kneading disc with 60° staggering angle	L=D/4	

3.2.3.1 Liquid feeder

The liquid binder (water) was administrated into the system using a peristaltic pump (101U, Watson-Marlow, UK). The output of the pump can be controlled by adjusting the

number of revolutions per minute (RPM) of the rotating device. The liquid mass flow rate at a specific RPM depends on the diameter of the used pipe. Two pipes were used to cover a range of mass flow rate of liquid binder. The output of the pump was regularly calibrated to ensure accurate liquid flow rate.

3.2.4 Drying method

The granules were directly collected from the granulator into flat trays. Then the granules were left to dry at room temperature for 72 hours. The moisture content was meseared using a loss on drying method to ensure that the granules were dried. The moisture content of the powder/granules was measured using a loss-on-drying analyser (MA37, Sartorius, Germany). The device was set to heat to 80°C for 45 minutes.

3.2.5 Granule characterisation

3.2.5.1 Granule sizing

The size of dry granules was measured using a CAMSIZER (Retsch Technology GmbH & Co. KG, Germany) which is a dynamic image analysis technology [169,170]. The particle/ granule size distribution (PSD) was presented as a frequency distribution based on volume vs size class.

3.2.5.2 Granule sieving

The sieve shaker (AS200, Retsch GmbH, Germany) was used to sieve the dry granules into two size classes: 300-500 µm and 1.18-1.40 mm. The sieving time was five minutes.

3.2.5.3 Granule Structure analysis

The internal structure of dry granules in the size class 1.18-1.40 mm was studied using X-ray tomography (µCT 35, SCANCO Medical AG, Switzerland). For dicalcium phosphate, the granule size fraction used was 300-500 µm since no larger granules were available. The X-ray tube was operated at a voltage of 45 kV, a current of 177 mA and a power of 8 W. Images from the X-ray machine were analysed using an image analysis software (Image J 1.49v, national institute of health, USA).

In the X-ray images, the white pixels represent the powder while the black pixels indicate the air voids within the granule. The total number of black pixels was determined and

divided by the total number of pixels; this ratio represents the porosity of the granule [82,171].

A comparison study for quantifying the porosity using X-ray and solid displacement pycnometer is provided in Appendix D.

3.2.5.4 Granule crushing force

The crushing force of 40 individual granules was measured using a materials testing machine (Z0.5, Zwick/Roell, Germany) fitted with a 500 N load cell [131]. The test speed was 50 µm/min, with a pre-load of 0.01 N. The size class of the tested granules was 1.18-1.40 mm.

3.2.6 Specific surface area measurement

The specific surface area (SSA) of the primary powders and the granules were measured using (TriStar II Plus, Micromeritics, USA). The granules were degassed for 16 hours using a degassing station which operates under vacuum at 30 °C. The SSA of 1 gram of powder/ granules were tested in duplicates using Nitrogen gas adsorption method. The Brunauer–Emmett–Teller (BET) equation (Eq 3.3) was used to calculate the BET specific surface area [68]. The measurements were performed at relative nitrogen pressure range (P/P^0) from 0.05 to 0.3 (multi point BET theory) at tempretuer of -196 °C [61].

3.2.6.1 Brunauer–Emmett–Teller (BET) theory

The BET method is based on the monolayer adsorption of an inert gas such as nitrogen on the solid surface at reduced temperatures. The BET surface area equation is based on Langmuir's kinetics theory which theorised that only a single layer of molecules can adsorb on the solid surface. In 1983 three scientist Brunauer–Emmett–Teller extended the Langmuir's theory to multimolecular layer adsorption [68]. The gas molecules adsorb and desorb at various rates until equilibrium is established. The quantity of molecules adsorbed when the system in equilibrium can be obtained by summing for an infinite number of layer [172].

$$V = \frac{v_m C P}{(P^0 - P)[1 + (C - 1)\frac{P}{P^0}]}$$ Eq 3.2

Where V is the quantity of the gas adsorbed at P/P^0 expressed as gas volume at the standard temperature and pressure. P is partial pressure of adsorbate and P^0 is the saturation pressure of the adsorbate at the experimental temperature. The v_m is the volume adsorbed in monolayer. Lastly C is the BET constant related to the heat of adsorption.

The linear form of the previous relationship is called the BET equation as described below

$$\frac{P}{V(P^0 - P)} = \frac{1}{v_m C} + \left(\frac{C-1}{v_m C}\right)\frac{P}{P^0} \qquad \text{Eq 3.3}$$

Plotting $\frac{P}{P^0}$ VS $\frac{P}{V(P^0 - P)}$ will enable the calculation of C and v_m.

The BET method has been proven to be an accurate method for calculating the surface area for the majority of materials [64,173].

3.2.7 Tablet compression and characterisation

3.2.7.1 Tablet compression

A materials testing machine (3367, dual column, Instron®, USA) was used to compress the granulated materials. Two size classes of granules (300-500 µm and 1.18-1.40 mm) were compressed at 5, 10, and 20 kN. A flat-face upper punch and a fixed 12 mm internal diameter cylindrical die were used. The compression speed was 1 mm/second, once a pre-load of 1 N was detected the force displacement data was recorded. The die and the punch were lubricated with a suspension of magnesium stearate in ethanol (1% w/w) before each compaction [64] and were dried using a source of hot air. The lubrication of the die and the punch (external lubrication) was used to overcome the stickiness of the materials on the tablet tooling. Each point in the tabletability and compactability profiles represent the average of five tablets.

3.2.7.2 Tablet tensile strength and porosity

The tensile strength of tablets was calculated using Eq (2.1) [33].

$$\sigma_T = \frac{2F}{\pi H T} \qquad \text{Eq 2.1}$$

Where σ_T is the tablet tensile strength in MPa, H is tablet diameter in mm, and T is the tablet thickness in mm. F is the force needed to break the tablet, measuered using a

materials testing machine (Z0.5, Zwick/Roell, Germany) fitted with a 500 N load cell [131]. The test speed was 0.5 mm/min, with a pre-load of 0.1 N.

The tablet porosity was calculated using equations Eq (3.4) and Eq (3.5) [174].

$$Apparent\ density = \frac{Tablet\ weight}{Tablet\ Volume} \qquad\qquad \text{Eq 3.4}$$

$$\varepsilon_T = \left(1 - \frac{Apparent\ density}{True\ Density}\right) * 100 \qquad\qquad \text{Eq 3.5}$$

3.2.7.3 Change in tabletability after granulation compared with tablets prepared by direct compression

The percentage of change in the tabletability was calculated using the following formula

$$\Delta Ts = \left(\frac{T_{DC} - T_g}{T_{DC}}\right) * 100 \qquad\qquad \text{Eq 3.6}$$

Where ΔTs is the percentage of the change in the tablet tensile strength after granulation compared with the table strength of the material when directly compressed. T_g is the tablet tensile strength of the granulated material, and T_{DC} is the tablet strength of the material when direct compression is used

3.2.8 Tablet dissolution

Sodium chloride was selected as a non-functional active ingredient to study the dissolution rate of tablets made from granulated materials [13]. The dissolution profile was measured using a conductivity probe (Jenway model 4520, Camlab, UK) by measuring the change in the conductivity of de-ionised water as a function of time. 250 ml of water was used as a dissolution medium 25 °C using a temperature controlled hot plate. The 250 ml was used to enable detection of a good conductivity signal. A data logging system was used to record the conductivity at three-second intervals until a constant reading was achieved.

0.5 gram of granules was compressed into tablets at different compression forces 5, 10, 20 kN.

The fraction of the dissolved sodium chloride, Y, after t, was determined as follows (Eq 3.7) [12].

$$Y = \left(\frac{x - x_0}{x_\infty - x_0}\right) * 100\%$$ Eq 3.7

Where x is the conductivity of the solution at time t, and x_0 and x_∞ are the initial and the final conductivity. The dissolution time was calculated based on the time needed for 90% of the sodium chloride to be dissolved from the compressed materials [175].

A range of concentrations of sodium chloride in de-ionised water were prepared. The conductivity of these solutions was measured to build a standard calibration curve. Figure 3.11 shows that there is a linear relationship between the concentration of sodium chloride and the conductivity, which indicates that the selected method is fit for purpose in the selected concentrations.
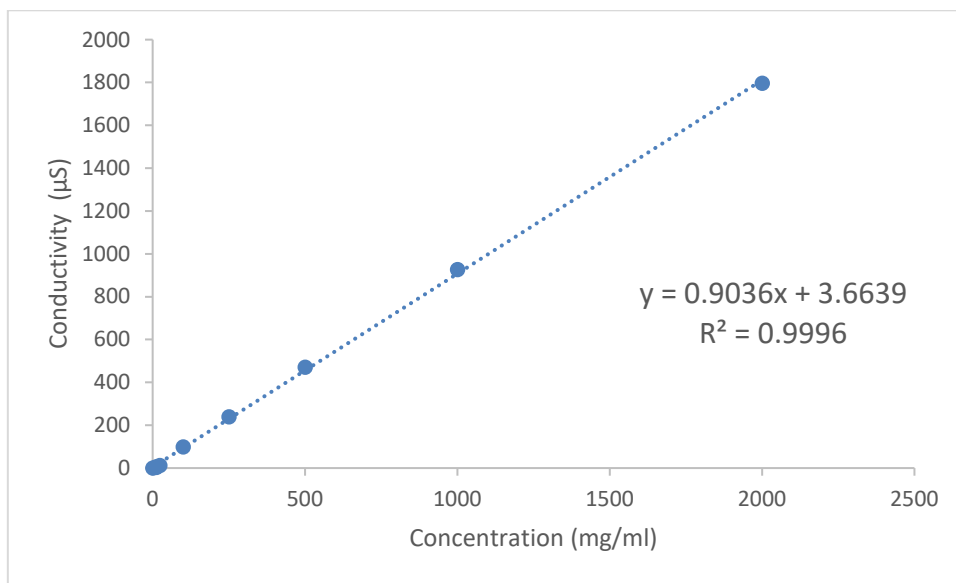
Figure 3.11 Conductivity of aqueous sodium chloride solutions at a range of concentrations.

3.2.9 Flow chart of the processing steps

Four pharmaceutical excipient were selected as explained in section 3.1. The excipients have different mechanical properties and water solubility as presented in Figure 3.12. MCC and DCP are non water soluble while mannitol is water soluble. In terms of deformability, MCC is the most deformable and DCP is the least as depicted in figure 3.12
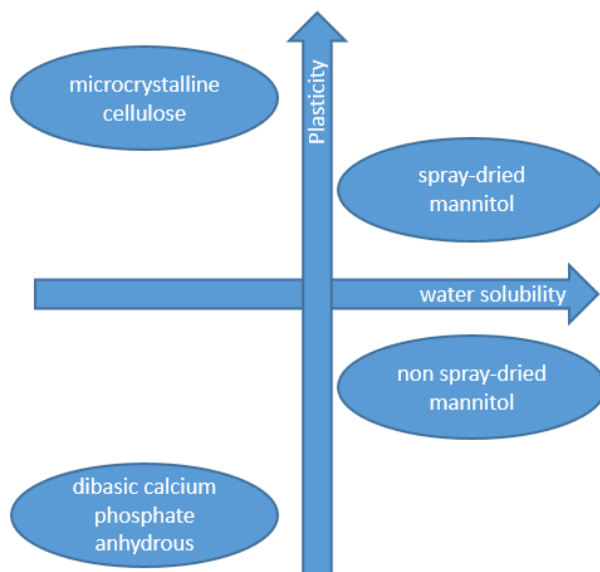
Figure 3.12 An illustration properties of the primary materials in terms of water solubility and mechanical deformability.

After the characterisation of the mechanical properties of the primary materials as described in section 3.2.1 the materials were subjected to several processes as presented in Figure 3.13. The primary material were granulated using a TSG then dried and sieved into two size classes after that the granule porosity, strength, and specific surface area were characterised. Tablets from the granulated materials and primary powder were prepared at a range of compression pressure (44-175 MPa). The tablet tensile strength and dissolution rate were measured as described in section 3.2.7.2 and 3.2.8 respectively.
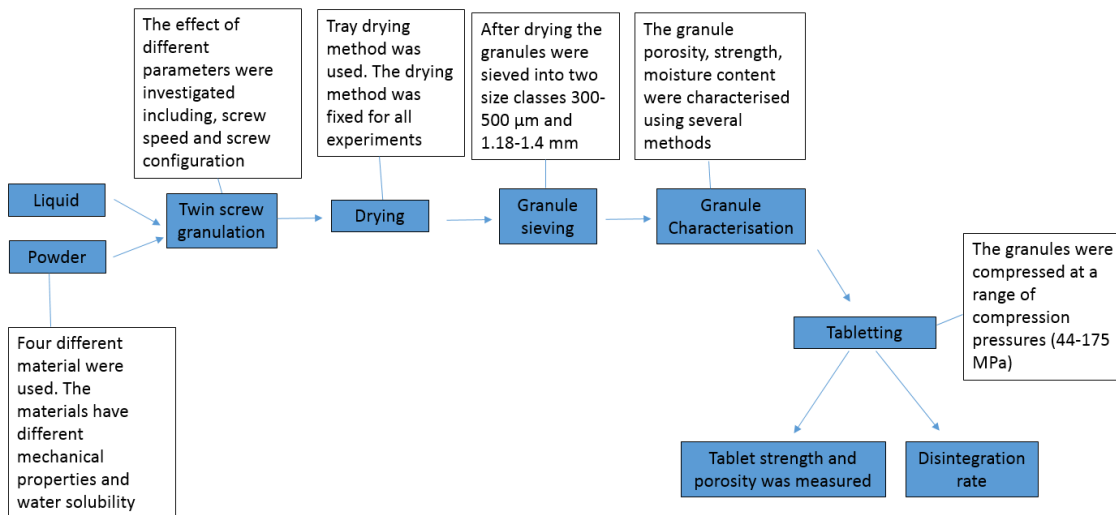
Figure 3.13 flow chart of the processing steps of the primary material starting from granulation until the characterising of tablets.

Chapter 4   The Effect of The Mechanical Properties of Primary Powder on The Tabletability of Twin Screw Granulated Materials

4.1   Summary

Granulation is a technique commonly used before tabletting because it solves powder handling problems and ensures uniform filling of the compression dies. However, granulation can have an adverse impact on powder transformation into a tablet; i.e. tabletability.

Therefore, the aim of this chapter is to examine the effect of continuous wet granulation using twin-screw granulator (TSG) on the tabletability of the granulated materials. Furthermore, the study investigates the mechanisms that dictate the change in tabletability after wet granulation.

Granules and tablet properties were characterised using a range of mechanical and X-ray analysis techniques. The presented work suggested that there is a correlation between the mechanical properties of the primary powder and the percentage of change in tabletability after granulation. The study found that plastically deformable materials like microcrystalline cellulose (MCC) experienced a significant reduction of tabletability when granulated compared with the direct compression of their powder. On the other hand, brittle materials like crystalline mannitol C160 or calcium phosphate dibasic anhydrous maintained their tabletability after twin-screw granulation.

4.2 Introduction

The effect of granulation on the tabletability of several materials using dry granulation (roller compaction or slugging) has been thoroughly investigated [38,130–132]. It is reported that dry granulation causes a reduction in tabletability and compactability of the granulated powder. Two principal mechanisms for the deterioration of compactability after dry granulation have been proposed: size enlargement (difference in size among granules, and between the granules and the primary powder), granule strength, or a combination of both [37,130,131].

The effect of wet granulation on the tabletability has been studied in a high shear mixer (HSM). It was reported that increasing the granules size caused a deterioration of the granule tabletability after granulation using HSM [127]. Badawy et al. associated the reduction in the tabletability of MCC granules with a reduction in the granule porosity [135]. Osei-Yeboah et al. reported that the decrease in the tablet strength of MCC granules produced using HSM correlates with the size enlargement, specific surface area, and porosity of the granules [128]. The motivation for this work was to try to deconvolute these effects.

TSG is distinctly different from roller compaction and HSM in the mechanisms of size enlargement, type and extent of the compression and shear stresses, and the residence time during granulation [4,11]. Also, the use of a granulation liquid can have a significant impact on the process when compared with roller compaction. Hence, the mechanisms that describe the reduction of the tabletability of granules made using roller compaction and wet granulation by HSM should not be extrapolated to wet granulation by TSG without a thorough investigation. There appear to be no reports in the available literature to the best of the author's knowledge, about the mechanisms which describe the change in tabletability of the granulated material using TSG, which is the focus of this work. Additionally, the work aims to understand the effect of the mechanical properties of the primary powder on the attributes of granules and tablets.

4.3   Materials

Four pharmaceutically-relevant excipients were chosen for use in this study: microcrystalline cellulose (Avicel PH-101), spray-dried mannitol (Pearlitol® 100 SD); crystalline mannitol (Pearlitol® 160 C) and dibasic calcium phosphate anhydrous (Calipharm® A). The four selected excipients were chosen for their differing mechanical properties and water solubilities. Regarding water solubility, mannitol is soluble, microcrystalline cellulose is insoluble but absorbs water, and dibasic calcium phosphate anhydrous is insoluble and does not absorb water. The applied method of granulating excipients alone allowed obtaining information about the behaviour of each material selected and classified by its mechanical properties and solubility.

4.4   Methodology

The study started by characterising the mechanical properties of the primary powders. Then the granules properties were analysed, i.e. porosity and crushing force as depicted in Figure 4.1. The produced granules were sieved into two size classes and compressed using a range of compression pressures.
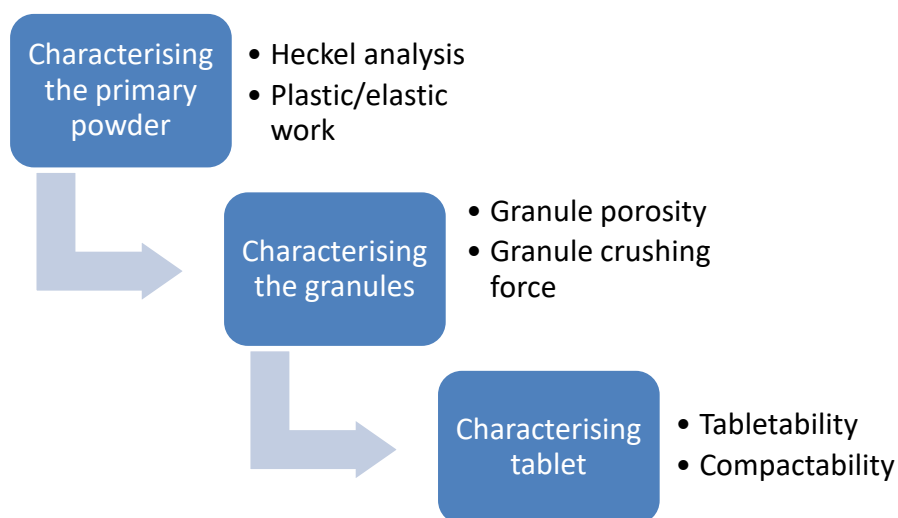
Figure 4.1 Flow chart of the used methodology to investigate the characteristic of primary powder, granules and tablets.

4.4.1 Primary powder characterisation

4.4.1.1 Heckel analysis

The primary powders were compressed then the yield pressure of the primary powders was calculated using the method outlined in the methodology section 3.2.1.1. Out-of-die Heckel analysis was used to analyse the powder compaction data. The reciprocal value of the Heckel coefficient is the yield pressure, Y_p, which is a measurement of the compressibility of the material.

4.4.1.2 Work of compaction

A compression-decompression method was used to calculate the percentage of the elastic and plastic work of the primary powders as presented in section 3.2.1.2. The plastic work can be used as a good indicator of a material's plasticity [168].

4.4.2 Granulation of primary powders

The four excipients were granulated using the TSG described in section 3.2.3. In order to keep the liquid-to-solid ratio (L/S) for each material constant, the optimum L/S ratio of each material was determined by prior experiments to allow the processing of the materials using different screw speed and configurations without changing the L/S ratio. For this study, two screw configurations were used; one with conveying elements only, and the second with conveying elements and two zones of kneading elements (32 kneading discs in total) as shown in Figure 4.2.
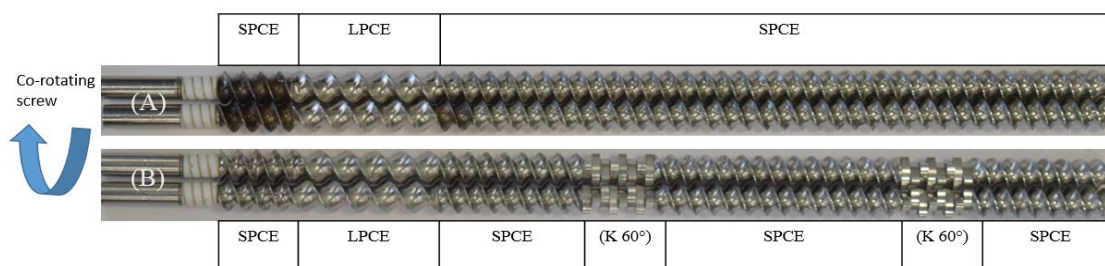
Figure 4.2 Illustration of the used screw elements. A) Conveying elements only. B) Conveying elements and two zones of kneading elements (32 kneading discs). LPCE: Long pitch conveying element (Length=2 x diameter), SPCE: Short pitch conveying element (length = diameter) and K 60° staggering angle: Kneading disc at 60° pitch (length=diameter/4).

Two granulation process parameters were investigated in this study as a means of achieving granules with different properties: screw configuration and screw speed. Both screw configuration and speed were changed to apply different stresses during the granulation process [11,176]. The granulation parameters for each experiment are detailed in Table 4.1.

Table 4.1 Granulation parameters for chapter four.

Set #	Abbreviation	Material	Screw configuration	Screw speed (RPM)	Liquid / solid ratio
1	MCC/C/200	Microcrystalline cellulose	Conveying elements	200	1.31
2	MCC/C/800		Conveying elements	800	
3	MCC/K/200		Conveying elements +32 Kneading discs	200	
4	M100/C/200	Mannitol 100 SD	Conveying elements	200	0.21
5	M100/C/800		Conveying elements	800	
6	M100/K/200		Conveying elements +32 Kneading discs	200	
7	M160/C/200	Mannitol 160C	Conveying elements	200	0.11
8	M160/C/800		Conveying elements	800	
9	M160/K/200		Conveying elements +32 Kneading discs	200	
10	DCP/C/200	Dicalcium phosphate, anhydrous	Conveying elements	200	0.32

4.4.3 Granules characterisation

4.4.3.1 Granule sieving

The granules were directly collected from the granulator into flat trays. Then the granules were left to dry at room temperature for 72 hours. The Sieve shaker was used to sieve the dry granules into several size classes. Two size classes: 300-500 µm and 1.18-1.40 mm.

4.4.3.2 Granule crushing force

The crushing force of 40 individual granules was measured using a materials testing machine (Z0.5, Zwick/Roell, Germany) fitted with a 500 N load cell [131]. The size class of the tested granules was 1.18-1.40 mm.

4.4.3.3 Granule structure analysis

The internal structure of dry granules in the size class 1.18-1.40 mm was studied using X-ray tomography as explained in section 3.2.5.3. For dicalcium phosphate, the granule size fraction used was 300-500 µm since no larger granules were available.

4.4.4 Tablet compression and characterisation

4.4.4.1 Tablet compression

The granulated materials were compressed as described in section 3.2.7.1 using a material testing machine. Two size classes of granules (300-500 µm and 1.18-1.40 mm) were compressed at 5, 10, and 20 kN.

4.4.4.2 Tablet tensile strength and porosity

The tensile strength of tablets was calculated using the equations presented in section 3.2.7.2.

4.5   Results and discussion

4.5.1 Primary powder characterisation by Heckel analysis and work of compaction

The mechanical properties of the primary powders were assessed by Heckel analysis and work of compaction. Out-of-die Heckel analysis was used to calculate the yield pressure (Yp) of the pharmaceutical powders. The Yp results of the primary powders are presented in Table 4.2. The results reveal that the four materials differ significantly in their yield pressure. The Yp of the primary powders is ranked with DCP (highest) > M160 > M100 > microcrystalline cellulose (lowest). The Heckel analysis indicates that the microcrystalline cellulose is the most deformable material among the materials analysed, and DCP is the least deformable. Therefore, the powders start to deform at different compression pressures. Hence, the materials are expected to respond differently to the same level of stress along the granulation barrel and upon compression during the tabletting process.

Force-displacement data during compression and decompression of powders was used to calculate the plastic and elastic work components. The percentage of the plastic and elastic work of the primary powders after compression and decompression method at 88 MPa are presented in Table 4.2. The analysis shows that the primary powders differ in their plastic work, the microcrystalline cellulose has the highest plasticity whereas DCP has the least plasticity in the range of the studied materials. The plasticity of the primary powders is ranked as microcrystalline cellulose (highest) > M100 > M160 > DCP (lowest) – the opposite trend to that observed for the Heckel analysis (Yield pressure). The range of the mechanical properties of the primary powders based on the Yp and the plastic work conforms to the literature - it has been reported that DCP is considered a brittle material and mannitol moderately brittle, while microcrystalline cellulose is typically classified as plastically deforming. The reported order of the studied materials is in agreement with the results reported in several other studies [149,183,190–192], although none of these studies has tested all of these materials together.

Table 4.2 Yield pressure (Heckel analysis) and the percentage of the plastic and elastic work of the primary powder.

Material	Yield Pressure, Yp (MPa)	R^2 for Yp determination	Work of Compaction				Coefficient of variation[2] of the work of compaction (%)
			Percentage of plastic work	Standard deviation of plastic work	Percentage of elastic work	Standard deviation of elastic work	
Microcrystalline cellulose	149	0.99	87.38	0.91	12.61	0.91	3.9
Mannitol 100 SD	181	0.99	84.85	0.76	15.14	0.76	1.1
Mannitol C160	333	0.94	71.31	0.62	28.68	0.62	2.2
Calcium phosphate, dibasic anhydrous	434	0.94	67.25	0.71	32.74	0.71	2.5

The correlation between the yield pressure of the compressed materials (powder and granules) and the percentage of their plastic and elastic work is presented in Figure 4.3. The R^2 value of the linear fitting is good, 0.84. It could be suggested that the powder characterisation using the uniaxial compression methods employed in this study can be used alternatively.

---

[2] Coefficient of variation also known as relative standard deviation is defined as the ratio of the standard deviation to the mean of the measurements.
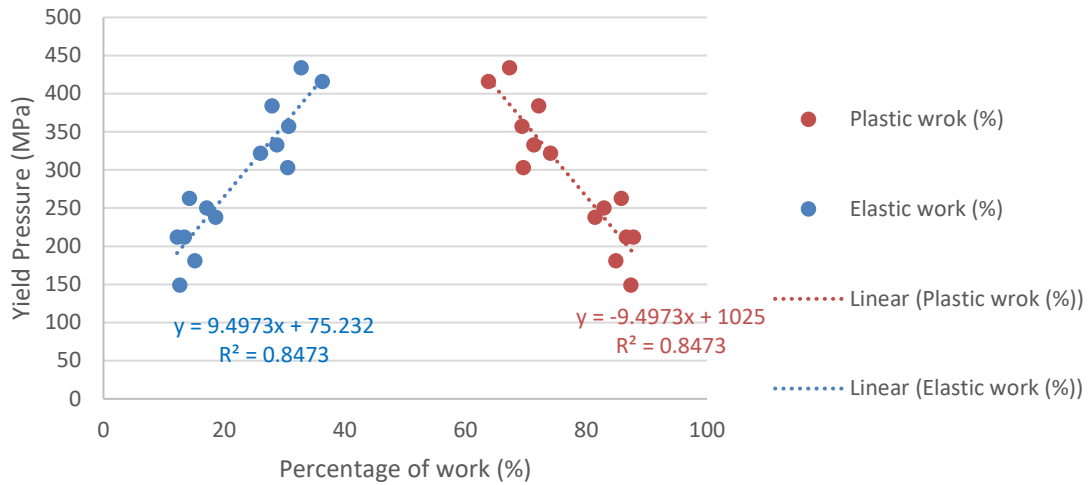
Figure 4.3 Correlation between the percentage of the elastic and the plastic work and the yield pressure of the granules and powders.

4.5.2 Granule characterisation

The effect of granule density (consolidation) on the tabletability of granules was investigated by measuring the crushing force and porosity of single granules. Granule porosity was characterised using X-ray tomography and subsequent image analysis. Figure 4.4 presents X-ray images representing the full set of materials and processing conditions. In general, it can be seen that as the granulation process intensity is increased (by increasing screw speed and introducing kneading zones – presented left to right in Figure 4.4), the granule density clearly increased for all materials (with the exception of dicalcium phosphate for which there was only one set of successful processing conditions). For some of the materials, this change was obvious (e.g., mannitol 100 SD), while for others it was more subtle (e.g., microcrystalline cellulose).
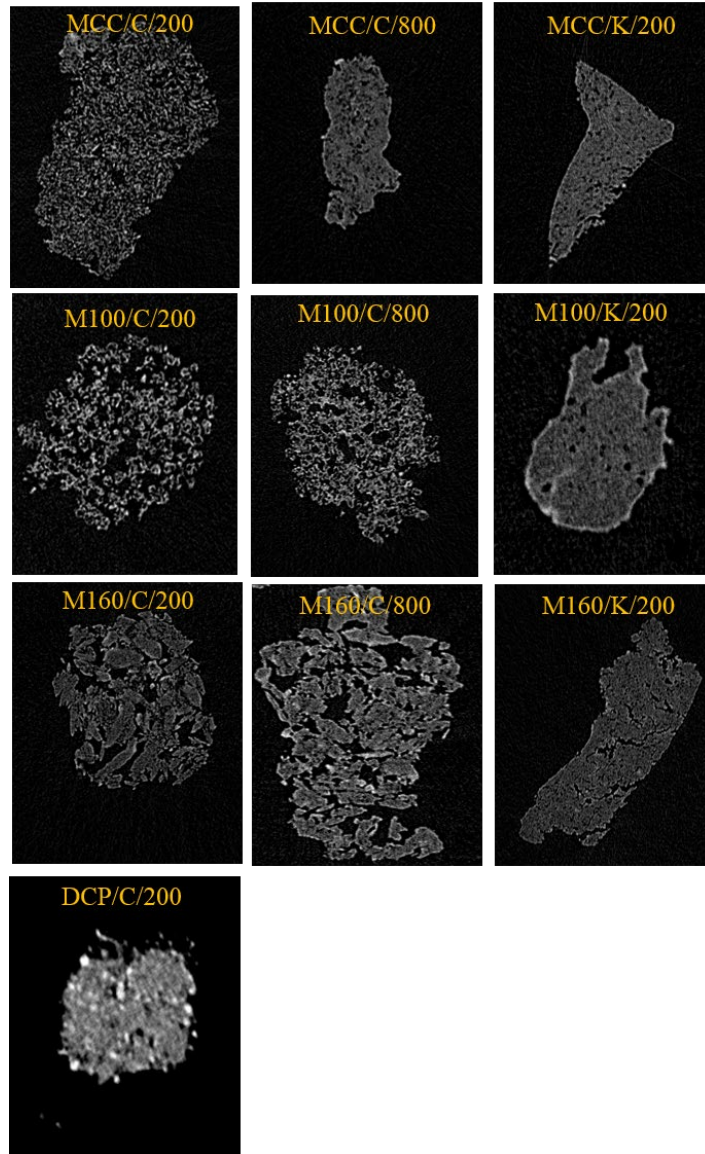
Figure 4.4 X-ray tomographic images of granules in the size class 1.18-1.40 mm (except DCP, which is 300-500 microns).

The porosity and crushing force of the 1.18-1.40 mm granules are presented in

Figure 4.5. The porosity of all granules decreased with increasing the intensity of granulation (with a corresponding increase in granule crushing force). For microcrystalline cellulose, both screw speed and element type (conveying vs kneading) had a detectable effect on granule porosity and strength. For mannitol (both 100 SD and 160 C grades), only the screw configuration had a significant effect on the porosity of the granules produced, although the crushing force was sensitive to higher screw speeds. This suggests that there was some further

densification of C/800 mannitol granules, but the X-ray derived porosity measurement could not detect it. The increased granule strength upon the use of kneading elements in the screw configuration has also been reported by others [176]. For dicalcium phosphate, a low value of granule porosity was measured even for the most gentle granulation condition.
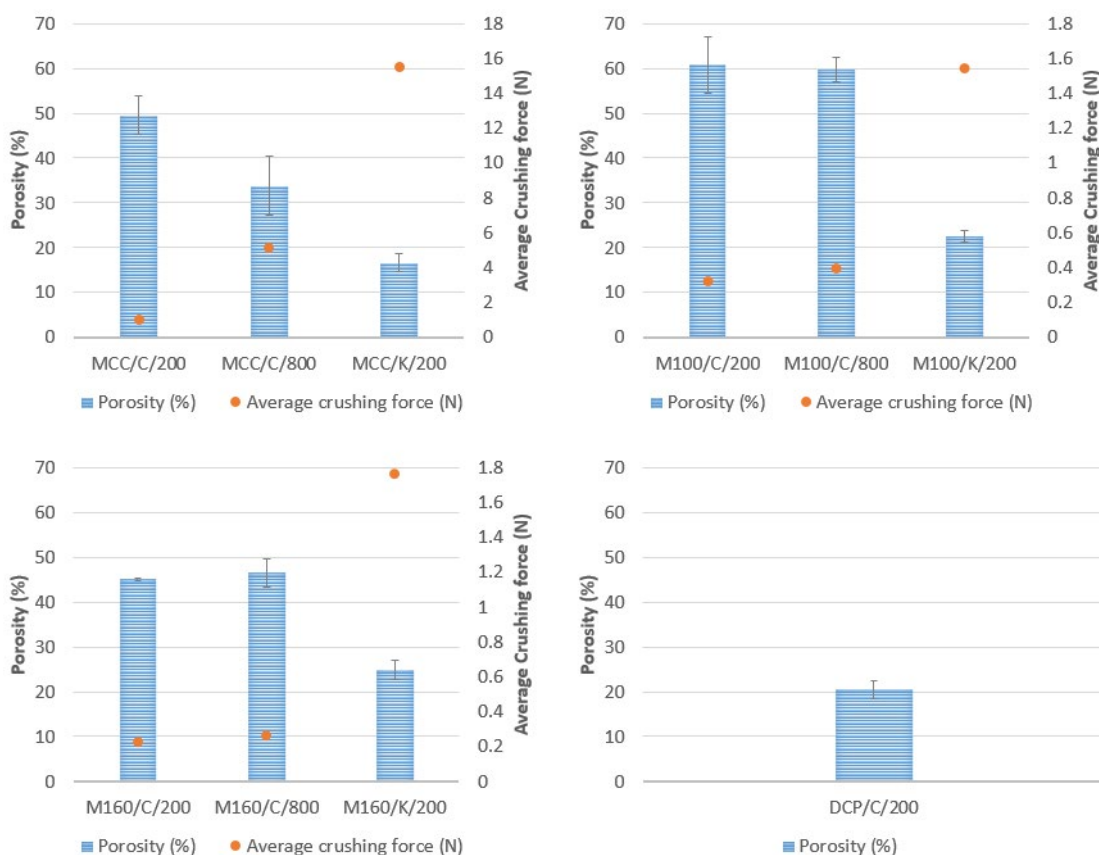
Figure 4.5 The average crushing force and porosity of granules in the size class 1.18-1.40 mm. (except dicalcium phosphate, anhydrous, which is 300-500 microns, porosity only).

4.5.3 Tablet compression and tablet characterisation

In many industries, granules are an intermediate produced to enhance the quality of the final product. It is therefore important to understand how the properties of the granules (and the powders used to make them) influence the properties of the final product. In the pharmaceutical industry, tabletability is defined as the relationship between tablet compaction pressure and tensile strength. It is usually presented as a graphical plot of tablet tensile strength versus the compaction pressure. Compactability is defined as the relationship between tablet solid fraction/porosity and tensile strength, and it is usually presented as a graphical plot of tablet

tensile strength versus its solid fraction (equal to 1 minus the pore fraction) [58,139]. In this discussion, we will use these two measures to examine how each of our materials (primary powders and granules) responds to tablet compression.

4.5.3.1 Microcrystalline cellulose

The tabletability and compactability results for microcrystalline cellulose powder by direct compression (DC) and microcrystalline cellulose granules were compared and are presented in Figure 4.6 and Figure 4.7, respectively. All variants of granulated microcrystalline cellulose show a loss in tabletability and compactability compared with the primary powder. However, the granulation conditions have had varying degrees of impact. The use of high screw speeds or kneading zones resulted in a bigger drop in tablet tensile strength than for conveying elements and slower screw speeds. At 44 MPa compaction pressure, the MCC/C/200 lost around 62% of tablet tensile strength compared with the MCC primary powder, while granules from MCC/C/800 and MCC/K/200 showed about a 75% reduction. It is worth mentioning that the direct compression MCC tablets made at 175 MPa did not break using the applied method with the 500 N load cell.

As shown in Figure 4.7, this significant change in tabletability is not explained by a difference in tablet solid fraction/porosity since there is a large difference in tablet tensile strength for the different input materials at the same tablet solid fraction. There is also no clear difference in the tabletability and compressibility profiles of the 300-500 µm and 1.18-1.40 mm granules for microcrystalline cellulose.
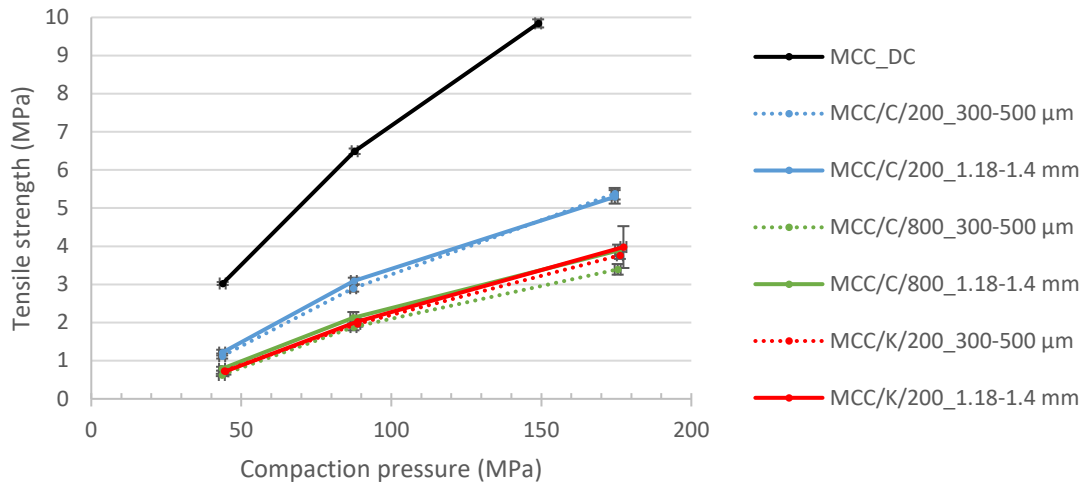
Figure 4.6 Tabletability of microcrystalline cellulose (MCC) granules and primary powder (DC).
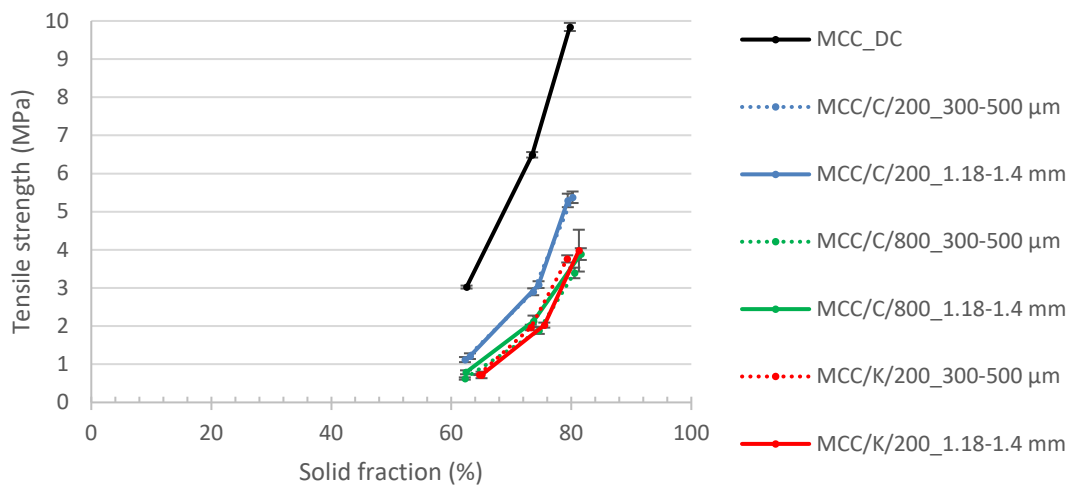
Figure 4.7 Compactability of microcrystalline cellulose (MCC) granules and primary powder (DC).

This decrease in tabletability for denser granules, independent of granule size suggests that particle or granule density/strength is the primary property for determining the tabletability of compacts made from microcrystalline cellulose.

4.5.3.2 Mannitol 100 SD

The tabletability and compactability results for the mannitol 100 SD powder by direct compression (DC) and mannitol 100 SD after granulation were compared and are presented in Figure 4.8 and Figure 4.9 respectively.
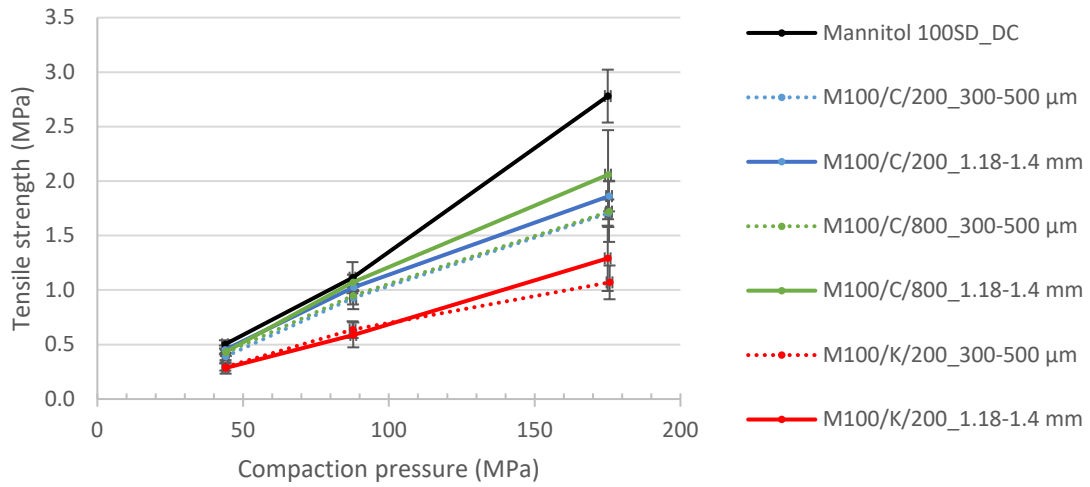
Figure 4.8 Tabletability of mannitol 100 SD (M100) granules and primary powder (DC).
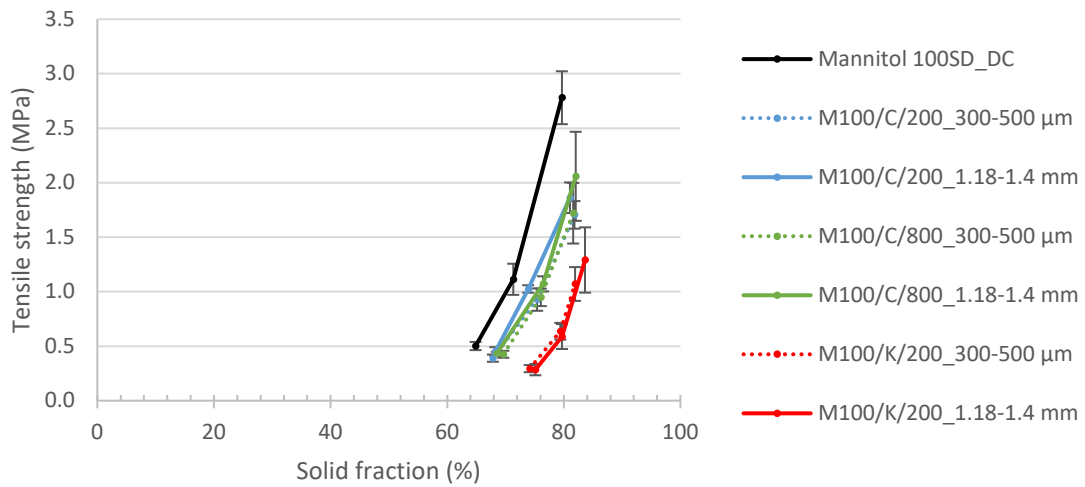
Figure 4.9 Compactability of mannitol 100 SD (M100) granules and primary powder (DC).

All variants of granulated mannitol 100 SD show a loss in tabletability and compactability compared with the primary powder. However, the granulation conditions have had varying degrees of impact. For the spray dried mannitol, the use of kneading zones resulted in a bigger drop in tablet tensile strength than for conveying elements, regardless of screw speed. At 44 MPa compaction pressure, the M100/K/200 lost around 43% of tablet tensile strength compared with the mannitol 100 SD primary powder, while granules manufactured using only conveying elements showed about 22% reduction at 200 RPM screw speed.

As shown by Figure 4.9, this significant change in tabletability is not explained by a difference in tablet porosity, since there is a large difference in tablet tensile strength for the different input materials for a given tablet solid fraction. There is also no clear difference in the tabletability and compressibility profiles of the 300-500 µm and 1.18-1.40 mm granules for mannitol 100 SD. The tabletability profiles of microcrystalline cellulose and mannitol 100 SD granules show that microcrystalline cellulose is more prone to reduction in tabletability after granulation. That could be explained by the fact that microcrystalline cellulose powder has a lower yield pressure and higher plasticity than mannitol 100 SD as depicted in Table 4.2. The applied shear stress during granulation due to the screw elements (predominantly kneading but also conveying) leads to densification of the materials inside the granulation barrel. The lower the yield pressure of the material the more densification it experiences during granulation. Hence, microcrystalline cellulose is more deformable than mannitol 100 SD, which resulted in denser and stronger MCC granules as seen in Figure 4.5. In the subsequent compression step, the dense MCC granules (which have lower deformability compared with the mannitol 100SD granules) then produced weaker tablets (which was seen as a greater reduction in tabletability). This relationship between the granule density and its deformability has been reported by several researchers [15,118,193]. The results are in agreement with another study in which it was found that the granule strength is the profound factor causing the deterioration of the tabletability of microcrystalline cellulose after dry granulation [148].

4.5.3.3 Mannitol 160 C

The tabletability and compactability of mannitol 160 C are presented in Figure 4.10 and Figure 4.11. It was found that granules manufactured from mannitol 160 C did not experience deterioration of tabletability following granulation, as observed with microcrystalline cellulose

and mannitol 100 SD. Mannitol 160 C granules produced using kneading elements (M160/K/200) showed an improvement in the tabletability compared with the primary powder and granules produced using only conveying elements. The granules produced using only conveying elements showed similar tabletability to the primary powder but allowed the use of increased compaction pressures without showing any signs of capping. On the other hand, the mannitol 160 C powder produced capped and laminated tablets when higher compression pressure (175 MPa) was used. It has been reported that several factors could lead to lamination and capping of tablets [194]. In the case of mannitol 160 C, the brittle nature of the crystalline mannitol, and the in-die elastic recovery could be the causes of the capping and lamination.
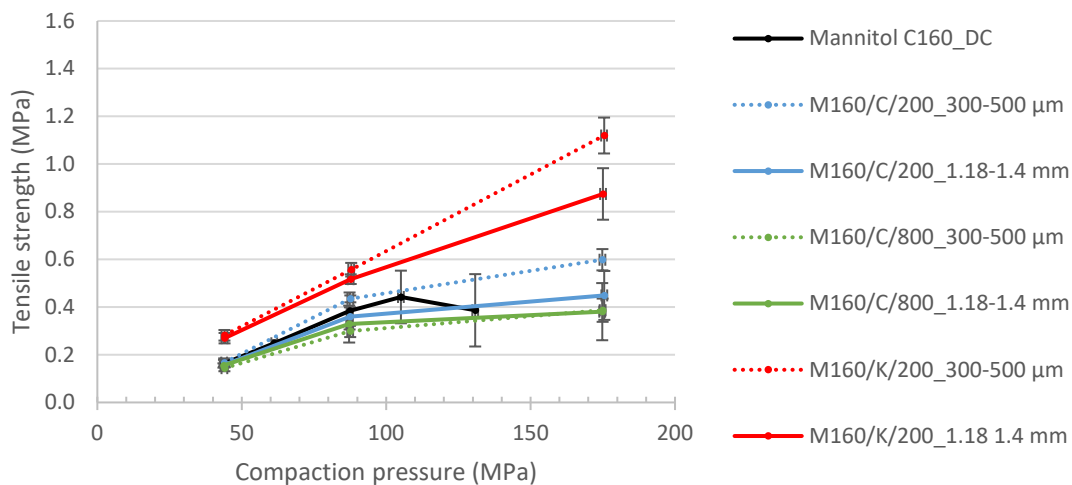
Figure 4.10 Tabletability of mannitol 160 C (M160) granules and primary powder (DC).
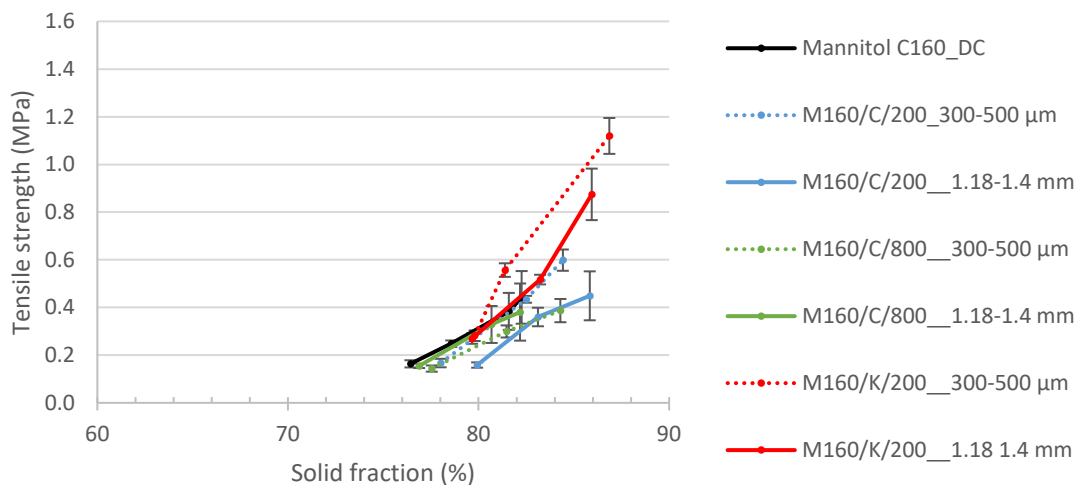
Figure 4.11 Compactability of mannitol 160 C (M160) granules and primary powder (DC).

It is evident that the granule size slightly affects the tabletability of mannitol 160 C granules - smaller granules produced stronger tablets. From the compactibility plot (Figure 4.11), it could be seen that this observation is not due to lower tablet solid fraction/porosity. Interestingly, granules from M160/K/200 were significantly denser than granules from M160/C/200 and M160/C/800 (see Figure 4.5). However, as discussed above, there was an improvement in the tabletability and compactability of M160/K/200 compared with M160/C/200 and M160/C/800. The macroscopic images of the granules from mannitol 160 C as well as mannitol 160 C powder are shown in Figure 4.12. It is noticed that the granules made using only conveying elements had structural similarities with the mannitol powder - the rectangularly shaped crystals are a common feature. This suggests that these granules are built by a fairly simple agglomeration of individual crystals which remain intact and largely unchanged by the agglomeration process. However, there is no evidence of a clear crystal shape for the M160/K/200 granules, which suggests that when kneading elements are used, there is a much more significant physical change for this material.
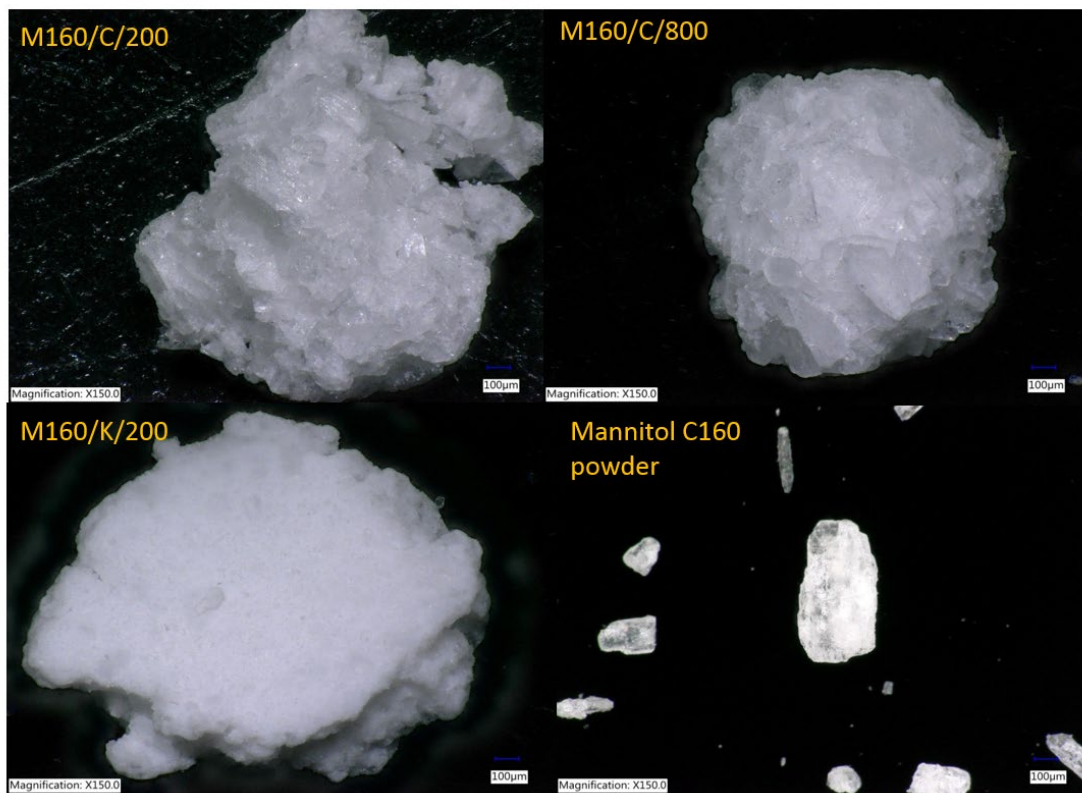
Figure 4.12 Macroscopic images of mannitol 160 C (M160) powder and granules produced using different twin-screw granulation configurations.

The SEM images shown in Figure 4.13 confirm the structural differences between the samples observed by X-ray computed tomography (Figure 4.4) and the optical microscope (Figure 4.12). In particular, the mannitol 160 C shows quite a significant transformation with increasing granulation intensity. The individual crystals for the M160/K/200 granules are much smaller compared with both M160/C/200 and M160/C/800. M160/K/200 granules have many tiny crystals or crystallites with an average size of around 1 µm (measured using Image J). Such crystallites are not found in this material at any of the other processing conditions. Based on this finding, we can infer that the use of kneading elements led to a higher degree of granulation liquid distribution, dissolving a significant proportion of the crystals in the mannitol 160 C primary powder. Following granulation and upon drying, the dissolved mannitol then recrystallises to smaller crystals and crystallites which gives the granules a much higher surface area than the primary powder, creating more bonding area and leading to better tabletability. To the best of the author's knowledge, this phenomenon as a mechanism for improved tabletability

78

has not been previously reported, and it can be easily missed since the crystallites adhere to larger particles and would therefore not be detected using conventional particle or granule size analysis techniques. This finding is in agreement with a recent study [195] in which it was reported that coating paracetamol (which has low compactability) with a sub-micron-sized binder could double the tensile strength of formulation made of the raw paracetamol and binder [195]. The fragmentation and breakage of the mannitol 160 C crystals to smaller crystals due to its brittle nature by the kneading elements is another possibility for the reduction in crystal size that cannot be ruled out. However, it is most likely that the dissolution and re-crystallisation to be the main mechanism for the reduction in the particle size. On the other hand, even though the M100/K/200 has some small crystals but it did experience a reduction in the tabletability which is likely to be due to the plasticity of the mannitol 100 SD. Within the ranges and materials studied, it is most likely that the negative effect of decreasing porosity due to granulation of M100 outweighs the benefits of the reduced particle size by dissolution/crystallisation.
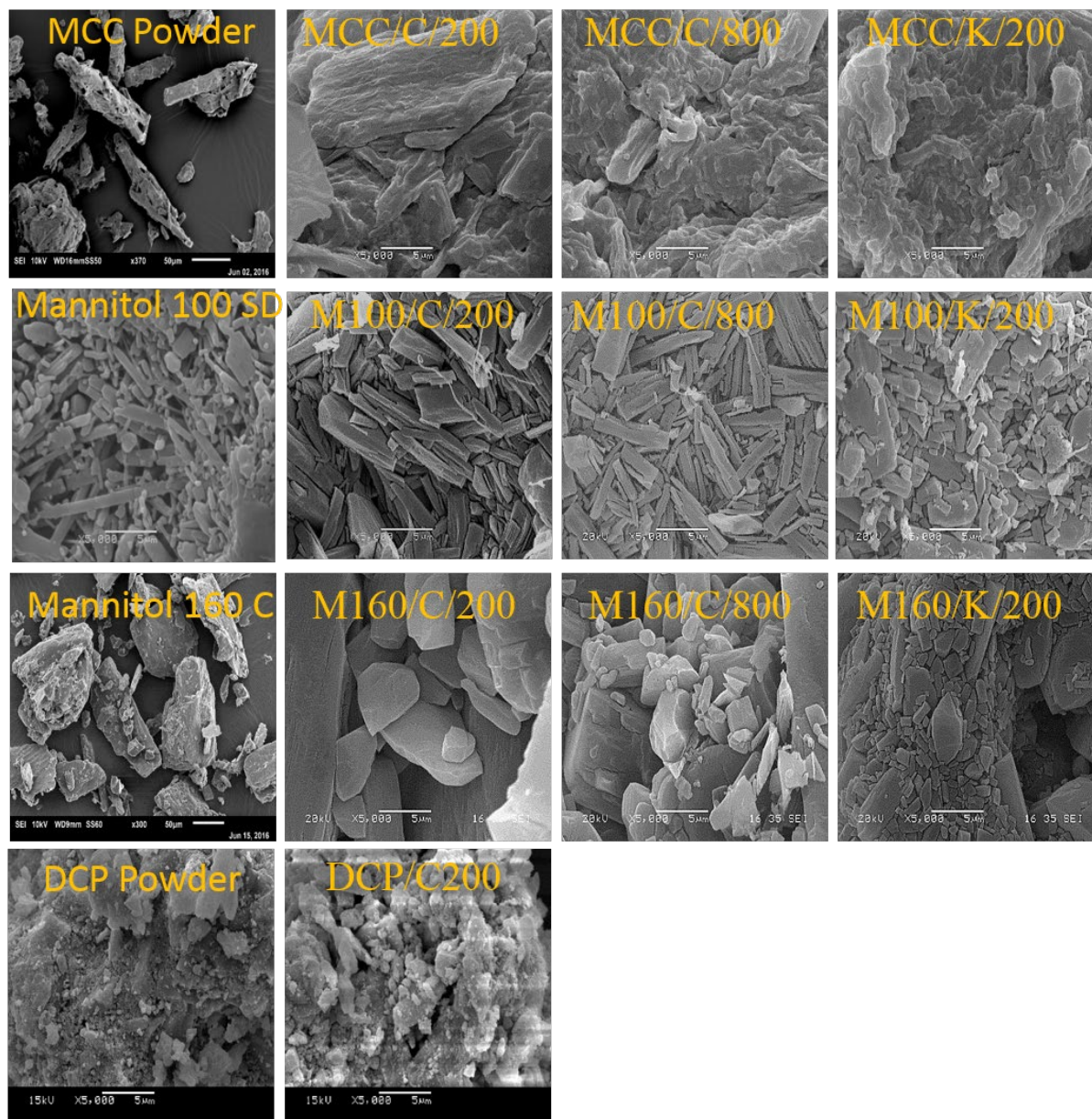
Figure 4.13 Scanning electron microscopy images of granules from each material and processing condition at 5000x magnification.

4.5.3.4 Dicalcium phosphate

DCP was granulated as described in Table 4.1. Since DCP is a relatively hard material, insoluble in the chosen liquid binder (water), it was not possible to granulate DCP using kneading elements at the required screw speeds. The non-deformable and insoluble nature of the powder particles means that the screw has a tendency to jam when a screw configuration including

kneading elements is used. Due to processing issues such as this, DCP, granules were only successfully produced using conveying elements at a screw speed of 200 RPM (DCP/C/200), and even then only in the size class 300-500 µm. Adding a binder could have allowed the better process of this material, but the addition of a second formulation component would have compromised the ability to draw sound conclusions from the results.

In a similar manner to mannitol 160 C granules, the DCP granules did not show a reduction in their tabletability compared with the direct compression powder. The tabletability and the compactibility of the DCP/C/200 are similar to that of the DCP powder, as can be seen in Figure 4.14 and Figure 4.15, respectively. The unchanged tabletability behaviour of the DCP granules is explained based on the non-deformable and insoluble nature of the powder particles – so no significant change in particle size (Figure 4.13) occurs. This is supported by the SEM images presented in Figure 4.13, which show no discernible difference in granule morphology between the primary powder and the material after passing through the wet granulator.
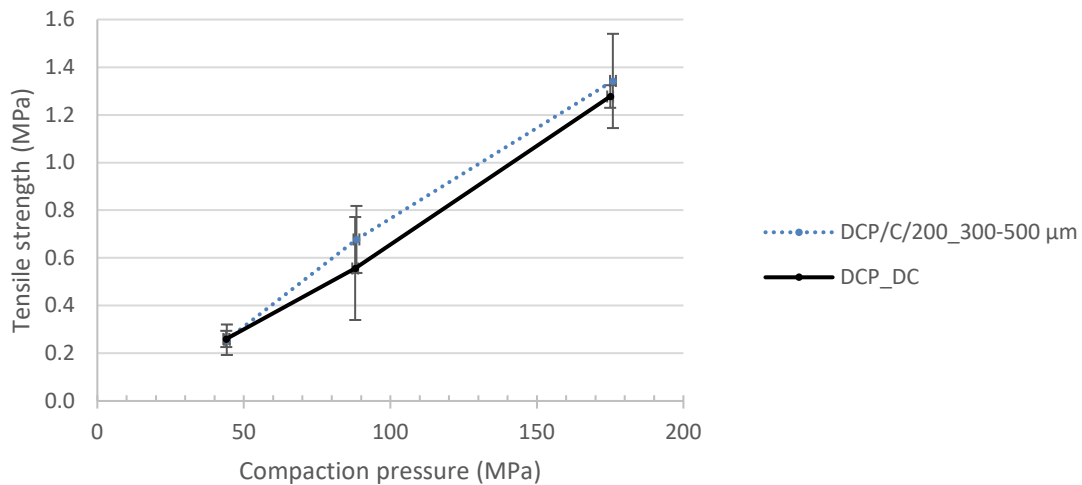
Figure 4.14 Tabletability of DCP granules and primary powder (DC).
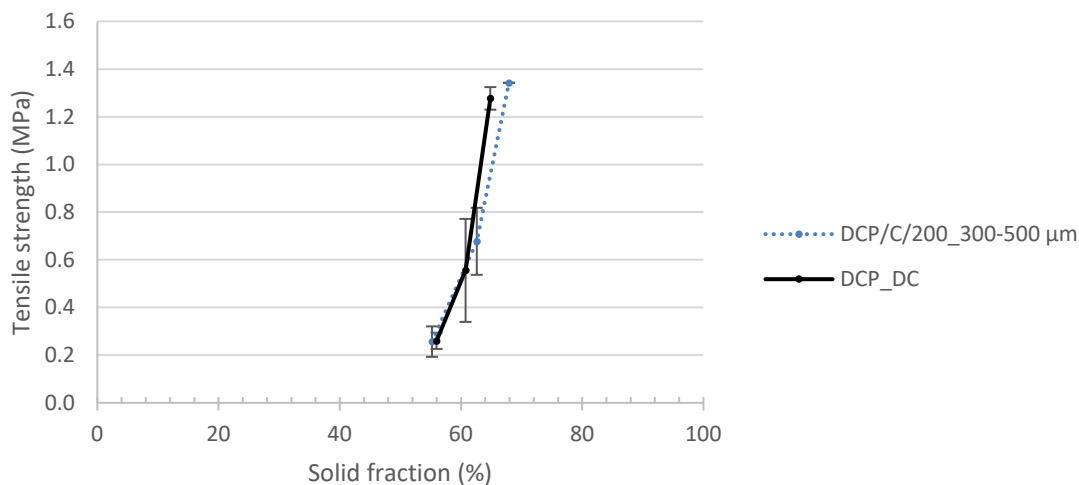
Figure 4.15 Compactability of DCP granules and primary powder (DC).

4.5.4 Development of a tabletability regime map based on material properties

Both MCC and mannitol 100 SD granules become less porous and stronger as the level of stress during granulation is increased, resulting in weaker tablets. The tensile strength of microcrystalline cellulose and mannitol 100 SD (MCC/K/200 and M100/K/200) tablets reduced by about 75% and 43% respectively at 44 MPa compaction pressure. Granule size did not strongly affect the tabletability and compressibility of these materials. MCC and mannitol 100 SD (which have high plasticity and low yield pressure) are prone to reduction in the tabletability and compactability after granulation compared with direct compression of the primary powder. The results suggest that materials that compress by plastic deformation such as microcrystalline cellulose and mannitol 100 SD would also consolidate and densify to a greater extent during granulation. This pre-compaction of the material then means that the granules lose their ability to form a tablet as strong as direct compression of the primary powder. This phenomenon has been reported previously by several workers [13].

In contrast, brittle materials with high elasticity and yield pressure such as mannitol 160 C and DCP maintained or improved their tabletability after granulation. The M160/K/200 experienced an improvement in tensile strength following granulation of around 73% when compressed at the same pressure (44 MPa).

82

The tabletability of mannitol 160 C granules were superior to their respective primary powders and also showed superior resistance to capping and lamination at higher compaction pressures (>150 MPa). In the case of M160/K/200, an increase in tabletability was observed despite a reduction in granule porosity - size reduction of the powder crystals is believed to be the mechanism for this improvement and was only detected upon examination of SEM images of the granules.

To visualise these different trends, effects and dependencies, a regime map showing the potential for improved or reduced tablet tensile strength following granulation, with materials classified by the yield pressure of the primary powder was developed (Figure 4.16). Calculation of the yield pressure of the primary powder not only gives a strong indication of the tabletability performance of the powder itself, but also a quantitative indication of how that powder is likely to granulate, and qualitative information about the likely most favourable granulation conditions and how the resultant granules are likely to compact. This finding, and its applicability across a wide range of pharmaceutically relevant materials is quite significant and provides a useful increase in predictive capability for the field.
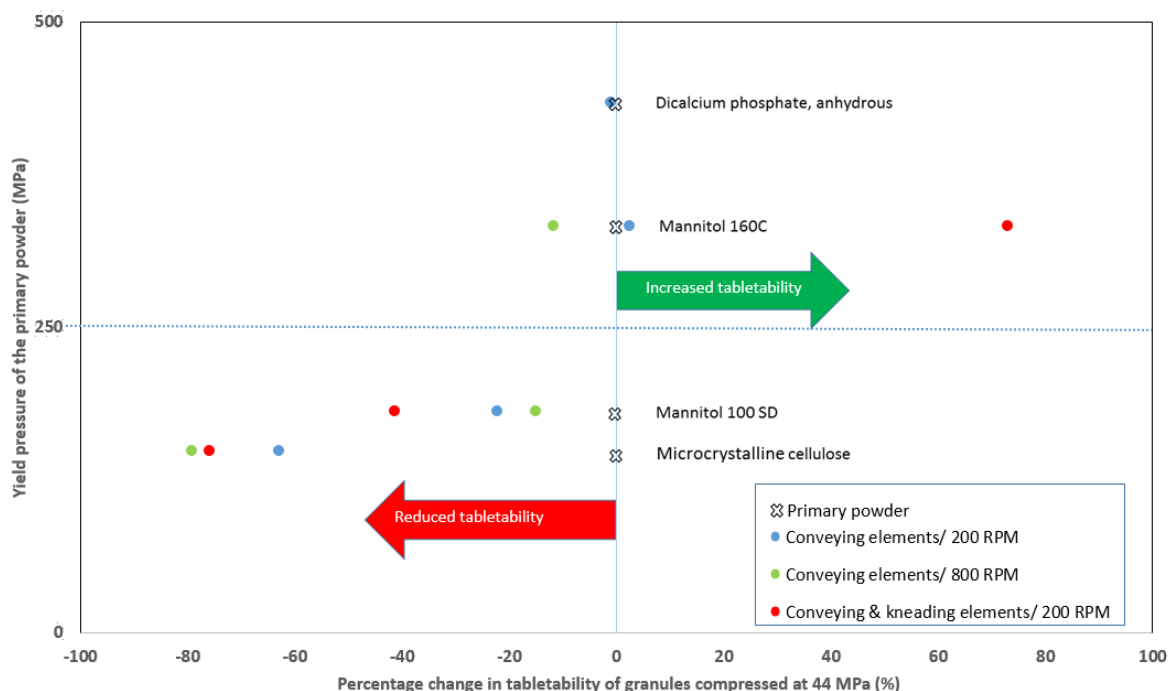
Figure 4.16 Tabletability regime map based on yield pressure of primary powder and relative change in tablet tensile strength at 44 MPa compaction pressure.

Furthermore, if the yield pressure of the intermediate granules is calculated, the resultant values can be used to quantitatively predict the resultant tablet tensile strength (Figure 4.17). Powder or granule yield pressures above 300 MPa can be seen to result in universally weak tablets. Powders or granules around 225 MPa yield mid-range tablet tensile strengths, while those around 150 MPa result in very strong compacts. The equation of best fit is given by equation 4.1.

$$\sigma = 10^{(35.25-27.35[\log_{10} Y_p]+5.206[\log_{10} Y_p]^2)} \qquad \text{Eq 4.1}$$

More supporting evidence for the relationship between the mechanical properties of the powder and the granules and their tablet tensile strength is provided in Appendix C.
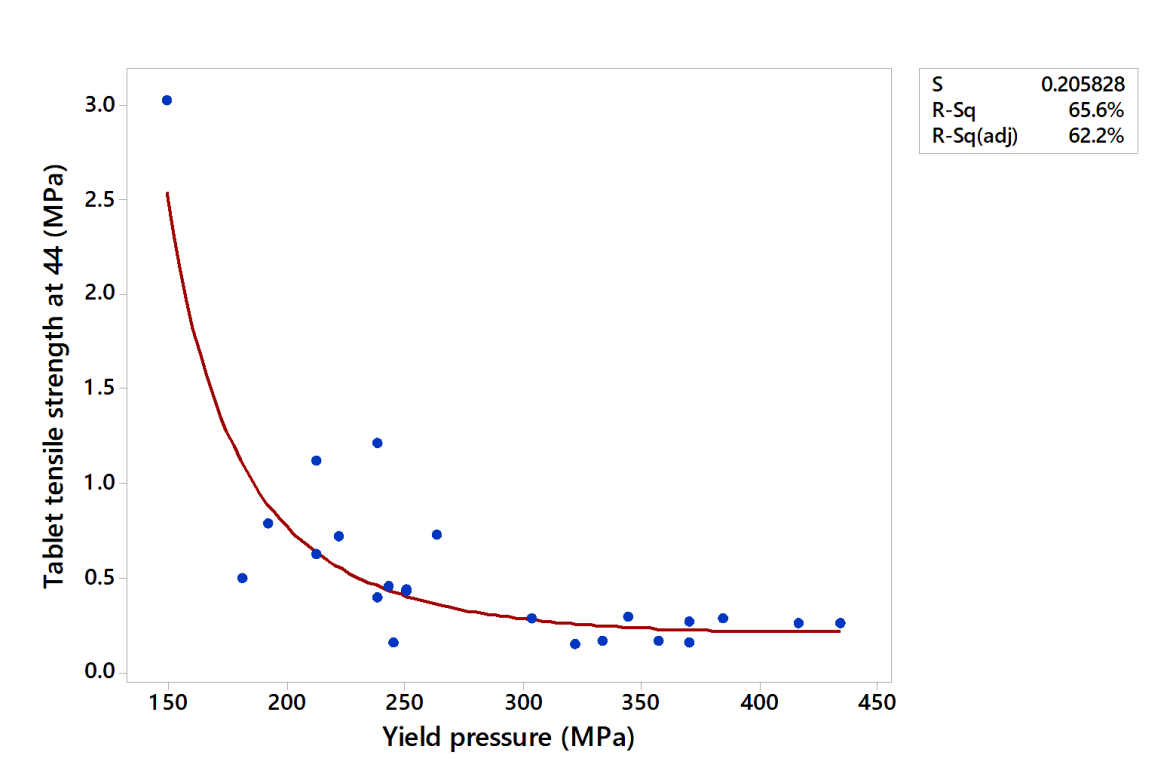
Figure 4.17 Yield pressure of compacted materials (primary powder and granules) vs tensile strength of tablets made from those materials at 44 MPa.

4.6   Conclusion

In conclusion, it was found that the analysis of the mechanical properties which are presented in Table 4.2 shows that the plasticity of the primary powders is ranked as microcrystalline cellulose (highest) > mannitol 100SD >Mannitol 160 C > DCP (lowest). Both microcrystalline cellulose and mannitol M100 granules experienced a reduction in the tabletability compared with the primary powder. Whereas the mannitol 160 C and DCP did not experience any reduction in tabletability which is related to the plastic behaviour of the MCC and the Mannitol 100 SD which deform plastically during granulation. It was found that the decrease in the tabletability of the plastically deforming materials (MCC, Mannitol 100SD) is caused by an increase in the granules density and is independent of the granule size as could be seen in figures 4.5-9. Whereas the DCP and mannitol 160 C which have higher yield pressure as presented in Table 4.2 did not experience a reduction in tabletability after granulation. On the contrary, the tabletability of mannitol 160 C improved due to the reduction of the primary particle size – which could be primarily due to dissolution and subsequent post-granulation crystallisation. The essentially solid crystals of mannitol 160 C cannot suffer from additional densification so there is no downside of wet granulating the crystalline grade of mannitol. The unchanged tabletability behaviour of the DCP granules is explained based on the non-deformable and insoluble nature of the powder particles – so no significant change in particle size or porosity occurs.

Chapter 5   The Role of Bonding Surface Area and Moisture Content on Tablet Strength

5.1   Summary

A novel approach/model to predict the tabletability of powders and granules is proposed. The approach provides a holistic and mechanistic understanding of the origins of tablet tensile strength. It was found that the specific surface area (SSA) available for bonding and the moisture content within the compressed materials (granules and powders) are together capable of explaining the tabletability of mechanically different materials.

5.2   Introduction

The physics of interparticle interactions are well documented [44,177]. However, a clear application of this physics to powder compaction has been limited to date, particularly in the pharmaceutical industry, which still relies heavily on compaction testing and trial and error methods to determine the best powder properties for compaction.

Two factors are primarily responsible for the tabletability of powders: the dominating bond mechanism, and the surface area over which these bonds are active [39,50] (i.e. the number and strength of bonds). The number and nature of contacts involved between particles are impossible to measure in-situ using current techniques. Add to that the complex nature of material rearrangement and deformation across the vast array of different materials. Instead, more indirect, secondary factors such as particle size, surface texture and the volume reduction behaviour have been studied in detail [50,57].

Solid bridges, the attraction between particles and mechanical interlocking, have been generally regarded as the dominant mechanisms for tablet formation [45]. Nonetheless, the presence of liquid/moisture in the compressed materials or in the tablets (absorbed during storage) may have a significant effect on the tablet strength [73,74,178]. However, the effect of moisture on the tabletability as a discrete mechanism has been overlooked. This study investigated the overall

contribution of the SSA and the commonly accepted bonding mechanisms as well as the effect of moisture on tablet strength.

5.3   Materials

In this project, two materials were selected based on their significantly different mechanical properties: microcrystalline cellulose (MCC) and mannitol (crystalline rather than spray-dried grades). MCC is a soft material which deforms plastically upon compression. In contrast, mannitol is more brittle and has a higher yield pressure than MCC. Four grades of MCC were selected covering a range of different powder particle sizes. Avicel PH-105 (mean diameter 20 µm), Avicel PH-101 (mean diameter 50 µm), Avicel PH-102 (mean diameter 100 µm) and Avicel PH-200 (mean diameter 180 µm) were supplied from FMC Corporation, Ireland. Three grades of crystalline mannitol were selected: mannitol PEARLITOL® 160 C (mean diameter 160 µm), PEARLITOL® 50 C (mean diameter 50 µm) and PEARLITOL® 25 C (mean diameter 25 µm) - all supplied from Roquette, France. Different primary particle sizes were used to cover a wide range of sceptic surface areas.

5.4   Methods

5.4.1   Granulation and granule analysis

5.4.1.1 Granulation of the primary powder

The powders were granulated using a TSG as described in section 3.2.3. A variety of screw configurations with an increasing number of kneading discs were used to apply different levels of stress during the granulation process [11,198,199]. Three screw configurations were used in this study: conveying elements only (set 1), conveying elements with 16 kneading discs (set 2) and conveying elements with 32 kneading discs (set 3) as presented in Figure 5.1. The granulation parameters for each experiment are detailed in Table 5.1. The optimum liquid-to-solid ratio (L/S) for each material was used (determined by prior experiment) enabling the processing of the materials using the three screw configurations presented in Figure 5.1. The MCC and mannitol grades were granulated with a liquid-to-solid ratio of 1.14, and 0.10 respectively. A screw speed of 200 RPM was used for all runs. And the feed rate was 1kg/h.

(1)	SPCE	LPCE	SPCE

(2)	SPCE	LPCE	SPCE	(K 60°)	SPCE

(3)	SPCE	LPCE	SPCE	(K 60°)	SPCE	(K 60°)	SPCE
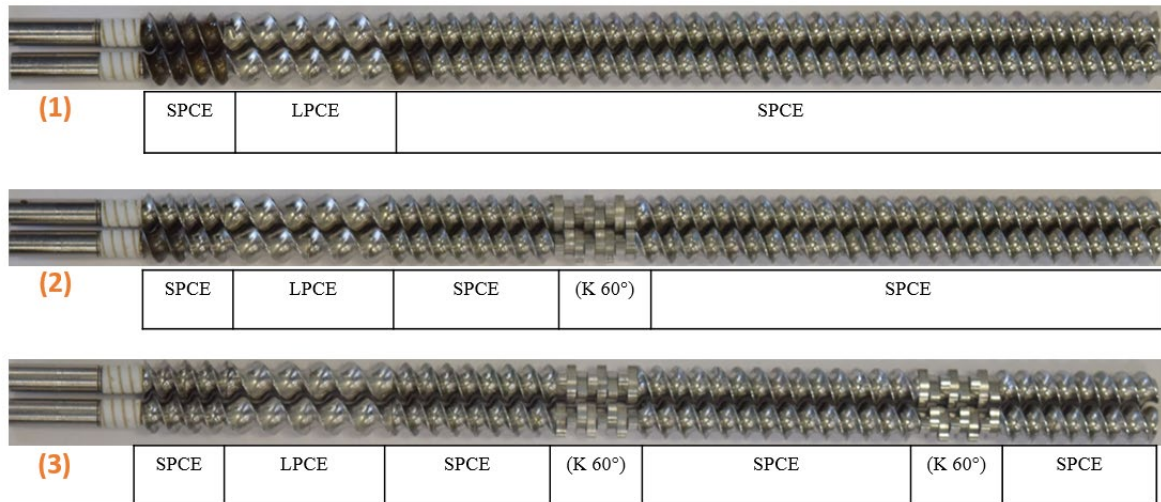
Figure 5.1 The screws configured with conveying elements only. (2) The screws configured with conveying elements and 16 kneading discs. (3) The screws configured with conveying elements and 32 kneading discs. LPCE: Long pitch conveying element (Length=2 x diameter), SPCE: Short pitch conveying element (length = diameter) and K 60° staggering angle: Kneading disc at 60° pitch (length=diameter/4).

88

Table 5.1 Granulation conditions

Abbreviation	Material	Screw configuration
101/C	Microcrystalline cellulose (Avicel PH-101)	Conveying elements
101/K16		Conveying elements+16 kneading discs
101/K32		Conveying elements+32 kneading discs
102/C	Microcrystalline cellulose (Avicel PH-102)	Conveying elements
102/K16		Conveying elements+16 kneading discs
102/K32		Conveying elements+32 kneading discs
105/C	Microcrystalline cellulose (Avicel PH-105)	Conveying elements
105/K16		Conveying elements+16 kneading discs
105/K32		Conveying elements+32 kneading discs
200/C	Microcrystalline cellulose (Avicel PH-200)	Conveying elements
200/K16		Conveying elements+16 kneading discs
200/K32		Conveying elements+32 kneading discs
25/C	Mannitol (PEARLITOL® 25 C)	Conveying elements
25/16K		Conveying elements+16 kneading discs
25/32K		Conveying elements+32 kneading discs
50/C	Mannitol (PEARLITOL® 50 C)	Conveying elements
50/16K		Conveying elements+16 kneading discs
50/32K		Conveying elements+32 kneading discs
160/C	Mannitol (PEARLITOL® 160 C)	Conveying elements
160/K16		Conveying elements+16 kneading discs
160/K32		Conveying elements+32 kneading discs

5.4.1.2 Granule sieving

The granules were collected on flat trays and left to dry at room conditions for 72 hours [5,82]. A sieve shaker (AS200, Retsch GmbH, Germany) was used to sieve the dry granules into two size classes: 300-500 µm and 1.18-1.40 mm.

5.4.2   Specific surface area

The specific surface area of the primary powders and granules was measured by nitrogen adsorption as described in section 3.2.6.

5.4.3   Moisture content analysis

The moisture content of the powder/granules was measured using a loss-on-drying analyser (MA37, Sartorius, Germany). The device was set to heat to 80°C for 45 minutes.

5.4.4   Tablet compression and characterisation

5.4.4.1 Tablet compression

The granulated materials were compressed as described in section 3.2.7.1. Two size classes of granules (300-500 µm and 1.18-1.40 mm) were compressed to a force of 5 kN. In the pharmaceutical industry, it is preferred to produce tablets which are strong but still week enough to break apart in the human body [179]. Generally, the optimum tablet strength is between 1.7-2 MPa [179]. Therefore, 44 MPa compression pressure was used which produce tablet in the range of 0.12 to 3.2 MPa. Before each compaction, the die and the punch were lubricated with a suspension of magnesium stearate in ethanol (1% w/w) and were dried using a source of hot air.

5.4.4.2 Tablet tensile strength

The tensile strength of tablets was calculated as described in section 3.2.7.2.

5.4.4.3 Work of compaction

The subtraction of the elastic work from the total work of compaction provides the plastic work. The method to calculate the plastic work is provided in section 3.2.1.2.

5.5   Results and discussion

5.5.1   Analysis of the effect of specific surface area

5.5.1.1 MCC

The SSA of the primary MCC powder and the granulated MCC are presented in Figure 5.2. It can be seen from Figure 5.5 that all the granulated MCC grades had a reduction in the SSA compared with the primary materials (none granulated). The usage of kneading elements (Figure 5.1, 2 and 3) to granulate the MCC grades resulted in a significant reduction in the specific surface area compared with granules made using only conveying elements and the ungranulated powder (see Table 5.2). There was little difference (decrease) in granule SSA for screw configurations containing 16 and 32 kneading elements, suggesting that the use of 16 kneading elements was sufficient to reach a high degree of deformation at the granulation conditions (i.e. L/S ratio, feed rate and screw speed). Also the granule size shows no apparent effect on SSA of the granules. Both small and big granules have similar SSA
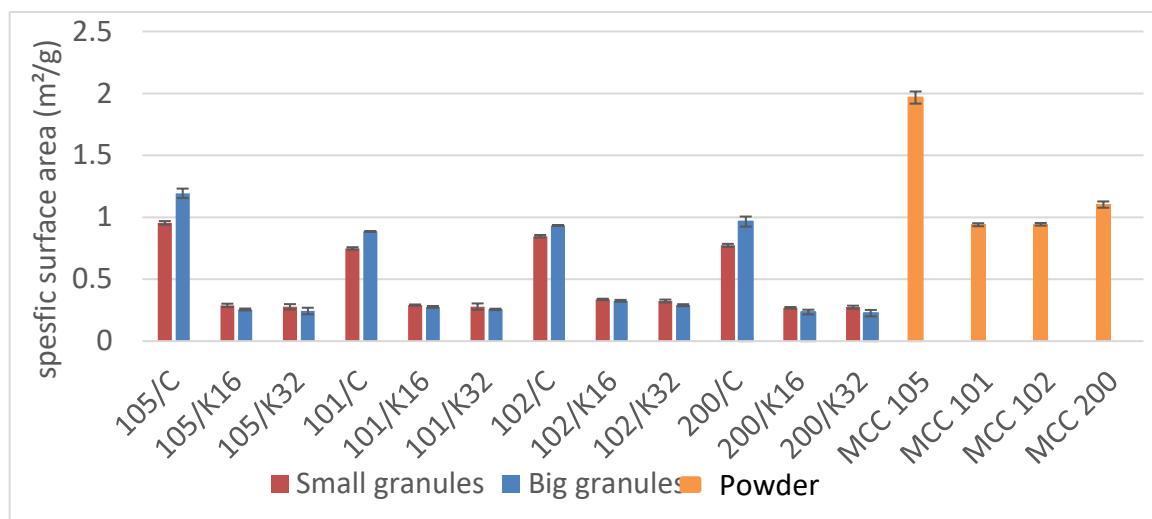
Figure 5.2 Specific surface area of MCC granules and powders. The small granules are 300-500 µm in size and the big granules are 1.18-1.4 mm.

5.5.1.2 Mannitol

The SSA of the primary mannitol powder and the granulated mannitol grades are presented in Figure 5.3. It could be seen that the smaller the size of mannitol powder the higher the SSA. For mannitol, the effect of granulation can be quite different compared with MCC. The use of

kneading elements in twin screw granulation led to an increase in the SSA of the granulated mannitol compared with granules made using only conveying elements as presented in Figure 5.3 and Table 5.2. Similar to the MCC granules, there was no effect of the mannitol granules size on the SSA.
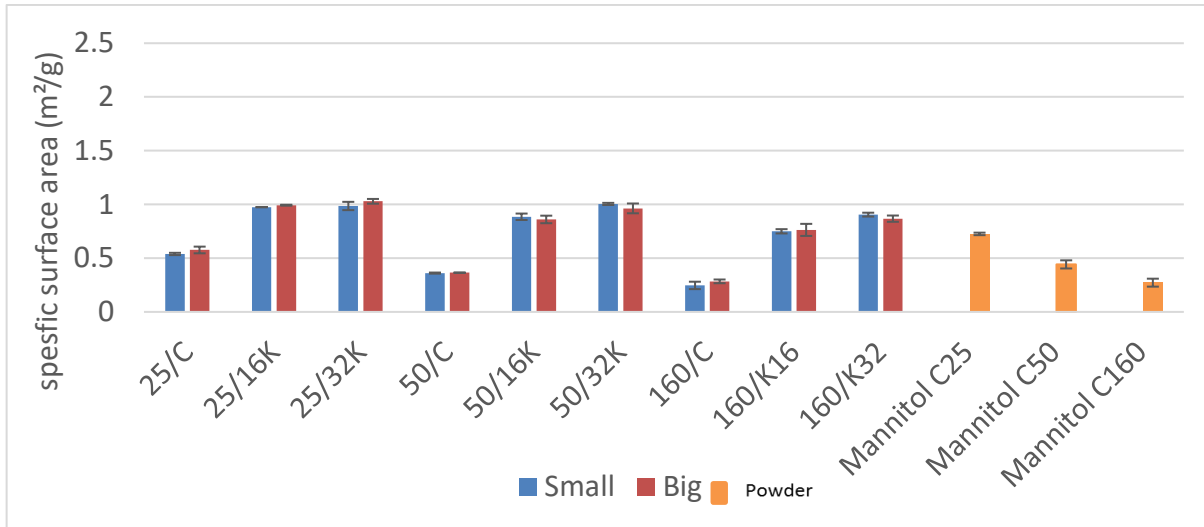
Figure 5.3 Specific surface area of mannitol granules and powders. The small granules are 300-500 μm in size, and the big granules are 1.18-1.4 mm.

Table 5.2 Granules specific surface area (m²/g) and moisture content (%w/w). (C) refers to convening elements only, (K) Refers to the use of conveying element and kneading elements, 16 refers to 16 kneading discs plus conveying elements, and K32 refers to 32 kneading discs plus conveying elements.

Material	Material grade	Abbreviation	Moisture content (% w/w)	Specific surface area (m²/g)	Specific surface area * moisture content (%w/w)	Tablet tensile strength @ 44(MPa)
Powder	MCC 101(D_{50}=50 μm)	MCC 101	4.65	0.94	4.37	2.47
	MCC 102(D_{50}=100 μm)	MCC 102	4.75	0.94	4.48	2.48
	MCC 105 (D_{50}=20 μm)	MCC 105	3.68	1.97	7.24	3.22
	MCC 200 (D_{50}=180 μm)	MCC 200	4.04	1.10	4.45	2.45
Granule	MCC 101(1.18-1.4 mm)	101/C/B	5.30	0.89	4.69	1.63
		101/K16/B	5.90	0.28	1.63	0.68
		101/K32/B	5.39	0.26	1.38	0.67
	MCC 102 (1.18-1.4 mm)	102/C/B	5.20	0.93	4.86	1.58
		102/K16/B	5.65	0.33	1.84	0.81
		102/K32/B	5.47	0.29	1.59	0.69
	MCC 105 (1.18-1.4 mm)	105/C/B	5.54	1.19	6.61	1.73
		105/K16/B	5.87	0.26	1.50	0.76
		105/K32/B	5.94	0.24	1.44	0.72
	MCC 200 (1.18-1.4 mm)	200/C/B	5.01	0.97	4.84	1.90
		200/K16/B	5.42	0.23	1.27	0.69

Material	Material grade	Abbreviation	Moisture content (% w/w)	Specific surface area (m²/g)	Specific surface area * moisture content (%w/w)	Tablet tensile strength @ 44(MPa)
Granule	MCC 200 (1.18-1.4 mm)	200/K32/B	5.34	0.23	1.21	0.68
	MCC 101 (300-500 μm)	101/C/S	5.70	0.75	4.27	1.30
		101/K16/S	5.98	0.29	1.74	0.70
		101/K32/S	5.89	0.28	1.64	0.73
	MCC 102 (300-500 μm)	102/C/S	5.43	0.85	4.60	1.22
		102/K16/S	5.48	0.34	1.84	0.74
		102/K32/S	5.93	0.32	1.92	0.67
	MCC 105 (300-500 μm)	105/C/S	5.43	0.95	5.19	1.51
		105/K16/S	5.63	0.29	1.63	0.76
		105/K32/S	6.19	0.28	1.72	0.82
	MCC 200 (300-500 μm)	200/C/S	5.55	0.77	4.29	1.49
		200/K16/S	5.84	0.27	1.57	0.70
		200/K32/S	5.94	0.27	1.63	0.70
Powder	Mannitol 25C (D_{50}=25 μm)	M25	0.16	0.73	0.12	0.15
	Mannitol 50C (D_{50}=50 μm)	M50	0.16	0.44	0.07	0.19
	Mannitol 160C (D_{50}=160 μm)	M160	0.27	0.27	0.07	0.16
Granule	Mannitol 25C (1.18-1.4 mm)	M25/C/B	0.21	0.58	0.12	0.14
		M25/16K/B	0.28	0.99	0.27	0.22

Material	Material grade	Abbreviation	Moisture content (% w/w)	Specific surface area (m²/g)	Specific surface area * moisture content (%w/w)	Tablet tensile strength @ 44(MPa)
Granule	Mannitol 25C (1.18-1.4 mm)	M25/32K/B	0.11	1.03	0.11	0.20
	Mannitol 50C (1.18-1.4 mm)	M50/C/B	0.18	0.36	0.06	0.12
		M50/16K/B	0.23	0.86	0.20	0.18
		M50/32K/B	0.17	0.96	0.16	0.17
	Mannitol 160C (1.18-1.4 mm)	M160/C/B	0.19	0.28	0.05	0.13
		M160/K16/B	0.31	0.76	0.24	0.18
		M160/K32/B	0.15	0.87	0.13	0.17
	Mannitol 25C (300-500 µm)	M25/C/S	0.26	0.54	0.14	0.15
		M25/16K/S	0.23	0.97	0.22	0.21
		M25/32K/S	0.20	0.99	0.19	0.22
	Mannitol 50C (300-500 µm)	M50/C/S	0.33	0.36	0.12	0.12
		M50/16K/S	0.21	0.89	0.19	0.19
		M50/32K/S	0.32	1.00	0.32	0.22
	Mannitol 160C (300-500 µm)	M160/C/S	0.21	0.25	0.05	0.11
		M160/K16/S	0.20	0.75	0.15	0.19
		M160/K32/S	0.44	0.91	0.40	0.23

5.5.2 The effect of specific surface area on tablet strength

Figure 5.4 presents the SSA of granulated MCC and mannitol versus the tablet tensile strength at 44 MPa. A reduction in the SSA of MCC grades for the small and the big granules due to granulation correlates with a reduction in the tabletability as seen in Figure 5.4 and Table 5.2. A similar observation has been reported previously by several other researchers. Osei-Yeboah et al., Herting and Kleinebudde, and Badawy et al. all reported that the tensile strength of tablets made from MCC granules is proportional to granule SSA [128,130,135].

As observed for MCC, the increase in the SSA correlates with an increase in the tensile strength of tablets manufactured from them (Figure 5.4 and Table 5.2), although the absolute values of the tensile strength are quite low. A similar observation was reported by Westermarck et al., who found that the wet granulation of mannitol using an aqueous polymeric binder solution in a high shear mixer resulted in a significant improvement in the SSA of the granules compared with the powder, which consequently led to a marked improvement in the breaking force of tablets produced from granules compared with tablets made from ungranulated powder [66]. Additionally, the improvement in the tabletability after granulation using kneading element is in agreement with the results presented in section 4.5.3.3 [82]. The tensile strength of tablets manufactured from granulated materials (at a given compaction pressure 44 MPa) is a linear function of the SSA available. The SSA is proportional to the area available for van der Waals type bonding, whereby higher SSA results in higher tablet tensile strength due to higher bonding area utilisation.

The proposed mechanism for this increase in true contact area is that the more porous and fragile nature of materials having higher specific surface area means that they are more likely to have a greater number of contact asperities which deform easily under an applied load, thereby increasing the fraction of surfaces which find themselves in sufficiently close proximity for attractive van der Waals type bonding to occur, ~1.65 to 4.0 Angstroms [46].
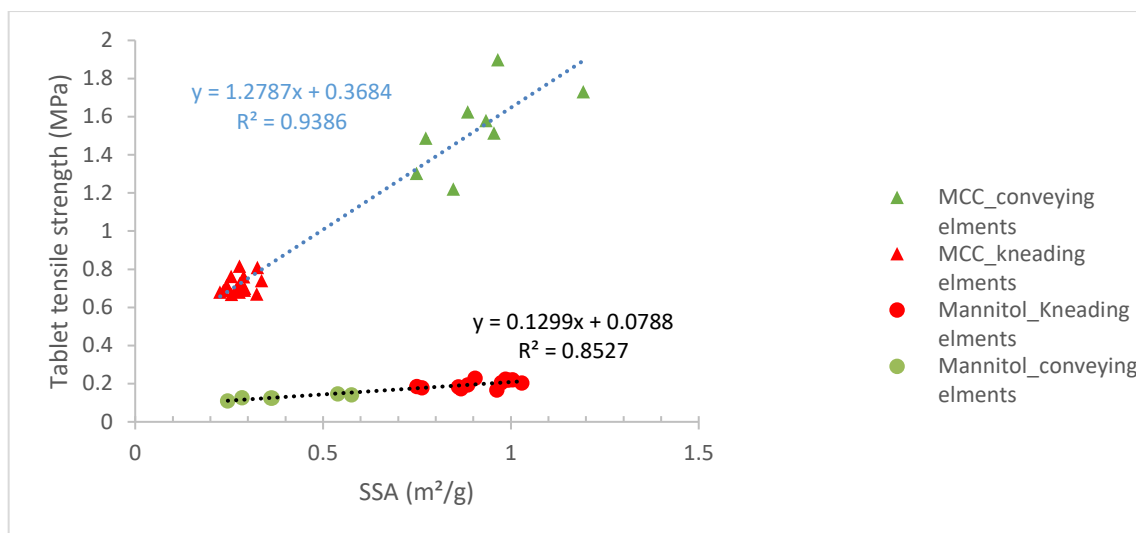
Figure 5.4 Specific surface area (SSA) vs the tablet tensile strength of tablets made of granules at 44 MPa.

However, from Figure 5.4 it is also evident that there is a significant difference in tablet tensile strength when comparing across material types (i.e. comparing mannitol with MCC), even when the surface area available for bonding is identical. This led to the conclusion that while SSA is a useful tensile strength predictor, there must be bonding mechanism which can explain why MCC and mannitol produce significantly different tablet properties when the surface area of the input material is the same.

5.5.3 Analysis of material moisture content

Based on the accepted physics of liquid-mediated bonding of solid surfaces (2.6 and section 2.7.2) and the wealth of reports in the literature about a correlation between moisture content and tablet tensile strength (2.8.2.4) a hypothesis was made. It was hypothesised that the difference in the tabletability between the MCC and mannitol that have similar SSA is due to the difference in their moisture content. This would not be unreasonable as MCC is widely known for being hygroscopic, while mannitol does not absorb much water unless relative humidity is high (approximately above 75 relative humidity) [180].

5.5.3.1 Qualitative assessment

A preliminary investigation of the proposed hypothesis was performed by testing samples of MCC granules from four different batches across the surface area spectrum available (i.e. covering the range ~0.2-1.0 m^2/g – as shown in Figure 5.5).The samples were dried using a moisture content analyser and then compressed into tablets.
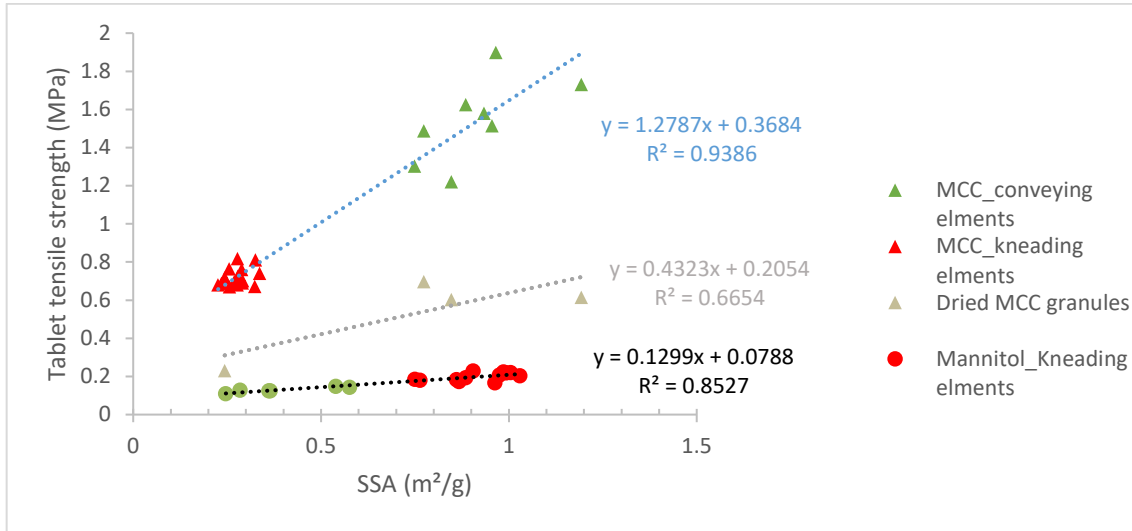
Figure 5.5 Specific surface area (SSA) vs the tablet tensile strength of tablets made of granules at 44 MPa.

The compaction of these dried MCC granules did drop from the MCC line (the grey points in Figure 5.5), confirming the hypothesis and indicating that moisture content does represent a second key bonding mechanism in tablet compacts. This should not have been a surprise – many other researchers have found a good correlation between the moisture content of a material and its tabletability as discussed in section 2.8.2.4 [50,55,73,107,122,181]. However, that it can describe the difference in tabletability between mannitol and MCC is quite surprising.

5.5.3.2 Quantitative assessment

The results from Figure 5.5 suggest that the quantification of the moisture content could be used to better describe the material tabletability, just as measurement and quantification of the specific surface area does. Figure 5.6 and Figure 5.7 confirm the hypothesis that by quantifying both the moisture content and specific surface area of the materials to be compressed, whether they are granules or powders, whether they are mannitol or MCC, it is possible to generate a good correlation with the tensile strength of the tablets formed at a given compaction pressure.

The correlation is a linear function with an R^2 value of 0.95. The majority of data fall within the prediction limits of the fitted line presented in Figure 5.6. To the best of the author's knowledge, this is the first time that such a unique, combined approach has been proposed, which can describe the compaction behaviour of materials based on the characterisation of their properties. Several attempts were done before the correlation between the tablet strength and the SSA multiplied by the moisture content of the compressed materials. For example the corelation between the SSA multiplied by plastic work is material dependant as presented in section 5.5.4.1.

In addition, the elastic work and total work of compaction were tried but no strong correlation was observed as could be seen in Appendix C
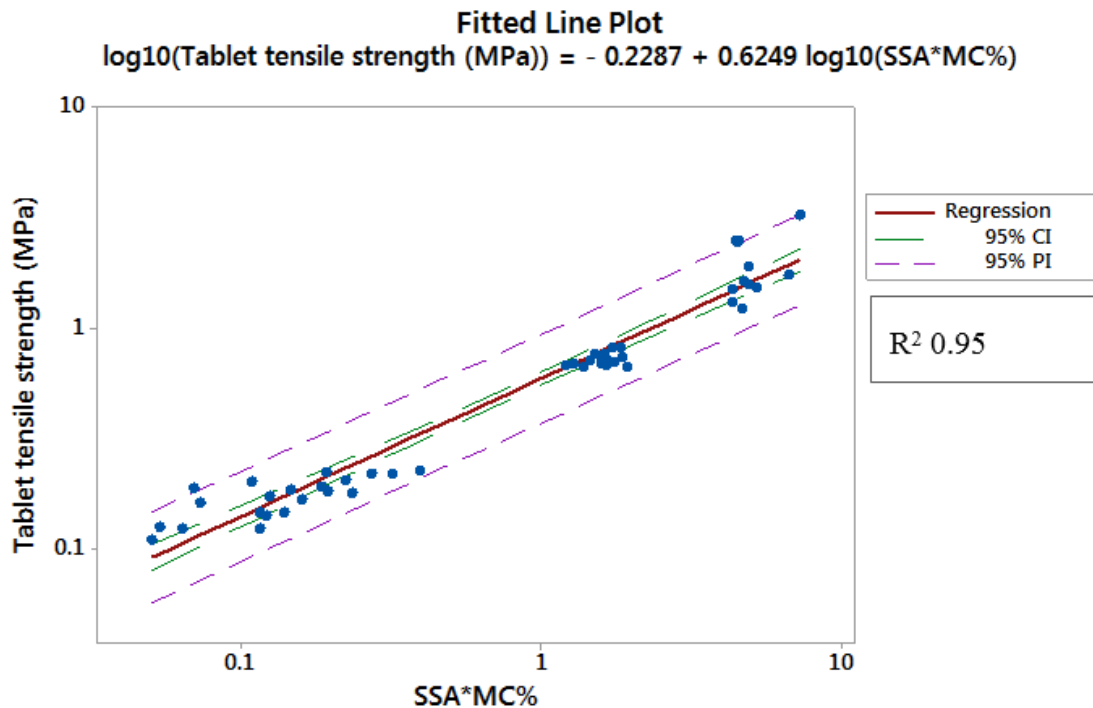
Figure 5.6 Tablet tensile strength made at 44 (MPa) vs specific surface area (SSA) * moisture content (MC) (%w/w). CI is the confidence interval, and PI is the prediction interval.
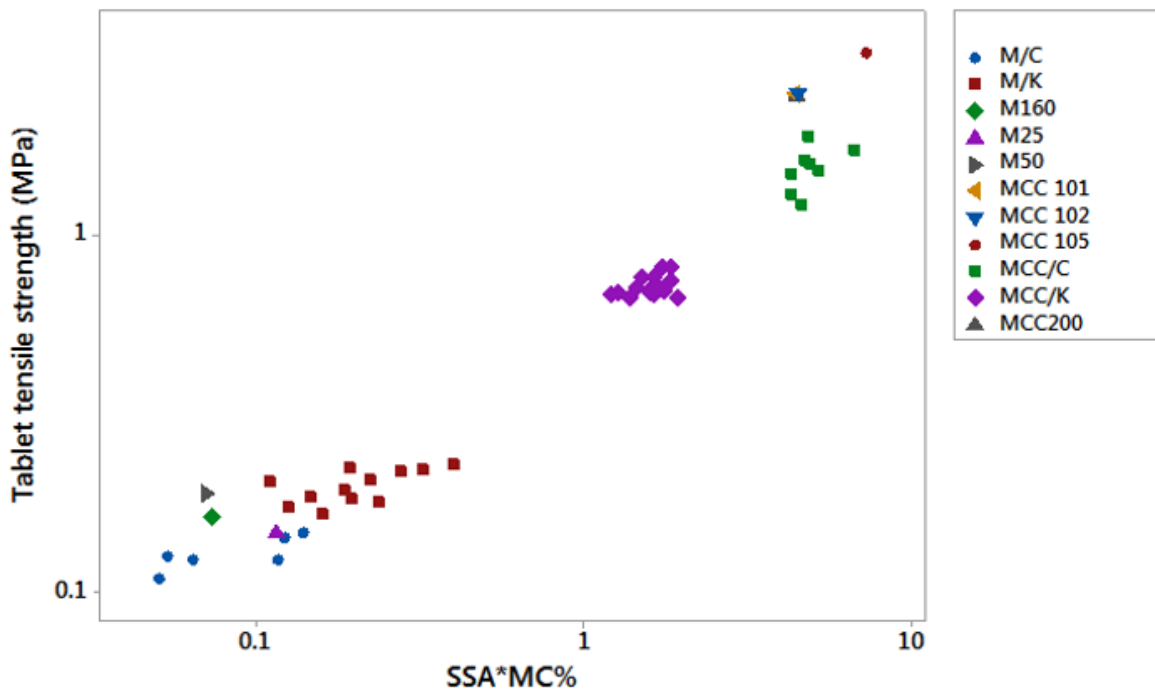
Figure 5.7 Tablet tensile strength made at 44 (MPa) vs specific surface area (SSA) * moisture content (MC) (%w/w).

Figure 5.7 includes the same data as in Figure 5.6, but the data is labelled for visual purposes. It could be seen that the SSA and the moisture content can be used to rank the MCC tablets in this order, MCC powder > MCC granules made using conveying elements > MCC granules made using kneading elements. Whereas, the mannitol tablets had a different order which is mannitol granules made using elements (M/C) > mannitol powder > mannitol granules conveying elements. The improved tablet strength of crystalline mannitol after granulation using kneading elements was also reported in section 4.5.3.3. This improvement in the tablet strength of the mannitol granules after granulation using kneading elements (Figure 5.7) can be also be explained by the improved SSA of the granules compared with the mannitol powder as shown in Figure 5.3. Measuring the moisture content in the compressed materials allowed for explaining the differences in the tabletability behaviour of mannitol and MCC which have different mechanical properties. The approach was investigated further using eight different materials and formulations as provided in Appendix E.

5.5.4 The role of moisture content – material plasticisation or liquid bridge formation

When considering the impact of material moisture content on compaction and the resulting tablet tensile strength, most researchers have so far attributed its impact to the plasticising effect on the material, facilitating greater solid:solid contact area and thus greater tensile strength (section 2.8.2.4). However, based on the bonding mechanisms reviewed in section 2.6, and the known significance of liquid bridge-based bonding in everyday situations (building sand castles, wetting a finger to open a plastic bag etc), and that they can have comparable bond strength to van der Waals forces [54], therefore further investigation is needed.

5.5.4.1 Assessment of the plasticising effect

To assess the plasticising effect directly, the plastic work of compaction of the MCC and mannitol granules produced during tabletting were extracted, which is a good indicator of the plasticity of the material [82,168]. From Figure 5.8, it can be seen that the SSA multiplied by the plastic work of the compressed MCC and mannitol granules does not provide any better correlation than that achieved in Figure 5.6. Thus, it suggests that the plastic work is not likely to be responsible for the improvement in tablet strength.
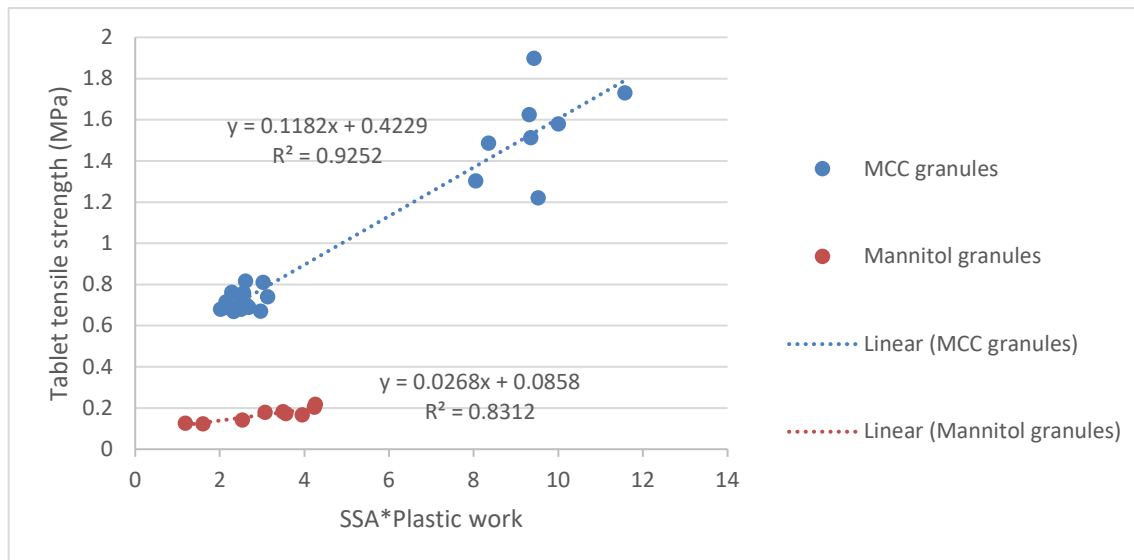
Figure 5.8 Specific surface area (SSA)* the plastic work vs the tablet tensile strength of tablets made of granules at 44 MPa.

In order to assess the plasticising effect from a different angle, the effect of lubricants on tabletability was reviewed. An interesting observation was reported by Lordi et al., the authours investigated the effect of hydrophilic and hydrophobic lubricants on the strength of potassium chloride compacts stored at different relative humidities [182]. The former study found that the reduction in tablet strength in the case of hydrophilic lubricant is less than the reduction in the case of the hydrophobic lubrication, which supports the proposed explanation for the role of moisture in the overall tablet strength. The use of hydrophilic lubricant promotes local wetting of particles (lower contact angle) compared with a hydrophobic lubricant [183].

5.5.4.2 Assessment of the liquid bridge contribution

To assess the effect of the moisture content on the total tablet strength MCC powder was compressed into tablets. Half of the tablets were stored at 80°C and 1-2 % relative humidity (which is the maximum limits of the automated storage cabinet) for five days. After drying, the tablet strength was measured as described in section 3.2.7.2. The strength of the remaining tablets was measured after compression as described in section 3.2.7.2. The moisture content of the tablets was measured directly after breakage using the LOD method (section 5.4.3). The moisture content of the tablets for the dried and non dried were 3.7% and 0.35% respectively.

Figure 6.9 shows the tablet tensile strength of dried and non dried MCC tablets. It can be seen that the strength of the dried tablet decreased approximately by 35%. This decrease in tablet strength can further support the importance of moisture in providing strength to the tablet by holding particle together by capillary forces.
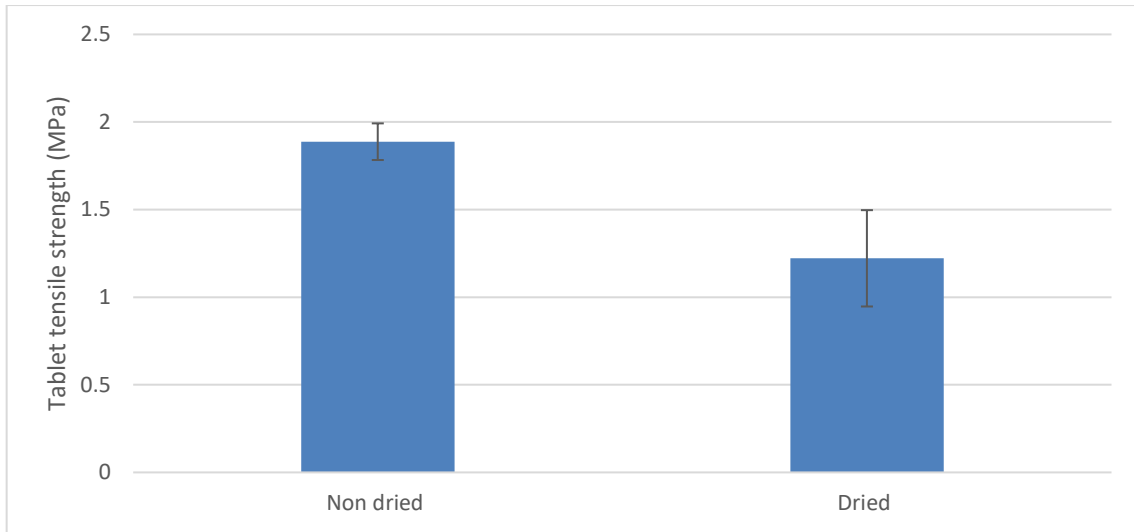
Figure 5.9 Tensile strength of MCC tablets immediately after compaction and following drying.

Based on the discussion presented above, it could be concluded that the most likely reason for increased tablet strength with increasing material moisture content is due to the presence of capillary forces (liquid bridges) and the negative Laplace pressures they generate rather than increased plasticity of the materials being compressed, leading to a greater bonding area.

5.5.5 Tablet bonding mechanism relationships

Based on the literature review provided in sections 2.5, 2.6, 2.7, and the findings from the experimental investigations, a tabletability relationship map is proposed in Figure 5.10 which describes the main contributors to tablet tensile strength and how they are inter-related with each other. The map highlights the role of capillary forces as a discrete bonding mechanism and the interaction it can have with other mechanisms. The capillary forces arise from moisture (or other liquid) adsorbed onto the surface of particles, squeezed out from the bulk during compression, or remaining in interstitial spaces as a result of incomplete drying processes further upstream [117]. Liquids with higher surface tension values such as water lead to stronger meniscus forces [76].

The fitting equation presented in Figure 5.6 has been shown to be valid for mechanically different materials which have different starting particle size and covers both granules and powders. The presented data shows that a new mechanistic approach based on a physical characteristic of the compressed materials, i.e. SSA available for bonding (both solid: solid and liquid-mediated) and average moisture content can be used to predict tabletability. The model has the potential to be applied to several industries where compaction of powders is performed.

However, there are still a number of unanswered questions and limitations with the approach presented in this paper. For example, it is well documented that for materials such as MCC, when an excess of water is present, the tensile strength of tablets formed can drop [55], therefore this approach is currently only valid for materials not having an excess of liquid present. In addition, the behaviour of materials such as hydrates in which the water molecules are an integral part of the crystal structure is not yet understood and requires further exploration.
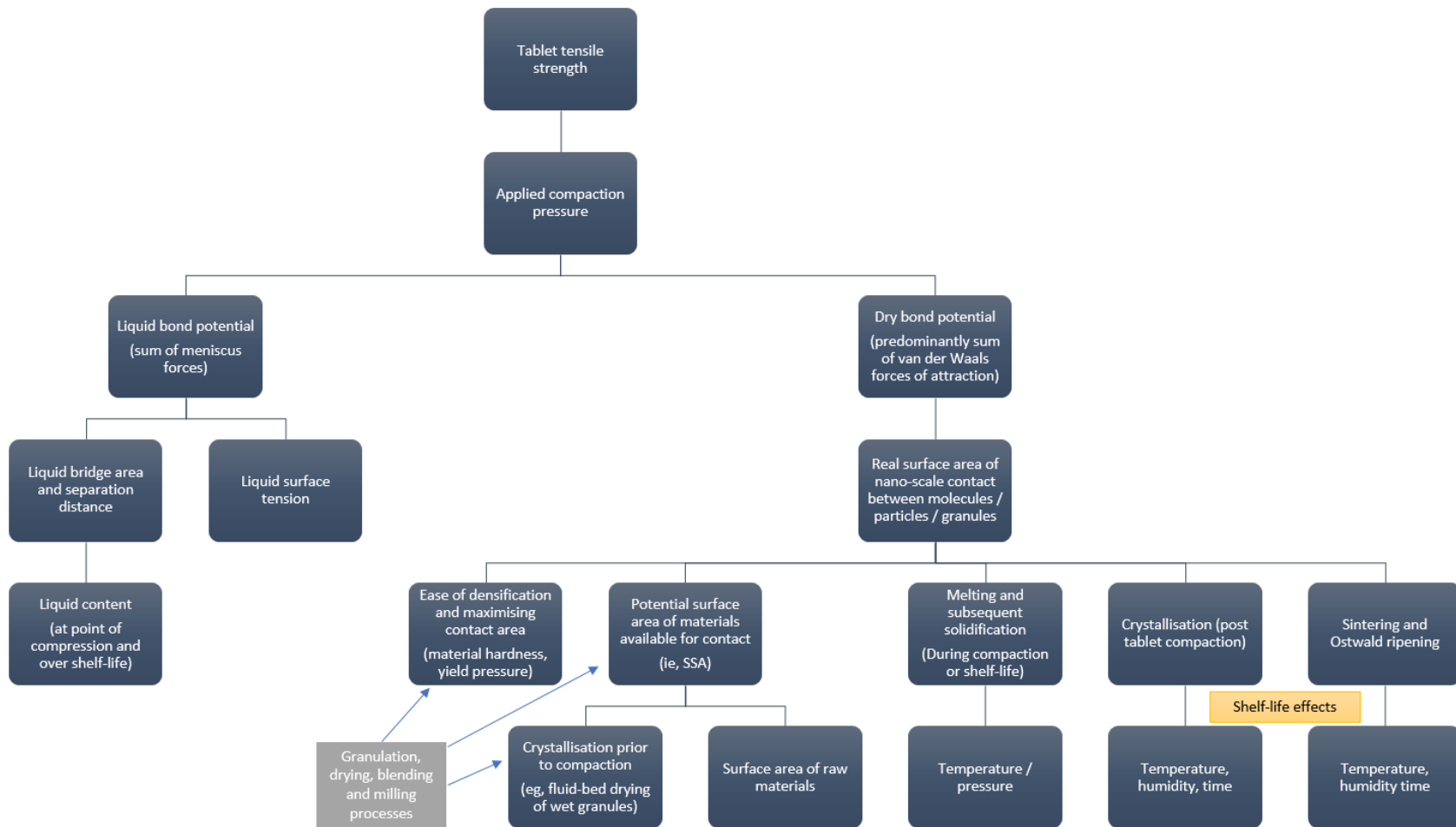
Figure 5.10 Main contributing material properties to tablet tensile strength-illustration of the 'dry and wet bond' model (DAWB).

5.6 Conclusions

The presented results have described an advance in the understanding of the most important bonding mechanisms for tablet compacts, particularly in the pharmaceutical industry. A novel approach/model to explain and predict the tabletability for a wide range of granular and powder materials is proposed. It was found that the tensile strength of tablets formed can be predicted using just two material properties – the specific surface area and the moisture content. The model can successfully predict the tabletability of plastically-deforming materials such as MCC as well as brittle materials like mannitol.

The findings presented in this chapter may have profound implications for:

- API manufacturing in the pharmaceutical industry – current initiatives around drug substance particle engineering can now have more precisely defined properties of interest and targets, namely specific surface area and moisture sorption characteristics.

- Process design and optimisation – the reported findings help to ensure that the most appropriate process parameter values are selected for a given process type and formulation. For example, crystalline materials having little internal surface area will be reliant on their external surface area and moisture content for tablet bonding. Therefore, one might reason that either milling or wet granulation of the material would help to maximise its surface area and that any subsequent processing should not remove too much moisture from the formulation.

Chapter 6 The Mechanical Properties of Formulations and their Tabletability

6.1 Summary

The change in tabletability after granulation of nine formulations was investigated. The tablet strength (TS) of the granulated materials was compared with the TS of the directly compressed tablets of the same formulation. It was found that the plasticity of the primary materials can be used to predict the percentage of change in tabletability after granulation compared with the direct compression method. The SSA*MC% approach/model was used to predict the tabletability of the granulated material at a range of compression pressures. In addition, tablet dissolution rate of granules made from mechanically different materials was investigated.

6.2 Introduction

In chapter four, the mechanisms that dictate the change in tabletability after wet granulation using TSG have been investigated. A strong correlation between the mechanical properties of the primary powders described by the yield pressure and the change in tabletability was described. It was found that the lower the yield pressure of the primary powder the higher the percentage of loss of tabletability after granulation. A few methods were proposed to restore the lost tabletability after granulation by milling the granulated material to increase the surface area available for bonding [135] or through coating the surface of the compressed materials [136]. In the pharmaceutical industry, it is very common to use a mixture of several components to make granules or tablets. Therefore, the aim of this chapter is to propose a formulation method to control the change in tabletability after granulation and to predict the tablet strength of the resulted granules. And furthermore, to investigate the dissolution rate of different formulations that have a range of mechanical properties.

6.3   Materials and methods

Binary mixtures from the four materials which are described in section 3.1 were prepared. The powders were mixed using a Y shaped mixer as described in section 3.2.2. The mass percentage (w/w %) of the mixtures are presented in Table 6.1.

Table 6.1 Mass percentage of the binary powder mixtures.

Abbreviation	Microcrystalline cellulose	Spray dried mannitol	Crystalline mannitol	Dibasic calcium phosphate anhydrous
M80/S20	80	20	0	0
M60/S40	60	40	0	0
M40/S20	40	60	0	0
M80/C20	80	0	20	0
M60/C40	60	0	40	0
M40/C60	40	0	60	0
M80/D20	80	0	0	20
M60/D40	60	0	0	40
M0/D60	40	0	0	60

6.3.1   Granulation of starting materials

The mixtures were granulated using TSG as described in section 3.2.3. For the study in this chapter, the screw configuration was made of conveying elements and one kneading zone, which includes eight kneading discs in each screw as depicted in Figure 3.10 (2). The kneading elements were used to ensure proper mixing of the materials within the granulating barrel. The screw speed was fixed at 400 RPM[3]. The powder feed rate was 1 Kg/h. Preliminary studies were conducted to select the best L/S ratio for each set of the

---

[3] The selected screw speed (400 RPM) allowed the granulation of the used formulation at the selected L/S ratios).

binary mixtures which allows successful granulation at different ratios. Deionised water was used as a liquid binder, to study the dissolution of compressed granules, 2% w/w sodium chloride (NaCl) as added to the liquid binder. The granulation conditions used in this study are described in Table 6.2

Table 6.2 Granulation conditions

Mixtures	Liquid to solid ratio
microcrystalline cellulose and spray-dried mannitol	0.64
Microcrystalline cellulose and crystalline mannitol	0.64
Microcrystalline cellulose and dibasic calcium phosphate anhydrous	0.84

6.3.2 Sieving

After the materials have been dried using tray method, the granules were sieved following the same method in section 3.2.5.2. A granule sieve cut (500-700 µm) was used for the work of compaction and tabletting (as at this sieve cut a good yield was achievable from the nine different formulations).

6.3.3 Work of compaction

The powder mixtures were compressed using a material testing machine as described in section 3.2.1.2.

6.3.4 Tabletting

The granulated and the primary formulations were compacted as described in section 3.2.7.1. No lubricant was used in order not to influence the dissolution of the tablets. Three compression pressures were used 44, 88, and 175 MPa.

6.3.5 Tablet Dissolution

The nine formulations presented in Table 6.1 were granulated (Section 6.3.1). After sieving the granules (500-700 µm), the granules were compressed using three compression pressures 44, 88, and 175 MPa. After that the dissolution tests were

performed on the tablets. The dissolution of the sodium chloride from the compressed granules was assessed using a conductivity method described in section 3.2.8. T_{90} was used to represent the dissolution rate of the compressed materials. T_{90} is defined as the time required for 90% of the sodium chloride to be dissolved from the compressed materials [177]. The dissolution test was performed in triplicate.

6.4 Results and discussion

6.4.1 Tabletability of the formulations

Sodium chloride (2% w/v) was used as a tracer to study the dissolution from the granulated formulations, as it was important to exclude the possibility that the tracer affects the tabletability of the granules. MCC was granulated with and without sodium chloride (NaCl) then the tablet tensile strength of the two granulated materials was compared as presented in Figure 6.1. It could be seen from Figure 6.1 that there is no difference in the tablet tensile strength between the tablets that have NaCl and the ones that do not. The former observation could be expected as a low concentration of sodium chloride was used, which did not impact the granules properties.
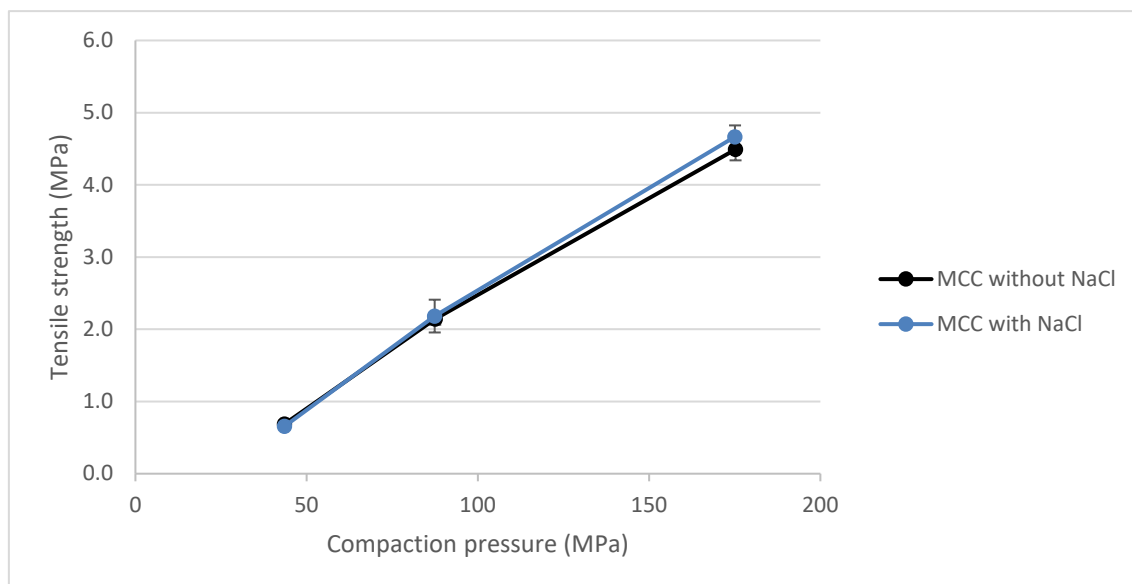
Figure 6.1 Tabletability of MCC granules with and without sodium chloride in the liquid binder.

6.4.2 Loss of tabletability after granulation

6.4.2.1 Loss of tabletability and plasticity of primary powders

The percentage of change in the tablet tensile strength (ΔTS) between the granulated formulations and the directly compressed formulation was calculated as described in section 3.2.7.3. ΔTS for all formulations was calculated at three compression pressures 44, 88 and 175 MPa as presented in Figure 6.2-6.4. It could be seen from Figure 6.2 and Figure 6.3 that the loss of compactability of the MCC granules after granulation decreased by adding a brittle material, the crystalline mannitol and the DCP. The improvement in the tabletability was found to be concentration-dependent of the brittle material. In all formulations, it was found that 40% of the brittle material (mannitol or DCP) in the formulation almost stopped the reduction in the tabletability. The formulation, which had 60% of the brittle material, showed no loss of tabletability (-ΔTS) but interestingly an improvement in the strength compared with the direct compression formulation.
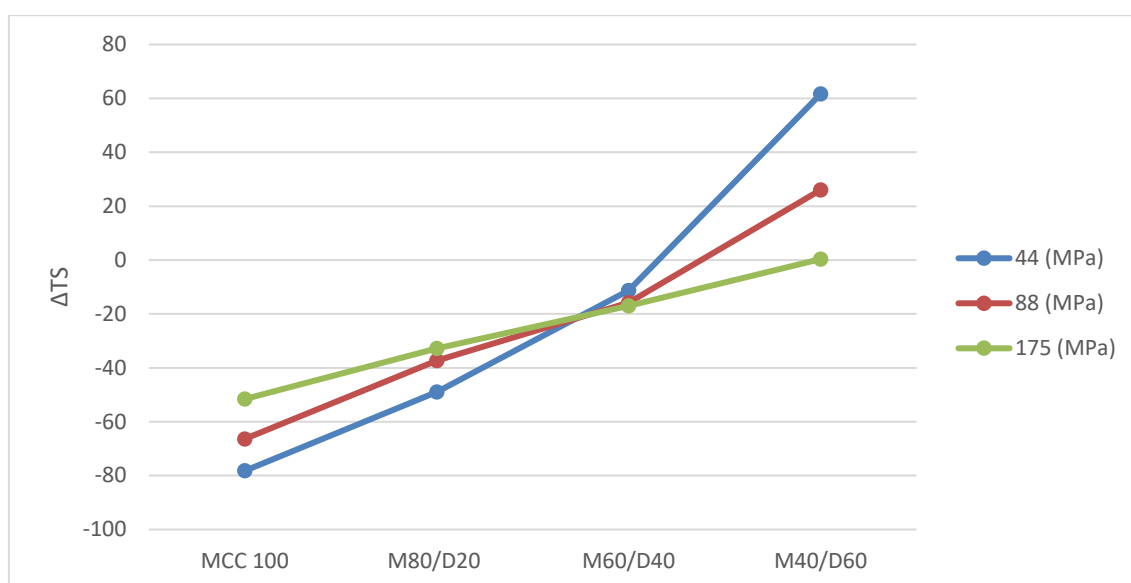
Figure 6.2 The percentage of change of the tabletability after granulation of microcrystalline cellulose (MCC) and dibasic calcium phosphate (DCP) mixtures compressed at different compression pressures.
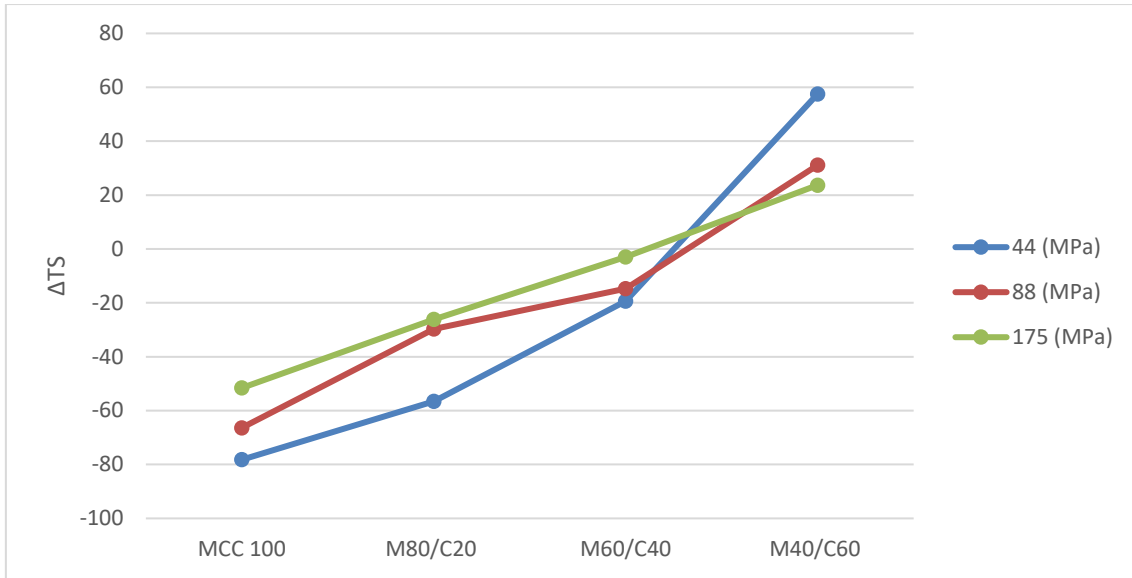
Figure 6.3 The percentage of change of tabletability after granulation of microcrystalline cellulose and crystalline mannitol mixtures compressed at different compression pressures.

Adding spray-dried mannitol (plastically deforming material) to the MCC formulation led to a reduction in the percentage of loss of tabletability as can be seen in Figure 6.4. A decrease in the tablet strength after granulation was always noticed when spray-dried mannitol was added (regardless of the added ratio) unlike the trend which was seen with the MCC/brittle material formulation.
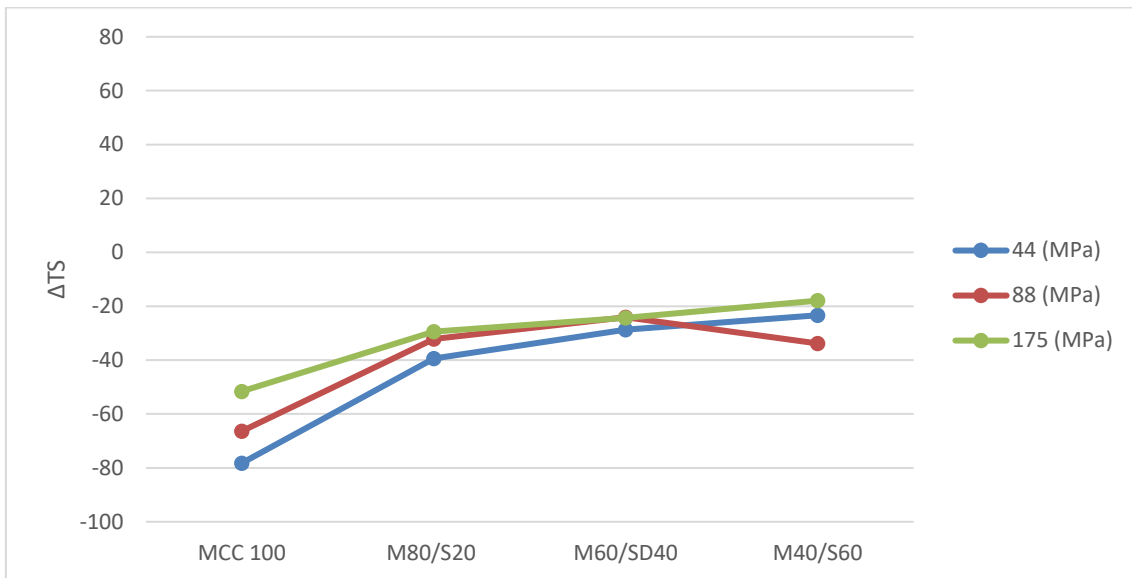
Figure 6.4 The percentage of change of tabletability after granulation of microcrystalline cellulose and spray-dried mannitol mixtures compressed at different compression pressures.

The plastic work of the primary formulation is presented in Figure 6.5. It could be seen that the percentage of the plastic work decreased as the percentage of the brittle material increased (mannitol and DCP). This trend agrees with the results presented in Table 4.2, which present the plastic work of the primary materials. The plasticity of the primary powders is ranked as microcrystalline cellulose (highest) > spray-dried mannitol (M100) >crystalline mannitol (M160) > DCP (lowest) as presented in Table 4.2. This trend is in agreement with previous studies [149,183,190].
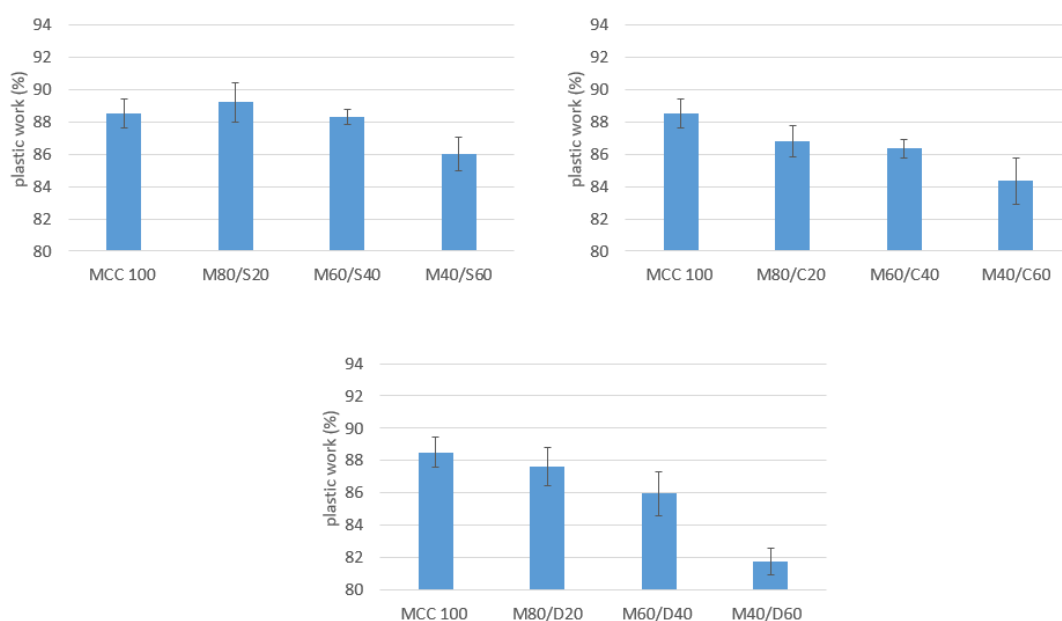
Figure 6.5 The percentage of the plastic work of the ungranulated formulations.

By comparing Figure 6.2, Figure 6.3, Figure 6.4, and Figure 6.5, a correlation between ΔTS and the percentage of the plastic work of the primary formulation is realised. As the percentage of the plastic work of the primary formulation increases, the percentage of loss of tabletability increases. Further investigation showed that there is a linear correlation between ΔTS and the percentage of the plastic work of the primary formulation when tablets are compressed at 44, 88, and 175 MPa as presented in Figure 6.6, Figure 6.7, and Figure 6.8.
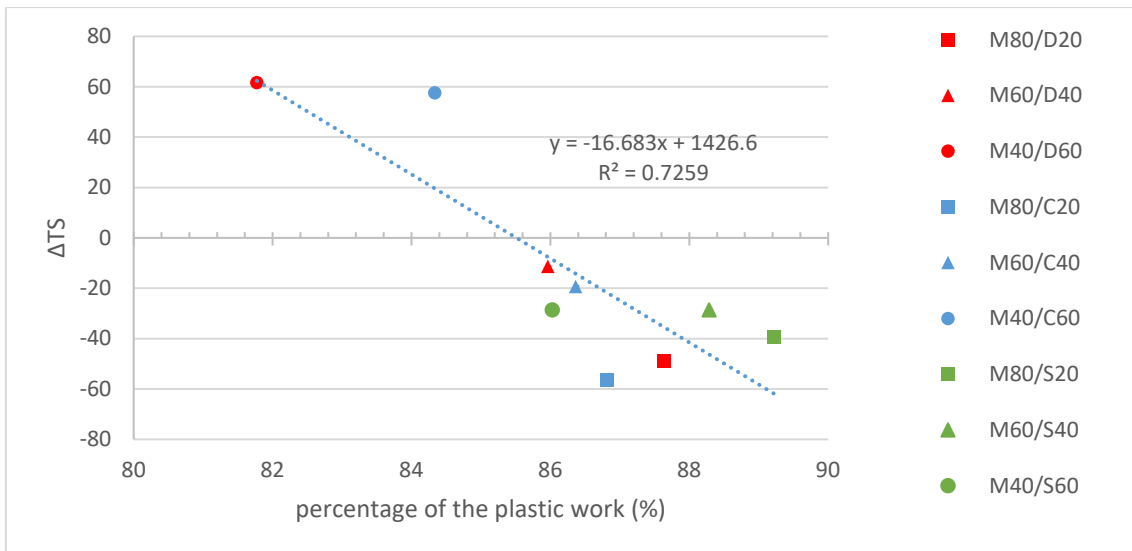
Figure 6.6 The relationship between the plastic work (%) of the primary formulation and the percentage of change in tabletability after granulation for the tablets compressed at 44 MPa.
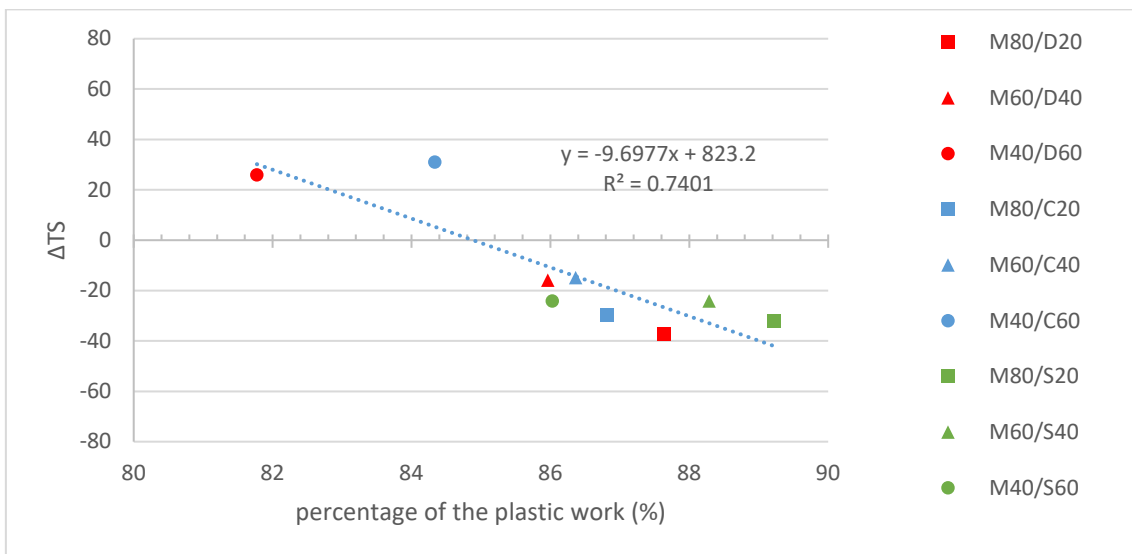
Figure 6.7 The relationship between the plastic work (%) of the primary formulation and the percentage of change in tabletability after granulation for the tablets compressed at 88 MPa.
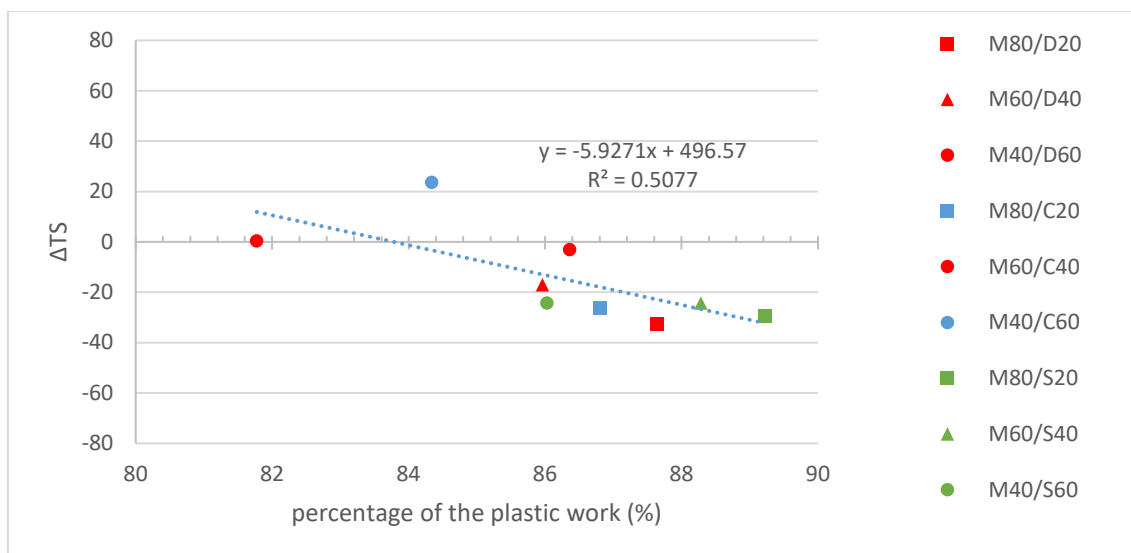
Figure 6.8 The relationship between the plastic work (%) of the primary formulation and the percentage of change in tabletability after granulation for the tablets compressed at 175 MPa.

This finding is in agreement with the tabletability regime map for the TSG granulated materials (Figure 4.16) in which it was presented that the yield pressure of the primary material has good correlation with the percentage of change in tabletability after granulation (ΔTS). The tabletability map presents the correlation between the yield pressures of a single component formulation with the percentage of change in the tabletability after granulation compared with the direct compression tablets [107]. The presented findind further supports the results presneted in Figure 4.3, which shows a good corelation btween the yield pressure and the percentage of plastic work as an good parameter to chractrise the mechanical properties of materials.

Furthermore, the results are in agreement with Osei-Yeboah work in which it was found that the addition of brittle material to a MCC formulation can increase the value of the minimum tablet tensile strength [152]. It was hypothesised that the brittle materials promote the brittle fracture of the granules during compaction leading to a higher tablet tensile strength by increasing bonding area at a varying level of liquid binder [152]. The presented data in this work explain what is most likely to be the significant reason for the loss of tablet strength, whereby the more plastically deformable the primary formulation, the more densification it can experience due to the stresses along the granulation barrel as seen in chapter four (Figure 4.4). Additionally, the results presented in Figure 6.6, Figure 6.7, and Figure 6.8 suggest that the ΔTS can be predicted for the studied formulations by measuring the plastic work of the primary formulations. This finding will

115

enable the development of tablets based on the knowledge of the properties of the components within the formulation rather than a trial and error method.

6.4.3   Specific surface area and moisture content: predicting tablet strength

In chapter five (Figure 5.6), it was found that the specific surface area available for bonding multiplied by the amount of moisture (SSA*MC %) in a compressed material can be a good predictor of the tablet tensile strength of primary powder and granulated materials.

In this section, the SSA*MC % model will be used to predict the tabletability of the nine formulations prepared as described in Table 6.1. Also, the validity of the DAWB model over different compression pressures will be assessed. The used formulations cover a wide range of mechanical properties and solubilities. The granulated formulations were compressed at a range of compression pressures, 44, 88, and 175 MPa.

Figure 6.9 shows the relationship between the SSA and the moisture content of the granules with the strength of the tablets made of granules of the different formulations compressed at 44 MPa. As could be seen from Figure 6.9, the relationship between the tablet strength and the specific surface area and moisture content SSA* MC% is linear with a R^2 of 0.93, which is very similar to the finding presented in Figure 5.6. By increasing the compression pressure at which the granules are compressed, it could be seen that the R^2 of the linear relationship decreased to 0.74 and 0.52 as Figure 6.10 and Figure 6.11 show, respectively.
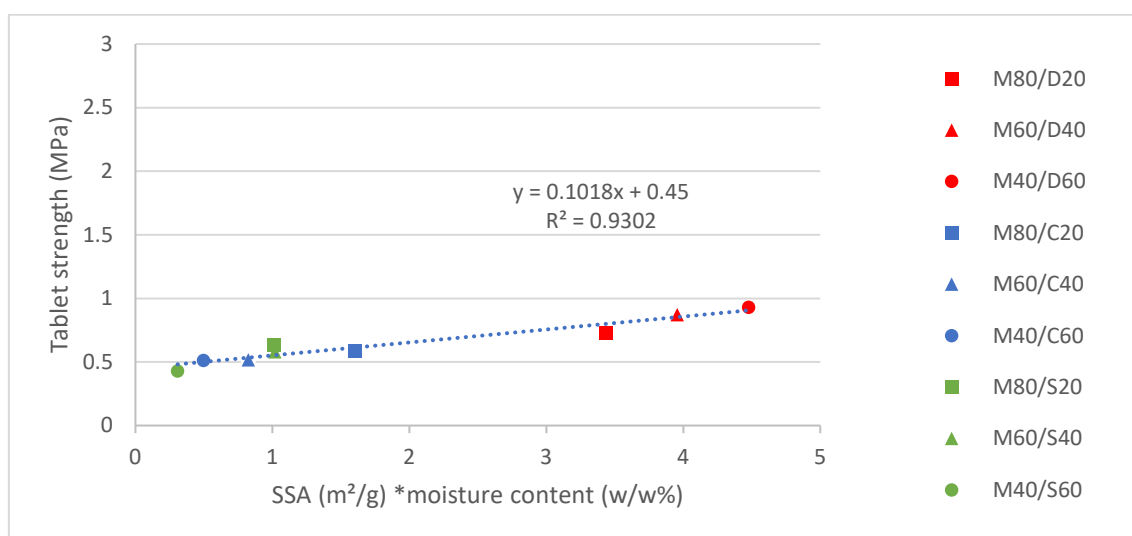
Figure 6.9 Tablet tensile strength made at 44 (MPa) vs specific surface area * moisture content (%w/w).
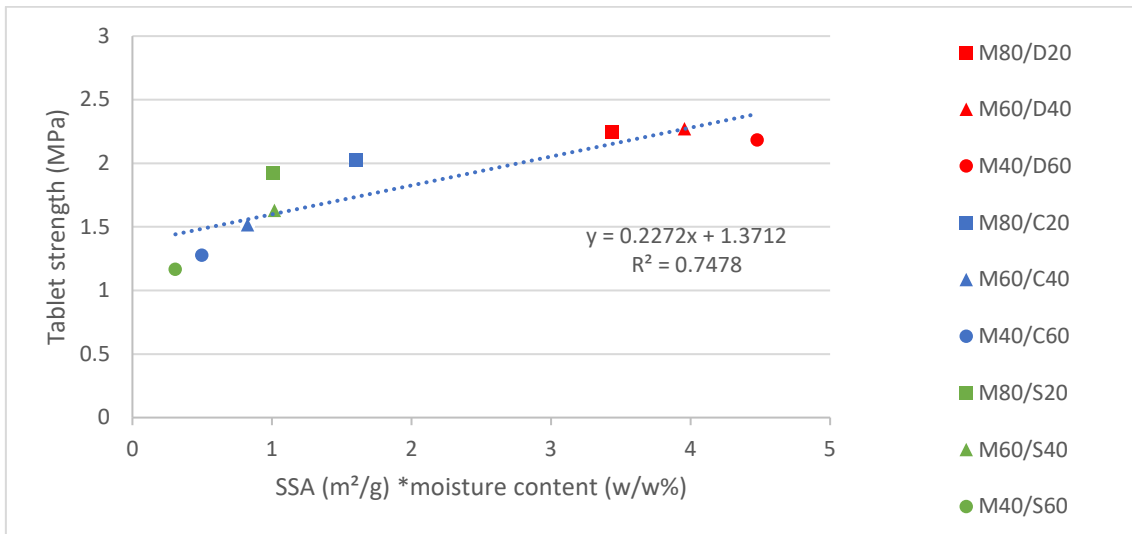
Figure 6.10 Tablet tensile strength made at 88 (MPa) vs specific surface area * moisture content (%w/w).
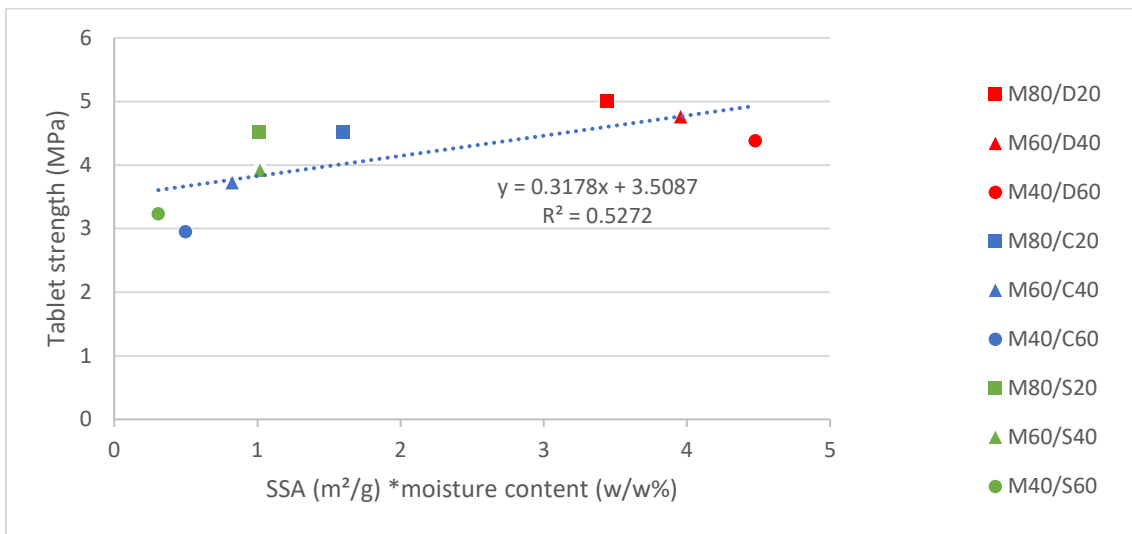
Figure 6.11 Tablet tensile strength made at 175 (MPa) vs specific surface area * moisture content (w/w%)

The R^2 of the relationship between the tablet strength (TS) and SSA*MC% at medium (88 MPa) and high (175 MPa) compression pressures increased from 0.74 to 0.91 and from 0.52 to 0.72 respectively when a logarithmic function was used instead of a linear function as shown by Figure 6.12 and Figure 6.13.
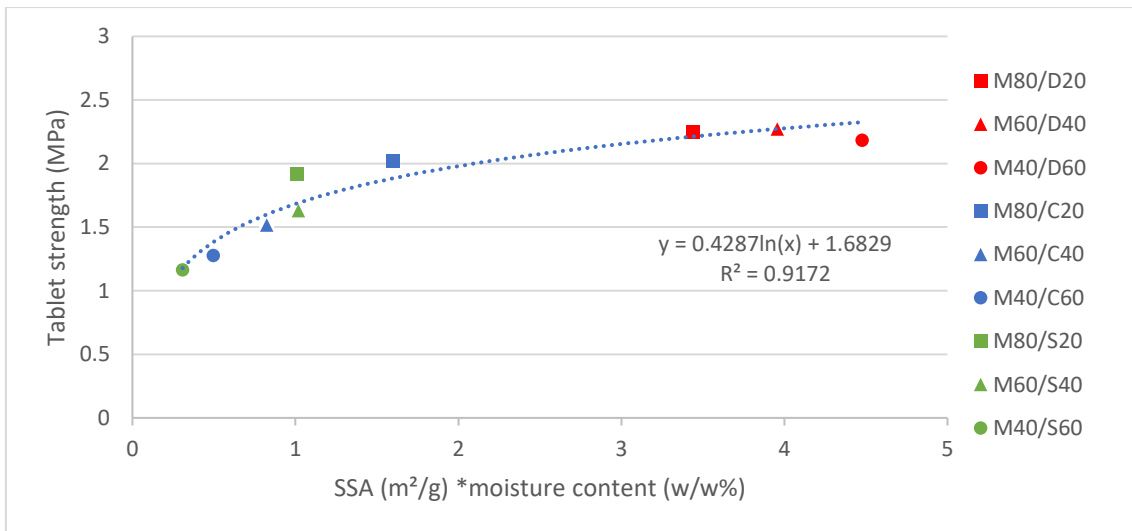
Figure 6.12 Tablet tensile strength made at 88 (MPa) vs specific surface area * moisture content (w/w%).
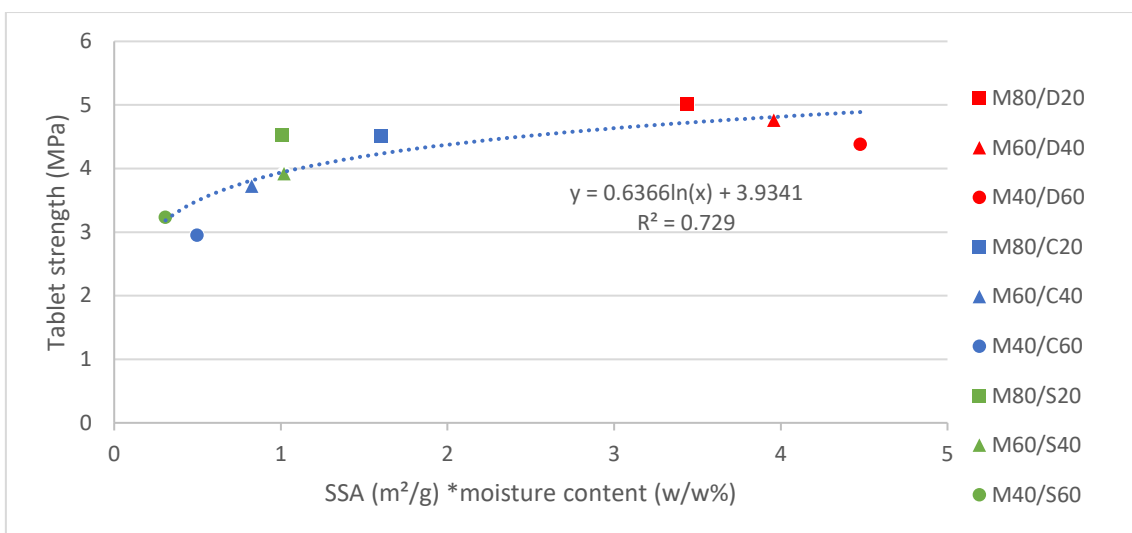
Figure 6.13 Tablet tensile strength made at 175 (MPa) vs specific surface area * moisture content (w/w%).

Based on the results presented in Figures 6.9-6.13, it can be concluded that the specific surface area and the moisture content of the granules could be used to predict the tablet strength of the granules at the studied range of compression pressures (44-175 MPa). To the best of our knowledge, this is a novel approach to predict the loss of tabletability based on the characterisation of the granules.

6.4.4 Tablets dissolution

6.4.4.1 The dissolution of granulated MCC & crystalline mannitol-based formulation

The dissolution measurements of the three granulated MCC/crystalline mannitol formulations compressed at 44, 88, and 175 MPa are presented in Figure 6.14, Figure 6.15, and Figure 6.16 respectively. From Figure 6.14, it can be realised that there is no significant difference between the dissolution profiles of the MCC/crystalline mannitol formulations when the granules are compressed at 44 MPa. In addition, the dissolution rates expressed as T_{90} of the three formulations were achieved in less than one minute.
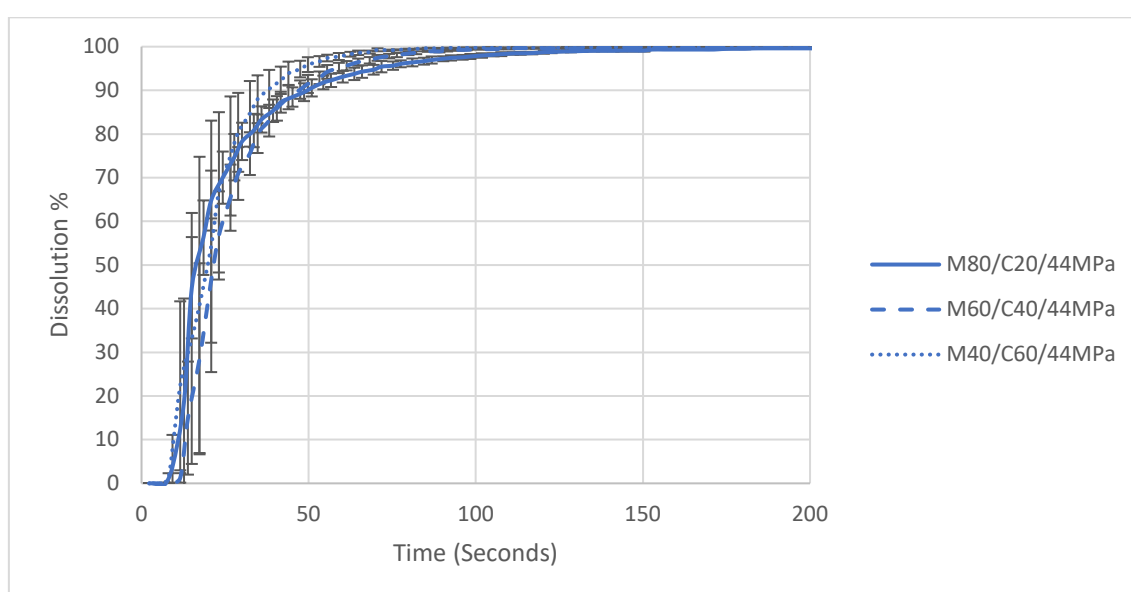
Figure 6.14 The dissolution rate of granulated microcrystalline cellulose and crystalline mannitol tablets compressed at 44 MPa.

The dissolution rates of the MCC/ crystalline mannitol tablets compressed at 88 MPa are presented in Figure 6.15. Increasing the compression pressure from 44 to 88 MPa led to a slower dissolution rate as could be seen from Table 6.3. The dissolutions of all the formulations compressed at 44, 88, and 175 MPa expressed as T_{90} are presented in Table 6.3. Furthermore, the dissolution rates of M40/C60 and M60/C40 are faster than the M80/C20. In other words, increasing the mannitol in the formulation leads to a faster dissolution rate, since the amount of the soluble material in the granules increases.
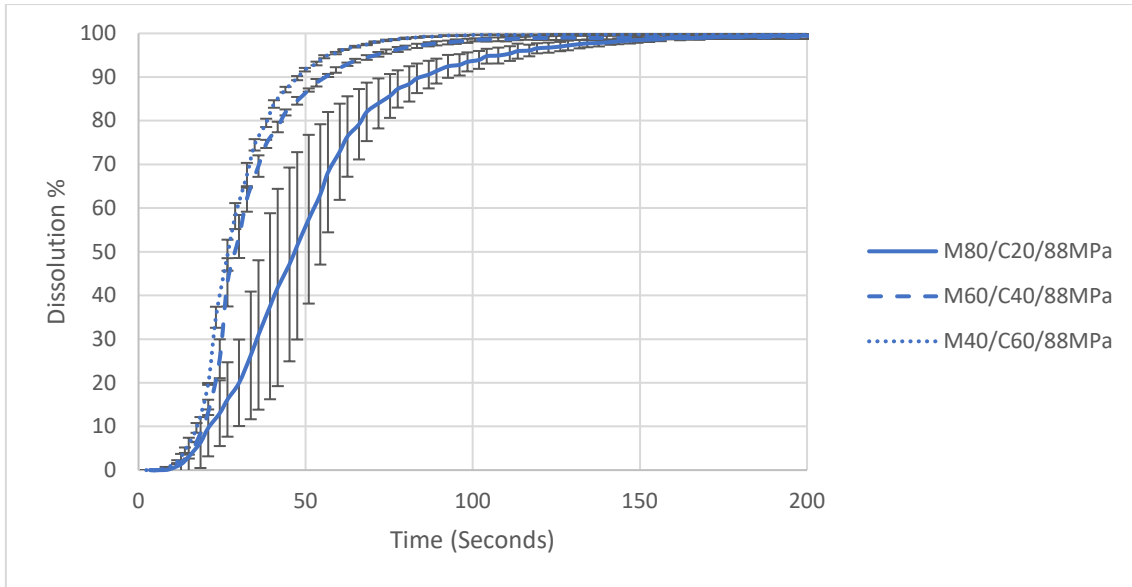
Figure 6.15 The dissolution rate of granulated microcrystalline cellulose and crystalline mannitol tablets compressed at 88 MPa.
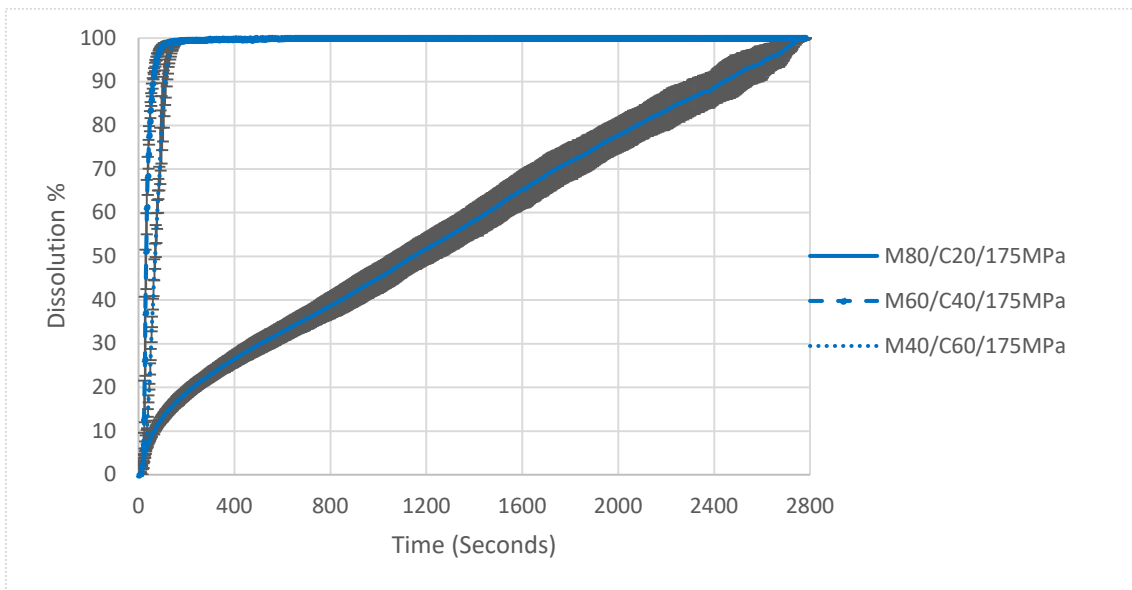
Figure 6.16 The dissolution rate of granulated microcrystalline cellulose and crystalline mannitol tablets compressed at 175 MPa.

By increasing the compression pressure to 175 MPa a significant delay in the dissolution rate of the granules made of high proportion of MCC (M80/C20) was noticed as presented in Figure 6.16. The T90 of the M80/C20 for the tablets compressed at 175 MPa are significantly slower than M60/40C and M40/C60 as presented in Table 6.3. The T90 of the M80/C20 is 2104 seconds while the M60/C40 and M40/C60 had T90 of 53 and 95 seconds, respectively.

Table 6.3   T90 of the formulations compressed at 44, 88, 175 MPa.

Microcrystalline cellulose and crystalline mannitol formulation			Microcrystalline cellulose and spray-dried mannitol formulation			Microcrystalline cellulose and DCP formulation		
Abbreviation	T_{90} (seconds)	Relative Standard deviation (%)	Abbreviation	T_{90} (seconds)	Relative Standard deviation (%)	Abbreviation	T_{90} (seconds)	Relative Standard deviation (%)
M80/C20/44MPa	43	13.9	M80/S20/44MPa	41	9.7	M80/D20/44MPa	1938	0.8
M60/C40/44MPa	42	4.7	M60/S40/44MPa	41	9.7	M60/D40/44MPa	2079	2.2
M40/C60/44MPa	33	15.1	M40/S60/44MPa	47	8.5	M40/D60/44MPa	2068	0.7
M80/C20/88MPa	74	13.5	M80/S20/88MPa	66	12.1	M80/D20/88MPa	1775	0.1
M60/C40/88MPa	49	1.2	M60/S40/88MPa	46	1	M60/D40/88MPa	1894	1.3
M40/C60/88MPa	41	2.4	M40/S60/88MPa	52	19	M40/D60/88MPa	2016	1.3
M80/C20/175MPa	2104	5.6	M80/S20/175MPa	2067	2.2	M80/D20/175MPa	1823	2.5
M60/C40/175MPa	53	1.8	M60/S40/175MPa	231	7.7	M60/D40/175MPa	1903	1.5
M40/C60/175MPa	95	9.4	M40/S60/175MPa	290	12.4	M40/D60/175MPa	2079	2.2

6.4.4.2 The dissolution of granulated MCC and spray dried mannitol-based formulation

The dissolution rate of the MCC/ spray-dried mannitol tablets compressed at 44, 88, and 175 MPa are presented in Figure 6.17, Figure 6.18, and Figure 6.19, respectively.

The tablets compressed at 44 and 88 MPa share a similar dissolution trend as seen in Figure 6.17 and Figure 6.18. The dissolution rate seems to be independent of the MCC to mannitol ratio at 44 and 88 MPa. The dissolution of the tablets made at 88 MPa is slightly slower than the tablets compresseed at 88 MPa as seen in Table 6.3. A clear effect of the ratio of the MCC to spray-dried mannitol on the dissolution rate of tablets compressed at 175 MPa is shown in Figure 6.19. M80/S20 has a significantly slower dissolution rate compared with M60/C40 and M40/C60. This observation can be expected as the percentage of the water soluble material is increased within the tablets. The T_{90} is increased with increasing the compression pressure of the tablets as seen in Table 6.3.
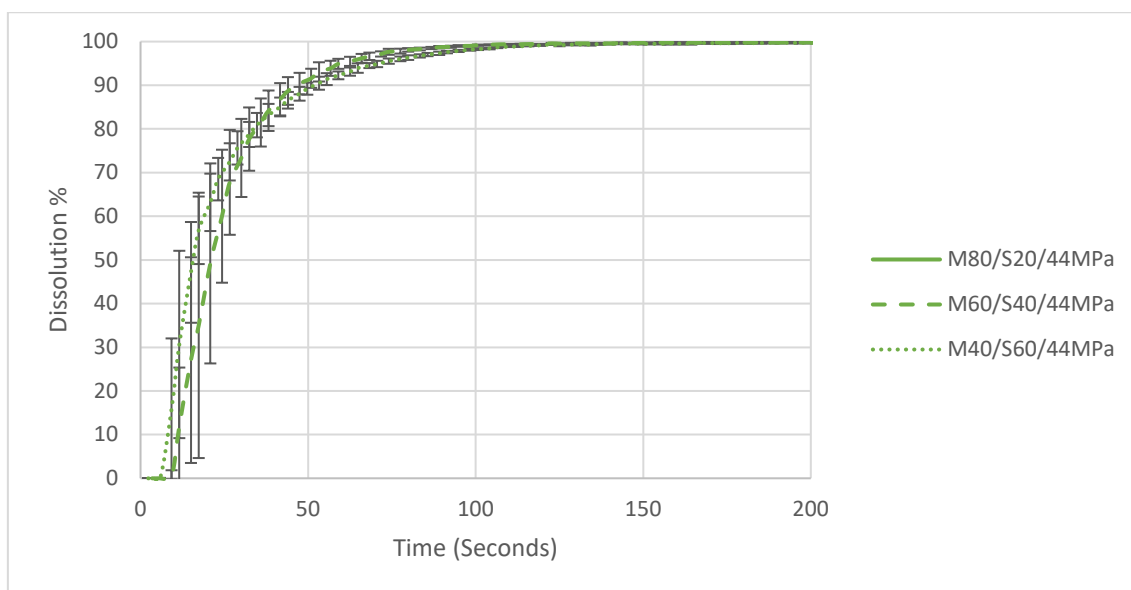
Figure 6.17 The dissolution rate of granulated microcrystalline cellulose and spray dried mannitol tablets compressed at 44 MPa.
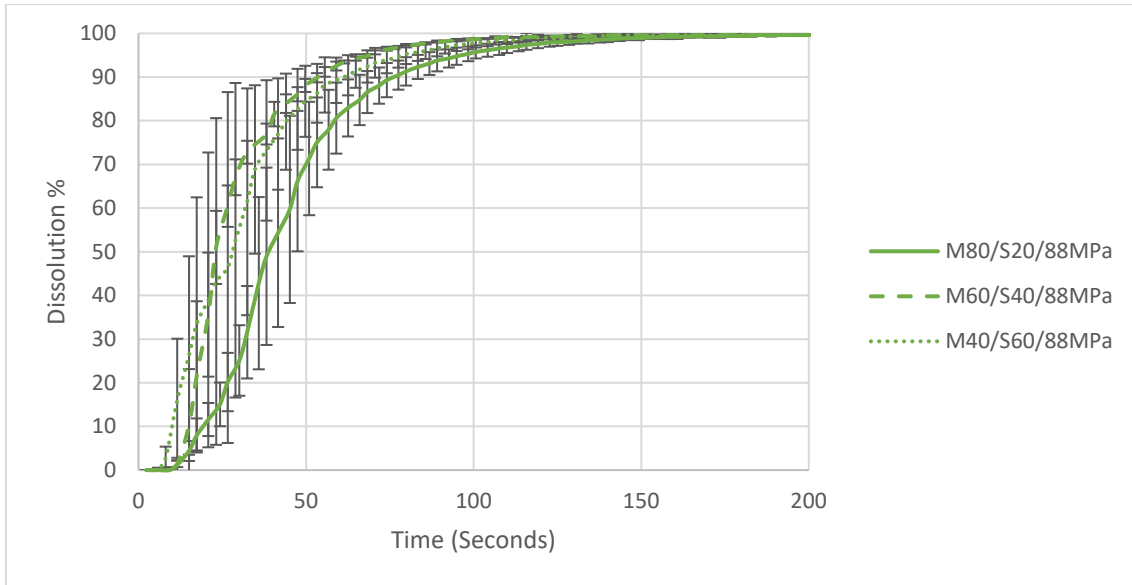
Figure 6.18 The dissolution rate of granulated microcrystalline cellulose and spray dried mannitol tablets compressed at 88 MPa.
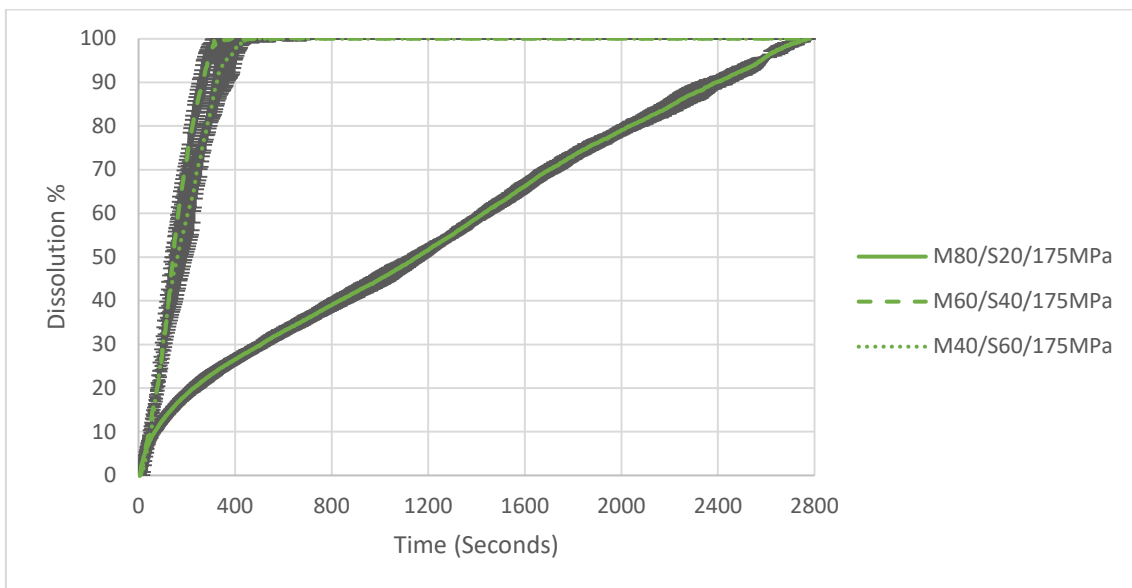
Figure 6.19 The dissolution rate of granulated microcrystalline cellulose and spray dried mannitol tablets compressed at 175 MPa.

6.4.4.3 The dissolution of granulated MCC & DCP based formulation

The dissolution of the MCC and DCP based formulation tablets compressed at 44, 88, and 175 MPa are presented in Figure 6.20, Figure 6.21, and Figure 6.22, respectively.

Unlike the tablets made from the MCC and mannitol formulations (which had a fast dissolution rate, shorter than 2 minutes in most cases), the MCC and DCP tablets have significantly longer T_{90} regardless of the compression pressure. Figure 6.20 presents the dissolution rate of tablets made of the MCC and DCP formulations at 44 MPa, which are very similar. The values for the T_{90} for the M80/D20/44MPa, M60/D40/44MPa, and M40/D60/44MPa are 1938, 2079, and 2068 seconds respectively, which are slightly similar with 130 second difference between the M80/D20 and the M40/D60. Although the T 90 was similar, however the ratio of the DCP in the tablet affects the early stages of the dissolution rate where it was found that the M60/D40 and M40/D60 had similar dissolution rate the T_{40} were approximately 800 second, whereas the M80/D20 at 800 second had already achieved its T_{60}.
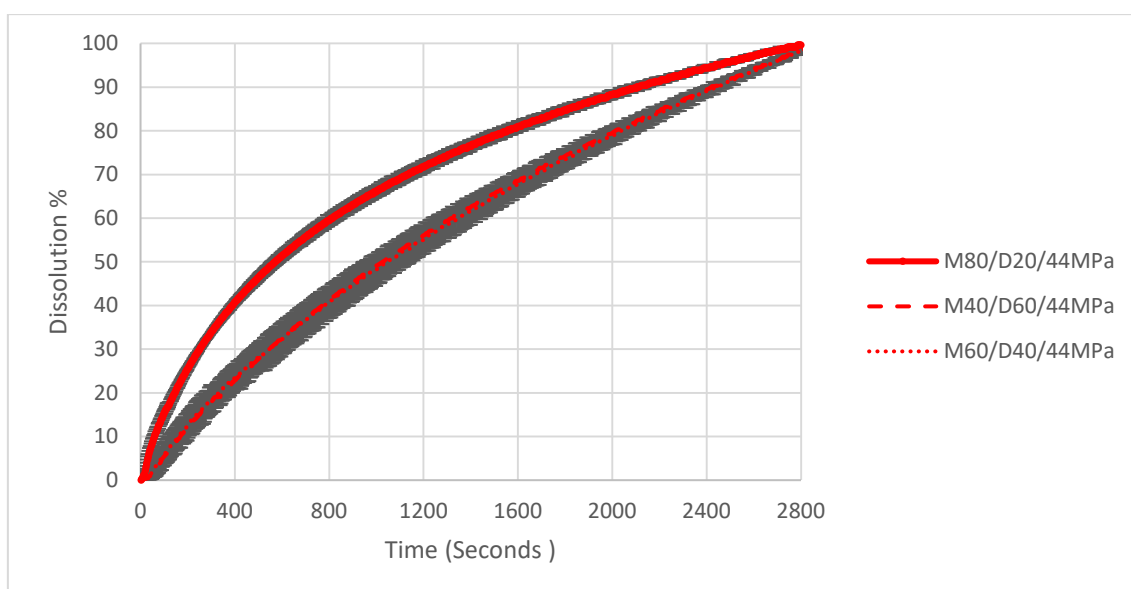
Figure 6.20 The dissolution rate of granulated microcrystalline cellulose and dibasic calcium phosphate anhydrous tablets compressed at 44 MPa.

By increasing the compression pressure to 88 and 175 MPa, the effect of the ratio of the MCC to DCP on the dissolution rate becomes more visible, in which increasing the DCP leads to slightly slower dissolution rate as shown in Figure 6.21-Figure 6.22. However, the difference in the T_{90} of the three different formulations tablets at the three compression pressures used is not as significant as the MCC and the mannitol based formulations. The difference between the minimum and the maximum value of the T_{90} at 175 MPa compression pressure for the MCC/DCP formulations is 256 seconds while it is 2051

seconds and 1836 seconds for the MCC/crystalline mannitol and the MCC/spray dried mannitol, respectively.
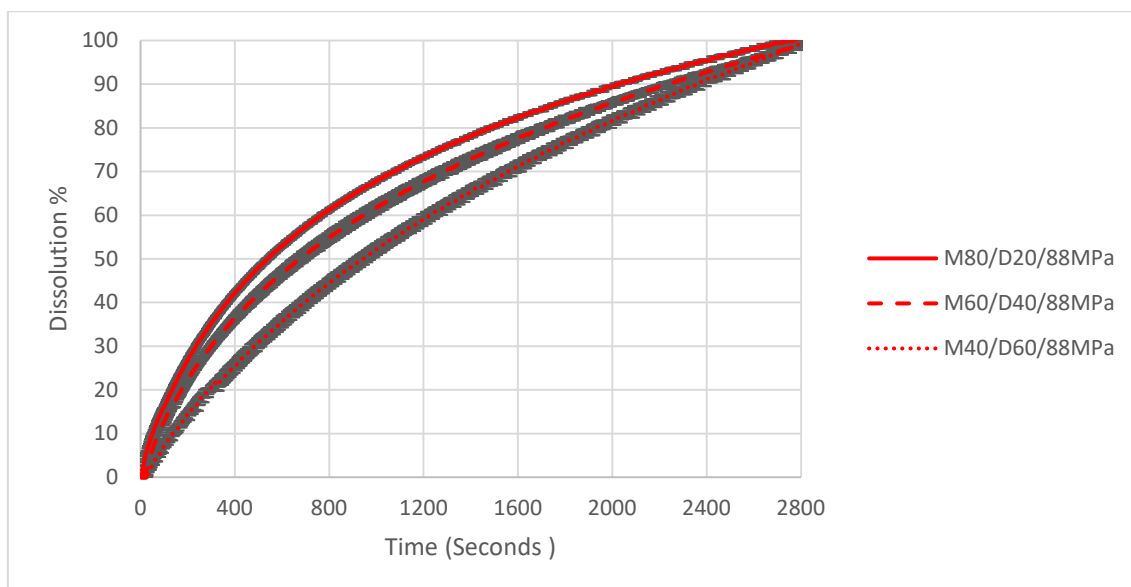
Figure 6.21 The dissolution rate of granulated microcrystalline cellulose and dibasic calcium phosphate anhydrous tablets compressed at 88 MPa.
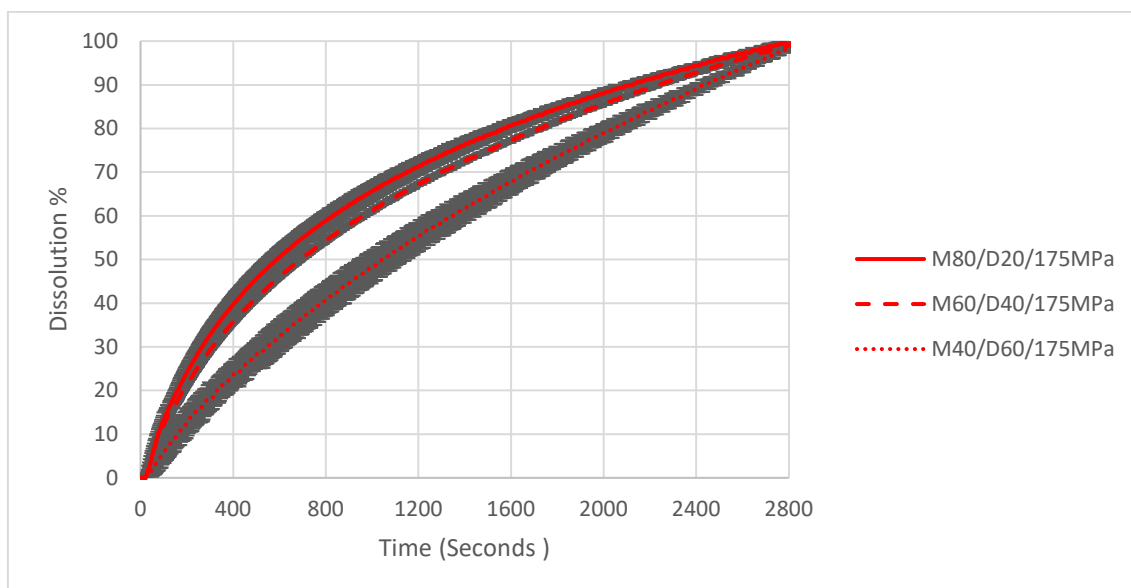
Figure 6.22 The dissolution rate of granulated microcrystalline cellulose and dibasic calcium phosphate anhydrous tablets compressed at 175 MPa.

6.4.4.4 Summary of the dissolution behaviour of the binary formulations

The dissolution rate of the water insoluble formulations (MCC and DCP) was significantly slower than the water soluble formulations (MCC and mannitol) as could be seen from Figure 6.23. For instance, T_{90} for the M80/20/44MPa and M80/S20/44MPa are

43 and 41seconds respectively, while the T_{90} of the M80/D20/44MPa is 1938 seconds. The same trend is seen with the other formulation ratios. The effect of the compression pressure on the dissolution rate of the MCC and both types of mannitol formulations was insignificant at low and medium compression forces (44, 88 MPa). However, a significant delay in the T_{90} was seen for the MCC and mannitol formulations compressed at 175 MPa as could be seen from Table 6.3 and Figure 6.23.
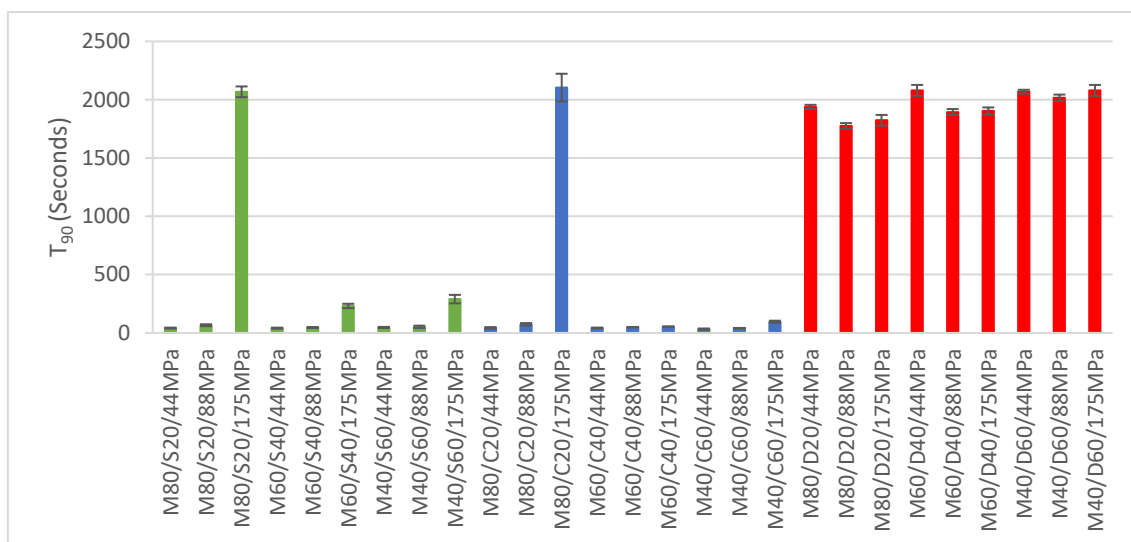
Figure 6.23 T90 of the formulations.

The apparent density (Eq 3.4) of the tablets made from the granulated formulations is presented in Figure 6.24. The apparent density of the tablet increased by increasing the compression pressure from 44 to 175 MPa.
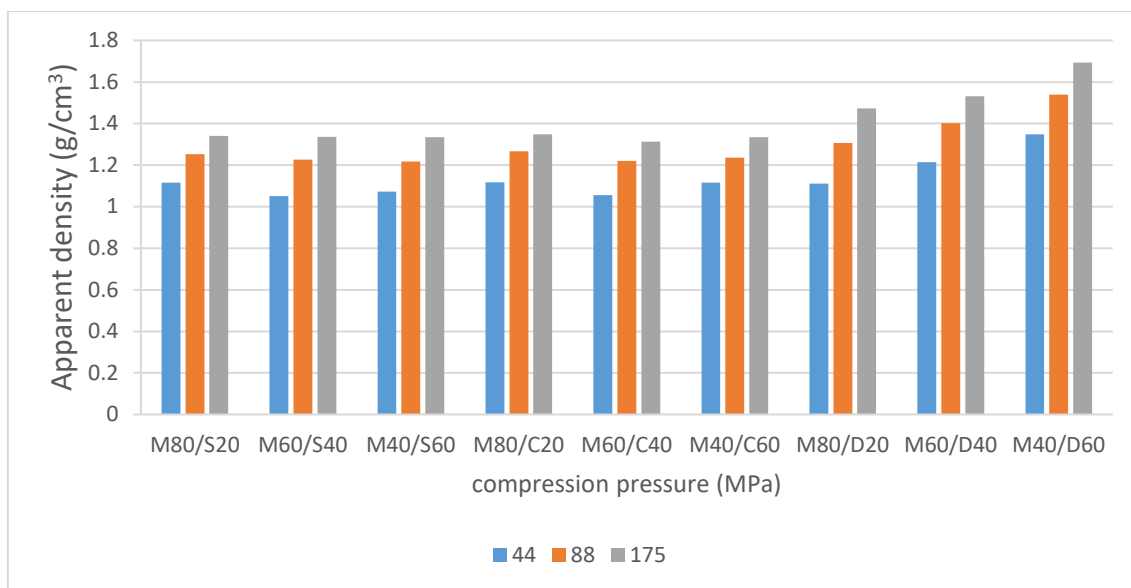
Figure 6.24 The apparent density of the tablets (of the granulated formulations) compressed at 44, 88, 175 MPa.

The formulations which include DCP have higher apparent density compared with the MCC/mannitol formulations, as DCP has the highest true density among the studied materials. The true density of the DCP, MCC and mannitol are 2.890, 1.670, and 1.514 g/cm^3 respectively. It could be seen from Figure 6.23 and Figure 6.24 that there is no clear relationship between the apparent density of the tablets and their T$_{90}$, which suggest that the difference in the T$_{90}$ of the tablets presented in Figure 6.23 is related to the solubility and the hydrophilicity/hydrophobicity of the materials used. Also, it was found that the MCC/DCP formulations have the larger T$_{90}$ value compared with the MCC/mannitol formulations.

6.5 Conclusion

The change in tabletability after granulation of nine formulations was investigated. The tablet strength of the granulated materials was compared with the tablet strength of the direct compression tablets of the same formulation. The formulations consist of binary mixtures prepared with different ratios of MCC, mannitol and DCP.

An inverse relationship between ΔTS and the plasticity of the primary powder was found which enables quantitative prediction of ΔTS after granulation.

In addition, the SSA*MC % model was also used to predict the tablet strength of nine granulated formulations that were compressed at 44, 88, and 175 MPa. The results showed that the model is valid at the studied compression pressures and can provide quantitative prediction of the tablet tensile strength.

The dissolution of the granulated materials was also investigated. It was found that the dissolution rate of the formulations which have mannitol (water soluble material), was independent from the percentage of the MCC to mannitol when compressed at 44 and 88 MPa. However, a significant delay was seen for the formulation that has a low ratio of mannitol (20%) when compressed at 175 MPa.

In conclusion, adding a brittle material such as mannitol or DCP to a plastically deformable material such as MCC can reduce the loss of tabletability after granulation. When a high proportion of brittle material is used, an improvement in the tabletability can be noticed. The water solubility and hydrophobicity of the added brittle material can impact the dissolution behaviour of the tablets. Selecting a water soluble material like mannitol leads to a relatively fast/instant dissolution rate compared with a non-water soluble material like DCP.

Chapter 7   Modelling of the Granulation and Tabletting Processes: Artificial Neural Network

Artificial neural network (ANN) is a powerful tool that can capture complex patterns and highly nonlinear relationships in an available data set that was collected from a process. Therefore, ANN has been used in several areas of science such as analytical chemistry, biomedical and powder technology [149,154]. Recently, ANN has been used in the field of processing powders, granules, and tablets [148,155–157]. This chapter aims to build and validate a fast, robust and accurate artificial neural network which can be used in a versatile way to predict the quality attributes of granules and tablets.

7.1   Methodology

7.1.1   Granulation

Microcrystalline cellulose (MCC, Avicel PH 101) was granulated using TSG, as described in section 3.2.3. Deionised water was used as a liquid binder. The screw configuration, which consists of conveying and kneading elements, was considered as an input parameter in addition to three other parameters, namely; liquid to solid (L/S) ratio, feed rate and speed, as presented in Table 7.1. Several input parameters can affect the TSG process. However, the aforementioned parameters have the most significant effect on the granule properties [4,184]. 36 experiments were conducted based on a full factorial design of experiments. Once each experiment was completed, the produced granules were left to dry at room temperature as described in section 3.2.4. The D values (D_{10}, D_{50}, and D_{90}) of the granules were measured as described in section 3.2.5.1.

Table 7.1 The investigated input parameters of the twin screw granulation process.

Inputs	Inputs' levels
Feed rate	1 and 4 (Kg/h)
Liquid to solid ratio	0.94 and 1.25
Screw speed	250, 500, and 750 (rpm)
Screw configuration	Conveying, conveying and 16 kneading elements, and conveying and 32 kneading elements

7.2   Results & discussion

7.2.1   Prediction of the granule size distribution

7.2.1.1 Statistical analysis

A correlation test (Pearson correlation)[4] between the inputs and the outputs was performed, the results for the granules D values are presented in Table 7.2. The results show that there is a correlation between few of the inputs and the outputs. L/S ratio has the highest R^2 value, which suggests that it has the strongest correlation with the outputs compared with the other inputs. The screw configuration has an inverse relationship with the output as well as the screw speed.

Table 7.2 Pearson correlation test between the inputs and the outputs. R^2 is used to express the degree of the correlation.

Output	Input			
	Liquid to solid ratio	Feed rate	Screw configuration	Screw speed
D_{10}	0.79	0.17	-0.10	-0.10
D_{50}	0.61	0.28	-0.12	-0.03
D_{90}	0.23	0.24	-.044	-0.08

7.2.1.2 Regression analysis

Linear regression was conducted to predict the D-values of the granule size (D_{10}, D_{50}, and D_{90}). Design expert which is a statistical software (version11, stat-Ease, USA) was used to develop a simple linear model to predict the D values of the granules.

The linear regression equations are presented in the Table 7.3. Analysis of variance (ANOVA) testing was performed to determine the significance of the terms for the linear model. The inputs with P values greater than 0.1 were not considered significant, and therefore were not included in the model. The L/S ratio and the feed rate were significant inputs for the D_{10} and $D_{50,}$ while the former inputs as well as the screw configuration were

---

[4] Pearson's correlation is used to access the strength and the direction of the association between two variables. It reflects the strength of a linear relationship between the compared variables.-1and +1 reflect perfect linear relationship while zero indicates no relationship.

significant inputs for the D_{90}. The higher the magnitude of the coefficient of the term, the more significant the term in the model in the studied granulation space. The most influential term of the model in predicting D_{10}, D_{50}, and D_{90} is the L/S ratio.

Table 7.3 The prediction equations of the linear regression for the granule D values.

output	Equation
D_{10}	$D_{10}=-498+649.3\text{L/S ratio}+14.33\text{Feed rate}$
D_{50}	$D_{50}=-154+792.13\text{L/S ratio}+38.17\text{Feed rate}$
D_{90}	$D_{90}=+1096+574.39\text{L/S ratio}+61.87\text{Feed rate}-203.22\text{screw configuration}$

The performance of the linear regression, the results of which are shown in Table 7.4, indicates that the linear model failed to accurately predict the granules size represented by the D-values, which means that the relationships between the granulation input parameters and the granule size are not linear. Therefore, there is a strong need to develop a more complex model to represent these nonlinear relationships.

Table 7.4 The performance (predicted R^2) of the regression analysis for the D-values of the granules (D_{10}, D_{50}, and D_{90}).

Model	D_{10}	D_{50}	D_{90}
Linear	0.57	0.28	0.07
Non linear	0.58	0.35	0.18

The nonlinear regression considers the significance of the inputs and their interactions. The terms of the model describing the influence of the granulation process on the D values of the granule size are given in Table 7.5. The higher the magnitude of the coefficient of the term, the more significant the term in the model in the studied granulation range. For example, the most influential term of the model in predicting D_{10} and D_{50} is the L/S ratio and the least significance is the screw speed, while for D_{90} the screw configuration[2] is most significant term in the model with the highest coefficient, and the screw speed is the least significant term. The equations of the nonlinear regression are presented in Table 7.5.

Table 7.5 The prediction equations of the nonlinear regression for the granule D values.

output	Equation
D_{10}	D_{10}=-980+1049.57 L/S ratio-41.09Feed rate+208.32screw configuration+1screw speed+83.94L/S ratio x Feed rate-205.18L/S ratio x screw configuration-0.81L/S ratio x screw speed-0.07feed rate x screw speed
D_{50}	D_{50}=-18+741.16L/S ratio-186.93Feed rate-702.68screw configuration+1.96screw speed+205.57L/S ratio x feed rate+453.14L/S ratio x screw configuration-1.83L/S ratio x screw speed+87.34screw configuration^2
D_{90}	D_{90}=+1505+355.08L/S ratio-407.25Feed rate-1549.21screw configuration+3.35screw speed+428.42L/S ratio x feed rate+755.72L/S ratio x screw configuration-3.21L/S ratio x screw speed+259.23screw configuration^2

The performance of the linear and the multi nonlinear regression is similar and reflect low capability for both regressions to enable accurate prediction of the D values.

7.2.1.3 Artificial neural network

7.2.1.3.1 Building the network

Matlab R2016a was used to develop an ANN model to predict the granule size represented by its D values. The ANN was developed using the NN toolbox. The liquid to solid (L/S) ratio, feed rate, screw speed and screw configurations were defined as inputs as presented in Table 7.1, whereas the granule size expressed by the main three diameters (D_{10}, D_{50}, and D_{90}) was considered as an output. In order to improve the network training process, the data were normalised (minimum maximum method) and then randomised.

A feedforward neural network was used. The network was first made of one hidden layer then adjustment was made to add a second hidden layer. The ANN consists of three layers, namely, the input layer, two hidden layers, and an output layer as presented in Figure 7.1
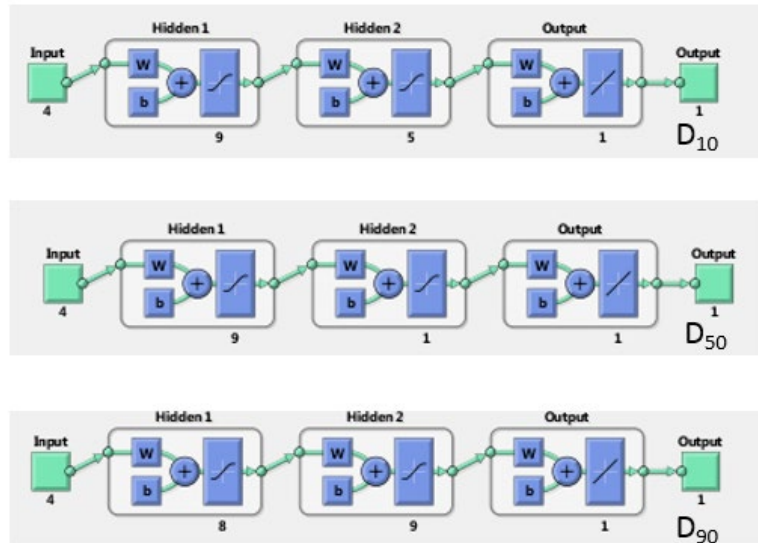
Figure 7.1 The best neural network topography for D10, D50, and D90 of the microcrystalline cellulose granules produced using Twin screw granulator.

The best number of hidden neurons corresponds to the minimum error measured via the mean square error (MSE)[5]. A scaled conjugate gradient algorithm was utilized in this research work. The data were divided into three sets, namely, training (70%), validation (15%) and testing (15%) sets. The training data allows the model to learn the relationship between the inputs and outputs. While the validation data helps in adjusting the weights associated with the inputs. The testing data set is used to assess the model generalisation.

Figure 7.2 presents the performance of the ANN (one hidden layer) in predicting the D_{10} of the granule size. The R values for the training, validation, testing and all points vary are in the range of 0.57-0.94, which reflect a not strong correlation between the output and the target values. The MSEs and their corresponding epoch numbers (i.e. forward and backward calculations) [185] for the best ANN for each output are presented in Appendix F.

---

[5] The mean square error (MSE) is the average squared difference between the estimated vale and what is estimated.
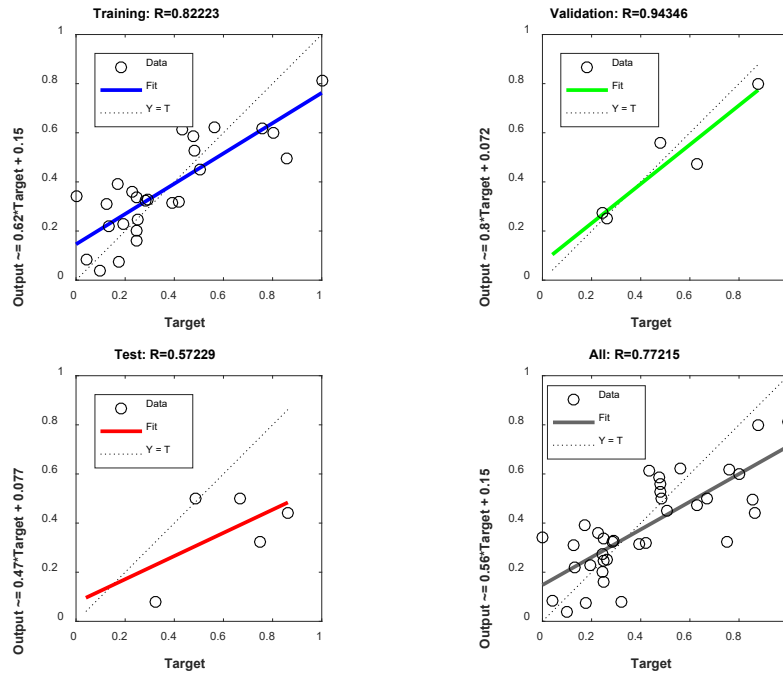
Figure 7.2 The performance of the neural network used to predict the D_{10} of the granules size. The performance is presented as R value (correlation coefficient).

The results of the prediction of the D_{50} are presented in Figure 7.3. The R value of the performance of the training, validation and testing varies between 0.57-0.94. The performance of the ANN to predict the D_{90} is presented in Figure 7.4, which lower than the previous two networks. By comparing the performance of the regression analysis and the performance of the single layer ANN, it could be seen that the performance of the ANN (D_{10} and D_{50}) is higher than the performance of the linear and nonlinear regression as presented in Table 7.6. The performance of the ANN was approximately 35 % higher for the prediction of D_{10} compared with the regression analysis, and approximately 95 % higher for D_{90}. However, both the performance of the single layer ANN and the regression were similar and no high enough to provide accurate prediction.
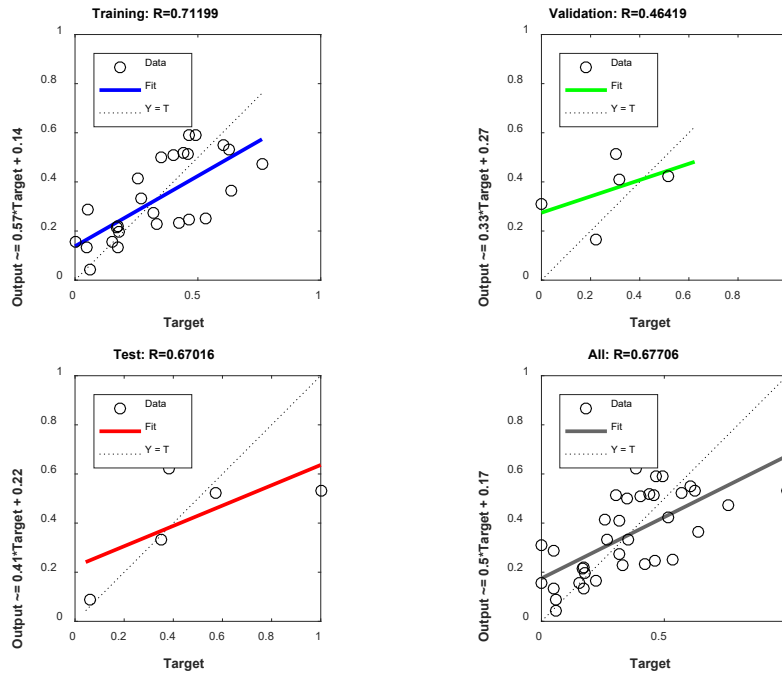
Figure 7.3 The performance of the neural network used to predict the D_{50} of the granules size. The performance is presented as R value (correlation coefficient).
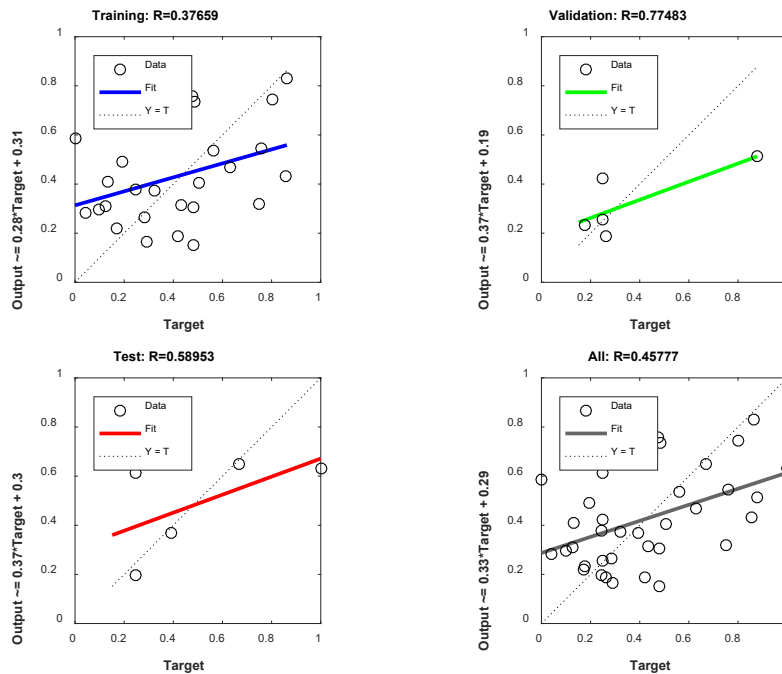
Figure 7.4 The performance of the neural network used to predict the D_{90} of the granules size. The performance is presented as R value (correlation coefficient).

Table 7.6 performance (R^2) of the regression analysis and single layer neural network to predict the granule D values.

	R^2 ANN(validation)	R^2 (predicted) Linear	R^2 (predicted) nonlinear
D_{10}	0.89	0.57	0.58
D_{50}	0.21	0.28	0.35
D_{90}	0.60	0.07	0.18

To improve the prediction performance of the neural network with one hidden layer, a neural network with two hidden layers was implemented, where the outputs of the first hidden layer are used as inputs to the second hidden layer. The numbers of hidden neurons are the ones that correspond to the minimum error measured via the mean square error and good generalization capabilities. Different values for the connecting coefficients were randomly initialized and then optimized using scaled conjugate gradient algorithm.

The results of the outputs D_{10}, D_{50}, and D_{90} are presented in figures 7.5, 7.6, and 7.7 respectively. The performance (R value) of the training, validation and testing from the previous Figures (7.5-7.7) are high, with range of R value from 0.80-0.99. The MSEs and their corresponding epoch numbers for the best ANN for each output are presented in Appendix F.
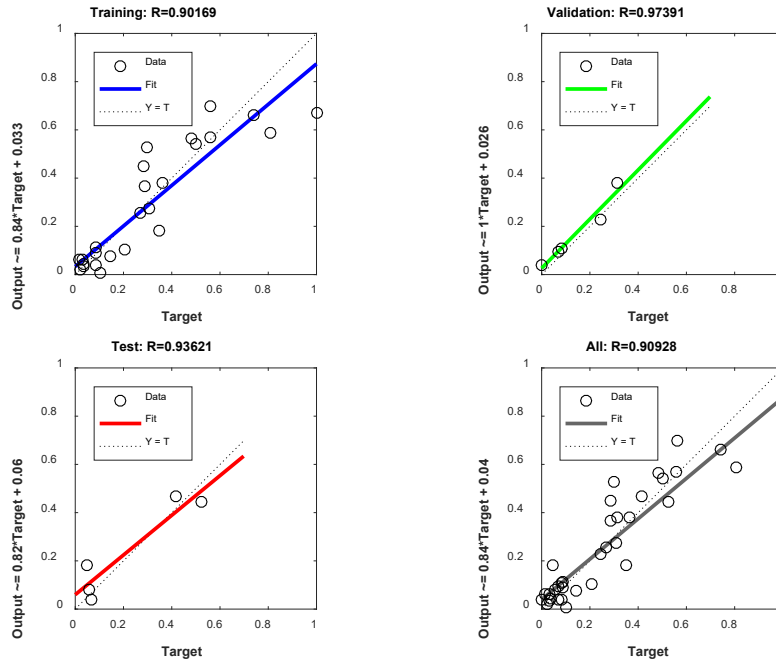
Figure 7.5 The performance of the neural network (two hidden layers) used to predict the D_{10} of the granules size. The performance is presented as R value (correlation coefficient).
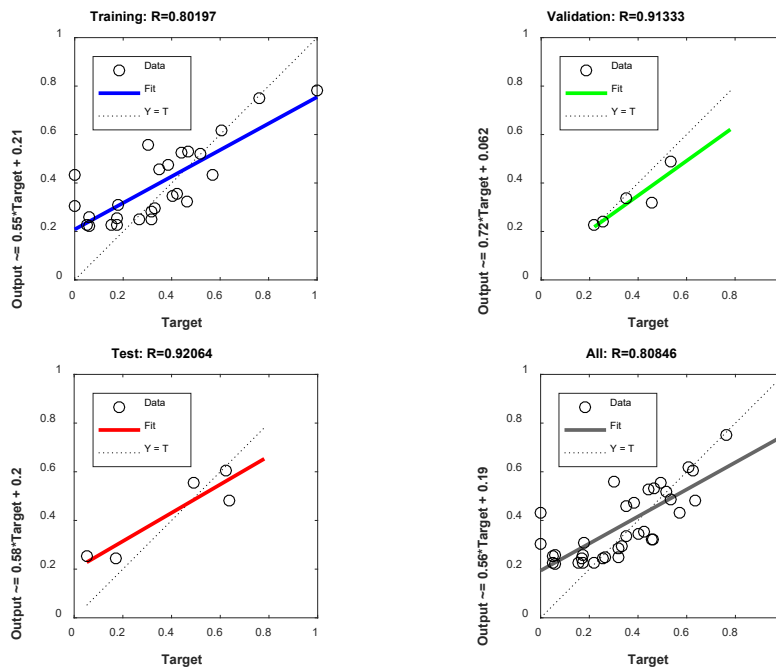
Figure 7.6 The performance of the neural network (two hidden layers) used to predict the D_{50} of the granules size. The performance is presented as R value (correlation coefficient).
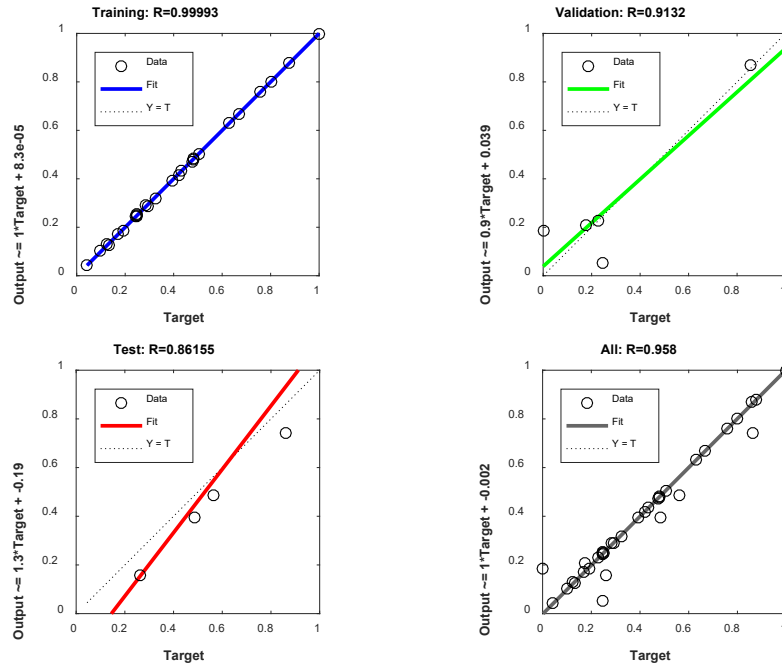
Figure 7.7 The performance of the neural network (two hidden layers) used to predict the D_{90} of the granules size. The performance is presented as R value (correlation coefficient).

The developed ANN with two hidden neurons are capable of predicting the granule size represented by the D_{10}, D_{50}, and D_{90} with small values of RMSE and high R^2 values as presented in Table 7.7. The performance of the 2 hidden layer is superior to the other prediction methods. From Table 7.7, it can be seen that the performance of the two hidden ANN is better than the single hidden layer ANN. The prediction of the D_{10} improved by adding a second hidden layer, it could be seen that the R^2 of the training, validation, testing, and all the points increased. The same observation is notised for the D_{50}, and D_{90}.

Table 7.7 The performance (R^2)of the one hidden layer, two hidden layer neural network, linear regression and nonlinear regression to predict the granule size represented by the D_{10}, D_{50}, and D_{90}. The

Output	One hidden layer				Two hidden layers				(predicted) Linear	(predicted) nonlinear
D10	0.68	0.89	0.33	0.60	0.81	0.95	0.88	0.83	0.57	0.58
D50	0.51	0.22	0.45	0.46	0.64	0.83	0.85	0.65	0.28	0.35
D90	0.14	0.60	0.35	0.21	1.00	0.83	0.74	0.92	0.07	0.18

The RMSE of the developed ANNs is similar to work done by Shirazian et al. on the prediction of the granules size (D_{10}, D_{50}, and D_{90}) of twin screw granulated MCC. R^2 values of Shirazian's work are higher than the ones presented in this work, due to the use of a boosting approach to the model, another reason could be due to difference in the data sets [148]. Boosting is used to build larger additive ANN models by fitting a series of smaller models. Shirazian et al. used 15 sub network with two neurons in each hidden layer in order to boost the performance of the ANN. Although the R^2 value from Shirazian's work are higher than the reported results in this work, however both have very similar RMSE. The RMSE indicates how close the predicted value to the real values are. Which could suggest similar performance in terms of the prediction error.

Table 7.8 Comparison between the performances reported results and the literature in predicting the D values of granules made by twin screw granulation.

Output	R^2 (validation)	RSME (Validation)	R^2 (Validation)	RSME (Validation)
D10	0.95	10.65	0.99	11.57
D50	0.83	22.32	0.99	22.05
D90	0.83	33.21	0.99	33.78

*The unit of the route mean square error (RMSE) values is μm.

7.2.2 Prediction of tablet tensile strength

To build a prediction model for the tablet strength, the tablet tensile strength of 49 experiments from chapter five were used. Seven attributes of the compressed materials were considered as an input, and the tablet tensile strength was considered as an output as presented in Table 7.9.

Table 7.9 inputs and output used for building a prediction model for the tablet tensile strength.

Experiment number	Output	Inputs						
	Tablet tensile strength (MPa)	specific surface area (m²/g)	Total work (milli joule)	Moisture content (% w/w)	Plastic work (milli joule)	Elastic work (milli joule)	Elastic work/Plastic work	specific surface area* Moisture content %
1	1.63	0.89	11.91	5.30	10.52	1.39	0.13	4.69
2	0.68	0.28	10.44	5.90	9.04	1.40	0.15	1.63
3	0.67	0.26	10.56	5.39	9.09	1.47	0.16	1.38

Experiment number	Output	Inputs						
	Tablet tensile strength (MPa)	specific surface area (m²/g)	Total work (milli joule)	Moisture content (% w/w)	Plastic work (milli joule)	Elastic work (milli joule)	Elastic work/Plastic work	specific surface area* Moisture content %
4	1.58	0.93	12.13	5.20	10.71	1.41	0.13	4.86
5	0.81	0.33	10.59	5.65	9.29	1.43	0.15	1.84
6	0.69	0.29	10.60	5.47	9.25	1.35	0.15	1.59
7	1.73	1.19	11.18	5.54	9.70	1.48	0.15	6.61
8	0.76	0.26	10.27	5.87	8.94	1.33	0.15	1.50
9	0.72	0.24	10.27	5.94	8.82	1.46	0.16	1.44
10	1.90	0.97	11.31	5.01	9.77	1.54	0.16	4.84
11	0.69	0.23	10.40	5.42	9.03	1.36	0.15	1.27
12	0.68	0.23	10.38	5.34	8.94	1.44	0.16	1.21
13	1.30	0.75	12.06	5.70	10.75	1.31	0.12	4.27
14	0.70	0.29	10.39	5.98	9.05	1.34	0.15	1.74
15	0.73	0.28	10.41	5.89	9.07	1.34	0.15	1.64
16	1.22	0.85	12.65	5.43	11.25	1.41	0.13	4.60
17	0.74	0.34	10.64	5.48	9.29	1.35	0.14	1.84
18	0.67	0.32	10.56	5.93	9.15	1.41	0.15	1.92
19	1.51	0.95	11.16	5.43	9.80	1.36	0.14	5.19
20	0.76	0.29	10.18	5.63	8.87	1.31	0.15	1.63
21	0.82	0.28	10.49	6.19	9.41	1.08	0.11	1.72
22	1.49	0.77	12.30	5.55	10.81	1.50	0.14	4.29
23	0.70	0.27	10.52	5.84	9.11	1.41	0.16	1.57
24	0.70	0.27	10.33	5.94	8.94	1.39	0.16	1.63
25	2.47	0.94	12.02	4.65	10.64	1.38	0.13	4.37
26	3.22	1.97	10.46	3.68	8.93	1.53	0.17	7.24
27	2.45	1.10	13.18	4.04	11.60	1.58	0.14	4.45
28	2.48	0.94	12.67	4.75	11.14	1.53	0.14	4.48
29	0.20	1.03	5.40	0.11	4.12	1.28	0.31	0.11
30	0.22	0.99	5.57	0.28	4.29	1.28	0.30	0.27
31	0.14	0.58	5.61	0.21	4.40	1.22	0.28	0.12
32	0.12	0.36	5.61	0.18	4.40	1.22	0.28	0.06
33	0.18	0.86	5.31	0.23	4.06	1.25	0.31	0.20
34	0.17	0.96	5.49	0.17	4.10	1.39	0.34	0.16
35	0.13	0.28	5.39	0.19	4.18	1.21	0.29	0.05

Experiment number	Output	Inputs						
	Tablet tensile strength (MPa)	specific surface area (m²/g)	Total work (milli joule)	Moisture content (% w/w)	Plastic work (milli joule)	Elastic work (milli joule)	Elastic work/Plastic work	specific surface area* Moisture content %
36	0.18	0.76	5.29	0.31	4.02	1.27	0.32	0.24
37	0.17	0.87	5.52	0.15	4.11	1.41	0.34	0.13
38	0.16	1.66	4.59	0.08	3.25	1.34	0.41	0.13
39	0.28	1.86	7.78	0.34	6.41	1.37	0.21	0.63
40	0.34	0.84	6.50	0.53	5.19	1.31	0.25	0.45
41	0.23	0.40	6.26	0.43	4.97	1.29	0.26	0.17
42	0.78	0.40	9.30	2.86	7.98	1.34	0.17	1.15
43	0.87	0.33	8.76	2.83	7.41	1.34	0.18	0.94
44	0.83	0.15	11.18	9.49	9.74	1.44	0.15	1.39
45	1.67	0.15	6.28	17.95	4.58	1.87	0.41	2.63
46	2.47	0.94	12.02	4.65	10.64	1.38	0.13	4.37
47	3.22	1.97	10.46	3.68	8.93	1.53	0.17	7.24
48	2.45	1.10	13.18	4.04	11.60	1.58	0.14	4.45
49	2.48	0.94	12.67	4.75	11.14	1.53	0.14	4.48

7.2.2.1 Statistical analysis

A correlation test (Pearson correlation) between the inputs and the outputs was performed, the results are presented in Table 7.10. The results show that there is a correlation between the inputs and the outputs. The highest correlation is between the tablet tensile strength and the specific surface area multiplied by the moisture content (SSA*MC %).

Table 7.10 Pearson correlation test between the inputs and the outputs. R^2 is used to express the degree of the correlation.

Output	Input						
	specific surface area (m²/g)	Total work of compaction (milli joule)	Moisture content (% w/w)	Plastic work (milli joule)	Elastic work (milli joule)	Elastic work/Plastic work	specific surface area* Moisture content %
Tablet tensile strength	0.46	0.69	0.37	0.67	0.62	-0.49	0.92

7.2.2.2 Regression analysis

Linear and non-linear Regressing analysis was conducted to predict the tablet tensile strength. Statistical software (Design expert, version11, stat-Ease, USA) was used to conduct the regression analysis. The R^2 of the regression analysis is approximately 0.84 for the linear and 0.37 for the nonlinear regression, hence, the linear regression performance was superior to the nonlinear regression. The equations of the linear regression are presented in Table 7.11. ANOVA testing was performed to determine the significance of the terms on the linear model. The inputs with P values greater than 0.1 were not considered significant, and therefore were not included in the model. Only three terms were significant for the linear regression model, while more terms were found to be significant for the nonlinear regression as seen in Table 7.11.

Table 7.11 The prediction equations of the linear and nonlinear regression for the tablet strength.

output	Equation
Linear regression	Tablet strength=-0.65+0.04Total work of compaction+0.65 Elastic work+0.12 specific surface area* Moisture content
nonlinear regression	Tablet strength=-1.48+0.55 Total work of compaction-0.09 Moisture content+7.12E/P-2.93Elastic work+1.40 specific surface area x Moisture content+2.80 (specific surface area x Moisture content)/ plastic work-0005 Total work of compaction x Moisture content+12.00E/P x (specific surface area x Moisture content)/ plastic work+0.79Elastic work x (specific surface area x Moisture content)

7.2.2.3 Artificial neural network

Two layers artificial neural network was implanted to predict the tablet strength. The first hidden layer was made of six neurons and the second layer contained eight hidden neurons. The best number of hidden neurons corresponds to the minimum error measured via the mean square error (MSE). A scaled conjugate gradient algorithm was utilized in this research work. The data were divided into three sets, namely, training (70%), validation (15%) and testing (15%) sets.

The results of the two hidden layer ANN for predicting the tablet strength are presented in Figure 7.8. The R value of the validations process was 0.75 with RMSE of 0.22 (MPa).
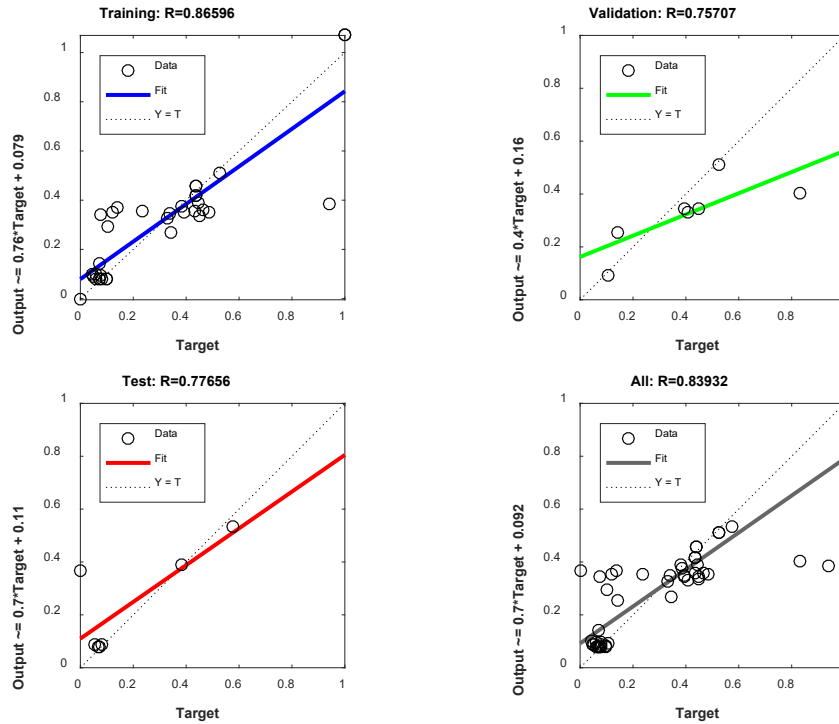
Figure 7.8 Output and target values of the tablet tensile strength based on the analysis of artificial neural network using two hidden layers.

In the previous chapter, it was found that the multiplication of the specific surface area available for bonding by the moisture content (SSA*MC %) of the compressed material is in a linear relationship with the tablet strength. Based on the previous finding, ANN with two layers was used to predict the tablet tensile strength, where by the value of SSA*MC% was used as an input for the 49 experiments. The results of the ANN are presented in Figure 7.9. The performance of the model was better compared with ANN when the seven inputs were used. The R of the validation process for the network using 7 inputs is 0.75 with and the RMSE was 0.22 (MPa) while the R of the validation process was 0.99 and the RMSE was 0.12 (MPa) when SSA*MC% was used an input. The improvement in the performance in the prediction of the tablet strength when only SSA*MC % was used as an input reflect the importance of the selection of the processed inputs. As shown earlier the term SSA*MC was the most significant as presented in Table 7.10. In addition, the previous observation supports the finding from Figure 5.6.

144
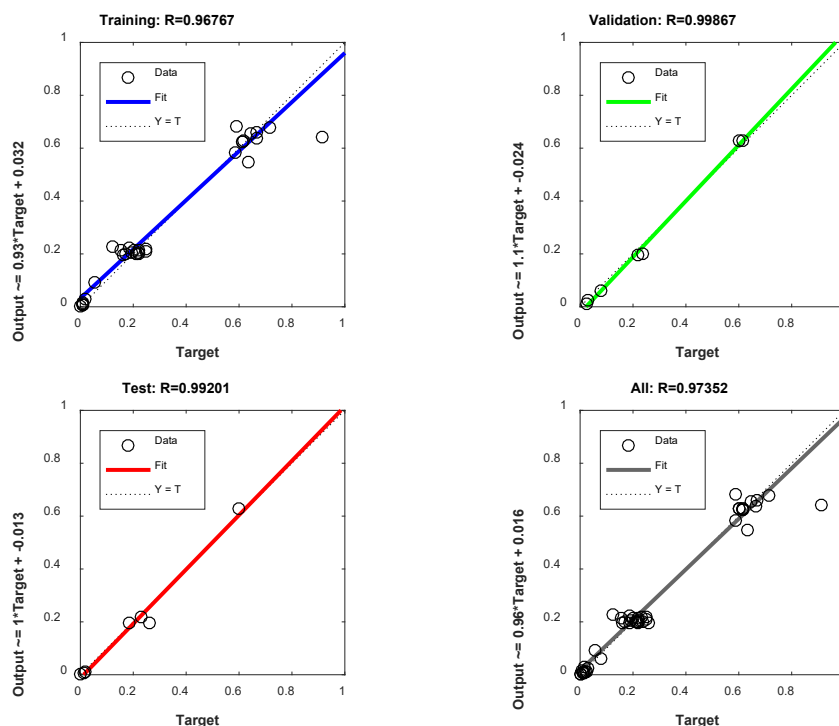
Figure 7.9 The artificial neural network based on two hidden neurons for the tablets tensile strength as an output and the specific surface area* moisture content as input.

The developed ANNs presented to be more accurate than other ANNs used to predict tablet strength, such as the work done by Bourquin et al. in which the maximum R^2 value for tablet strength was 0.86 [186]. Kesavan et al., applied ANN to predict the tablet strength of wet granulated materials using high shear mixer. It was found that the designed neural network produced less accurate than the one designed in this work, the values of the R^2 are 0.70 and 0.98 respectively [162]. One reason for this improvement in the performance of the ANN is the topography of the network and the optimisation method of the number of neurons in each layer as Kesavan et al. used one layer network [162]. More reasonable explanation for the improved performance of the presented work could be due to the relevance of the selected inputs which correlate well to the tabletability of the material such as the SSA and work of compaction, while the inputs in Kesavan work was less relevant such as the bulk density , tap density and particle size. In another work Bourquin et al., predicted the tablet crushing force using two ANN models (R^2 0.85, 0.91) which are lower than the presented results [187].

7.3 Conclusion

The utilised artificial neural network using two hidden layers has shown to be suitable for quantitative prediction of the granules size distribution represented by the D_{10}, D_{50}, and D_{90} and the tablet tensile strength. The performance for both outputs was acceptable and compared with the literature. Neural networks can provide accurate, quick, and cost-effective predictive tools especially when the mechanistic understanding is not fully developed. The implemented methodology could be useful in predicting other granule attributes such as flowability, and granule strength.

Chapter 8   Summary, Conclusion and Future Work

8.1   Summary

The main outcomes of this research are:

- Investigating the effect of the mechanical properties of primary powder/ mixtures on the attributes of the granules and the tablet strength.
- Defining the mechanisms that could lead to a decrease or increase in tabletability after twin screw granulation.
- Presenting solutions for loss of tabletability after granulation by using brittle materials.
- Developing a predictive model/approach for tablet strength based on specific surface area available for bonding and the percentage of the moisture content of the compressed materials.
- Assessing the applicability of artificial neural network in prdicting the granule size and tablet strength.

8.2   Conclusions

In the first experimental chapter (chapter four) the effect of the mechanical properties of the primary powder on the tabletability of twin screw granulated materials was investigated. The main conclusions from chapter four are:

- A quantitative prediction of the tablet strength of materials (both granulated and primary) has been developed based on measuring the yield pressure.

- A regime map presenting the potential for improved or reduced tablet tensile strength following granulation was proposed. The materials included in the map were classified by the yield pressure of the primary powder.

- Some materials such as MCC and spray dried sugars should be teamed with low-energy granulation processes (using conveying elements) to reduce the loss of tabletability after granulation; While some materials such as soluble, crystalline

mannitol should be teamed with high-energy granulation processes (using kneading elements) – since granulation can improve their compaction behaviour.

Chapter five investigated the effect of specific surface area and moisture content on tablet tensile strength of the compressed materials:

- The presented results show that the SSA*MC% of granulated and non-granulated materials can be used to predict the tablet tensile strength for a range of mechanically different materials.

Chapter six further investigated the model proposed in chapter five by studying several formulations that differ in the mechanical properties and water solubility. The main findings in this chapter are:

- Changing the plasticity of a formulation, by changing the ratio of plastically deformable material to brittle material in a formulation can be used to control the change in tabletability after granulation.
- The plasticity of a formulation could be used for quantitative prediction of the change in tablet strength after granulation.
- The SSA*MC% approach/model was successfully able to predict the change in the tabletability behaviour of mechanically different formulations after wet granulation using TSG. The approach was valid at a range of tablet compression pressures (44-175 MPa).

The conclusion from chapter seven is:

- The artificial neural network can be implemented to predict the size of granules made by TSG. Additionally it can successfully predict with high accuracy the tablet tensile strength of powders or granules (R^2 0.99).

8.3 Future work

8.3.1 Impact of the granulation stresses on the hardness of the granulated materials

In this work the loss of tabletability was investigated to define the significant contributors to the change in tabletability either in a positive or a negative way. Based on the materials and the methodology used in this work it was concluded that the change in the specific surface area available for bonding leads to loss or improvement in the tabletability. In addition, dense granules will result in weaker tablets compared with porous granules. The available literature has not answered an important question which is: does wet granulation lead to a change in the hardness of the material? The concept of the change of tabletability after wet granulation could be further investigated by performing nano-indentation to the primary powder, and the granules to detect any changes in the hardness of the single particle or crystal. This method could differentiate between the densification of the granulated materials due to granulation, which makes the granules denser and stronger, and any possible changes in the hardness of the materials itself due to plastic deformation.

8.3.2 Improving the proposed SSA*MC% approach/model

The SSA*MC% approach was developed based on thorough controlled experiments and a deep understanding of the mechanisms of tablet formation. Even though the suggested model showed good predictive capabilities, there is still room for further improvements. The effect of varying moisture content by conditioning the powders and the granules at different relative humidity could improve the predictive capabilities of the model. Additionally, the model could be more improved by:

- Investigating the effect of the surface energy of the primary powder by examining a range of materials that have different surface energy and its interaction with relative humidity. This approach will enable making evidence based conclusions about the significance of the surface energy in the tabletability behaviour of materials. Inverse gas chromatography could be used as a method to measure the surface energy of powders at of relative humidity.

- Investigating the relationship between the hardness of the compressed material or granules (using nanoindentation) with relative humidity and the ability of the materials to uptake moister. If a relationship was found between the ability of a

material to uptake moisture and its hardness, this would provide a very simple, cheap and fast approach to get an initial understanding of the mechanical properties of a material.

- Measuring the difference between the surface area available for bonding and the surface area after compression at different compression pressures and relative humidity. This will help to deconvolute the effect of SSA, moisture content, and compression pressures on the tablet tensile strength.

- Investigating the interaction between hydrophobic and hydrophilic lubricants on the amount of moisture content within the compressed materials which could be a potential mitigation strategy to control the tablet strength.

- Using modelling capabilities such as discrete element method (DEM) to further investigate the DAWB model and compare it with the experimental data. This approach will enhance the understanding of the role of water content/ capillary forces in the overall magnitude of tablet strength.

8.3.3 Improving the artificial neural network

- ANN can be coupled with other modelling approaches such as neuro fuzzy logic. The combination enables the generation of rule sets representing the cause-effect relationships contained in the analysed data.

References

[1]   R.M. Dhenge, Twin screw granulation : A detailed study, University of Sheffield, 2012.

[2]   J.B. Ennis, Theory of Granulation : An Engineering Perspective, in: D. Parikh (Ed.), Handbook of Pharmaceutical Granulation Technology, Informa, 2010.

[3]   M. Aulton, Dissolution and Solubility, in: Aulton's Pharmaceutics [Electronic Resource] : The Design and Manufacture of Medicines, Fourth, London, 2013.

[4]   R.M. Dhenge, J.J. Cartwright, M.J. Hounslow, A.D. Salman, Twin screw granulation: steps in granule growth., International Journal of Pharmaceutics. 438 (2012) 20–32.

[5]   R.M. Dhenge, K. Washino, J.J. Cartwright, M.J. Hounslow, A.D. Salman, Twin screw granulation using conveying screws: Effects of viscosity of granulation liquids and flow of powders, Powder Technology. 238 (2013).

[6]   R.M. Dhenge, J.J. Cartwright, M.J. Hounslow, A.D. Salman, Twin screw wet granulation: Effects of properties of granulation liquid, Powder Technology. 229 (2012).

[7]   R.M. Dhenge, J.J. Cartwright, M.J. Hounslow, A.D. Salman, Twin screw wet granulation: Effects of properties of granulation liquid, Powder Technology. 229 (2012) 126–136.

[8]   W. Da Tu, A. Ingram, J. Seville, Regime map development for continuous twin screw granulation, Chemical Engineering Science. 87 (2013) 315–326.

[9]   A. Kumar, J. Dhondt, J. Vercruysse, F. De Leersnyder, V. Vanhoorne, C. Vervaet, J.P. Remon, K. V. Gernaey, T. De Beer, I. Nopens, Development of a process map: A step towards a regime map for steady-state high shear wet twin screw granulation, Powder Technology. 300 (2015) 73–82.

[10]   R.M. Dhenge, K. Washino, J.J. Cartwright, M.J. Hounslow, A.D. Salman, Twin screw granulation using conveying screws: Effects of viscosity of granulation liquids and flow of powders, Powder Technology. 238 (2013) 77–90.

[11] K.T. Lee, A. Ingram, N.A. Rowson, Comparison of granule properties produced using Twin Screw Extruder and High Shear Mixer: A step towards understanding the mechanism of twin screw wet granulation, Powder Technology. 238 (2013) 91–98.

[12] C. Mangwandi, M.J. Adams, M.J. Hounslow, A.D. Salman, Effect of impeller speed on mechanical and dissolution properties of high-shear granules, Chemical Engineering Journal. 164 (2010) 305–315.

[13] R.M. Dhenge, J.J. Cartwright, D.G. Doughty, M.J. Hounslow, A.D. Salman, Twin screw wet granulation: Effect of powder feed rate, Advanced Powder Technology. 22 (2011) 162–166.

[14] D. Djuric, P. Kleinebudde, Impact of Screw Elements on Continuous Granulation With a Twin-Screw Extruder, Pharmaceutical Technology. 97 (2008) 4934–4942.

[15] K. Lee, Continuous granulation of pharmaceutical powder using a twin screw granulator, University Of Birmingham, 2013.

[16] E.. Keleb, A. Vermeire, C. Vervaet, J.. Remon, Continuous twin screw extrusion for the wet granulation of lactose, International Journal of Pharmaceutics. 239 (2002) 69–80.

[17] E.I. Keleb, A. Vermeire, C. Vervaet, J.P. Remon, Twin screw granulation as a simple and efficient tool for continuous wet granulation., International Journal of Pharmaceutics. 273 (2004) 183–94.

[18] D. Djuric, B. Van Melkebeke, P. Kleinebudde, J.P. Remon, C. Vervaet, Comparison of two twin-screw extruders for continuous granulation., European Journal of Pharmaceutics and Biopharmaceutics. 71 (2009) 155–60.

[19] J. Vercruysse, M. Toiviainen, M. Fonteyne, N. Helkimo, J. Ketolainen, M. Juuti, U. Delaet, I. Van Assche, J.P. Remon, C. Vervaet, T. De Beer, Visualization and understanding of the granulation liquid mixing and distribution during continuous twin screw granulation using NIR chemical imaging., European Journal of Pharmaceutics and Biopharmaceutics. 86 (2014) 383–92.

[20] S. V Lute, R.M. Dhenge, Twin Screw Granulation : Effects of Properties of

Primary Powders, Pharmaceutics. 10 (2018) 68.

[21] M. Fonteyne, A. Correia, S. De Plecker, J. Vercruysse, I. Ilić, Q. Zhou, C. Vervaet, J.P. Remon, F. Onofre, V. Bulone, T. De Beer, Impact of microcrystalline cellulose material attributes: a case study on continuous twin screw granulation., International Journal of Pharmaceutics. 478 (2015) 705–17.

[22] T. Schaefer, C. Mathiesen, Melt pelletization in a high shearmixer. IX. Effects of binder particle size, International Journal of Pharmaceutics. 139 (1996) 139–148.

[23] R.M. Dhenge, R.S. Fyles, J.J. Cartwright, D.G. Doughty, M.J. Hounslow, A.D. Salman, Twin screw wet granulation: Granule properties, Chemical Engineering Journal. 164 (2010) 322–329.

[24] M.F. Saleh, R.M. Dhenge, J.J. Cartwright, M.J. Hounslow, A.D. Salman, Twin screw wet granulation: Binder delivery., International Journal of Pharmaceutics. 487 (2015) 124–34.

[25] B. Johansson, G. Alderborn, The effect of shape and porosity on the compression behaviour and tablet forming ability of granular materials formed from microcrystalline cellulose, European Journal of Pharmaceutics and Biopharmaceutics. 52 (2001) 347–357.

[26] H. Ma, G.P. Andrews, D.S. Jones, G.M. Walker, Low shear granulation of pharmaceutical powders: Effect of formulation on granulation and tablet properties, Chemical Engineering Journal. 164 (2010) 442–448.

[27] C. Mangwandi, M.J. Adams, M.J. Hounslow, A.D. Salman, Effect of batch size on mechanical properties of granules in high shear granulation, Powder Technology. 206 (2011) 44–52.

[28] J. Vercruysse, D. Córdoba Díaz, E. Peeters, M. Fonteyne, U. Delaet, I. Van Assche, T. De Beer, J.P. Remon, C. Vervaet, Continuous twin screw granulation: influence of process variables on granule and tablet quality., European Journal of Pharmaceutics and Biopharmaceutics. 82 (2012) 205–211.

[29] D. Djuric, Continous Granulation with a twin-screw extruder, Universität Düsseldorf, 2008.

[30] B. Van Melkebeke, C. Vervaet, J.P. Remon, Validation of a continuous granulation process using a twin-screw extruder., International Journal of Pharmaceutics. 356 (2008) 224–30.

[31] M. Fonteyne, H. Wickström, E. Peeters, J. Vercruysse, H. Ehlers, B.-H. Peters, J.P. Remon, C. Vervaet, J. Ketolainen, N. Sandler, J. Rantanen, K. Naelapää, T. De Beer, Influence of raw material properties upon critical quality attributes of continuously produced granules and tablets., European Journal of Pharmaceutics and Biopharmaceutics. 87 (2014) 252–63.

[32] R. Meier, M. Thommes, N. Rasenack, M. Krumme, K.-P. Moll, P. Kleinebudde, Simplified formulations with high drug loads for continuous twin-screw granulation., International Journal of Pharmaceutics. 496 (2015) 12–23.

[33] K. Pitt, C. Sinka, Tabletting, in: A. Salman, D, M. Hounslow, J, J. Seville, K, P (Eds.), Handbook of Powder Technology, Granulation, Elsevier, Amsterdam, 2007.

[34] G. Alderborn, Tablets and compaction, in: M.E. Aulton, K. Taylor (Eds.), Aulton's Pharmaceutics: The Design and Manufacture of Medicines, Fourth, London, 2013.

[35] A.R. Webster, N.J. Van Abbé, A Test for the Mechanical Strength of Compressed Tablets, Journal of Pharmacy and Pharmacology. 7 (1955) 882–891.

[36] G. Alderborn, Tablets and compaction, in: M.E. Aulton, K. Taylor (Eds.), Aulton's Pharmaceutics: The Design and Manufacture of Medicines, Fourth Edi, Lond, 2013.

[37] C.C. Sun, M.W. Himmelspach, Reduced tabletability of roller compacted granules as a result of granule size enlargement, Journal of Pharmaceutical Sciences. 95 (2006) 200–206.

[38] C.C. Sun, P. Kleinebudde, Mini review: Mechanisms to the loss of tabletability by dry granulation, European Journal of Pharmaceutics and Biopharmaceutics. 106 (2016) 9–14.

[39] C.C. Sun, Decoding Powder Tabletability: Roles of Particle Adhesion and Plasticity, Journal of Adhesion Science and Technology. 25 (2011) 483–499.

[40] G. Alderborn, G. Frenning, Mechanical Strength of Tablets, in: L.L. Augsburger, W.S. Hoag (Eds.), Pharmaceutical Dosage Forms: Tablets, Volume 3, Boca Raton, 2008.

[41] W.S. Hoag, S.V. Dave, V. Moolchandani, Compression and Compaction, in: L.L. Augsburger, W.S. Hoag (Eds.), Pharmaceutical Dosage Forms: Tablets, Third, Boca Raton, 2008.

[42] C. Nyström, G. Alderborn, M. Duberg, P.-G. Karehill, Bonding Surface area and Bonding Mechanism-Two Important Factors for the Understanding of Powder Compactability, Drug Development and Industrial Pharmacy. 19 (1993) 2143–2196.

[43] J. Fell, J.M. Newton, Determination of tablet strength by the diametral-compression test, Journal of Pharmaceutical Sciences. 59 (1970) 688–691.

[44] R.H. decker, M. Van Den Tempel, structure of matter in relation to its elastic and plastic behaviour and failure, in: Elasticity, Plasticity and Structure of Matter, Third, Cambridge University press, Cambridge, 1971.

[45] G. Buckton, Intermolecular bonding forces : where materials and process come together, in: M. Celik (Ed.), Pharmaceutical Powder Compaction Technology, second, CRC Press, London, 2011.

[46] J.P.K. Seville, C.D. Willett, P.C. Knight, Interparticle forces in fluidisation: A review, Powder Technology. 113 (2000) 261–268.

[47] R. (Honorary D. at E. Houwink, N.Y. De Decker, H.K. (Uniroyal International, Elasticity, Plasticity & Structure of Matter, Third, Cambridge University press, London, 1971.

[48] H. Olsson, Å. Adolfsson, C. Nyström, Compaction and measurement of tablets in liquids with different dielectric constants for determination of bonding mechanisms - Evaluation of the concept, International Journal of Pharmaceutics. 143 (1996) 233–245.

[49] C.M. Mate, Tribology on the Small Scale - a bottom up approach to friction, lubrication and wear, first edit, Oxford University Press, Oxford, 2013.

[50]   C. Nyström, G. Alderborn, M. Duberg, P.-G. Karehill, Bonding Surface area and Bonding Mechanism-Two Important Factors for the Understanding of Powder Comparability, Drug Development and Industrial Pharmacy. 19 (1993) 2143–2196.

[51]   E.N. Hiestand, Principles, tenets and notions of tablet bonding and measurements of strength, European Journal of Pharmaceutics and Biopharmaceutics. 44 (1997) 229–242.

[52]   L. Bocquet, E. Charlaix, S. Ciliberto, J. Crassous, Moisture-induced ageing in granular media and the kinetics of capillary condensation, Nature. 396 (1998) 735–737.

[53]   M.C. Coelho, N. Harnby, The effect of humidity on the form of water retention in a powder, Powder Technology. 20 (1978) 197–200.

[54]   S. You, M.P. Wan, Mathematical models for the van der waals force and capillary force between a rough particle and surface, Langmuir. 29 (2013) 9104–9117.

[55]   C.C. Sun, Mechanism of moisture induced variations in true density and compaction properties of microcrystalline cellulose, International Journal of Pharmaceutics. 346 (2008) 93–101.

[56]   C. Fuhrer, Interparticle Attraction Mechanisms, in: G. Alderborn, C. Nyström (Eds.), Pharmaceutical Powder Compaction Technology, First Edit, Marcel Dekker, New York, 1996.

[57]   Å. Adolfsson, C. Gustafsson, C. Nyström, Use of tablet tensile strength adjusted for surface area and mean interparticulate distance to evaluate dominating bonding mechanisms, Drug Development and Industrial Pharmacy. 25 (1999) 753–764.

[58]   C.C. Sun, Decoding Powder Tabletability: Roles of Particle Adhesion and Plasticity, Journal of Adhesion Science and Technology. 25 (2011) 483–499.

[59]   P.G. Karehill, M. Glazer, C. Nyström, Studies on direct compression of tablets. XXIII. The importance of surface roughness for the compactability of some directly compressible materials with different bonding and volume reduction properties, International Journal of Pharmaceutics. 64 (1990) 35–43.

[60]   C. NYSTROM, P.-G. Karehill, The importance of intermolecular bonding forces and the concept of bonding surface area, in: G. Alderborn, C. Nyström (Eds.), Pharmaceutical Powder Compaction Technology, Marcel Dekker, New York, 1996.

[61]   V. Busignies, B. Leclerc, S. Truchon, P. Tchoreloff, Changes in the specific surface area of tablets composed of pharmaceutical materials with various deformation behaviors, Drug Development and Industrial Pharmacy. 37 (2011) 225–233.

[62]   H. Vromans, G.K. Bolhuis, C.F. Lerk, K.D. Kussendrager, Studies on tableting properties of lactose. VIII. The effect of variations in primary particle size, percentage of amorphous lactose and addition of a disintegrant on the disintegration of spray-dried lactose tablets, International Journal of Pharmaceutics. 39 (1987) 201–206.

[63]   A.W. Newman, Micromeritics, in: H.G. Brittain (Ed.), Physical Characterization of Pharmaceutical Solids, Marcel Dekker, New York, 1995.

[64]   G. Alderborn, M. Duberg, C. Nyström, Studies on direct compression of tablets X. Measurement of tablet surface area by permeametry, Powder Technology. 41 (1985) 49–56.

[65]   U. V. Shah, Z. Wang, D. Olusanmi, A.S. Narang, M.A. Hussain, M.J. Tobyn, J.Y.Y. Heng, Effect of milling temperatures on surface area, surface energy and cohesion of pharmaceutical powders, International Journal of Pharmaceutics. 495 (2015) 234–240.

[66]   S. Westermarck, A.M. Juppo, L. Kervinen, J. Yliruusi, Pore structure and surface area of mannitol powder, granules and tablets determined with mercury porosimetry and nitrogen adsorption, European Journal of Pharmaceutics and Biopharmaceutics. 46 (1998) 61–68.

[67]   D. Markl, A. Strobel, R. Schlossnikl, J. Bøtker, P. Bawuah, C. Ridgway, J. Rantanen, T. Rades, P. Gane, K.E. Peiponen, J.A. Zeitler, Characterisation of pore structures of pharmaceutical tablets: A review, International Journal of Pharmaceutics. 538 (2018) 188–214.

[68]   S. Brunauer, P.H. Emmett, E. Teller, Adsorption of Gases in Multimolecular Layers, Journal of the American Chemical Society. 60 (1938) 309–319.

[69]   H. Rumpf, The Strength of Granules and Agglomerates, Agglomeration. (1962) 379–413.

[70]   M. Rhodes, Size Enlargement, in: Martin J. Rhodes (Ed.), Introduction to Particle Technology, John Wiley & Sons, Chishester, 1998.

[71]   P.G. Karehill, C. Nyström, Studies on direct compression of tablets. XXII. Investigation of strength increase upon ageing and bonding mechanisms for some plastically deforming materials, International Journal of Pharmaceutics. 64 (1990) 27–34.

[72]   M. Anan, J. Fell, Bonding mechanisms in tabletting, International Journal of Pharmaceutics. 60 (1990) 197–202.

[73]   C. Ahlneck, G. Alderborn, Moisture adsorption and tabletting. I. Effect on volume reduction properties and tablet strength for some crystalline materials, International Journal of Pharmaceutics. 54 (1989) 131–141.

[74]   G.R.B. Down, J.N. McMullen, The effect of interparticulate friction and moisture on the crushing strength of sodium chloride compacts, Powder Technology. 42 (1985) 169–174.

[75]   T. Sebhatu, A.A. Elamin, C. Ahlneck, Effect of Moisture Sorption on Tabletting Characteristics of Spray Dried (15% Amorphous) Lactose, Pharmaceutical Research: An Official Journal of the American Association of Pharmaceutical Scientists. 11 (1994) 1233–1238.

[76]   C. Fuhrer, Interparticle Attraction Mechanisms, in: G. Alderborn, C. Nyström (Eds.), Pharmaceutical Powder Compaction Technology, Marcel Dekker, London, 1996.

[77]   P.M. Desai, C.V. Liew, P.W.S. Heng, Review of Disintegrants and the Disintegration Phenomena, Journal of Pharmaceutical Sciences. 105 (2016) 2545–2555.

[78]   M.J. Mollan, M. Çelik, The effects of humidity and storage time on the behavior

of maltodextrins for direct compression, International Journal of Pharmaceutics. 114 (1995) 23–32.

[79]   E. Horisawa, K. Danjo, H. Sunada, Influence of granulating method on physical and mechanical properties, compression behavior, and compactibility of lactose and microcrystalline cellulose granules., Drug Development and Industrial Pharmacy. 26 (2000) 583–593.

[80]   S. Patel, A.M. Kaushal, A.K. Bansal, Compression Physics in the Formulation Development of Tablets, Critical Reviews™ in Therapeutic Drug Carrier Systems. 23 (2006) 1–66.

[81]   F. Podczeck, Particle adhesion in powder assemblies, in: Particle-Particle Adhesion In Pharmaceutical Powder Handling, Imperial College Press, London, 1998.

[82]   B. Khorsheed, I. Gabbott, G.K. Reynolds, S.C. Taylor, R.J. Roberts, A.D. Salman, Twin-screw granulation: Understanding the mechanical properties from powder to tablets, Powder Technology. 341 (2019) 104–115.

[83]   G.K. Reynolds, J.I. Campbell, R.J. Roberts, A compressibility based model for predicting the tensile strength of directly compressed pharmaceutical powder mixtures, International Journal of Pharmaceutics. 531 (2017) 215–224.

[84]   J. Ilkka, P. Paronen, Prediction of the compression behaviour of powder mixtures by the Heckel equation, International Journal of Pharmaceutics. 94 (1993) 181–187.

[85]   G. Frenning, J. Nordström, G. Alderborn, Effective Kawakita parameters for binary mixtures, Powder Technology. 189 (2009) 270–275.

[86]   M. Šantl, I. Ilić, F. Vrečer, S. Baumgartner, A compressibility and compactibility study of real tableting mixtures: the effect of granule particle size, Acta Pharmaceutica. 62 (2012) 325–340.

[87]   Discussion of Ryshkewitch Paper by Winston Duckworth, Journal of the American Ceramic Society. 36 (1953) 68–68.

[88]   C.Y. Wu, S.M. Best, A.C. Bentham, B.C. Hancock, W. Bonfield, Predicting the

tensile strength of compacted multi-component mixtures of pharmaceutical powders, Pharmaceutical Research. 23 (2006) 1898–1905.

[89] F.M. Etzler, T. Bramante, R. Deanne, S. Sienkiewicz, F.J. Chen, Tablet tensile strength: An adhesion science perspective, Journal of Adhesion Science and Technology. 25 (2011) 501–519.

[90] M.J. Adams, M.A. Mullier, J.P.K. Seville, Agglomerate strength measurement using a uniaxial confined compression test, Powder Technology. 78 (1994) 5–13.

[91] J.. Sonnergaard, A critical evaluation of the Heckel equation, International Journal of Pharmaceutics. 193 (1999) 63–71.

[92] A.-S. Persson, J. Nordström, G. Frenning, G. Alderborn, Compression analysis for assessment of pellet plasticity: Identification of reactant pores and comparison between Heckel, Kawakita, and Adams equations, Chemical Engineering Research and Design. 110 (2016) 183–191.

[93] J. Nordström, K. Welch, G. Frenning, G. Alderborn, On the physical interpretation of the Kawakita and Adams parameters derived from confined compression of granular solids, Powder Technology. 182 (2008) 424–435.

[94] F. Osei-Yeboah, S.Y. Chang, C.C. Sun, A critical examination of the phenomenon of bonding area - Bonding strength interplay in powder tableting, Pharmaceutical Research. 33 (2016) 1126–1132.

[95] M.A. Al-Nasassrah, F. Podczeck, J.M. Newton, The effect of an increase in chain length on the mechanical properties of polyethylene glycols, European Journal of Pharmaceutics and Biopharmaceutics. 46 (1998) 31–38.

[96] L. Farber, K.P. Hapgood, J.N. Michaels, X.Y. Fu, R. Meyer, M.A. Johnson, F. Li, Unified compaction curve model for tensile strength of tablets made by roller compaction and direct compression, International Journal of Pharmaceutics. 346 (2008) 17–24.

[97] T.H. Nguyen, D. a. V. Morton, K.P. Hapgood, Application of the unified compaction curve to link wet granulation and tablet compaction behaviour, Powder Technology. 240 (2013) 103–115.

160

[98]   T.H. Nguyen, D.A.V. Morton, K.P. Hapgood, Predicting Tablet Strength from the Wet Granulation Conditions via the Unified Compaction Curve, Procedia Engineering. 102 (2015) 517–526.

[99]   A. MCKENNA, D.F. MCCAFFERTY, Effect of particle size on the compaction mechanism and tensile strength of tablets, Journal of Pharmacy and Pharmacology. 34 (1982) 347–351.

[100] G.M. Walker, C.R. Holland, M.M.N. Ahmad, D.Q.M. Craig, Influence of process parameters on fluidised hot-melt granulation and tablet pressing of pharmaceutical powders, Chemical Engineering Science. 60 (2005) 3867–3877.

[101] A. Kelemen, A. Szalay, T. Sovány, K. Pintye-Hódi, Role of the particle size of sorbitol during the compression of common tablets and prediction of mini-tablet compression parameters, Chemical Engineering Research and Design. 104 (2015) 814–818.

[102] K.J. Paluch, L. Tajber, O.I. Corrigan, A.M. Healy, Impact of alternative solid state forms and specific surface area of high-dose, hydrophilic active pharmaceutical ingredients on tabletability, Molecular Pharmaceutics. 10 (2013) 3628–3639.

[103] E.I. Keleb, A. Vermeire, C. Vervaet, J.P. Remon, Single-step granulation/tabletting of different grades of lactose: A comparison with high shear granulation and compression, European Journal of Pharmaceutics and Biopharmaceutics. 58 (2004) 77–82.

[104] F. Fichtner, Å. Rasmuson, G. Alderborn, Particle size distribution and evolution in tablet structure during and after compaction, International Journal of Pharmaceutics. 292 (2005) 211–225.

[105] K.A. Macias, M.T. Carvajal, The influence of granule density on granule strength and resulting compact strength, Chemical Engineering Science. 72 (2012) 205–213.

[106] D.M. Morkhade, Comparative impact of different binder addition methods, binders and diluents on resulting granule and tablet attributes via high shear wet granulation, Powder Technology. 320 (2017) 114–124.

[107] I.P. Gabbott, F. Al Husban, G.K. Reynolds, The combined effect of wet granulation process parameters and dried granule moisture content on tablet quality attributes, European Journal of Pharmaceutics and Biopharmaceutics. 106 (2016) 70–78.

[108] B. Johansson, G. Alderborn, The effect of shape and porosity on the compression behaviour and tablet forming ability of granular materials formed from microcrystalline cellulose., European Journal of Pharmaceutics and Biopharmaceutics. 52 (2001) 347–57.

[109] S.I.F. Badawy, A.S. Narang, K. LaMarche, G. Subramanian, S.A. Varia, Mechanistic basis for the effects of process parameters on quality attributes in high shear wet granulation., International Journal of Pharmaceutics. 439 (2012) 324–33.

[110] D. GANDERTON, B.M. HUNTER, A comparison of granules prepared by pan granulation and by massing and screening, Journal of Pharmacy and Pharmacology. 23 (1971) 1S-10S.

[111] L. Shi, Y. Feng, C.C. Sun, Massing in high shear wet granulation can simultaneously improve powder flow and deteriorate powder compaction: a double-edged sword., European Journal of Pharmaceutical Sciences. 43 (2011) 50–56.

[112] S. Grote, P. Kleinebudde, Roll Compaction/Dry Granulation of Dibasic Calcium Phosphate Anhydrous—Does the Morphology of the Raw Material Influence the Tabletability of Dry Granules?, Journal of Pharmaceutical Sciences. 107 (2018) 1104–1111.

[113] T. Yoshinari, The improved compaction properties of mannitol after a moisture-induced polymorphic transition, International Journal of Pharmaceutics. 258 (2003) 121–131.

[114] K.A. Riepma, K. Zuurman, G.K. Bolhuis, A.H. de Boer, C.F. Lerk, Consolidation and compaction of powder mixtures. I. Binary mixtures of same particle size fractions of different types of crystalline lactose, International Journal of Pharmaceutics. 66 (1990) 47–52.

[115] K.A. Riepma, J. Veenstra, C.F. Lerk, Consolidation and compaction of powder mixtures II. Binary mixtures of different particle size fractions of α-lactose monohydrate, 76 (1991) 9–15.

[116] K.A. Riepma, K. Zuurman, G.K. Bolhuis, A.H. de Boer, C.F. Lerk, Consolidation and compaction of powder mixtures: III. Binary mixtures of different particle size fractions of different types of crystalline lactose, International Journal of Pharmaceutics. 85 (1992) 121–128.

[117] F. Podczeck, Fundamentals of Adhesion of Particles to Surfaces, in: Particle-Particle Adhesion In Pharmaceutical Powder Handling, Imperial College Press, London, 1998.

[118] A. Gupta, G.E. Peck, R.W. Miller, K.R. Morris, Effect of the variation in the ambient moisture on the compaction behavior of powder undergoing roller-compaction and on the characteristics of tablets produced from the post-milled granules, Journal of Pharmaceutical Sciences. 94 (2005) 2314–2326.

[119] M.C. Coelho, N. Harnby, Moisture bonding in powders, Powder Technology. 20 (1978) 201–205.

[120] M. Eriksson, G. Alderborn, The effect of original particle size and tablet porosity on the increase in tensile strength during storage of sodium chloride tablets in a dry atmosphere, International Journal of Pharmaceutics. 113 (1995) 199–207.

[121] C. Ahlneck, G. Zografi, The molecular basis of moisture effects on the physical and chemical stability of drugs in the solid state, International Journal of Pharmaceutics. 62 (1990) 87–95.

[122] L. Stubberud, H.G. Arwidsson, A. Larsson, C. Graffner, Water solid interactions II. Effect of moisture sorption and glass transition temperature on compactibility of microcrystalline cellulose alone or in binary mixtures with polyvinyl pyrrolidone, International Journal of Pharmaceutics. 134 (1996) 79–88.

[123] G. Alderborn, C. Ahlneck, Moisture adsorption and tabletting. III. Effect on tablet strenght-post compaction storage time profiles, International Journal of Pharmaceutics. 73 (1991) 249–258.

[124] R.J. Roberts, R.C. Rowe, P. York, The relationship between the fracture properties, tensile strength and critical stress intensity factor of organic solids and their molecular structure, International Journal of Pharmaceutics. 125 (1995) 157–162.

[125] G.M. Walker, Drum granulation processes, in: A.D. Salman, M.J. Hounslow, J.P.K. Seville (Eds.), Granulation, First Edit, Elsevier B.V., London, 2007.

[126] G.K. Bolhuis, D.H. Waard, Compaction properties of directly compressible materials, in: M. Çelik (Ed.), Pharmaceutical Powder Compaction Technology, Second Edi, CRC Press, London, 2012.

[127] L. Shi, Y. Feng, C.C. Sun, Roles of granule size in over-granulation during high shear wet granulation, Journal of Pharmaceutical Sciences. 99 (2010) 3322–3325.

[128] F. Osei-Yeboah, Y. Feng, C.C. Sun, Evolution of structure and properties of granules containing microcrystalline cellulose and polyvinylpyrrolidone during high-shear wet granulation, Journal of Pharmaceutical Sciences. 103 (2014) 207–215.

[129] M.G. Herting, P. Kleinebudde, Studies on the reduction of tensile strength of tablets after roll compaction/dry granulation, European Journal of Pharmaceutics and Biopharmaceutics. 70 (2008) 372–379.

[130] M.G. Herting, P. Kleinebudde, Studies on the reduction of tensile strength of tablets after roll compaction/dry granulation, European Journal of Pharmaceutics and Biopharmaceutics. 70 (2008) 372–379.

[131] S. Patel, S. Dahiya, C. Calvin Sun, A.K. Bansal, Understanding Size Enlargement and Hardening of Granules on Tabletability of Unlubricated Granules Prepared by Dry Granulation, Journal of Pharmaceutical Sciences. 100 (2011) 758–766.

[132] N. Souihi, M. Dumarey, H. Wikström, P. Tajarobi, M. Fransson, O. Svensson, M. Josefson, J. Trygg, A quality by design approach to investigate the effect of mannitol and dicalcium phosphate qualities on roll compaction, International Journal of Pharmaceutics. 447 (2013) 47–61.

[133] L. Perez-Gandarillas, A. Perez-Gago, A. Mazor, P. Kleinebudde, O. Lecoq, A. Michrafy, Effect of roll-compaction and milling conditions on granules and tablet

properties, European Journal of Pharmaceutics and Biopharmaceutics. 106 (2016) 38–49.

[134] B. Johansson, M. Wikberg, R. Ek, G. Alderborn, Compression behaviour and compactability of microcrystalline cellulose pellets in relationship to their pore structure and mechanical properties, International Journal of Pharmaceutics. 117 (1995) 57–73.

[135] S.I.F. Badawy, D.B. Gray, M.A. Hussain, A study on the effect of wet granulation on microcrystalline cellulose particle structure and performance, Pharmaceutical Research. 23 (2006) 634–640.

[136] F. Osei-Yeboah, C.C. Sun, Tabletability Modulation Through Surface Engineering, Journal of Pharmaceutical Sciences. 104 (2015) 2645–2648.

[137] F. Osei-Yeboah, M. Zhang, Y. Feng, C.C. Sun, A Formulation Strategy for Solving the Overgranulation Problem in High Shear Wet Granulation, Journal of Pharmaceutical Sciences. 103 (2014) 2434–2440.

[138] V. Vanhoorne, B. Bekaert, E. Peeters, T. De Beer, J.-P. Remon, C. Vervaet, Improved tabletability after a polymorphic transition of delta-mannitol during twin screw granulation., International Journal of Pharmaceutics. 506 (2016) 13–24.

[139] T. Kuntz, M.A. Schubert, P. Kleinebudde, Increased compactibility of acetames after roll compaction, European Journal of Pharmaceutics and Biopharmaceutics. 77 (2011) 164–169.

[140] D. Brannegan, C. Lee, J. Wang, L. Taylor, Extraction Techniques Leveraging Elevated tempertuer and pressure, in: Beverly Nickerson (Ed.), Sample Preparation of Pharmaceutical Dosage Forms: Challenges and Strategies for Sample Preparation and Extraction, Springer, New York, 2011.

[141] A.D. Rajkumar, G.K. Reynolds, D. Wilson, S.A.C. Wren, A.D. Salman, The effect of roller compaction and tableting stresses on pharmaceutical tablet performance, Powder Technology. 341 (2018) 23–37.

[142] G. Lewis, A.Simpkin, Tabletting- An Industrial Viewpoint, in: D. Chulia, M. Deleuil, Y. Pourcelot (Eds.), Powder Technology and Pharmaceutical Processes,

Elsevier B.V., Oxford, 1994.

[143] I. Gabbott, Designer granules : beating the trade-off between granule strength and dissolution time. PhD thesis, (2007).

[144] A.Z. Al hassn, S. Jeßberger, M.J. Hounslow, A.D. Salman, Multi-stage granulation: An approach to enhance final granule attributes, Chemical Engineering Research and Design. 134 (2018) 26–35.

[145] V. Vanhoorne, L. Janssens, J. Vercruysse, T. De Beer, J.P. Remon, C. Vervaet, Continuous twin screw granulation of controlled release formulations with various HPMC grades, International Journal of Pharmaceutics. 511 (2016) 1048–1057.

[146] S.H. Kim, K.M. Hwang, C.H. Cho, T.T. Nguyen, S.H. Seok, K.M. Hwang, J.Y. Kim, C.W. Park, Y.S. Rhee, E.S. Park, Application of continuous twin screw granulation for the metformin hydrochloride extended release formulation, International Journal of Pharmaceutics. 529 (2017) 410–422.

[147] M. Asadi-Eydivand, M. Solati-Hashjin, A. Farzadi, N.A.A. Osman, Artificial neural network approach to estimate the composition of chemically synthesized biphasic calcium phosphate powders, Ceramics International. 40 (2014) 12439–12448.

[148] S. Shirazian, M. Kuhs, S. Darwish, D. Croker, G.M. Walker, Artificial neural network modelling of continuous wet granulation using a twin-screw extruder, International Journal of Pharmaceutics. 521 (2017) 102–109.

[149] M.H. Cartwright, Artificial Neural Networks in Biology and Chemistry: The Evolution of a New Analytical Tool, in: J.D. Livingstone (Ed.), Artificial Neural Networks Methods and Applications, Humana Press, Totowa, 2008.

[150] M. Celik, Expert systems and their use in pharmaceutical application, in: M. Celik (Ed.), Pharmaceutical Powder Compaction Technology, Second, Informa Healthcare USA, Inc, London, 2012.

[151] J. Zou, Y. Han, S.-S. So, Overview of Artificial Neural Networks, in: J.D. Livingstone (Ed.), Artificial Neural Networks Methods and Applications, Humana Press, Totowa, 2008.

[152] D. Svozil, V. Kvasnicka, J. Pospichal, Introduction to multi-layer feed-forward neural networks, Chemometrics and Intelligent Laboratory Systems. 39 (1997) 43–62.

[153] W.H. AlAlaween, B. Khorsheed, M. Mahfouf, I. Gabbott, G.K. Reynolds, A.D. Salman, Transparent Predictive Modelling of the Twin Screw Granulation Process using a Compensated Interval Type-2 Fuzzy System, European Journal of Pharmaceutics and Biopharmaceutics. 124 (2017) 138–146.

[154] N.M. Halberstam, I.I. Baskin, V.A. Palyulin, N.S. Zefirov, Neural networks as a method for elucidating structure–property relationships for organic compounds, Russian Chemical Reviews. 72 (2003) 629–649.

[155] E. Murtoniemi, P. Kinnunen, K. Leivisk, P. Merkku, The advantages by the use of neural networks in modelling the fluidized bed granulation process, 108 (1994) 155–164.

[156] M. Turkoglu, I. Aydin, M. Murray, A. Sakr, Modeling of a roller-compaction process using neural networks and genetic algorithms, European Journal of Pharmaceutics and Biopharmaceutics. 48 (1999) 239–45.

[157] M. Landin, Artificial Intelligence Tools for Scaling Up of High Shear Wet Granulation Process, Journal of Pharmaceutical Sciences. 106 (2017) 273–277.

[158] P. Barmpalexis, F.I. Kanaze, K. Kachrimanis, E. Georgarakis, Artificial neural networks in the optimization of a nimodipine controlled release tablet formulation, European Journal of Pharmaceutics and Biopharmaceutics. 74 (2010) 316–323.

[159] M. Sajjia, S. Shirazian, C.B. Kelly, A.B. Albadarin, G. Walker, ANN Analysis of a Roller Compaction Process in the Pharmaceutical Industry, Chemical Engineering and Technology. 40 (2017) 487–492.

[160] H. Yu, J. Fu, L. Dang, Y. Cheong, H. Tan, H. Wei, Prediction of the Particle Size Distribution Parameters in a High Shear Granulation Process Using a Key Parameter Definition Combined Artificial Neural Network Model, Industrial & Engineering Chemistry Research. 54 (2015) 10825–10834.

[161] S.S. Behzadi, J. Klocker, H. Hüttlin, P. Wolschann, H. Viernstein, Validation of

fluid bed granulation utilizing artificial neural network, International Journal of Pharmaceutics. 291 (2005) 139–148.

[162] J.G. Kesavan, G.E. Peck, Pharmaceutical granulation and tablet formulation using neural networks, Pharmaceutical Development and Technology. 1 (1996) 391–404.

[163] G. Thoorens, F. Krier, B. Leclercq, B. Carlin, B. Evrard, Microcrystalline cellulose, a direct compression binder in a quality by design environment-a review, International Journal of Pharmaceutics. 473 (2014) 64–72.

[164] C.R. Rowe, J.P. Sheskey, G.W. Cook, E.M. Fenton, A.P. Association, Handbook of Pharmaceutical Excipients, Seventh, APhA/Pharmaceutical Press, London, 2012.

[165] S.K. Kochhar, M.H. Rubinstein, D. Barnes, The effects of slugging and recompression on pharmaceutical excipients, International Journal of Pharmaceutics. 115 (1995) 35–43.

[166] Open chmistry database, Anhydrous Dibasic Calcium Phosphate, Pubchem. (201AD).

[167] M. Šantl, I. Ilić, F. Vrečer, S. Baumgartner, A compressibility and compactibility study of real tableting mixtures: The impact of wet and dry granulation versus a direct tableting mixture, International Journal of Pharmaceutics. 414 (2011) 131–139.

[168] A. Aburub, D. Mishra, I. Buckner, Use of Compaction Energetics for Understanding Particle Deformation Mechanism, Pharmaceutical Development and Technology. 12 (2007) 405–414.

[169] R. Meier, M. Thommes, N. Rasenack, K.P. Moll, M. Krumme, P. Kleinebudde, Granule size distributions after twin-screw granulation – Do not forget the feeding systems, European Journal of Pharmaceutics and Biopharmaceutics. 106 (2016) 59–69.

[170] O.-R. Arndt, R. Baggio, A.K. Adam, J. Harting, E. Franceschinis, P. Kleinebudde, Impact of different dry and wet granulation techniques on granule and tablet

properties: A comparative study, Journal of Pharmaceutical Sciences. (2018) 1–10.

[171] C.S. Omar, R.M. Dhenge, J.D. Osborne, T.O. Althaus, S. Palzer, M.J. Hounslow, A.D. Salman, Roller compaction: Effect of morphology and amorphous content of lactose powder on product quality, International Journal of Pharmaceutics. 496 (2015).

[172] P.A. Webb, Surface Area, Porosity, and Related Physical Characteristics, in: L.L. Augsburger, W.S. Hoag (Eds.), Pharmaceutical Dosage Forms: Tablets, Third, CRC Press, Boca Raton, 2008.

[173] A.Y. Gore, G.S. Banker, Surface chemistry of colloidal silica and a possible application to stabilize aspirin in solid matrixes, Journal of Pharmaceutical Sciences. 68 (1979) 197–202.

[174] A.D. Rajkumar, G.K. Reynolds, D. Wilson, S. Wren, M.J. Hounslow, A.D. Salman, Investigating the effect of processing parameters on pharmaceutical tablet disintegration using a real-time particle imaging approach, European Journal of Pharmaceutics and Biopharmaceutics. 106 (2016) 88–96.

[175] P.K. Le, P. Avontuur, M.J. Hounslow, A.D. Salman, A microscopic study of granulation mechanisms and their effect on granule properties, Powder Technology. 206 (2011) 18–24.

[176] S. V. Lute, R.M. Dhenge, M.J.H.& A.D. Salman, Twin Screw Granulation: understanding the Mechanism of granule formation along the barrel length, Chemical Engineering Research and Design. 110 (2016) 43–53.

[177] C.M. Mate, Mechanical properties of solids and real area of contact, in: C.M. Mate (Ed.), Tribology on the Small Scale, Oxford university Press, Oxford, 2008.

[178] T. Sebhatu, A.A. Elamin, C. Ahlneck, Effect of moisture sorption on tabletting characteristics of spray dried (15% amorphous) lactose., Pharmaceutical Research. 11 (1994) 1233–8.

[179] K.G. Pitt, M.G. Heasley, Determination of the tensile strength of elongated tablets, Powder Technology. 238 (2013) 169–175.

[180] S. Airaksinen, M. Karjalainen, A. Shevchenko, S. Westermarck, E. Leppänen, J. Rantanen, J. Yliruusi, Role of water in the physical stability of solid dosage formulations, Journal of Pharmaceutical Sciences. 94 (2005) 2147–2165.

[181] G. Alderborn, C. Ahlneck, Moisture adsorption and tabletting. III. Effect on tablet strength-post compaction storage time profiles, International Journal of Pharmaceutics. 73 (1991) 249–258.

[182] N. Lordi, P. Shiromani, Mechanism of hardness of aged compacts, Drug Development and Industrial Pharmacy. 10 (1984) 729–752.

[183] J. Dun, F. Osei-Yeboah, P. Boulas, Y. Lin, C.C. Sun, A systematic evaluation of dual functionality of sodium lauryl sulfate as a tablet lubricant and wetting enhancer, International Journal of Pharmaceutics. 552 (2018) 139–147.

[184] A. Kumar, J. Vercruysse, G. Bellandi, K. V. Gernaey, C. Vervaet, J.P. Remon, T. De Beer, I. Nopens, Experimental investigation of granule size and shape dynamics in twin-screw granulation, International Journal of Pharmaceutics. 475 (2014) 485–495.

[185] R. Han, Y. Yang, X. Li, D. Ouyang, Predicting oral disintegrating tablet formulations by neural network techniques, Asian Journal of Pharmaceutical Sciences. 13 (2018) 336–342.

[186] J. Bourquin, H. Schmidli, P. Van Hoogevest, H. Leuenberger, Comparison of artificial neural networks (ANN) with classical modelling techniques using different experimental designs and data from a galenical study on a solid dosage form, 6 (1998) 287–300.

[187] J. Bourquin, H. Schmidli, P. Van Hoogevest, H. Leuenberger, Application of Artificial Neural Networks (ANN) in the development of solid dosage forms, Pharmaceutical Development and Technology. 2 (1997) 111–121.

[188] J.N. Israelachvili, Intermolecular and Surface Forces, Third, Academic Press, Waltham, 2011.

[189] R.B. Al-Asady, R.M. Dhenge, M.J. Hounslow, A.D. Salman, Roller compactor: Determining the nip angle and powder compaction progress by indentation of the

pre-compacted body, Powder Technology. 300 (2016) 107–119.

[190] R.M. Dhenge, J.J. Cartwright, D.G. Doughty, M.J. Hounslow, A.D. Salman, Twin screw wet granulation: Effect of powder feed rate, Advanced Powder Technology. 22 (2011) 162–166.

[191] M. Leitritz, M. Krumme, P.C. Schmidt, Force-time curves of a rotary tablet press. Interpretation of the compressibility of a modified starch containing various amounts of moisture, Journal of Pharmacy and Pharmacology. 48 (1996) 456–462.

Appendix A

Type of bonds

There are two main groups of bonds of that keep matter together. The stronger one is called the primary bonds. The second category which is weaker is often denoted as secondary bonds.

Primary bonds

Ionic bonding

Ionic bonds occur where an atom or covalently-bonded molecule *donates* one or more of its electrons to its neighbouring atom or covalently-bonded molecule (e.g. NaCl). Ionic bonds are of comparable strength (and sometimes stronger than) covalent bonds, ranging from about 600 to 1000 kJ/mol for LiF, inversely proportional to the ionic size [188].

Covalent bonding

Covalent bonding occurs between atoms which share one or more of their electrons. Covalent bonding makes a very strong connection between atoms and so it requires much energy to break these molecules apart (e.g. carbon atoms covalently bonded to each other as in diamond). Covalent bond strength typically ranges from about 150 to 870 kJ/mol [188].

Metallic bonding

In metallic bonding, all atoms share all of the electrons in their outer (valence) electron shells. This 'gas' of free electrons gives rise to the high conductivity of metals. Broadly, the number of electrons an atom releases for bonding and the atomic number of the atom are proportional to the bond strength and therefore the melting point of the metal. Metallic bonds strengths are of the same order of magnitude as ionic and covalent bonds, depending on the atomic configuration [47]

Appendix B

Figure B.1 and Figure B.2 show the internal structure of the mannitol 100 SD particle. It could be seen that the internal particle is made of needle shape crystals which could be seen as well in Figure 4.13.
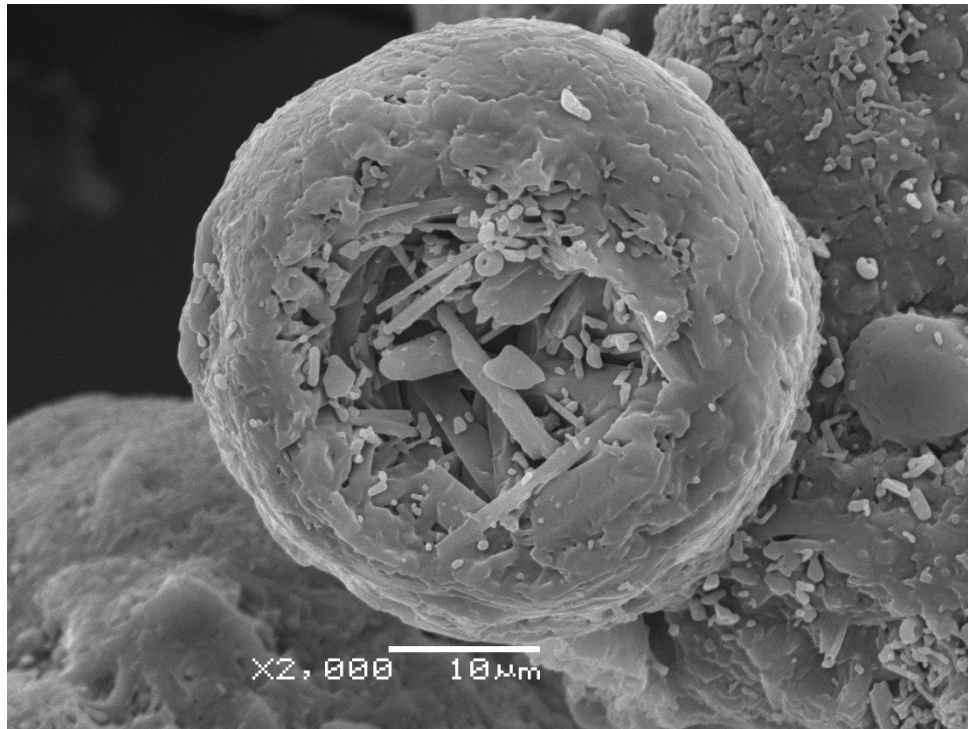

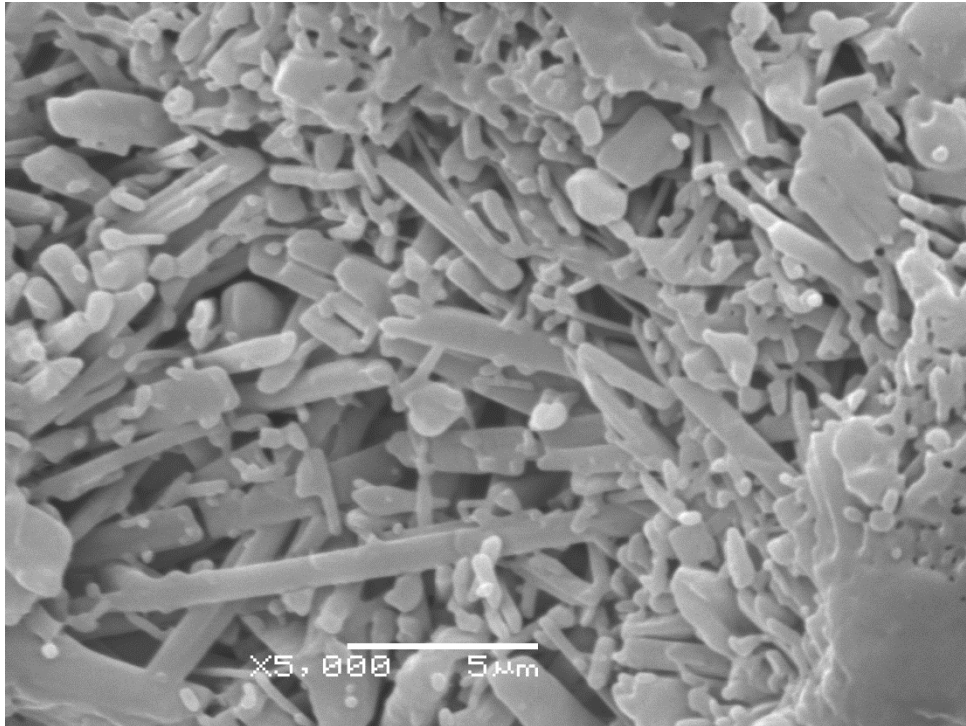Figure B. 1 SEM image of 100 SD mannitol at 2000x magnification.

Figure B. 2 SEM image of 100 SD mannitol at 5000x magnification.

Appendix C

In section 4.5.4 the relationship between the yield pressure of compressed materials (powder and granules) at 44 MPa and their tablets strength were presented in

Figure 4.17. In this appendix more supporting evidence of the relationship between the mechanical properties of the compressed materials and their tablet tensile strength is presented. The compressed granules all have the same size (300-500 µm) and the primary powders are compressed as received. The following figures present the relationship between the yield pressure, the percentage of the plastic and the elastic work versus the tablet tensile strength compressed at 88 MPa. The figures below (C.1 and C.2) suggest that both the yield pressure and the ratio of the elastic work to the plastic work of compressed materials (the primary powder and granules) are good predictors of their tablets tensile strength.
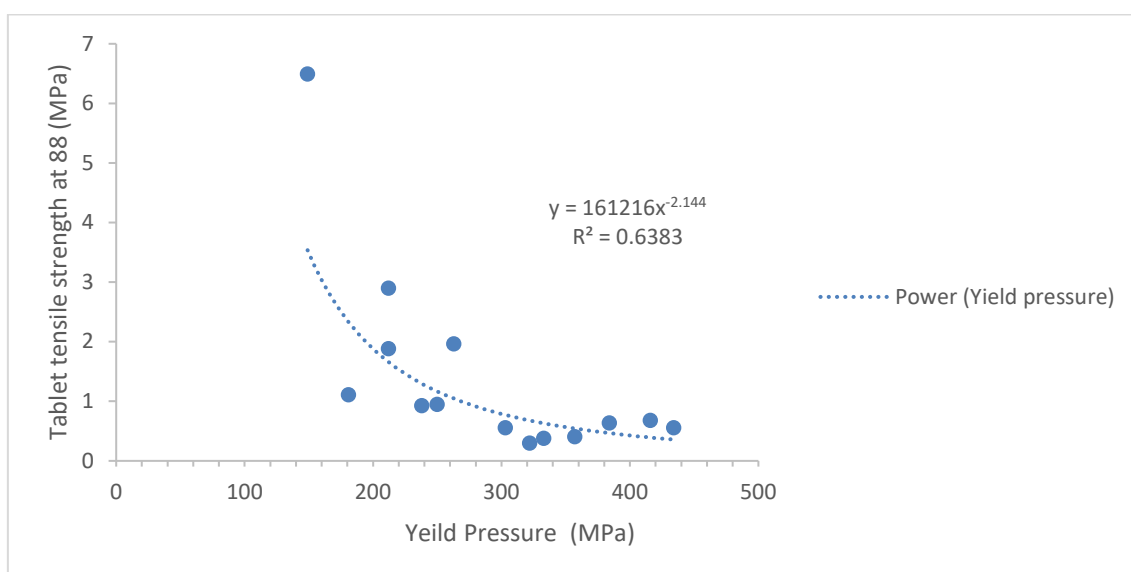

Figure C. 1 Yield pressure of compacted materials (primary powder and granules) vs tensile strength of tablets made from those materials at 88 MPa.
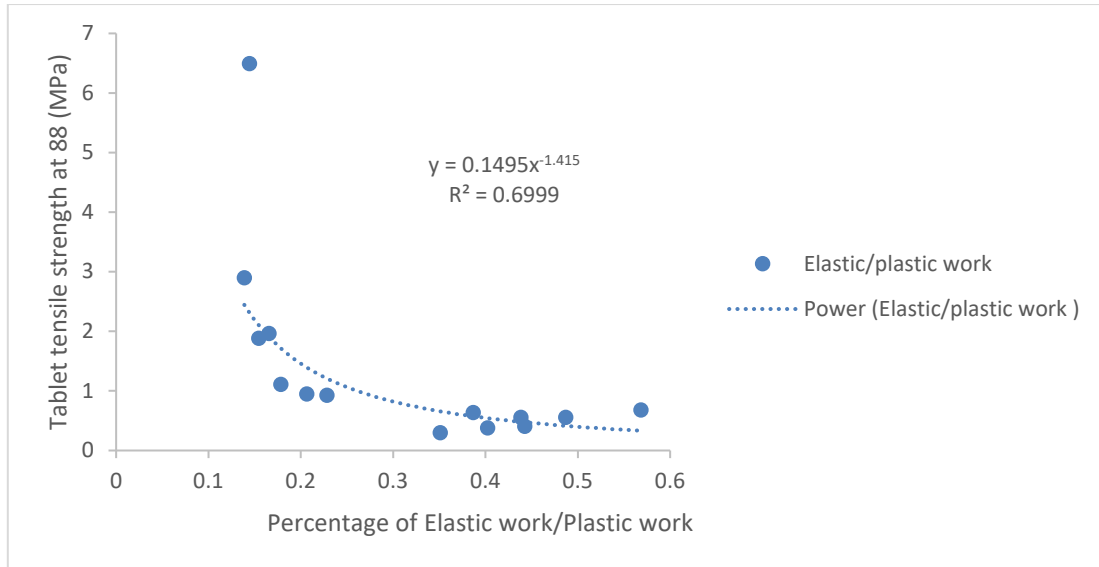
Figure C. 2 Percentage of the elastic work/the plastic work of the primary powder and granules vs tensile strength of tablets made from those materials at 88 MPa.

Appendix D

Porosity

X-ray tomography has shown to be useful to determine the porosity of granules and compacted bodies qualitatively and quantitatively [11,171,189,190]. The porosity of the granulated materials using X-ray analysis and pycnometer (GeoPyc, micromeritics, USA) were measured. Pearson correlation was performed using a statistical software (Minitab), the Pearson correlation between the X-ray and GeoPec is 0.922 and the R-squared is 85%. It can be concluded that the both techniques could be used alternatively.
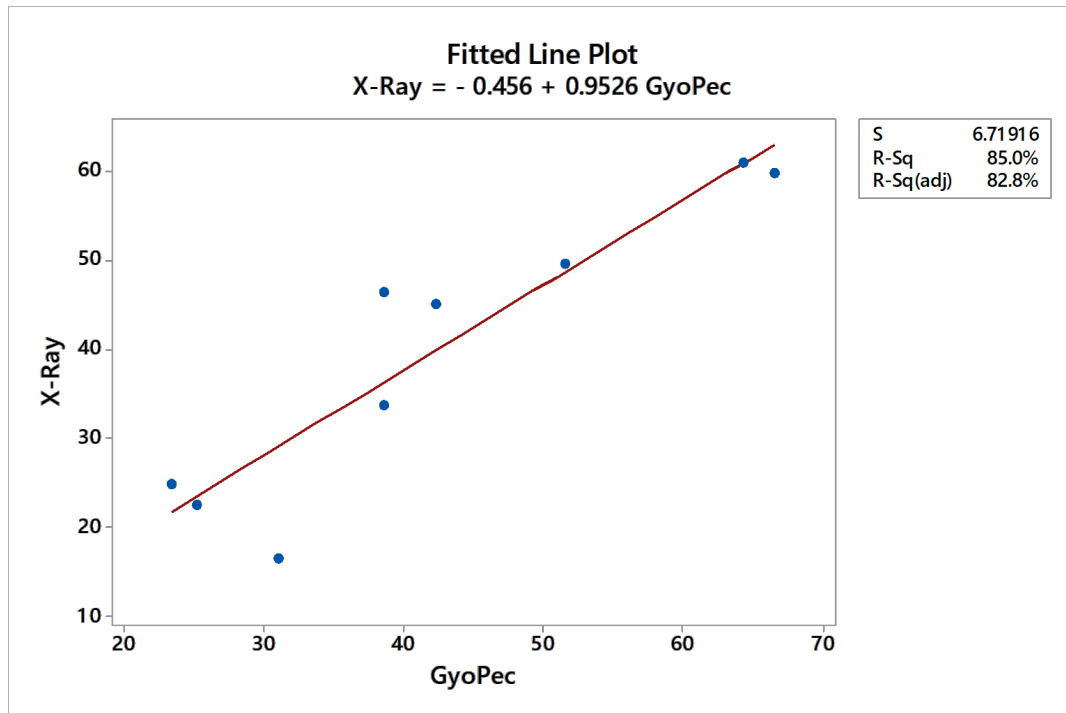

Figure D. 1 The correlation between granule porosity calculated using X-Ray topography and volume displacement method (Gyopec).

Appendix E

Validation of tabletability predictions for additional materials

Recognising that this relationship was based on just two materials (albiet with granulated and ungranulated variants), additional validation tests were performed by compressing granules made from other materials such as, spray dried mannitol lactose, starch and mixtures of components as presented in Tablet E.1. The results, also shown in Figure 5.6, indicate that this approach is capable of describing the compaction behaviour of these additional materials and mixtures of materials as well.

Table E. 1 granules used for the validation experiments

Abbreviation	Material	Granulation conditions
M100/K	Pearlitol® 100 SD	Conveying elements and 32 kneading discs
M100/C	Pearlitol® 100 SD	Conveying elements only
L/C	lactose anhydrous	Conveying elements only
L/K	lactose anhydrous	Conveying elements and 32 kneading discs
MCC50% & SD50%	50% MCC& 50% 100SD (granule)	Conveying elements and 16 kneading discs
0.64MCC50% & SD50%	50% MCC& 50&C160 (granule)	Conveying elements and 16 kneading discs
STA	Starch	Conveying elements only
STA-85% RH	Starch	Conveying elements only

For even further validation of this approach, starch granules were conditioned at 85% relative humidity in order to significantly increase their moisture content. The tablet strength of the conditioned starch granules showed an increase in the tablet strength in a linear manner compared with the starch granules equilibrated to ambient conditions (Figure E.1). Similar observations were reported by other researchers, whereby the strength of tablets made from starch increased after an increase in the moisture content of starch from 7.8 to 14.2% w/w [191].

As a result the extensive testing, it can be suggest that the two-parameter approach is capable of predicting the tensile strength of tablet compacts for wide range of materials material.
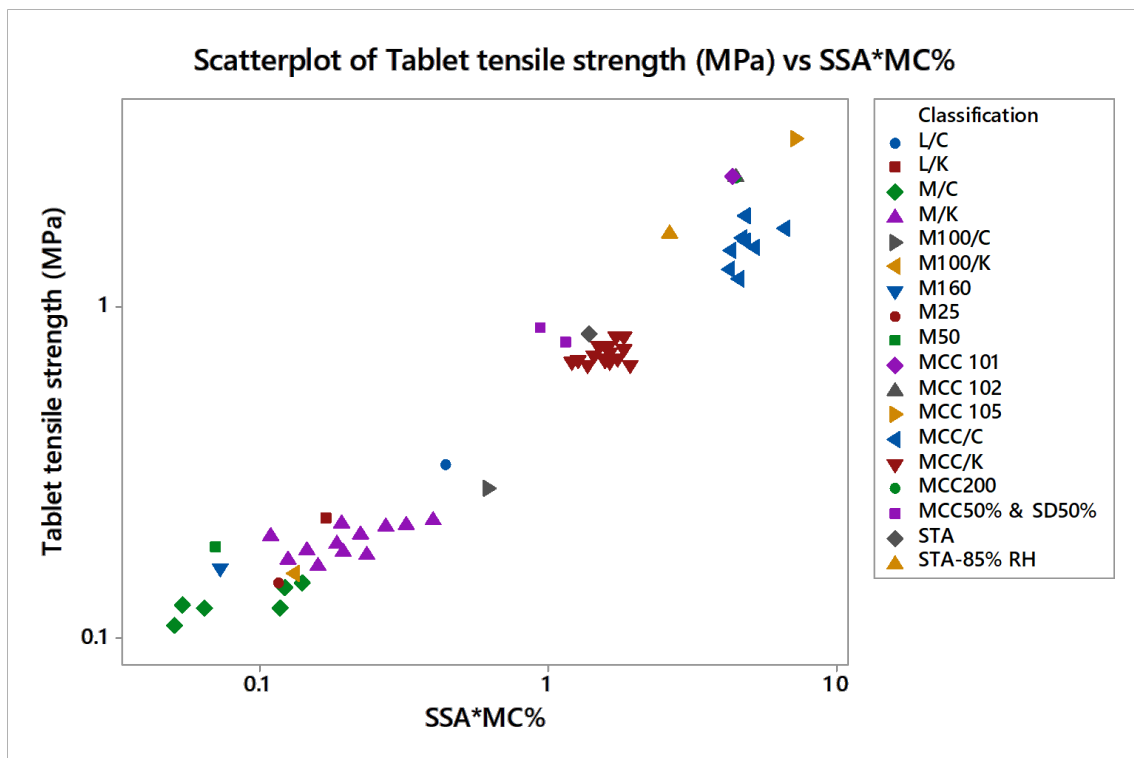

Figure E. 1 Tablet tensile strength at 44 (MPa) vs specific surface area multiplied by moisture content.

In figure E.2 the linear function of the relationship between the Tablet strength and the SSA*MC% is presented. The R^2 of the linear function (0.94) is very similar to the function presented in Figure 5.6. The fitted data in Figure E.1 and E 1.2 is presented in Table E.2.
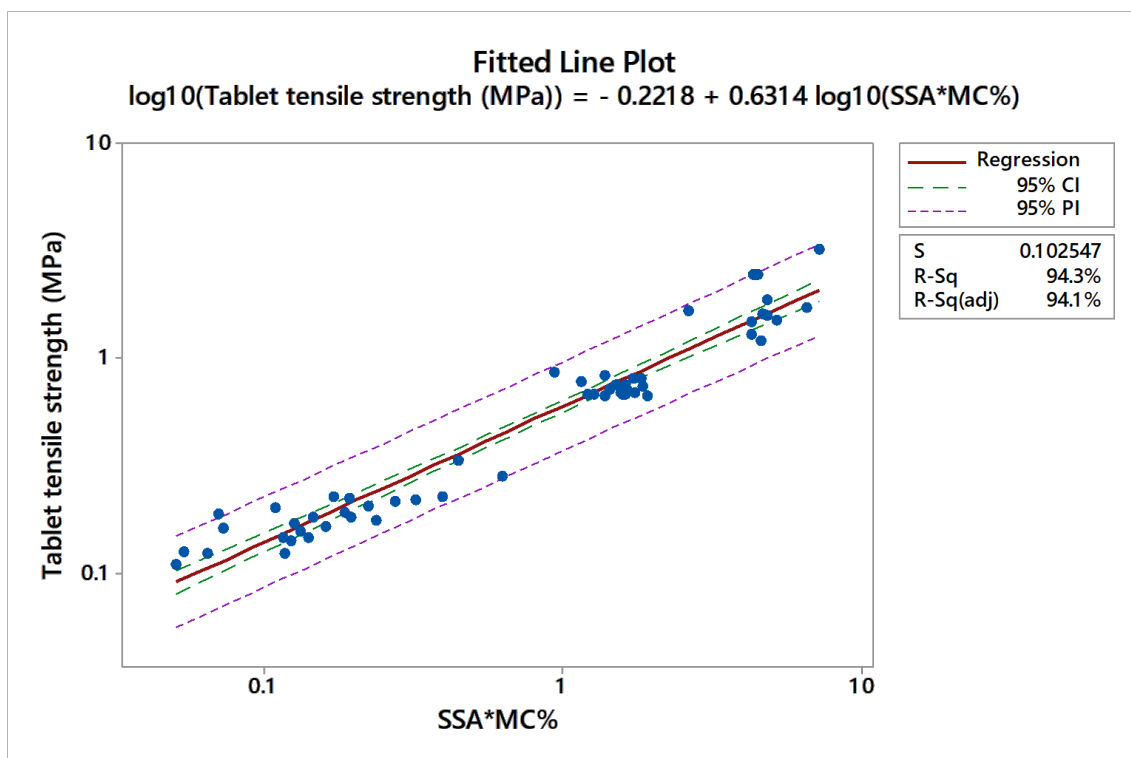
Figure E. 2 Tablet tensile strength made at 44 (MPa) vs specific surface area multiplied by moisture content.

Table E. 2 Granules specific surface area (m²/g) and Moisture content (%w/w).

Set	Moisture content (% w/w)	Specific surface area (m²/g)	Specific surface area * moisture content (%w/w)	Tablet tensile strength @ 44(MPa)
101/C/B	5.30	0.89	4.69	1.63
101/K16/B	5.90	0.28	1.63	0.68
101/K32/B	5.39	0.26	1.38	0.67
102/C/B	5.20	0.93	4.86	1.58
102/K16/B	5.65	0.33	1.84	0.81
102/K32/B	5.47	0.29	1.59	0.69
105/C/B	5.54	1.19	6.61	1.73
105/K16/B	5.87	0.26	1.50	0.76
105/K32/B	5.94	0.24	1.44	0.72
200/C/B	5.01	0.97	4.84	1.90
200/K16/B	5.42	0.23	1.27	0.69
200/K32/B	5.34	0.23	1.21	0.68
101/C/S	5.70	0.75	4.27	1.30
101/K16/S	5.98	0.29	1.74	0.70
101/K32/S	5.89	0.28	1.64	0.73
102/C/S	5.43	0.85	4.60	1.22
102/K16/S	5.48	0.34	1.84	0.74

180

Set	Moisture content (% w/w)	Specific surface area (m²/g)	Specific surface area * moisture content (%w/w)	Tablet tensile strength @ 44(MPa)
102/K32/S	5.93	0.32	1.92	0.67
105/C/S	5.43	0.95	5.19	1.51
105/K16/S	5.63	0.29	1.63	0.76
105/K32/S	6.19	0.28	1.72	0.82
200/C/S	5.55	0.77	4.29	1.49
200/K16/S	5.84	0.27	1.57	0.70
200/K32/S	5.94	0.27	1.63	0.70
MCC 101	4.65	0.94	4.37	2.47
MCC 105	3.68	1.97	7.24	3.22
MCC200	4.04	1.10	4.45	2.45
MCC 102	4.75	0.94	4.48	2.48
25/32K/B	0.11	1.03	0.11	0.20
25/16K/B	0.28	0.99	0.27	0.22
25/C/B	0.21	0.58	0.12	0.14
50/C/B	0.18	0.36	0.06	0.12
50/16K/B	0.23	0.86	0.20	0.18
50/32K/B	0.17	0.96	0.16	0.17
160/C/B	0.19	0.28	0.05	0.13
160/K16/B	0.31	0.76	0.24	0.18
160/K32/B	0.15	0.87	0.13	0.17
25/32K/S	0.20	0.99	0.19	0.22
25/16K/S	0.23	0.97	0.22	0.21
25/C/S	0.26	0.54	0.14	0.15
50/C/S	0.33	0.36	0.12	0.12
50/16K/S	0.21	0.89	0.19	0.19
50/32K/S	0.32	1.00	0.32	0.22
160/C/S	0.21	0.25	0.05	0.11
160/K16/S	0.20	0.75	0.15	0.19
160/K32/S	0.44	0.91	0.40	0.23
C25	0.16	0.73	0.12	0.15
C50	0.16	0.44	0.07	0.19
C160	0.27	0.27	0.07	0.16
M100/K	0.08	1.66	0.13	0.16
M100/C	0.34	1.86	0.63	0.28
L/C	0.53	0.84	0.45	0.34
L/K	0.43	0.40	0.17	0.23
MCC50% & SD50%	2.86	0.40	1.15	0.78

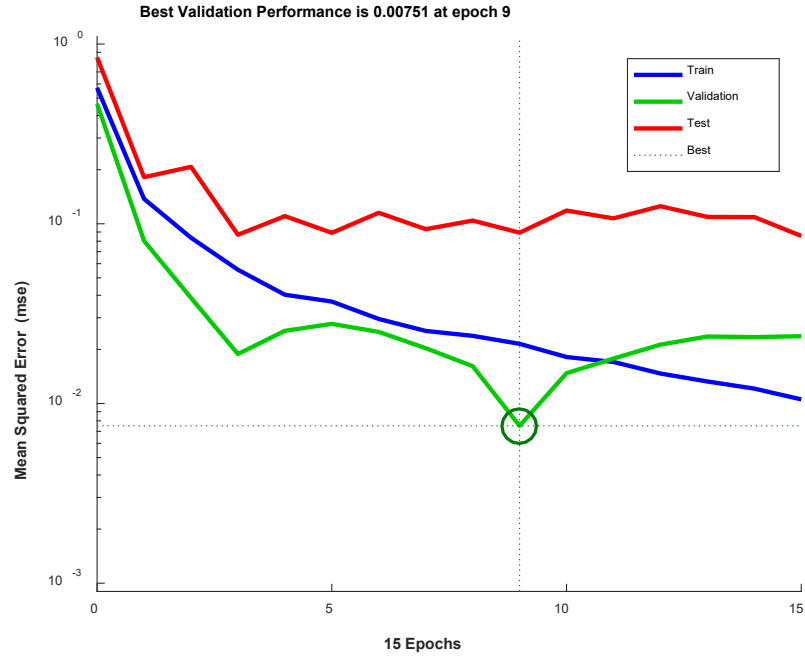| Set	Moisture content (% w/w)	Specific surface area (m²/g)	Specific surface area * moisture content (%w/w)	Tablet tensile strength @ 44(MPa)
MCC50% & SD50%	2.83	0.33	0.94	0.87
STA	9.49	0.15	1.39	0.83
STA-85% RH	17.95	0.15	2.63	1.67

Appendix F

Figure F. 1 The mean squared error for the training, validation, testing vs their corresponding epochs to predict the D10 via single hidden layer network.
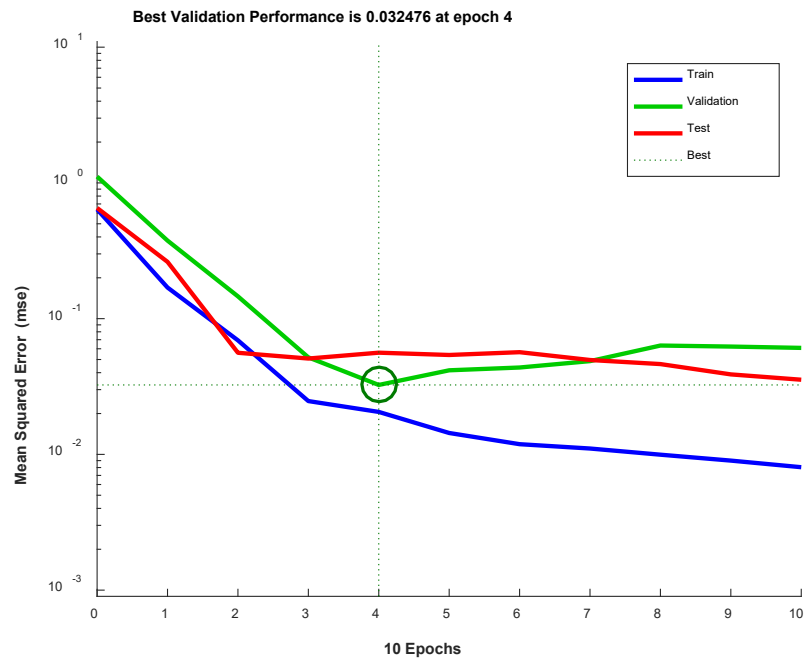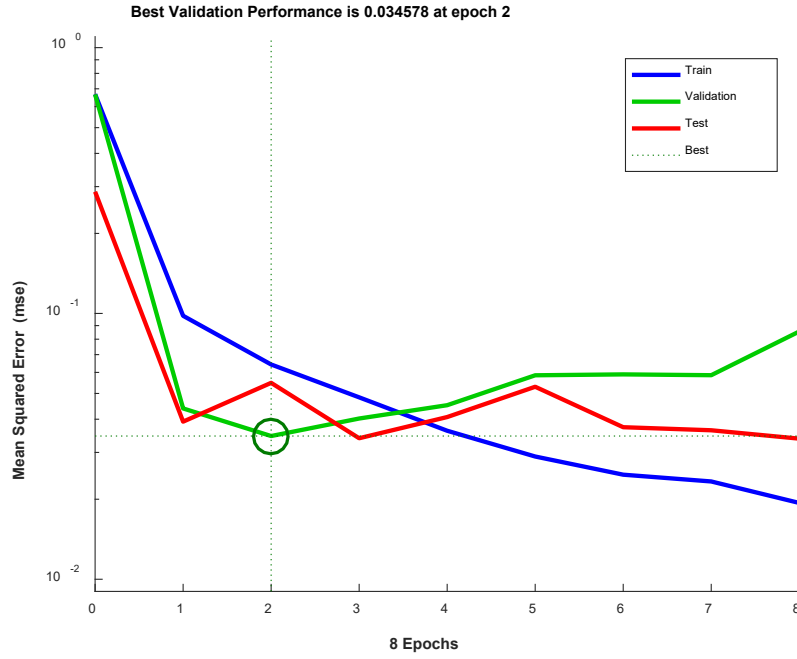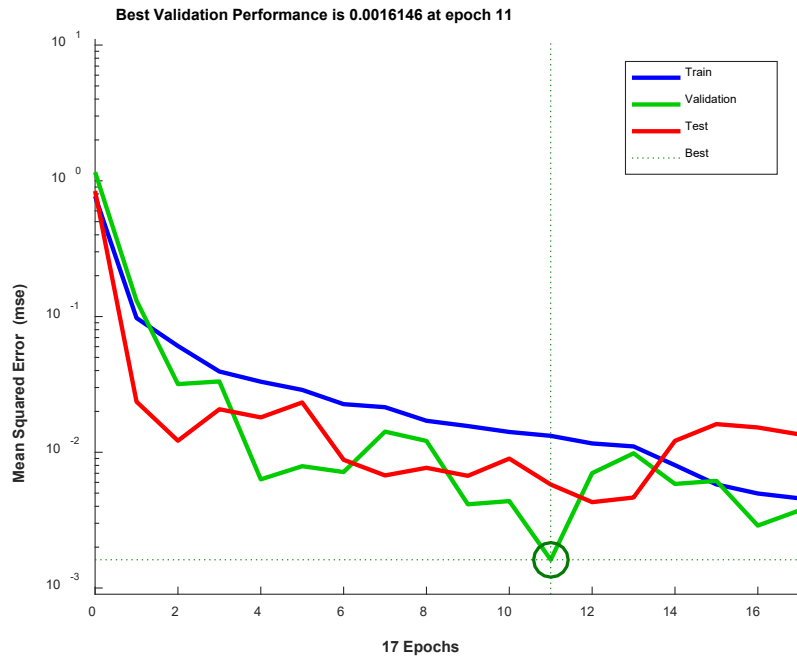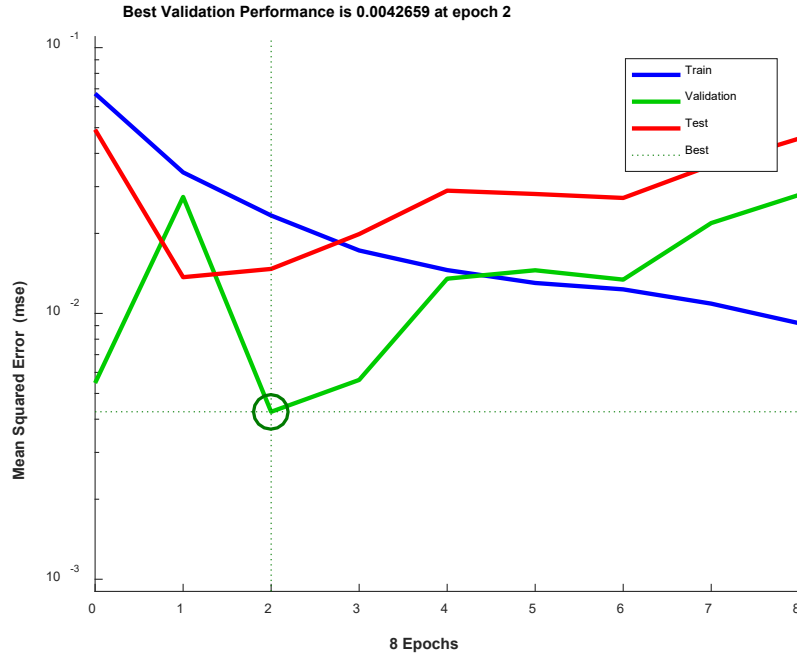

Figure F. 2 The mean squared error for the training, validation, testing vs their corresponding epochs to predict the D50 via single hidden layer network.

Figure F. 3 The mean squared error for the training, validation, testing vs their corresponding epochs to predict the D90 via single hidden layer network.
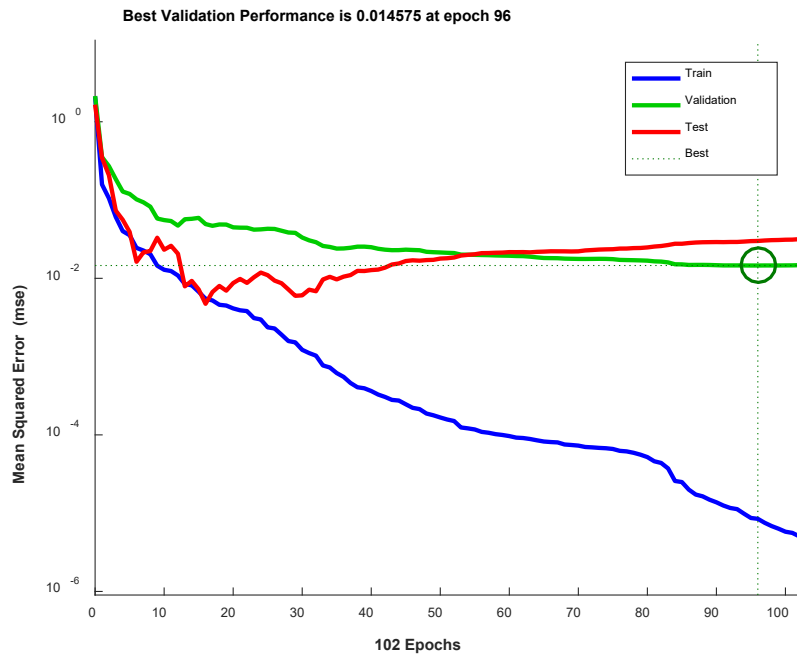

Figure F. 4 The mean squared error for the training, validation, testing vs their corresponding epochs to predict the D10 via two hidden layer network.

Figure F. 5 The mean squared error for the training, validation, testing vs their corresponding epochs to predict the D50 via two hidden layer network.

Figure F. 6 The mean squared error for the training, validation, testing vs their corresponding epochs to predict the D90 via two hidden layer network.
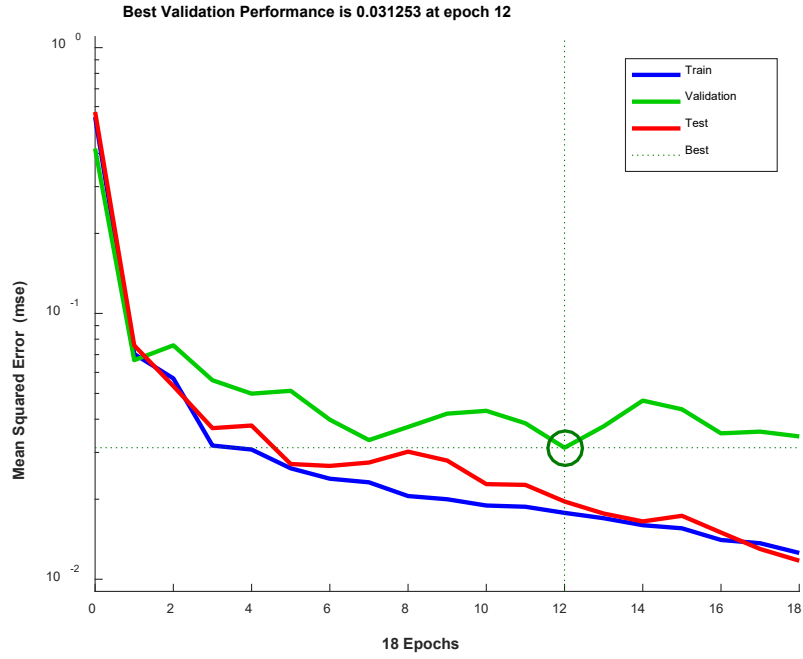
Figure F. 7 The mean squared error for the training, validation, testing vs their corresponding epochs to predict tablet strength using 7 inputs.
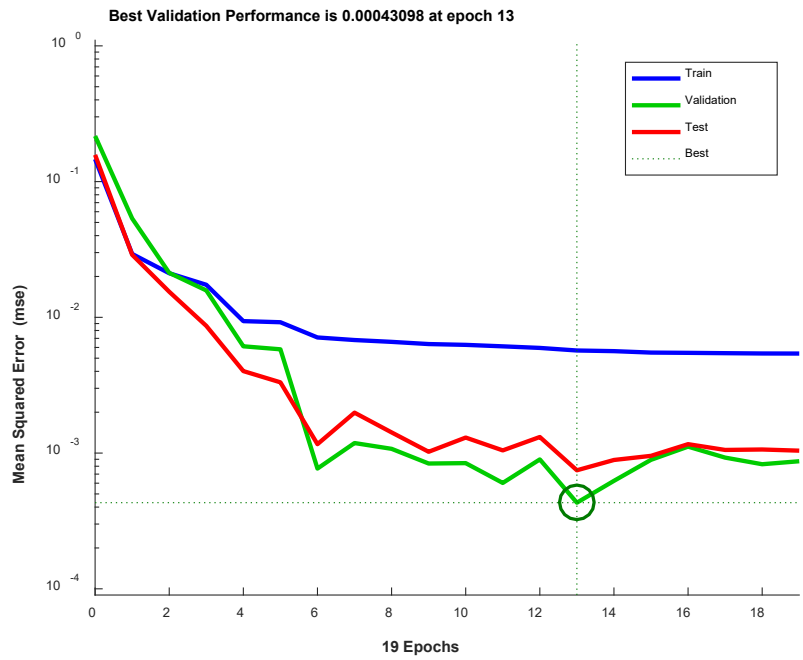

Figure F. 8 The mean squared error for the training, validation, testing vs their corresponding epochs to predict the tablet strength using specific surface area* moisture content as input.

186

Appendix G

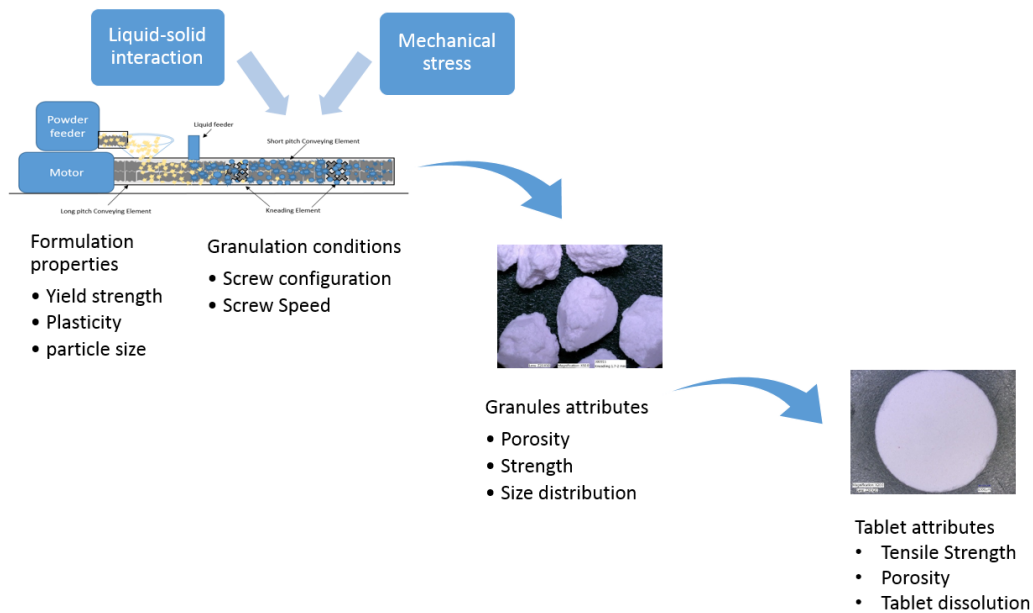Figure G.1 is a graphical abstract which shows briefly the work flow in this thesis.

Figure G. 1 Graphical abstract of the work conducted in this thesis.